PET studies on the aetiology of Parkinson's disease and on the efficacy of cell transplantation therapy ~~in Parkinson's disease.~~

Paola P. Piccini

Thesis submitted in fulfilment of the requirements for the degree of Doctor in Philosophy

Imperial College Faculty of Medicine,

Hammersmith Hospital,

University of London

BIBL.
LONDON.
UNIV.

Abstract

The aims of this thesis are, using positron emission tomography (PET), to increase our understanding of: 1.The role of genetic factors in the aetiology of Parkinson's disease (PD). 2. The role of cell transplantation as a therapy for PD.

^{18}F-dopa PET has been used to measure dopamine storage, ^{11}C-raclopride PET with amphetamine challenges to measure the capacity to release endogenous dopamine within the central dopaminergic systems, and $H_2{}^{15}O$ PET to localise patterns of cortical activation during specific motor tasks.

The main findings are as follows. (1) Longitudinal ^{18}F-dopa PET studies performed in mono- and dizygotic twins clinically discordant for idiopathic PD and in subjects heterozygous and homozygous for mutations in the *parkin* gene indicate that: (a) Genetic factors play an important role in the aetiology of "sporadic" PD and (b) Heterozygous *parkin* mutation carriers have subclinical dopamine degeneration and may be at risk for late-onset PD. (2) Fetal mesencephalic grafts implanted into the striatum of PD patients are able to: (a) Restore normal levels of dopamine storage capacity. (b) Release normal levels of dopamine after an amphetamine challenge. (c) Restore movement-related frontal cortical–activation. Taken together, my findings suggest that, despite an ongoing disease process, grafted human foetal DA neurones continue functioning over 10 years and that functional integration of the grafted neurones into the host brain is necessary in order to produce substantial clinical recovery in PD. 3. "Off" phase dyskinesias have been reported in transplanted PD. I have demonstrated that this is correlated with the amount of fetal material implanted but not with levels of graft dopamine storage capacity.

Table of contents

Abstract 2

List of tables 11

List of figures 15

Publications arising from thesis 20

Acknowledgements 22

1. Introduction and aims 24

1.1 The role of PET in understanding the genetic contribution to the causes of Parkinson's disease 24

1.1.1 The role of inheritance in sporadic Parkinson`s Disease 24

1.1.2 Dopaminergic function in twins 27

1.1.3. Genetic mutations 28

1.1.4 Studies in parkin-linked parkinsonism 36

1.1.4.1 Progression of nigrostriatal dysfunction in a *parkin* kindred 36

1.1.4..2. Striatal and cortical pre-and postsynaptic dopaminergic dysfunction in sporadic *parkin*-linked parkinsonism 38

1.2. PET studies on the efficacy of cell transplantation therapy in Parkinson' s disease 39

1.2.1 Neurosurgical approach to the treatment of Parkinson's disease 39

1.2.2 Replacement therapies 41

1.2.3 Dopamine release from nigral transplants 49

1.2.4 Recovery of movement-related cortical function following neural transplants 50

1.2.5 Dyskinesias following neural transplantation 50

2. Methodology 53

2.2 Positron Emission Tomography (PET) 53

2.2.1. Introduction 53

2.2.2. The cyclotron 53

2.2.3. Positron detection 54

2.2.4 Coincidence detection 56

2.2.5 Image reconstruction 58

2.2.6 Attenuation correction 58

2.2.7 Image resolution following reconstruction 59

2.2.8 The PET scanner 59

2.3 L-6-[18F]-fluorodopa (^{18}F-dopa) 62

2.3.1 Introduction 62

2.3.2 The Metabolism of intravenously injected ^{18}F-dopa 63

2.3.2.1 Peripheral Metabolism of ^{18}F –dopa 63

2.3.2.2 Blood Brain Barrier Transport of ^{18}F –dopa 63

2.3.2.3 Cerebral Metabolism of ^{18}F –dopa 64

2.3.4 Patient preparation and scan protocol 64

2.3..5 Data analysis 65

2.4 ^{11}C-raclopride 68

2.4.1 Introduction 68

2.4.2 Preparation 69

2.4.3 Safety and Tolerability 69

2.5 Displacement studies 70

2.5.1 Introduction 70

2.5.2 Validation of the method: Studies with normal volunteers and patients with Parkinson's disease 72

2.5.2.1 Subjects 72

2.5.2.2 Experimental design 73

2.5.2.3 Data acquisition 74

2.5.2.4 Tracer kinetic modelling 74

2.5.2.5 Region of interest analysis 75

2.6 H_2O^{15} activation studies 76

2.6.1 Measurement of regional cerebral blood flow (rCBF) 76

2.6.2 Relationship of rCBF to neuronal activity 77

2.6.3 Interpretation of rCBF changes 77

2.6.4 Statistical analysis of rCBF activation studies 78

2.6.4.1 Realignment of rCBF studies 79

2.6.4.2 Stereotactic normalisation 79

2.6.4.3 Smoothing 80

2.6.4.4 Statistical analysis 81

2.6.4.5 Statistical inferences 82

3. The role of PET in understanding the genetic contribution to the causes of Parkinson's disease 84

3.1 The role of inheritance in sporadic Parkinson's disease: Evidence from a longitudinal study of dopaminergic function in twins. 84

3.1.1 Subjects 84

3.1.2 Specific methods 85

3.1.3 Results 86

3.1.3.1 PD co-twins 85

3.1.3.2 Asymptomatic co-twins 87

3.1.3.2.1 Baseline 86

3.1.3.2.2 Repeat scanning 89

3.1.4 Discussion 94

3.2 Studies in *parkin*-linked parkinsonism 97

3.2.1 Progression of nigrostriatal dysfunction in a *parkin* kindred: an ^{18}F-dopa PET and clinical study 97

3.2.1.1 Subjects 97

3.2.1.2 Specific methods 97

3.2.1.2.1 PARK2 molecular data 97

3.2.1.2.2 Scanning protocol 99

3.2.1.3 Results 101

3.2.1.3.1 Clinical findings 101

3.2.1.3.1.1 Patients 102

3.2.1.3.1.2 Asymptomatic cases 104

3.2.1.3.2 PET data 106

3.2.1.3.2.1 Patients 106

3.2.1.3.2.2 Clinically asymptomatic cases 109

3.2.1.4 Discussion 110

3.2.2 Striatal and cortical pre-and postsynaptic dopaminergic dysfunction in sporadic *parkin*-linked parkinsonism 114

3.2.2.1 Subjects 114

3.2.2.2 Specific methods 116

3.2.2.2.1 Molecular analysis 116
3.2.2.2.2 Scanning protocol 116
3.2.2.3 Data analysis 117

3.2.2.3 Results 119
3.2.2.3.1 ROI analysis of ^{18}F-dopa 119
3.2.2.3.2 ROI analysis of ^{11}C-raclopride 120
3.2.2.3.3 ^{18}F-dopa SPM findings 121
3.2.2.3.4 ^{11}C-raclopride SPM findings 124

3.2.2.4 Discussion 127

4. Measuring striatal and cortical dopamine release in normals and in Parkinson's disease patients 131

4.1 Subjects 131

4.2 Specific methods 133

4.3 Results 134
4.3.1 Region of interest analysis 134
4.3.2 Statistical parametric mapping 142

4.4 Discussion 145

5. PET studies on the efficacy of cell transplantation therapy in Parkinson disease 149

5.1 Demonstrating dopamine release from striatal implants in a patient with Parkinson's disease 149

5.1.1 The subject 149

5.1.2 Specific Methods 149

5.1.2.1 Transplantation procedure 150

5.1.2.2 Clinical evaluation 151

5.1.2.3 Scanning procedure 151

5.1.3 Results 151

5.1.4 Discussion 157

5.2 Delayed recovery of movement-related cortical function in Parkinson's disease following striatal dopaminergic grafts 162

5.2.1 Subjects 162

5.2.2 Specific Methods 163

5.2.2.1 Graft preparation and neurosurgical procedure 163

5.2.2.2 Clinical evaluation 164

5.2.2.3 PET scanning procedures and data analysis 164

5.2.3 Results 167

5.2.4 Discussion 172

5.3 Dyskinesias following neural transplantation in Parkinson's disease 175

5.3.1 Subjects 175

5.3.2 Specific Methods 175

5.3.3 Results 177

5.3.4 Discussion 183

6. Conclusions. Review of the Major Findings 186

6.1 The role of PET in understanding the genetic contribution to PD 186

6.2 PET studies in transplantation therapy 187

7. References 190

List of tables

Table 1. Parkinson's disease loci. 30

Table 2. Functional outcome after bilateral transplantation in open label trials and in one double-blind placebo-controlled trial 47

Table 3. Displacement studies: clinical characteristics of the PD patients 73

Table 4. Mean putamen ^{18}F-dopa uptake in control subjects, in monozygotic and in dizygotic co-twins of clinically affected Parkinson's disease subjects. 87

Table 5. Concordance levels of nigro-striatal dopaminergic dysfunction in monozygotic and dizygotic twin pairs at baseline discordant for clinical Parkinson's disease. 89

Table 6. Clinical characteristics for each of the clinically affected subjects with parkin mutations and for a group of seven patients with idiopathic Parkinson's disease. 99

Table 7. Mean percentage reductions relative to the mean of normal subjects in caudate and putamen ^{18}F-dopa Ki values in the four parkin patients and in the group of seven patients with idiopathic Parkinson's disease (IPD), at the time of the first and the second scan with the interval in years between scans. 105

Table 8. Clinical, genetic and striatal ^{18}F-dopa PET characteristics of the asymptomatic members of the family. 108

Table 9. *Parkin* mutations identified in 13 cases with young onset PD. 113

Table 10. Demographic and clinical characteristics of parkin positive, parkin negative YOPD, IPD and control subjects. 114

Table 11. Mean regional putamen (anterior, posterior) and caudate ^{18}F-dopa K_i min^{-1} and ^{11}C-raclopride binding potential values in *parkin* positive YOPD, *parkin* negative YOPD, idiopathic Parkinson's disease and control subjects. 119

Table 12. (A) Between-group SPM findings showing significant decreases and increases of ^{18}F-dopa Ki in *parkin* positive, *parkin* negative YOPD, and control subjects. 122

Table12 (B) Between-group SPM showing of significant decreases of ^{11}C-raclopride BP in *parkin* positive, *parkin* negative YOPD, and control subjects. 124

Table 13. Clinical characteristics of PD patients 132

Table 14. Mean caudate and putamen ^{11}C-raclopride BP (± SD) for the normal subjects and for the Parkinson' s disease (PD) patients after saline and after methamphetamine i.v. infusion. 135

Table 15. SPM co-ordinates 142

Table 16. ^{18}F-dopa uptake in a PD patient before and after unilateral transplantation of fetal mesencephalic cells in the right putamen. 152

Table 17. Values of striatal ^{11}C-raclopride BP and relative tracer delivery (R_I) after intravenous infusion of m-amphetamine or saline in a PD patient 10 years after transplantation of embryonic mesencephalic tissue into the right putamen. 154

Table 16. Characteristics of PD patients PD patients 162

Table 19. Locations and peak-Z-scores of areas in which rCBF during joystick movements was significantly greater 18.3 months after bilateral implantation of embryonic mesencephalic tissue into caudate and putamen as compared to preoperatively in four PD patients. 168

Table 20. Mean striatal ^{18}F-dopa uptake in four PD patients before and after bilateral implantation of mesencephalic tissue in the caudate nucleus and putamen. 169

Table 21. PD patients transplanted in Lund included in this study. 177

Table 22. Clinical characteristics of the patients (n = 14) at the time of transplantation group and at the time of maximum post-operative 'off' phase dyskinesias. 178

Table 23. Exploratory correlation analyses for the highest observed postoperative "off" phase global CDRS score. 180

List of figures

Figure 1. Impaired ubiquitin-proteasome degradation pathway in PD. 35

Figure 2. Cortico-basal ganglia circuits: hypothetic effects of intrastriatal dopaminergic graft. 42

Figure 3. Schematic representation of the different steps in transplantation 45

Figure 4. Serial ^{18}F-dopa PET images in a PD patient before and after transplantation of human embryonic mesencephalic cells into putamen. 48

Figure 5. PET: production of radioisotopes. 55

Figure 6. Schematic representation of detectors in a tomograph. 57

Figure 7. The ECAT EXACT HR++ scanner. 61

Figure 8. Integral images of ^{18}F-dopa in a normal volunteer superimposed onto the subject MRI. 67

Figure 9. Two scan ^{11}C-raclopride model. 70

Figure 10. Discriminant analysis in 18 asymptomatic monozygotic and 16 dizygotic co-twins of Parkinson's disease patients. 89

Figure 11. Putamen ^{18}F-dopa uptake in 10 asymptomatic monozygotic (A) and 9 dizygotic (B) co-twins of Parkinson's disease patients scanned twice. 90

Figure 12. ^{18}F-dopa images in a twin with PD and in his asymptomatic MZ co-twins at baseline (A) and after 6 years (B). 92

Figure 13. Pedigree of the family with *Parkin* disease. 97

Figure 14. ^{18}F-dopa images for a patient with idiopathic PD (A) and for a patient with Parkin mutation (B) with similar age duration and similar disease severity. 104

Figure 15. Individual rate of decline over time in ^{18}F-dopa putamen uptake in *parkin* patients (A) and in patients with idiopathic Parkinson's disease (IPD) (B) 106

Figure 16. Mean percentage reductions per annum in ^{18}F-dopa caudate and putamen uptake in the group of *parkin* and in the IPD group. 107

Figure 17. Mean caudate and putamen ^{18}F-dopa uptake in four *parkin* heterozygous carriers and in 14 age matched normal controls. 109

Figure 18. SPM transverse and sagittal maximum intensity projection maps rendered on to a stereotactically normalized MRI scan, showing areas of significant decreases in

midbrain and caudate ^{18}F-dopa K_i uptake in *parkin*-linked parkinsonism compared with *parkin* negative YOPD. 121

Figure 19. SPM transverse maximum intensity projection maps rendered on to a stereotactically normalized MRI scan, showing areas of significant decreases in RAC-BP in parkin-linked parkinsonism compared with parkin negative YOPD. 125

Figure 20 (A) Individual caudate and putamen ^{11}C-raclopride binding potentials after injection of saline and after injection of m-amphetamine in the 6 normal volunteers. (B) Individual caudate and putamen ^{11}C-raclopride binding potentials after injection of saline and after injection of m-amphetamine in the 6 patients with PD 136-137

Figure 21. ^{11}C-raclopride binding potential parametric images in a normal subject after saline and after 0.3 mg/kg methamphetamine. 138

Figure 22. Correlation between left and right putamen ^{18}F-dopa uptake (Ki) and % reduction in left and right putamen ^{11}C-raclopride binding potentials (BP) after methamphetamine in individual patients with Parkinson's disease. 139

Figure 23. Images of ^{18}F-dopa uptake and ^{11}C-raclopride Binding Potential (BP) following administration of saline and following administration of 3 mg/kg methamphetamine in a PD patient. 140

Figure 24 Sagittal and transaxial projections of statistical parametric maps. A. Within group comparisons: Areas of significant decreases in ^{11}C-raclopride binding potential

after methamphetamine as compared to after saline in 6 normal volunteers and in 6 patients with Parkinson's disease. B. Between group comparisons: Areas of significant differences in ^{11}C-raclopride binding potential after methamphetamine between the groups of normal subjects and patients with Parkinson's disease 144

Figure 25. Percentage of the day spent in "off" (open squares) and UPDRS motor score (filled circles) in the practically defined "off" phase. 150

Figure 26 ^{18}F-dopa uptake in the grafted and in the ungrafted putamen (open squares) before transplantation and at one, three, six and ten years follow-up. 153

Figure 27. ^{11}C-raclopride time active curves after saline and after methamphetamine injection in a PD patient with transplantation of embryonic mesencephalic tissue to the right putamen.. 155

Figure 28. Integral images of ^{18}F-dopa and parametric images of ^{11}C-raclopride binding potential (BP) at the level of the basal ganglia for the PD patient 10 years after transplantation of embryonic mesencephalic tissue into the right putamen. In the baseline condition (after saline infusion). 156

Figure 29. Images of ^{18}F-dopa uptake and ^{11}C-raclopride Binding Potential (BP) following administration of saline and following administration of 3 mg/kg methamphetamine in a PD patient before and after transplantation of human embryonic mesencephalic cells into the right putamen. 161

Figure 30. Areas of activation associated with freely selected joystick movements before (left), at 6.5 months (centre), and at 18.3 months (right) after bilateral implantation of embryonic mesencephalic tissue into the caudate nucleus and putamen in four PD patients 167

Figure 31. Areas of increased movement-related activation at a mean of 18.3 months after bilateral implantation of embryonic mesencephalic tissue into the caudate nucleus and putamen as compared to preoperatively in four PD patients. 169

Figure 32. ^{18}F-dopa scans for a PD patient before and after bilateral implantation of human foetal dopamine cells in caudate and putamen bilaterally. 170

Figure 33. Caudate and putaminal ^{18}F-dopa K_i values, UPDRS motor score and percentage of movement-associated levels of rCBF in comparison to rest in SMA and DLPFC preoperatively and at 6.5 and 18.3 months after bilateral implantation of embryonic mesencephalic tissue into the caudate nucleus and putamen. 171

Figure 34. Hyperkinesias and dystonia during practically defined "off" and peak "on" phases before transplantation and the latest assessment after transplantation (mean 44.6 months). 181

Figure 35. Negative correlation between severity of postoperative "off" dyskinesias and preoperative ^{18}F-dopa uptake in the putamen. 182

Publications arising from this thesis

1. **Piccini P**, Pavese N, Brooks DJ. An *in vivo* study of striatal and cortical endogenous dopamine release following pharmacological challenges in Parkinson's disease. ***Ann Neurol***. 2003; 53: 647-653
2. **Piccini P.** Dyskinesias after transplantation in Parkinson`s disease. ***The Lancet*** Neurology 2002;1(8):472
3. Khan NL, Brooks DJ, Pavese N, Sweeney MG, Wood NW, Lees AJ, **Piccini P.** Progression of nigrostriatal dysfunction in a parkin kindred: an [(18)F]dopa PET and clinical study**.** ***Brain***. 2002;125: 2248-56.
4. Hagell P, **Piccini P**, Bjorklund A, Brundin P, Rehncrona S, Widner H, Crabb L, Pavese N, Oertel WH, Quinn N, Brooks DJ, Lindvall O. Dyskinesias following neural transplantation in Parkinson's disease. ***Nature Neuroscience***. 2002;5(7):627-8.
5. **Piccini P**, Lindvall O, Björklund A, Brundin P, Hagell P, Oertel W, Quinn N, Ceravolo R, Rehncrona S, Widner H, Brooks DJ. Delayed Recovery of Movement-related Cortical Function in Parkinson's Disease following Striatal Dopaminergic Grafts. ***Ann Neurol*** 2000; 48(5): 689-695.
6. Brundin P, Pogarell O, Hagell P, **Piccini P**, Widner H, Bjorklund AH, Brooks DJ, Quinn NP, Schrag A, Rehncrona S, Lindvall O. Bilateral Caudate and Putamen Grafts of Embryonic Mesencephalic Tissue Treated with Lazaroids in Parkinson's disease. ***Brain*** 2000; 123: 1380-1390.
7. **Piccini P**, Brooks DJ, Bjorklund A, Gunn RN, Grasby PM, Rimoldi O, Brundin P, Hagell P, Rehncrona S, Lindvall O. Dopamine release from nigral

transplants visualized *in vivo* in Parkinson's disease. ***Nature Neuroscience*** 1999; 2 (12): 1137-1140.

8. **Piccini P**, Burn DJ, Ceravolo R, Maraganore D, Marsden CD, Brooks DJ. The role of inheritance in Parkinson's disease: evidence from a longitudinal study of dopaminergic function in twins. ***Ann. Neurol.*** 1999; 45(5): 577-582.

9. Hagell P, Schrag A, **Piccini P**, Jahanshani M, Brown R, Odin P, Wenning GK, Morrish P, Rehncrona S, Widner H, Brundin P, Rothwell J, Gustavii B, Biorklund A, Brooks D, Marsden CD, Quinn NP, Lindvall O. Sequential bilateral transplantation in Parkinson's disease: effects of the second graft. ***Brain*** 1999; 122: 1121-1132.

Acknowledgements

There are so many people that have played some kind of part in the preparation of this thesis that I am virtually bound to leave many out of these pages. All colleagues, co-workers, friends that I have met and interacted with ever since I first came to the "MRC Cyclotron Unit" and during the following years as a PhD student, have contributed in one way or another.

First and foremost my gratitude goes to my supervisor, David Brooks. I could not have wished for a better supervisor. My gratitude goes also to the support and trust he has provided me with during all these years at the "Hammersmith".

I also would like to thank all the people whom I had the pleasure of collaborating with throughout this work. The Lund group and particularly Professor Olle Lindvall for his encouragement, support and expert advice without which important parts of this thesis would have not been written, but also Peter Hagell and Professor Anders Bjorkland.

The Institute of Neurology group, Professor Andrew Lees, Professor Niall Quinn and Professor Nicholas Wood for useful suggestions and help.

I am grateful to the many Research Fellows who have worked or are still working at the Cyclotron Unit and with whom I have shared not just the Unit rooms and scanner "slots" but lengthy discussions and mutual support. I am indebted to them for their valuable help and useful comments as well as being good friends: Henning Boecker, Harri Jenkins, Alain Dagher, Michael Samuel, Michele Hu, Thomasin Andrews, Jeremy Stern, Alex Hammers, Gary Hotton, Alan Whone, Naheed Kahn and Nicola Pavese.

A special thank you to Hyacinth Henry who has been always supportive throughout both good and bad days.

I would like to thank the radiographers for their considerable help with scanning and all the chemists and physicists who have made the scans possible.

Finally I am very grateful to the patients who traveled often and far (some of them from USA, Sweden, Italy, and Germany) in order to enable the completion of these studies.

Introduction and aims

1

1.1 The role of PET in understanding the genetic contribution to the causes of Parkinson's disease

1.1.1 The role of inheritance in sporadic PD.

Idiopathic (or sporadic) PD is one of the commonest neurodegenerative disorders with a clear age dependent prevalence of 1-2 percent after age 65 years (De Rijk 1997). The phenotype of idiopathic PD is characterized by asymmetric resting tremor, rigidity and bradykinesia, which respond well to levodopa treatment. Parkinsonism is the term used to describe this costellation of clinical signs but is also manifested by a number of other neurodegenerative disease which are generally less responsive to levodopa and have different neuropathological findings. PD has been found in all ethnic groups and geographical areas with lowest prevalences in China, Japan, and Africa (Zhang &Roman 1993) though this may reflect ascertainment bias. Since its description by James Parkinson nearly 200 years ago (Parkinson 1817) intense efforts have been made to establish its aetiology. The discovery that N-methyl-4-phenyl-1,2,3,6-tetrahydropyridine (MPTP) can cause clinical parkinsonism (Irwin et al 1987) refocused the environmental debate, but the absence of a diagnostic test or bioassay for PD has meant that epidemiological studies tend to underestimate the

prevalence of PD in population. To date, the only unequivocally accepted risk factors for PD are increasing age and a family history.

Several case-control studies have consistently indicated that PD is more common among relatives of index patients with PD compared with matched control population, as between 6 and 30% of index patients had first-or second degree affected relatives (Lazzarini 1994, Payami 1994, Bonifati 1995, De Michele1996, Marder 1996). However these studies were subjected to recall bias. A recent large population based case-control study found that PD significantly aggregated in families, the strength of the association being age-dependent. This is keeping with the fact that familial factors, which can be genetic , environmental, or both play a role in PD (Elbaz 1999). Overall the relative risk in first degree relative of probands with PD is in the range of 2-3 which is similar to that found in AD (Farrer et al 1989).

Sporadic PD patients are considered to be those cases where a familial aggregation for the disease is not clinically manifest; it is, nevertheless, unclear whether the apparent lack of familial aggregation only reflects our inability to detect subclinical disease in at-risk PD relatives who die from other disorders without ever manifesting parkinsonism. It has been estimated that, while 10% of 70 year olds show evidence of subclinical PD at autopsy, only 1% ever manifest clinical symptoms (Golbe, 1990). ^{18}F-dopa PET is a technique which is a marker of nigral pathology, albeit an indirect one. The striatal uptake of ^{18}F-dopa reflects the capacity of the striatum to form and store exogenous dopamine (Garnett et al., 1983), and so provides a measure of the functional integrity of the nigrostriatal dopaminergic projections. Following intravenous injection, the positron emitting tracer is taken up by nigrostriatal nerve terminals in the caudate and putamen, where it is converted by aromatic amino acid decarboxylase to ^{18}F-dopamine and its metabolites. Although considered in more detail

later, it should be stressed that ^{18}F-dopa PET does not represent the endogenous synthesis of dopamine, since the rate-limiting enzyme in this synthesis, tyrosine hydroxylase, is by-passed.

A number of groups have reported reduced striatal ^{18}F-dopa uptake in patients with PD (Nahmias et al,1985; Brooks et al 1990; Martin et al, 1989; Eidelberg et al,1990; Otsuka et al 1991). Brooks and colleagues (1990) reported that patients with a clinical diagnosis of sporadic PD had a mean 50% and a minimum 35% reduction in putamen tracer uptake when compared with normal. ^{18}F-dopa PET, therefore, should be capable of detecting preclinical disruption of nigrostriatal projections, if present.

In 1985, Calne *et al.* reported the results of ^{18}F-dopa PET studies in four human subjects who had been exposed to MPTP but who had no evidence of parkinsonism. Two of these subjects had striatal tracer uptake within the 'normal' range, and two within the range shown for PD patients. Guttman *et al* (1988) subsequently reported serial ^{18}F-dopa PET scans in two cynomolgus monkeys who were given small doses of MPTP, insufficient to cause signs of parkinsonism. One animal received three injections, spaced two weeks apart, and was scanned approximately 10 days after each injection. Striatal ^{18}F-dopa uptake was reduced to 97%, 59% and 38% of control values in these sequential scans. The animal subsequently became parkinsonian after a fourth injection of MPTP. The second monkey remained asymptomatic after a single injection of MPTP, but became parkinsonian after the second injection. Specific striatal signal was decreased to 77% of control values 11 days after the first injection. Subclinical nigrostriatal dopaminergic dysfunction has also been shown using ^{18}F-dopa PET in Guamanians (Snow et al, 1990). In this study four Guamanians with an amyotrophic lateral sclerosis syndrome, eight Guamanians with parkinsonism and seven clinically normal Guamanians underwent PET. Results were compared with data from nine Canadian control subjects. The parkinsonian

subjects all had significantly reduced striatal ^{18}F-dopa uptake. The group with amyotrophic lateral sclerosis had significantly reduced tracer uptake that was intermediate between that of the control group and the parkinsonian group. Two of the seven clinically normal Guamanians had significantly reduced striatal ^{18}Fdopa uptake.

Finally, in 1997 we used ^{18}F-dopa PET to investigate subclinical nigrostriatal dopaminergic function in asymptomatic members of 7 unrelated kindreds in which at least 2 members had parkinsonism. We found that eight (25%) of the 32 asymptomatic relatives showed abnormal putamen ^{18}F-dopa uptake (2.5 SD below the normal mean). When discriminant function analysis was applied all these eight subjects plus another three were classified with high probability as having PD (Piccini et al., 1997). Four of these subjects subsequently went on to develop clinical Parkinson's disease.

^{18}Fdopa PET can therefore provide a means of assessing severity of preclinical PD.

1.1.2 Dopaminergic function in twins

Twin studies have long served as a mean of examining the relative roles of genetic and environmental factors in a given disorder. However, classical cross-sectional surveys of the clinical concordance of PD in twins suffer from an inability to detect cases with subclinical disease. Latencies for clinical concordance vary greatly within PD twin pairs and one identical pair reportedly only became clinically concordant for parkinsonism after an interval approaching three decades (Zimmermann et al 1991).

Here I report serial clinical and ^{18}Fdopa PET findings collected over seven years for a PD twin population without familial aggregation of the disease in order to investigate the genetic contribution to the aetiology of this disorder. I hypothesised that if genetic factors are more important than environmental factors in idiopathic PD the

concordance for clinical and subclinical nigro-striatal dopaminergic dysfunction would be higher in MZ than DZ twin pairs and tend to increase over time.

1.1.3 Genetic mutations

Over the past few years several genes for monogenically inherited forms of parkinsonism have been mapped and/or cloned.

α-synuclein (PARK1). The first levodopa-responsive PD gene was found to map to 4q21-22 in a large Mediterranean kindred, the Contursi family (Polymeropoulos et al., 1996). In this family the parkinsonism was being inherited in autosomal dominant fashion. The clinical expression of the disease and pathology were consistent with sporadic PD except for a young mean age at onset of 46 years and a rapid disease course of 10 years from onset to death (Golbe et al., 1990). Subsequently, in this pedigree and three Greek families, a single common alanine to threonine substitution at position 53 within the gene coding from α-synuclein was identified (Polymeropoulos et al., 1997). Interestingly, the wild-type sequence in mouse, rat and canary has a threonine at amino acid 53. A second independent mutation has since been identified (Ala39Pro) in a small German kindred (Kruger et al., 1998). Large numbers of PD patients have been screened for mutations in the α-synuclein gene and the absence of additional mutations suggests that PD patients whose disease is caused by alterations in α-synuclein are rare (Farrer et al., 1998; Chan et al., 1998). However, recently it has been shown that certain polymorphisms of the α-synuclein gene may confer risk for the development of PD and, therefore, be a susceptibility factor in non-familial cases (Kruger et al., 1999; Farrer et al., 2001). Also a triplication of a section of the α-synuclein gene caused PD in one kindred - PARK4.

The finding of a mutation in the α-synuclein gene provided the first demonstration that genes can play a role in the pathogenesis of PD. Quickly following this discovery, it was recognized that α-synuclein was a major component of Lewy bodies in not only dominantly inherited PD but also in sporadic PD (Spillantini et al., 1997). The accumulation of α-synuclein in pathologic inclusions in the brain is not limited to PD. Immunohistochemical studies have demonstrated this protein in the inclusion of diffuse Lewy body disease (Hashimoto et al., 1999), the senile plaques of Alzheimer' s disease (Hashimoto et al., 1999), and Down's syndrome (Lippa et al., 1999) as well as the glial cytoplasmic inclusions of multisystem atrophy (Gai et al., 1998). This has led to development of a new pathological classification of neurodegenerative disorders, so-called " synucleinopathies" (Galvin et al., 2001). Both murine (Masliah et al., 2000) and a *Drosophila* (Feany et al., 2000) model of PD have now been developed and are proving to be useful. In particular, the *Drosophila* model is attractive in that it demonstrates age dependence, disease progression, selective loss of dopaminergic neurones, and the formation of fibrillar α-synuclein inclusions.

Parkin (PARK2). This autosomal recessive, classically juvenile onset form of PD maps to chromosome 6q25.2-q27 (Matsumine et al., 1997). A positional cloning approach identified a microdeletion and resulted in the isolation of a cDNA clone of 2.9kb with a 1395-base-pair open reading frame. The gene designated *parkin*, consisted of 12 exons and spanned more than 500kb. The resulting protein consisted of 465 amino acids with moderate similarity to ubiquitin at the amino terminus and a RING-finger motif at the carboxy terminus, predicting that *parkin* likely possesses DNA-binding and transcriptional activities (Kitada et al., 1998). Mutations in the *parkin* gene are responsible for the pathogenesis of autosomal recessive parkinsonism first described in Japanese families (Ishikawa et al., 1996). Clinically the disease has an early age of

onset with a mean of 24.6 years, prominent dystonia, diurnal fluctuations with a slow progression but early severe levodopa-induced dyskinesias.

Table 1. Parkinson's disease loci

LOCUS	GENE	MAP position	Inheritance	Phenotype	Pathology
PARK1	a-synuclein	4q21-22	AD	L-dopa responsive, early onset PD	Lewy bodies
PARK2	*parkin*	6q25.2-27	AR	L-dopa responsive, early onset PD*	No Lewy bodies
PARK3		2p13	AD	Typical PD	Lewy bodies
PARK4	Now known to be a-synuclein triplication	4q	AD	L-dopa responsive PD, postural tremor, dementia	Lewy bodies
PARK5	UCH-l	4p16	AD	Typical PD	Not reported
PARK6		1p36	AR	L-dopa responsive, early onset PD	Not reported
PARK7	DJ-1	1p35-36	AR	L-dopa responsive, early onset PD	Not reported
PARK8		12p11.2-q13.1	AD	Typical PD, but early age of onset	Nigral degeneration, no Lewy bodies

AD= autosomal dominant, AR= autosomal recessive, * additional clinical features reported in text.

In a study of 73 families in which at least one affected family member showed symptoms before the age of 45 and where the parents were not affected, 49% had *parkin* mutations demonstrating that this is a major cause of early onset autosomal recessive PD (Lucking et al., 2000). Among these patients, mutations were detected in 10 out of 13 patients (77%) with an age of onset of 20 years or younger, but in only 2 of 64 patients (3%) with an age at onset of more than 30 years. The mean age at onset in the patients with *parkin* mutations was younger than in those without mutations (32 vs 42 years), and they were more likely to have asymmetric involvement and dystonia at onset, to have hyperreflexia, to have a good response to levodopa therapy, and to have levodopa-induced dyskinesias. Numerous different mutations in *parkin* have now

been detected in individuals from diverse ethnic backgrounds (Leroy et al., 1998; Abbas et al., 1999).

PARK 3. In 1998 a susceptibility locus for PD was mapped to a 10.6 CM region of chromosome 2p13 in a subset of families with autosomal dominant inheritance (Gasser et al., 1998). In the original paper the authors described a genetic locus that appeared to be involved in the development of a disease closely resembling typical PD. This locus was detected in a group of six families of European origin and in two of these (families B and C) from a relatively small area in Northern Germany and Southern Denmark, there was a genetic evidence for a common founder. The penetrance of the disease at this locus was estimated to be 40% because of the relatively frequent occurrence of affected haplotype in clinically asymptomatic members in two of the linked families. To date the founder haplotype has not been identified in other German patients with familial or sporadic PD suggesting that it is not a prevalent founder effect in Germany (Klein et al., 1999). Further follow-up and molecular analysis suggests that one of these families of English descent may not be linked to this locus (Wszolek et al., 2001). This locus has been further refined, reducing the minimum common haplotype to eight markers spanning a physical distance of 2.5 Mb. The sequencing of 14 candidate genes within the region did not reveal any potentially pathogenic mutations segregating with the disease, implying that none of these genes are likely to be candidates for *PARK3* (West et al., 2002).

PARK4. In another linkage study, centred on a large family with levodopa responsive Lewy body parkinsonism , the disease segregated as an apparent autosomal dominant trait (Farrer et al., 1999). However, this family had other atypical features such as dysautonomia and dementia. On pathological examination in addition to Lewy bodies and nigral cell loss unusual vacuoles were seen in the hippocampus and other brain

areas. In this family the halpotype also occurred in individuals who do not have parkinsonism, but rather suffer from a postural and kinetic tremor, consistent with essential tremor, suggesting that essential tremor could be an alternative phenotype (Farrer et al., 1999).

Ubiquitin carboxy-teminal hydrolase L1 (UCH-L1) (PARK5). The *UCH-L1* gene which maps to 4p16 was sequenced in probands of 72 families with PD and a missense mutation, isoleucine to methionine at residue 93 (Ile93Met), and was identified in one sibling pair of German origin with atypical PD (Leroy et al., 1998). Symptoms began with resting tremor at age 51 in the sister and age 49 in the brother, and progessed to rigidity, bradykinesia and postural instability with a beneficial response to levodopa. No pathologic information is available yet to determine the presence of Lewy bodies associated with the mutation. The Ile93Met amino acid substitution was not present in 500 control chromosomes. Molecular modelling of the mutation was consistent with an alteration in the geometry of the active site, while functional studies demonstrated approximately 50% reduction in the catalytic activity (Leroy et al., 1998). *UCH-L1* is an abundant brain protein accounting for 1-2% of total soluble brain proteins, it is present in all the neurons and is also present in Lewy bodies. *UCH-L1* is a thiol protease belonging to the family of deubiquinating enzymes. The Ile93Met substitution in this gene has yet to be identified in other individuals with PD and suggest that it is either a very rare cause of PD or could in fact just be a rare non-pathologic polymorphism. An association study using a polymorphism within this gene demonstrated that it may confer a protective effect (Maraganore et al., 1999).

PARK 6 and PARK7. Two separate regions have been linked in different families as being associated with a levodopa-responsive parkinsonism on the short arm of chromosome 1 (*PARK6* an d *PARK 7*). The*PARK6* locus (1p35-36) was identified

through a genome-wide linkage in a consanguineous Italian family (Valente et al., 2001). This report was quickly followed by the identification of the*PARK7* locus in one family from southwest Netherlands with four affected individuals (van Duijn et al., 2001). These families have an early onset asymmetric disease (,50 years old) with good response to levodopa and slow disease progression. In the *PARK6* locus has subsequently been linked to an additional eight of 28 families screened from four different European countries, suggesting that it may be a common cause of recessively inherited PD in cases where the parkin gene has been excluded as a cause (Valente et al., 2002). Four of the 16 affected individuals had an age of onset above 45 years, with the oldest being 68. In the late-onset case the clinical features were indistinguishable from idiopathic PD suggesting that may be many individuals who harbour this yet to be identified mutation. Recently, mutations in the *DJ*-1 gene have been found to be associated with *PARK7* (Bonifati et al.,2003). *DJ*-1 gene encodes a ubiquitous , highly conserved protein, whose function is unknown but normally exists as a membrane bound dimer and is involved in oxidative stress response. The PARK7 mutations prevent dimerisation. In neither the *PARK6* nor *PARK7* families has pathology been documented.

PARK8. A genome–wide analysis identified a 13.6 cM region on chromosome 12p11.2-q13.1 in a Japanese family with autosomal dominant levodopa responsive parkinsonism (Funayama et al., 2002). All affected individuals shared a common haplotype but some unaffected individual also carried the disease haplotype suggesting that the penetrance of the disease is incomplete. The mean age of onset was 51±6 years, with unilateral onset of the disease. Four cases in this family have had neuropathological examination which showed mild to moderate loss of melanin-

containing cells but no Lewy bodies. These individuals were diagnosed as having 'pure nigral degeneration' (Hasegawa et al., 1997).

Molecular genetic studies on the familial forms of PD have advanced our understanding of the molecular mechanisms of selective dopaminergic neurones in the midbrain and have provided into the pathophisiology of this disorder. To date, there are still many questions to be answered but a common theme that is beginning to emerge is that PD may be caused by the neurone's inability to clear protein effectively. Figure 1 illustrates this hypothesis.

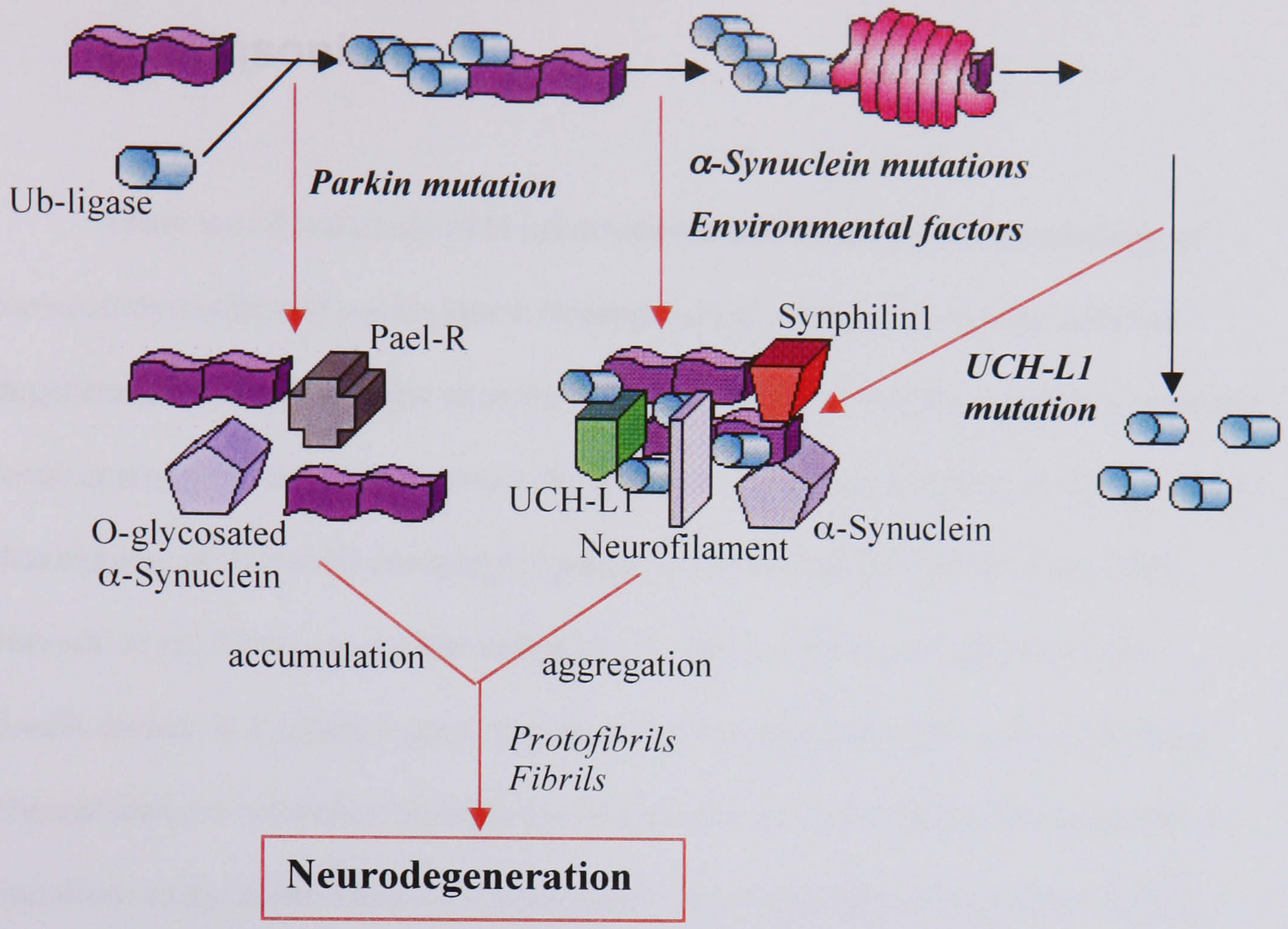


Figure 1. Impaired ubiquitin-proteasome degradation pathway in PD. Misfolded proteins (e.g. α-synuclein) undergo permanent degradation, and the ubiquitin-proteasome degradation pathway is the most important mediator of this turnover. Defects in this pathway, such as the increased generation of misfolded proteins or an impairment of ubiquitination or proteasomal function, might result in an accumulation and aggregation of misfolded proteins. Mutations in the a-synuclein gene lead to an increased tendency of spontaneous aggregation, and exogenic toxins (free radicals, MPP+) lead to increased expression of wild-type a-synuclein. As *parkin* has E3 ubiquitin ligase activity, loss-of-function mutations might result in impaired ubiquitination and accumulation of (non-ubiquinated) protein substrates (e.g. *O*-glycosylated a-synuclein, Pael-R) that cannot be degraded. Synphilin-1 is both an a-synuclein-interacting protein and a substrate of the ubiquitin ligase activity of *parkin*. Co-expression of synphilin-1 and a-synuclein results in the formation of intracytoplasmic aggregations. UCH-L1 plays a role in ubiquitin re-utilization, and mutations in *UCH-L1* might reduce its enzymatic activity (Modified Kruger et al., 2002).

1.1.4 Clinical and PET studies in *parkin*-linked parkinsonism

There is still relatively little information available on the neuropathology of molecularly confirmed *parkin* cases. Neuropathological features include selective degeneration of dopaminergic neurons in the zona compacta of the substantia nigra and locus coeruleus with reactive gliosis. No Lewy bodies were identified in the pathologic descriptions of the initial documented *parkin* mutation families (Mori et al., 1998; Hayashi et al., 2000; van de Warrenburg et al., 2001), leading to suggestions that *parkin* disease is a separate pathological entity from idiopathic PD with overlapping clinical features. However, an older individual who was a compound heterozygote for mutations in the *parkin* gene has subsequently been reported with nigral cell loss as well as α-synuclein positive Lewy bodies (Farrer et al., 2001).

In a few other cases that have been reported there was a severe and generalised loss of dopaminergic neurones in the substantia nigra pars compacta without Lewy body inclusions (Mori *et al,* 1998, Hayashi *et al*., 2000,) implying that *parkin* disease is a separate pathological entity from idiopathic PD with overlapping clinical features. ^{18}F-dopa PET examinations of *parkin* cases are limited (Broussolle *et al*., 2000, Hilker *et al*., 2001, Portman *et al*., 2001) , however, they reveal a severe reduction of caudate and putaminal ^{18}F-dopa uptake.

1.4.1.1 Progression of nigrostriatal dysfunction in a *parkin* kindred

In 1991 an Irish kindred with young-onset levodopa-responsive parkinsonism was studied with ^{18}F-dopa PET (Sawle *et al.*, 1992). At that time the four clinically affected siblings showed severely reduced ^{18}F-dopa influx in striatum. Moreover, putamen ^{18}F-dopa uptake was also mildly reduced in two asymptomatic members but normal in another asymptomatic sibling. Following the identification of *parkin* mutations causing early onset parkinsonism in 1998 (Kitada *et al.*, 1998), an affected individual in this kindred has been shown to be a compound heterozygote, having a deletion in exon 8 (personal communication C Lucking) and a splice site point mutation in intron 5 (personal communication M Farrer). This *parkin* family satisfied UK Brain Bank criteria for clinically probable Parkinson's disease (Gibb *et al.*, 1988) with rest tremor, dystonia and early complications as striking features. We have now repeated ^{18}F-dopa PET, 10 years later, in all four clinically affected cases with *parkin* disease. We have also studied four asymptomatic relatives who carry a single *parkin* mutation and one sibling who has a normal genotype. Two of the *parkin* carriers and the relative with a normal genotype had serial ^{18}F-dopa PET seven years apart. The aims were to study the pattern and rate of progression of the nigro-striatal dopaminergic dysfunction in clinically affected *parkin* cases and to assess the presence and possible changes with time of subclinical nigrostriatal dysfunction in carriers of a single *parkin* mutation.

1.1.4.2 Striatal and cortical pre-and postsynaptic dopaminergic dysfunction in sporadic *parkin*-linked parkinsonism

The purpose of the present study was to twofold:

1) To examine patterns of disruption of pre- and postsynaptic dopaminergic function in striatal and cortical regions in a group of unrelated *parkin* patients using ^{18}F dopa as a marker of dopaminergic function and ^{11}C-raclopride as a marker of post-synaptic D2 receptor function.

2) To determine whether differences in dopaminergic status were evident between *parkin* patients and young-onset PD patients (YOPD) negative for *parkin* mutations.

1.2 PET studies on the efficacy of cell transplantation therapy in Parkinson' s disease

1.2.1 Neurosurgical approaches to the treatment of Parkinson's disease.

Levodopa and dopaminergic drugs are very effective during the early stages of PD, however, the duration of their efficacy generally declines as the disease progresses. After several years of treatment with levodopa many PD patients develop severe side effects, most notably dyskinesias at peak dose and 'on-off' fluctuations in drug responsiveness (Poewe and Granata, 1997; Marsden and Parkes, 1977). Dyskinesias may, therefore, force patients to reduce the dosage at a time when they need increased antiparkinsonian medication. These problems have spurred renewed interest in pharmacological and neurosurgical interventions that might arrest, reverse or repair the progress of the disease.

Before levodopa came into use a variety of surgical approaches were explored. The pioneering studies by Meyers of stereotaxic lesions in the caudate nucleus and ansa lenticularis were followed by the identification of ventral thalamic nuclei as effective surgical targets (thalamotomy) for the treatment of tremor. In the absence of modern imaging techniques, placement and size of lesions were not particularly reliable. Moreover, although tremor could be controlled thalamotomy did not alleviate parkinsonian akinesia (Marsden et al, 1997).

The recent revival of stereotaxic surgery in PD has derived from three converging factors:

First, improved understanding of the functional organization of the basal ganglia and the functional changes induced by destruction of the nigral dopaminergic neurones has provided important clues for the identification of critical targets for neurosurgical intervention, in particular the internal segment of the globus pallidus and the subthalamic nucleus (DeLong, 1990, Starr et al, 1998).

Second, several important technical developments now allow surgery to be far more accurate in its selections of targets. MR imaging and electrophysiological monitoring during surgery now allow more precise positioning in deep-brain nuclei. Indeed, in certain targets recording can be combined with stimulation-induced movements to confirm the target site functionally (Starr et al, 1998).

Finally, the introduction of chronic deep-brain stimulation (DBS) as an alternative to destructive lesions has provided a new approach for the control of symptoms in advanced PD. High-frequency (130 Hz) stimulation produces a functional reversible lesion in the target area, perhaps by depolarisation block.

Deep-brain stimulation was first introduced as an alternative to thalamotomy for the control of tremor, but has been applied subsequently to both the globus pallidus internus and subthalamic nucleus resulting in a more general improvement of parkinsonism and also dyskinesias (Pollak et al, 1997). DBS has the dual advantages that the stimulation parameters can be titrated to yield an optimum response over time and that it is reversible if adverse effects occur.

One the primary applications of DBS now is not relief of parkinsonism, but the control of levodopa-induced dyskinesias by targeting the postero-ventral globus pallidus , thereby allowing more effective pharmacotherapy to be extended to advanced patients.

1.2.2 Replacement therapies

The nervous system, unlike many other tissues, has limited capacity for self-repair; mature nerve cells lack the ability to regenerate and neural stem cells, although they exist even in the adult brain, have limited ability to transform into functional neurones in response to injury. For this reason there is great interest in the possibility of repairing the nervous systems by transplanting new cells that can replace those lost through damage or disease.

The therapeutic effects of implanted dopamine neurones or neuronal precursors are likely to depend on their becoming structurally and functionally integrated into the host brain. Neurones survive and grow well after transplantation only if they are immature, that is at a developmental stage when they are differentiated but have not yet formed extensive axonal connections. Their ability to establish reciprocal connectivity with the host brain also depends on the age of the host: it is maximal during the fetal period and gradually diminishes during postnatal development. Nevertheless, grafted fetal neurones can establish functionally appropriate connections even in adult brain, and this capacity is much increased when the host circuitry is damaged, suggesting that the mechanisms regulating neuronal differentiation and connectivity during development may be reactivated by lesions or degenerative changes (Sotelo and Alvarado-Mallart, 1991; Hernit-Grant and Macklis, 1996; Snyder et al., 1997). For example, host cells that have lost their normal inputs may release neurotrophic factors that stimulate axon outgrowth, thereby promoting their reinnervation by grafted cells (Dunnett and Bjorklund, 1994).

However, reconstruction of neural circuitry is not always a prerequisite for functional recovery. Transplanted cells may release neurotransmitters (such as dopamine, acetylcholine or GABA) in a non-regulated tonic manner, or they may produce (or engineered to produce) neurotrophic or neuroprotective factors that can counteract degeneration or promote regeneration. Moreover, transplanted glial cells may be used to modify the response to injury and assist in structural repair (Raisman 1997). Thus cell replacement can improve functional deficits in the adult brain through different mechanisms.

Cell replacement therapy for PD has been developed over the past three decades within a relative simple conceptual framework: if the human disease is attributable to a primary degeneration of the dopamine neurons in the substantia nigra and a corresponding loss of dopaminergic innervation in the neostriatum, then replacement of lost dopamine neurones by transplantation should yield recovery of associated motor symptoms (Figure 2).

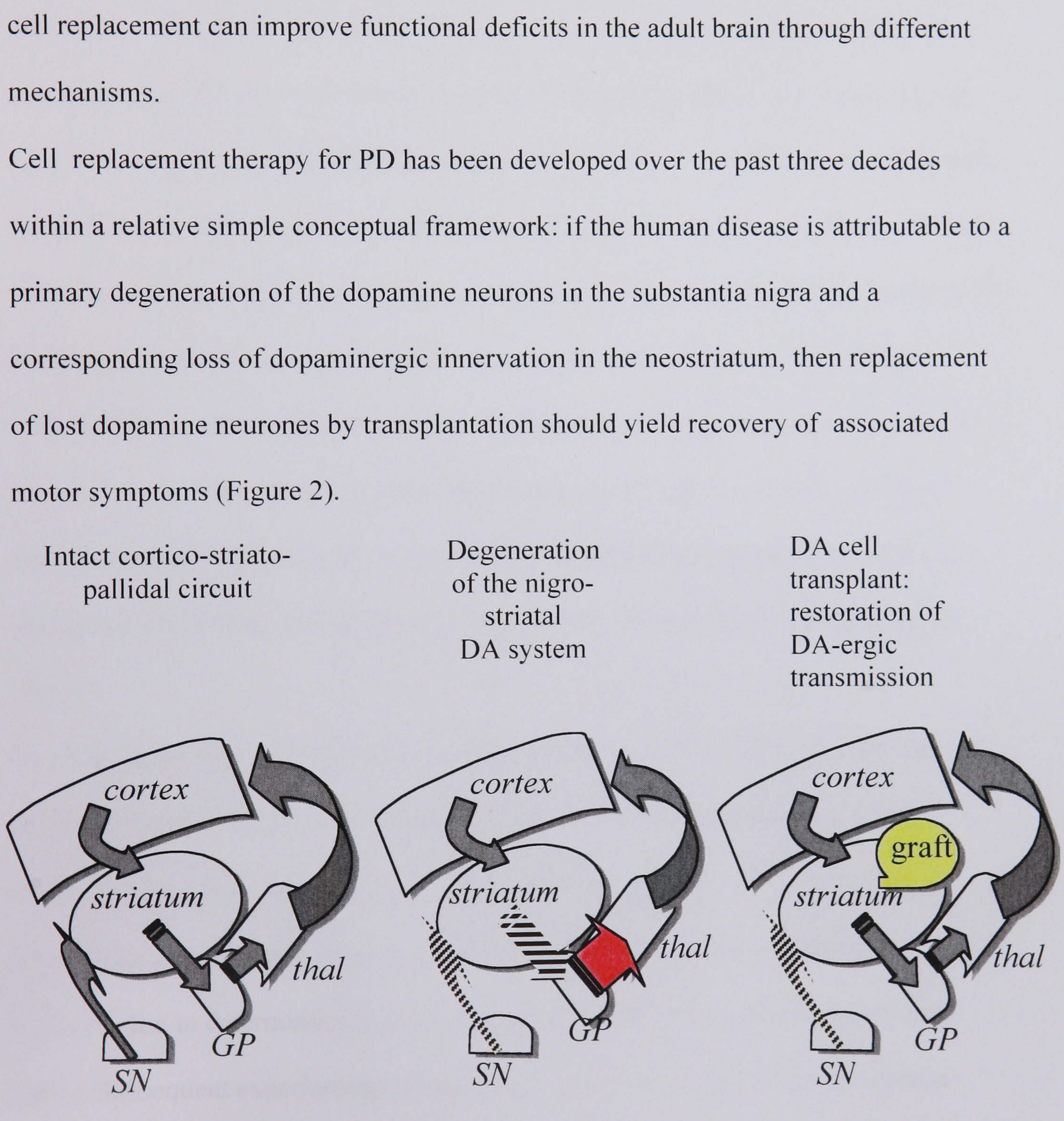


Figure 2 Cortico-basal ganglia circuits: hypothetical effects of intrastriatal dopaminergic graft.

PD is particularly suited for cell-replacement approaches for several reasons: The degenerating dopaminergic neurones of the substantia nigra are clearly circumscribed and their main target, the striatum, is anatomically well defined and easily accessible. Successful transplantation of cathecholamine-secreting cells in the nervous systems was first achieved by Oslon and colleagues in the 1970s by grafting adrenal chromaffin cells or embryonic dopamine neurones into the rat anterior eye chamber (Olson and Malmfors, 1970, Olson and Seiger, 1972). These studies established that survival, neurite outgrowth, and formation of contacts with the host nervous systems are best achieved using developing embryonic neurones. The fate of implanted dopamine cells depends on accurate dissection of the relevant ventral mesencephalic cell groups from embryos harvested during a critical stage of development. Initial attempts to transplant embryonic neurones into adult brain proved problematic and required complex technical protocols to provide adequate nutrient support for newly grafted tissue pieces (Stenevi et al, 1976). However, these limitations were largely overcome with the development of techniques for preparation of dissociated cell suspensions, allowing stereotaxic implantation of embryonic dopamine neurones directly into deep brain sites.

The first report of functional recovery after grafting was in 6-OHDA hemiparkinsonian rat model of PD involving mesencephalic solid tissue implants into the lateral ventricles (Perlow et al, 1979). This was soon replicated using cell-suspension technology, revealing the importance of topographic placement and terminal reinnervation in determining functional efficacy of the grafted cells (Dunnett et al, 1981). Subsequent experimental studies have developed methods for cool storage (hibernation) of donor tissue (Frodl et al, 1995), refinements in cell preparation and implantation, and improved trophic/neuroprotective support of grafted tissue (Brundin

et al 2000). Further studies have demonstrated recovery of a range of more complex behavioural functions in rodent model of PD after grafting and extended functional validation to non-human primates (Taylor et al 1991, Annett et al, 1995). In parallel, a combination of electrophysiological, *in vivo* neurochemistry and behavioural analyses have provided a clearer understanding of the mechanisms of graft function (Dunnett and Bjorklund, 1994). It is not simply sufficient for the grafted cells to secret topically dopamine at physiological levels into the host neuropil; rather full functional activity is dependent on a synaptic integration of the grafted cells into the host neural circuitry.

The first clinical trials of cell transplantation in PD used adrenal autografts (Backlund et al, 1985). In this procedure, one adrenal medulla of the PD patient was removed for dissection of the relevant cells which were then implanted into the brain, either as solid pieces into a ventricular cavity or by stereotaxic injections of cell suspensions into the striatal neuropil. Following a single report of apparently profound effect (Madrazo et al, 1987), several hundred patients received this operation in the late 1980s in a series of poorly controlled trials worldwide. However, it soon became apparent that the grafts did not survive long-term and that, at best, modest clinical effects were accompanied by significant side effects and an unacceptable level of morbidity and mortality. This procedure, therefore, is generally not considered to be acceptable.

The alternative was to pursue a clinical strategy based on one that works in experimental lesion model systems, namely human embryonic mesencephalic tissue allografts. The complex ethical and legal issues associated with use of human embryonic tissue from elective abortions have been considered in detail in most western countries, resulting in approved guidelines that permit use of embryonic

tissues subject to stringent conditions of selection, consent, collection, handling and application (Boer, 1994).

The cells used for transplantation are taken from the ventral midbrain (which include the substantia nigra) during fetal development at the time when nigral dopaminergic neurones are undergoing terminal differentiation. The fetal cells are grafted into the host striatum, allowing them to establish functional synaptic contacts with the denervated striatal neurones.

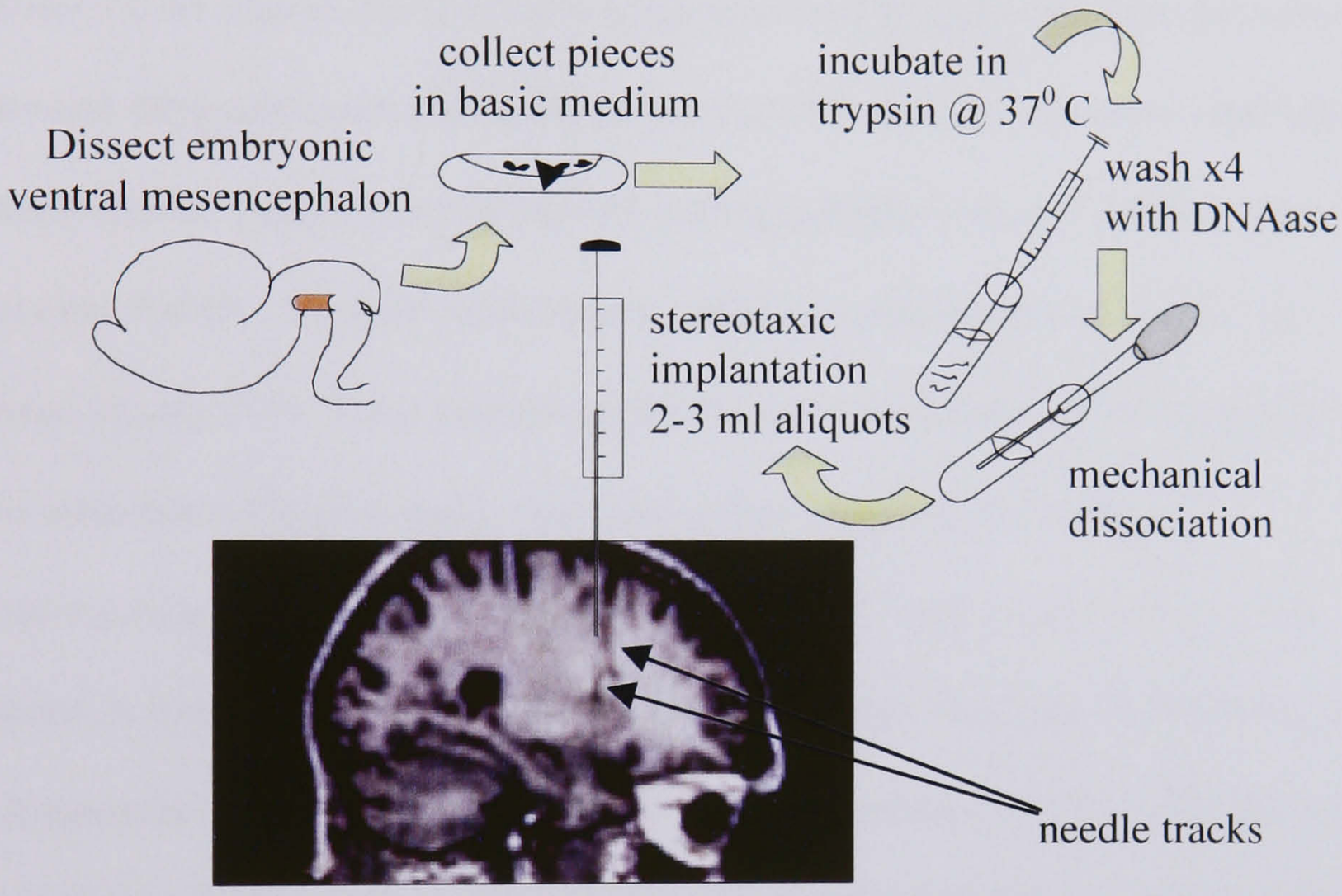


Figure 3. Schematic representation of the different steps in transplantation: from dissection of the embryonic ventral mesencephalon to the stereotactic injection of tissue into the striatum. Arrows: needle tracks on the MR image. (Modified from Dunnett 1997)

Unfortunately, the first patients to receive human embryonic nigral grafts, in Mexico and in Sweden, derived very limited benefit (Madrazo et al, 1988; Lindvall et al, 1989). However, subsequent improvements in technique have resulted in clear-cut and long lasting symptomatic improvement in subsequent open label trials. Clinical improvement after intrastriatal human embryonic graft transplantation has been

reported by research groups in Paris, Tampa and Lund (Lindvall et al., 1989, 1990, 1992, 1994; Peschanski et al., 1994; Freeman et al., 1995; Remy et al., 1995; Defer et al., 1996; Wenning et al., 1997; Brundin et al., 2000; Mendez et al., 2000).

The issue of how to determine whether a novel surgical treatment in PD is having significant clinical benefit is not straightforward. PD is a slowly progressive disorder and symptoms can fluctuate markedly depending on the day and drug intake as well as being sensitive to mood and motivation. Placebo effects are well known. Moreover, transplanted cells require many months to develop and integrate into the host nervous systems and the grafts cannot be easily removed (other than as a result of graft failure or rejection) so an experimental design for testing patients with and without grafts is not possible. Finally, the graft technologies, although quite advanced, are not yet optimised as only 10% of cells survive and so need to be refined and developed on a case-by-case basis. Consequently most centres have adopted the strategy of undertaking detailed longitudinal analysis of individual cases under well-defined conditions. A consortium of European and US centres has developed a standardized Core Assessment Protocol for Intracerebral Transplantations (CAPIT). This designates regular neurological and imaging assessments at defined time points with baseline measures extended over a three months pre-operation period (Langston et al., 1992; Defer et al., 1999).

Adoption of the CAPIT protocol provides two distinct advantages: it allows data to be pooled from several centres to provide large samples sizes even when each contributing centre might study only a few cases and it allows direct comparison between different tissue preparation and surgical methods used in different centres according to a common set of baseline and outcome assessments. On the basis of such open-label longitudinal analyses of small number of cases using this defined

assessment protocol there is now strong evidence in open trials of both clinical benefit and graft survival after embryonic tissue transplantation (table 2).

Table 2. Functional outcome after bilateral intrastriatal transplantation in open label trials and in one double-blind placebo-controlled trial.
(Modified from Dunnett et al., 2001)

Centre	Trial design	No cases	No ventral mesencephalon per putamen	^{18}F-dopa % increase	UPDRS % change	Time in 'off' % change
Lund	open-	4	4.9	+60	-30	-59
Lund	label	2	2.5	+87	-50	-50
Lund		5	2.8 (+lazaroid)	+55	-40	-43
Tampa	open-					
	label	6	3.0-4.0	+61	-30	-43
Creteil	open-	3	1.0-1.5	NR	-6	15
Creteil	label	6	3.0		-33	-66
Halifax	open-					
	label	2	3.25 (+GDNF)	+107	-32	-50
Denver	DBPC	19	2.0	+40	-18	NR
		47		+68	-30	-45
				(±24)	(±13)	(±19)

DBPC: Double-blind placebo-controlled, NR: non reported

This can be illustrated from the series of 18 patients transplanted in Lund with the collaboration of our Unit where the patients have had ^{18}F-dopa PET before and after transplantation. These patients have been followed up for over 10 years: the majority showed significant increases in the proportion of time spent in the 'on' phase, improvements in the speed and accuracy of movements in defined 'off' and maintenance of the improvement with progressive reduction or complete cessation in several cases of concurrent L-dopa therapy (Lindvall et al., 1990, 1994; Wenning et al., 1997, Hagell et al., 1998; Brundin et al., 2000). In parallel with neurological testing the patients have been studied serially with ^{18}F-dopa PET (table 2, figure 4). Increases in

putamen ^{18}F-dopa uptake ranged from 55 to 80% of the baseline value in these patients reaching levels that were 48 to 68% of the normal mean.

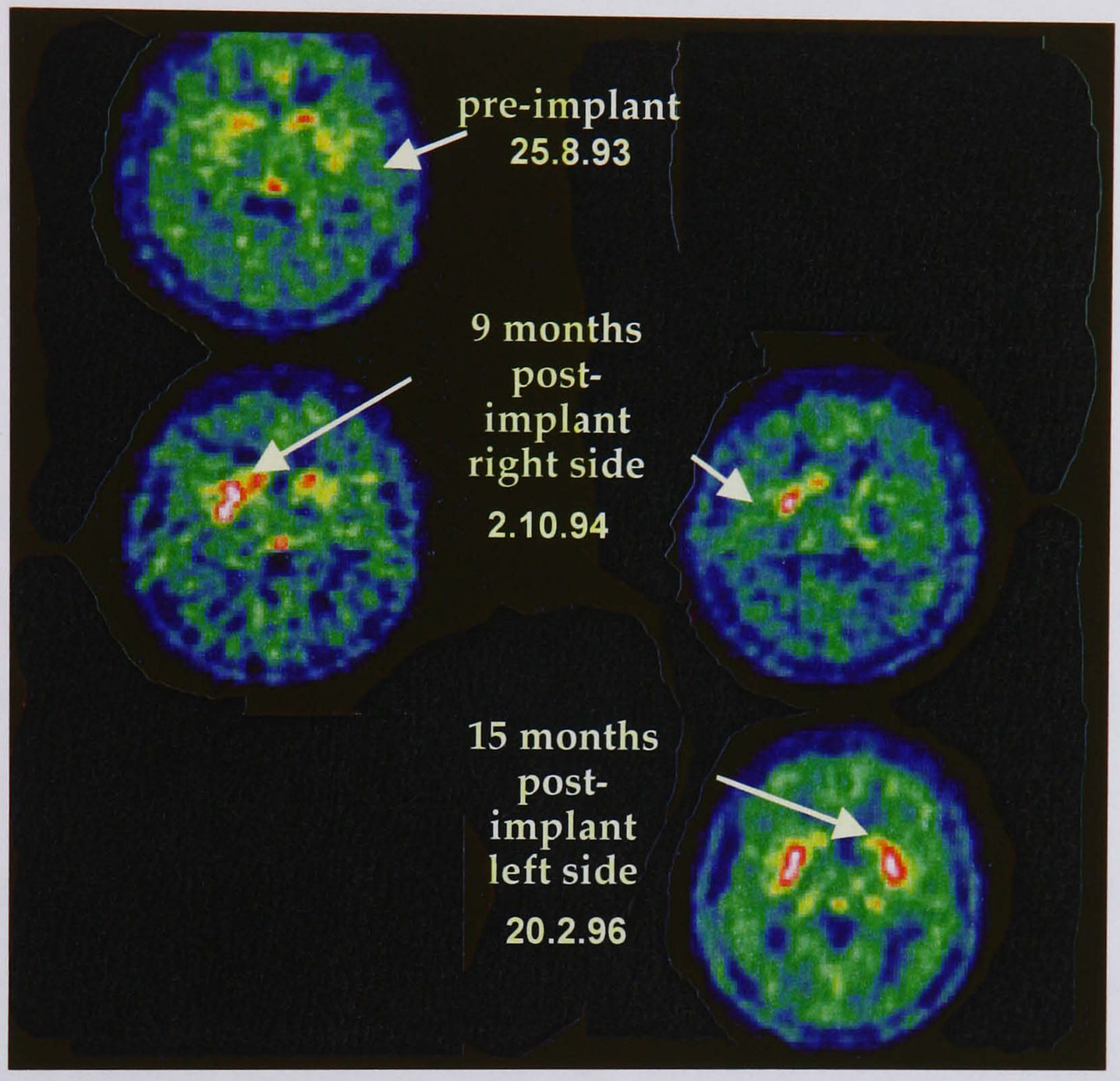


Figure 4. Serial ^{18}F-dopa PET images in a PD patient before and after transplantation of human embryonic mesencephalic cells into putamen. Top: before transplantation Middle: 12 months later and 9 months after unilateral transplantation into the right putamen. Note the increase in ^{18}F-dopa signal in the implanted putamen and for comparison the decline in signal in the ungrafted side. Bottom: 15 months after implantation into the left putamen and 2 years after implantation into the right putamen.

The only double-blind placebo-controlled trial (Freed et al., 2001) published so far showed that transplanted fetal cells survived in 85% of patients regardless of age and

without immunosuppression. UPDRS scores significantly improved in all PD patients but most markedly in those under the age of 60. Unfortunately the trial failed to meet its primary end point - significant improvement in patients' clinical global impression. Post-mortem data have confirmed graft survival in transplanted patients who have died of causes unrelated to the surgical procedure at different time points after transplantation (Kordower et al., 1995; 1996; 1998; Freed et al., 2001). In one subject survival was documented 8 years after transplantation (Freed 2002).

1.2.3 Dopamine release from nigral transplants

The gradual clinical improvement observed in many cases in open series over the first 6-24 months after transplantation of human embryonic nigral neurons is compatible with the protracted development, growth and maturation of a new striatal dopaminergic innervation provided by the grafted neurons. The magnitude of the transplant-induced effect is likely to be due to the ability of grafted neurons to release dopamine in a regulated fashion at regenerated synaptic sites. As mentioned above, the survival of the grafted dopamine neurons, reinnervation of the host striatum and formation of synaptic connections have all previously been shown in PD autopsy cases (Kordower et al., 1995; 1996; 1998; Freed et al., 2001). However, it has not yet been possible to demonstrate dopamine release from transplants *in vivo* in humans.

I have used ^{11}C-raclopride PET as a marker of the availability of dopamine D2 receptors to investigate *in vivo* synaptic dopamine release from intraputaminal nigral grafts.

BIBL.
LONDIN.
DIVY.

1.2.4 Recovery of movement-related cortical function following neural transplantation

The major output of the neostriatum via pallido-thalamic connections is to premotor and prefrontal cortical areas. Regional cerebral blood flow (rCBF) studies in PD patients have shown relatively impaired activation of the supplementary motor area (SMA) and dorsolateral prefrontal cortex (DLPFC) during performance of volitional movements (Playford et al., 1992; Jahanshahi et al., 1995). The impairment of function in these association areas is postulated to underlie the akinesia of internally generated movements observed in PD patients (Dick et al., 1989; Playford et al., 1992; Jahanshahi et al., 1995). Dopaminergic drugs, such as apomorphine, give marked symptomatic relief in PD and are able to restore activation of these cortical areas (Jenkins et al., 1992).

The objective of my study was to explore whether dopaminergic grafts improve movement-related frontal cortical function in PD patients and whether this improvement occurs in parallel with an increase of striatal dopamine storage capacity and amelioration of parkinsonian symptoms.

1.2.5 Dyskinesias following neural transplantation

Recently the results from the first double-blind placebo-controlled trial using grafts of embryonic tissue in PD have been published (Freed et al., 2001). In this study severe "off" phase dyskinesias were described in 15% of cases following transplantation and proposed to be due to graft-derived dopamine excess.

The design of the study differed from previous open-label trials in many ways: Clinical assessment was not conducted according to established CAPIT protocols, preventing comparison with previous open studies. Assessments were reported up to one year after grafting, which would emphasise placebo effects but which is likely to be too early to detect the full level of slowly developing graft-induced therapeutical benefit. Finally, patients' retrospective global self-assessment was selected as the primary outcome measure; this showed considerable variation and no difference between placebo and control groups.

Moreover, the technique for cell transplantation in this trial differed from other studies with fewer number of donors, idiosyncratic methods of cells preparation and storage for 4 weeks, absence of immunosuppression and the use of an unconventional frontal surgical approach. Nevertheless, even at the early one-year time point significant improvement was seen using two neurological rating scales in patients younger than 60. There was no improvement in the sham-operated patients. Improvement in the active arm was accompanied by a 40% increase in ^{18}F-dopa uptake and survival of 7,000-40,000 tyrosine-hydroxylase-positive neurons per side in two post-mortem cases compared with 80,000-135,000 cells per side using conventional methods in other post-mortem analyses (Kordower et al., 1995).

The outcome using this distinctive surgical approach, therefore, parallels that seen in the open–label trials with a level of functional benefit compatible with the modest survival of the grafted cells obtained. However, what has attracted widespread scientific and media attention has been the reports of severe and uncontrollable 'off' dyskinesias following transplantation in five out of 33 patients. Such severe side effects were not reported in the open-label trials and amelioration rather than induction of dyskinesias has been observed after dopamine neuron transplantation in animal

models of PD (Lee et al., 2000). Freed et al. (2001) have suggested that the dyskinesias observed in their study might be due to a dopamine overdose effect in the transplanted patients.

With the intention of clarifying whether 'off' dyskinesias are a common side-effect of transplantation and whether this results from a graft-derived dopamine excess I have retrospectively analysed clinical and ^{18}F-dopa PET data from 14 patients from our open series followed for up to 11 years after grafting.

Methodology

2

2.2 Positron Emission Tomography (PET)

2.2.1 Introduction

Positrons were first identified in 1932 when scattering of high energy gamma rays by "a positively charged particle having a mass comparable with that of an electron" was demonstrated. Positrons are particles of equal mass but opposite charge to electrons and are their anti-matter equivalent. When emitted from an unstable nucleus a positron travels one to three mm before colliding with an electron in the outer shell of an atom. This results in annihilation and the energy is emitted as two 511 keV gamma rays, released at 180 degrees to each other.

2.2.2 The cyclotron

A cyclotron is a particle accelerator which generates a static magnetic and electric field between specifically designed electrodes within a vacuum chamber (Birattari et al., 1987). Following emission from an ion source a charged particle, generally a proton or deuteron, is accelerated by the electric field along a path which is made circular by the presence of the magnetic field. As the particle gains energy it

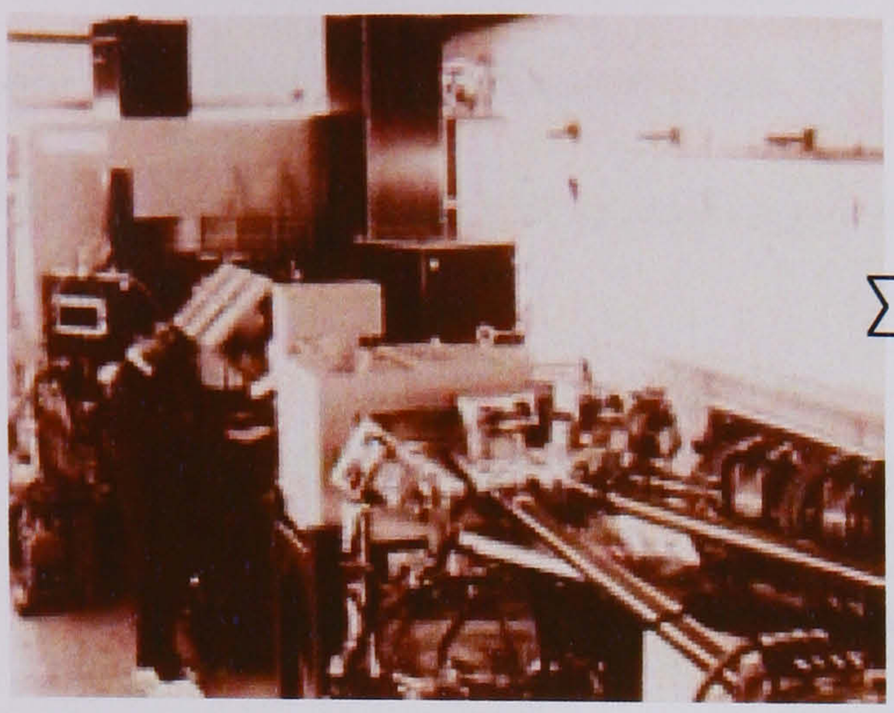
follows a spiral path from the centre of the cyclotron to a maximum radius from where it is then focused by an electrostatic deflecting beam to bombard a target.

2.2.3 Positron detection

The PET detector of the 511 keV gamma ray emissions created by positron annihilation consists of a scintillation bismuth germanate (BGO) crystal connected to a photomultiplier tube. The scintillation crystal emits low energy photons (visible light) after interaction with high energy photons (gamma rays). The photomultiplier tube then converts the scintillation events into electrical pulses.

The size of the crystal detection system is a major factor in the resolution of the PET camera and the maximal physical image resolution is approximately 1.1 to 1.2 times greater than the width of the individual detector crystals.

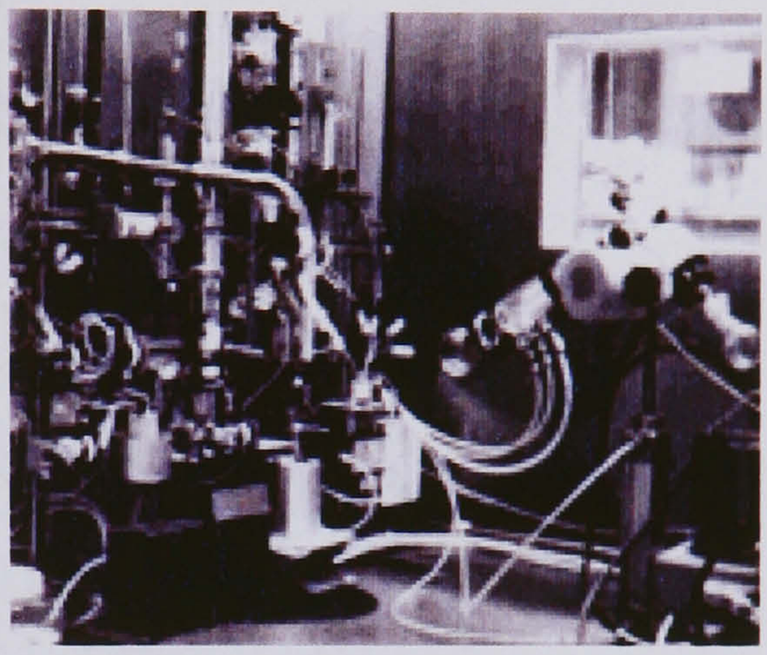
In current PET scanners multiple rings of detectors are stacked to assess volumetric data from a wide field of view. In two dimensional scanning the coincidences within the same ring define an intra-ring image and coincidences between adjacent rings form independent inter-ring images (cross-plane). PET can also be operated in a more sensitive 3D mode where coincident detections between all rings are counted (Cherry et al., 1993). This results in a six fold increase in signal but also increases counts due to scatter. When scattered events are subtracted the efficiency of coincidence detection at the centre of the field of view increases by a factor of 4.8 (Spinks et al., 1992). There are several ways of estimating the scatter component of PET data acquisition. We have used an approach in which data is acquired using a dual energy window technique. A lower energy data set, representing scatter, is subtracted from the main upper energy 511 keV window data set (Grootoonk et al., 1992).



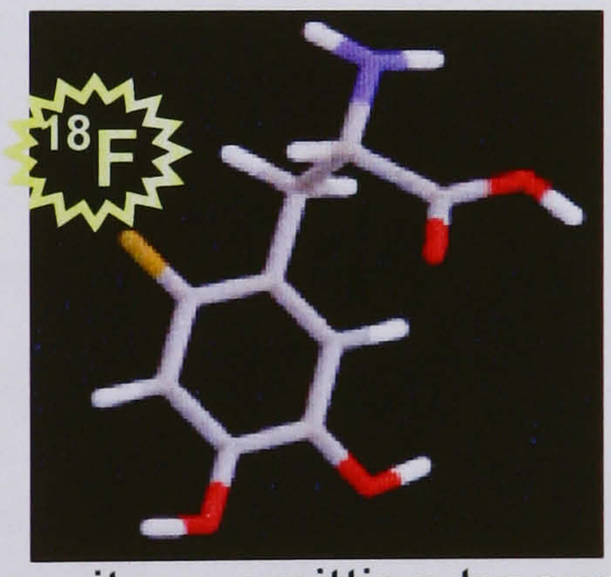
Cyclotron

positron-emitting radioisotopes

^{18}F ^{11}C ^{15}O



Chemistry hot cell



positron-emitting tracer
(^{18}F-dopa)

Figure 5.

PET: production of radioisotopes

The importance of 3D acquisition is that scans of comparable quality to 2D mode can be obtained after administration of approximately four times less radiation. This allows more scan repetitions to be performed. Use of 3D mode acquisition also enhances the ability to perform voxel rather than region based analyses.

2.2.4 Coincidence detection

When emitted positrons are annihilated by collision with an adjacent electron two 511 keV gamma rays are emitted at 180°. Consequently, if one event (photon) is detected, an event in the opposite detector is sought within a +/- 4 nanosecond (nsec) time window – so-called coincidence detection. 'Random' as opposed to 'true' coincidences can occur when two photons from separate annihilation events are detected simultaneously at opposing detectors. These are identified by introducing a delay into one side of the coincidence detection circuit by 48 nsec; coincidences resulting from a single annihilation event are not detected under these circumstances. The 'true' coincidence rate is then calculated by subtracting the number of random events from the total number of detections (Dyson 1960).

Annihilation events in which one of the photons is deflected (scattered) but in which the two photons are nevertheless detected simultaneously at opposing detectors can still constitute a proportion of the true rate. However, scattered photons tend to have lower energy and so the scatter fraction may be minimised by energy windowing. True coincidence events at detector pairs are then histogrammed by a real-time sorter into sinograms which are subsequently attenuation corrected and reconstructed into images by back projection.

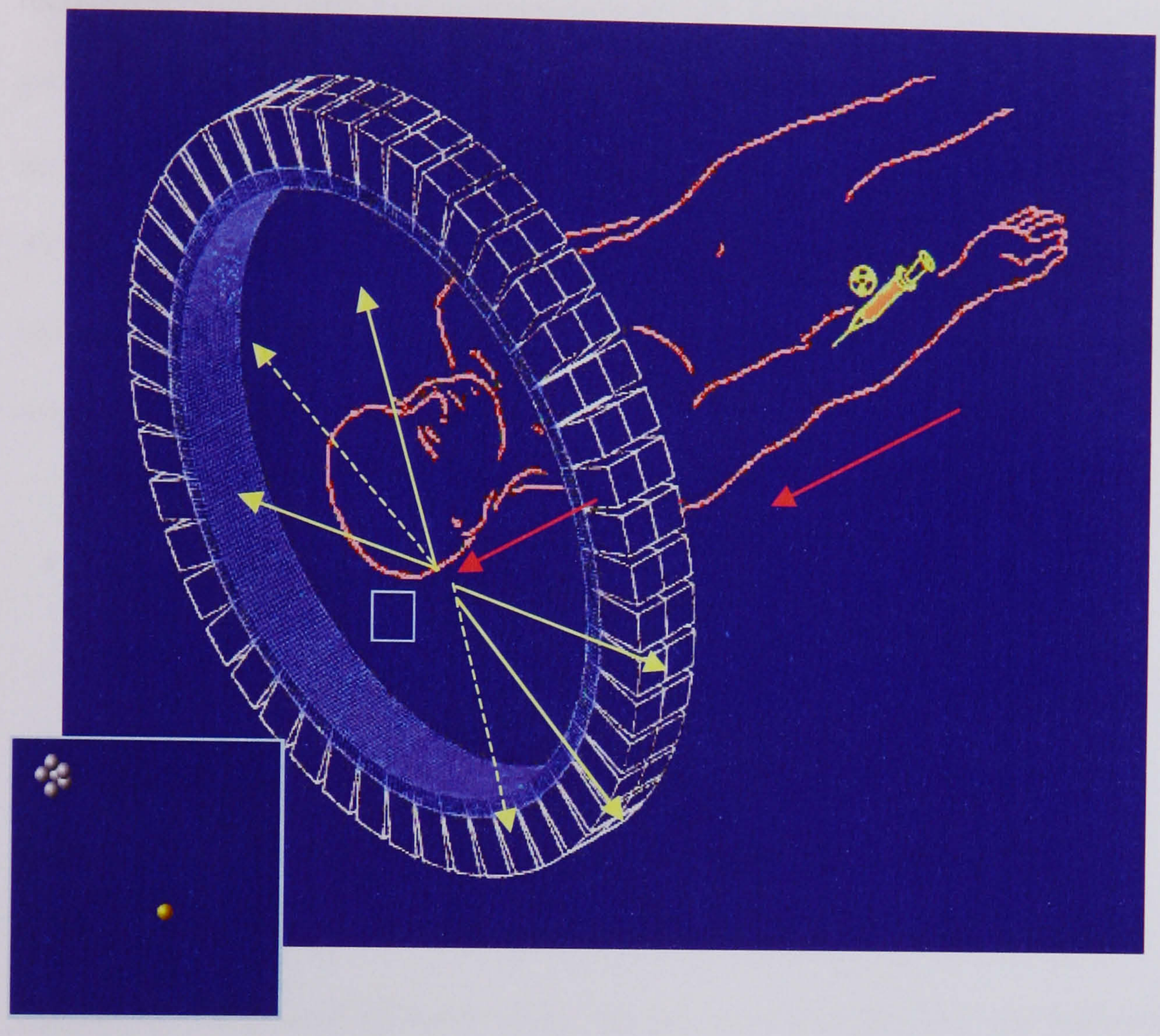


Figure 6. Schematic representation of detectors in a tomograph and the annhilation of a positron with an electron and the resulting pair of 511 keV gamma rays released at 180° (yellow arrows).

2.2.5 Image reconstruction

The radiation emission profiles acquired by the PET detector system are recorded in digital form by a computer system. From this data, the computer system generates 3D images through the application of a "filtered back projection" reconstruction algorithm similar to that used in computed tomography (CT) (Phelps 1977). The algorithm consists of the projection of a series of radiation profiles (sinograms) recorded at different angles to produce a cross-sectional image of the original distribution of radioactivity.

2.2.6 Attenuation correction

The sinograms used in image reconstruction in PET represent the distribution of activity in the scanned tissues, reduced by tissue attenuation. It is, therefore, necessary to correct for this attenuation in order to allow true quantitative reconstruction (Phelps 1977). The tissue attenuation is measured by performing transmission and blank emission scans. In a transmission scan the tissue attenuation of 511 keV photons along all coincidence lines is calculated by exposing the subject to be imaged to an external ring or rotating point positron source emitting 511 keV gamma radiation, usually ^{68}Ge-^{68}Ga. The blank emission scan is performed with no tissue between the detector rings to detect levels of background radiation. The ratio of the blank and transmission scan data provides attenuation coefficients for 511 keV g rays on a voxel basis for the object to be studied.

2.2.7 Image resolution following reconstruction

The intrinsic spatial resolution of a PET scanner is usually expressed in terms of its full width at half-maximum (FWHM), dictated by a number of physical factors. The average distance the positron travels before annihilation (≈2mm) determines the absolute resolution of the camera system but in practise the most important physical factor is the width of the detector crystals in the camera. The FWHM may be derived from "phantom" experiments where a line source of a positron-emitting isotope is scanned by the PET camera and reconstructed into a tomographic image. The degree of gaussian spread of the signal from the line source defines the FWHM of the machine. In practical terms, two line sources of radioactivity need to be separated by at least one full width half-maximum in order to be spatially resolved from one another.

In biological imaging other factors apart from the physical resolution of the PET camera contribute to the effective image resolution. Object size, contrast with surrounding objects and levels of smoothing necessary for statistical comparison all contribute to image resolution (Hoffman et al., 1979). In general, the effective spatial resolution of biological imaging is around 1.3 times the physical resolution unless deliberately smoothed to lower resolution to increase the signal to noise.

2.2.8 The PET scanner

The PET cameras used in this project were the CTI/Siemens 953B (CTI, Knoxville, Tenn., USA) and the CTI/Siemens EXACT HR+ scanner. The characteristics of both scanners have been described previously (Spinks et al., 1992 and Spinks et al., 1996)

The CTI/Siemens 953B camera consists of sixteen rings of bismuth germanate (BGO) detectors of width 5.6 mm (transaxial) and height 6.1 mm (axial). The basic detector

unit consists of a block of BGO cut into 64 elements viewed by 4 photomultiplier tubes. The detectors are mounted in rings and collimated by removable tungsten septa. In the studies to be described the scanner was operated with the septa retracted (3D mode). This permits the acquisition of 256 (16x16) inter-ring coincidences. The 256 sinograms were reconstructed using a three-dimensional algorithm and a 3D image volume is then formed by filtered back-projection (Townsend et al., 1991).

The EXACT HR+ scanner has 6 rings of BGO blocks without interplane septa, allowing the acquisition of data exclusively in 3D mode.

Following reconstruction, which includes filtering, the 953 scanner has an image resolution of 8.5 mm (x dimension) x 8.5 (y dimension) x 4.3 mm (z dimension) FWHM. For the 966 scanner , spatial resolution at FWHM is 4.7 mm (transaxial) and 4.8 (axial), the pixel size is 2.09 mm (x dimension) x 2.09 (y dimension) x 2.43 mm (z dimension) (Spinks et al., 1996).

The axial field of view (FOV) of the 953B scanner allows approximately 10.6 cm of brain to be imaged. Careful positioning in the scanner is required to ensure that data from the appropriate regions of interest within the brain is collected. The axial field of view for the 996 scanner is 23.4 cm, therefore the entire brain and upper cervical cord can be easily imaged. The 953 scanner also contains three retractable, rotating germanium rod sources which are used for measurement of attenuation correction in 2D mode. In addition these rods are used for a short transmission scan to ensure correct positioning of the subject's head within the camera prior scanning. In the EXACT HR+ scanner transmission data is acquired using a single photon point source (^{137}Cs) which is rotated just inside the detector ring (Spinks et al.. 1996).

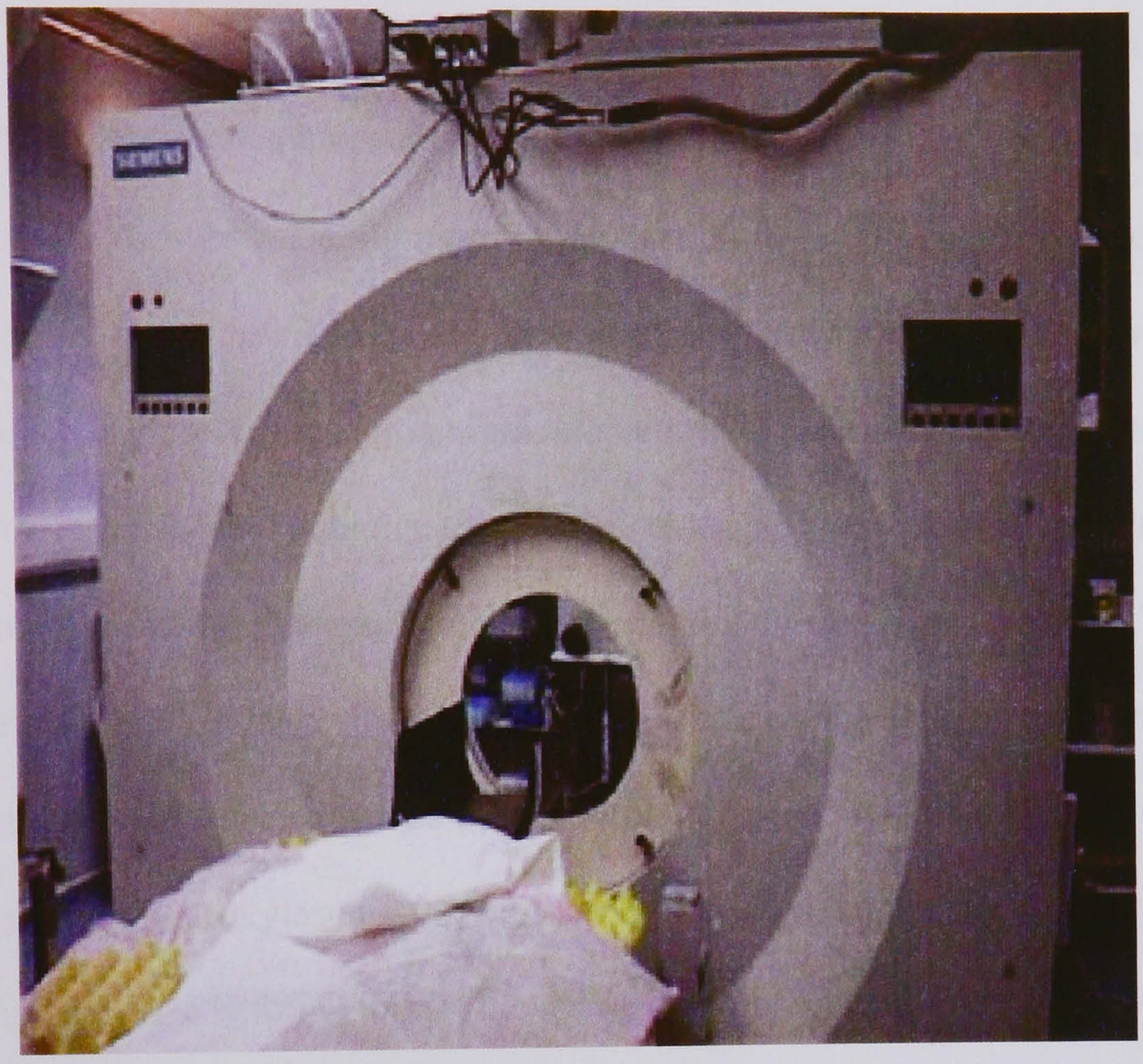


Figure 7

The ECAT EXACT HR++ scanner

2.3 L-6-[18F]-fluorodopa (^{18}F-dopa)

2.3.1 Introduction

The cell bodies of the 600,000 dopaminergic neurons in the human mesencephalon are located in four groups, comprising the 'nigral complex' (Agid et al, 1991): the substantia nigra pars compacta, the ventral tegmental area, the peri- and retrorubral region and finally the central grey substance. Axons from these cell groups, in particular the substantia nigra and ventral tegmental area, project to the striatum (i.e., caudate and putamen), pallidum, as well as to the frontal, cingulate and olfactory cortices. These neurons synthesize dopamine *in situ* , from tyrosine. Tyrosine is formed in the liver via hydroxylation of the aromatic amino acid, phenylalanine, and is actively transported across the blood brain barrier. It is then further hydroxylated by tyrosine hydroxylase to 3,4,-dihydroxy-L-phenylalanine (L-dopa). Tyrosine hydroxylase is found within the cytosol of catecholaminergic neurones. This enzyme is the rate limiting step in the synthesis of dopamine, since it is virtually saturated by the tissue concentrations of tyrosine. L-dopa is then decarboxylated by aromatic L-amino acid decarboxylase to form dopamine. This reaction has a high velocity with respect to L-dopa formation so that very little unchanged L-dopa remains in catecholaminergic tissue. Dopamine is then concentrated within neuronal vesicles by an ATP dependent process. The metabolic fate of dopamine is conversion to homovanillic acid and DOPAC via the enzymes catechol-*O*-methyl transferase (COMT) and monoamine oxidase (MAO). Homovanillic acid may be detected in the cerebrospinal fluid and has been used as an indirect marker of dopaminergic function.

Garnett *et al*, in 1983, first reported the use of ^{18}F-dopa to visualise the nigrostriatal dopaminergic system *in vivo*. In an elegant description they addressed many of the practical issues of ^{18}F-dopa PET scanning and explained why they believed that the distribution of fluorine-18 in the tomographic slices reflected the distribution of the dopaminergic pathways.

2.3.2 The metabolism of intravenously injected ^{18}F-dopa

The metabolic fate of intravenously injected ^{18}F-dopa in blood and brain tissue is qualitatively very similar to exogenous L-dopa (Firnau et al, 1988; Melega et al 1990), although at several steps there are quantitative differences in transportation and transformation.

2.3.2.1 Peripheral metabolism of ^{18}F-dopa

After injection, there are two enzymes which degrade the ^{18}F-dopa. Aromatic amino acid decarboxylase (AAAD) converts ^{18}F-dopa to ^{18}F-dopamine. The position of the fluorine-18 at the 6 position on the aromatic ring results in a Km for AAAD that is within the range published for L-dopa (Cumming et al, 1988). Peripheral ^{18}F-dopamine formed is unable to cross the blood brain barrier. Carbidopa, a peripheral inhibitor of AAAD, is routinely administered to block the formation of ^{18}F-dopamine during PET scanning (Bartholini and Pletscher, 1968). 100 mg of carbidopa are given one hour, and a further 50mg ten minutes before ^{18}F-dopa injection.

2.3.2.2 Blood Brain Barrier Transport of ^{18}F-dopa

As mentioned above, any ^{18}F-dopamine formed in the plasma is unable to cross the blood brain barrier. However, both ^{18}F-dopa and its metabolite 3-*O*-methyl-^{18}F-dopa compete for the neutral amino acid transport system into the brain. This system

is non-energy requiring and sodium independent. The transport of the 6-isomer of ^{18}F-dopa in man occurs at the same rate as L-dopa (Reith et al, 1990), while the transfer of 3-*O*-methyl-^{18}F-dopa has been shown in rats to be twice as rapid as for ^{18}F-dopa. In addition, dietary derived amino acids may compete with the ^{18}F-dopa for access to the brain (Adam et al, 1986). One ingenious way of utilising the blood brain barrier to improve ^{18}F-dopa PET signals was reported by Doudet *et al.* (1991). Reasoning that, for the first 20 minutes after injection ^{18}F-dopa levels are highest in the plasma (and, therefore, it is transported into the brain most rapidly), these workers started an i.v. infusion of L-phenylalanine after this time to block subsequent blood to brain transfer of the metabolite 3-*O*-methyl-^{18}F-dopa. This approach worked but is of limited practical use.

2.3.2.3 Cerebral metabolism of ^{18}F-dopa

Having reached the brain, ^{18}F-dopa is converted by centrally located AAAD to ^{18}F-dopamine. AAAD is an ubiquitous enzyme, and it is the high levels of this enzyme in the nigrostriatal nerve terminals which 'drive' the formation of the decarboxylated product. AAAD activity is the rate limiting step in ^{18}F-dopamine formation. There is some debate as to the subsequent rate of metabolism of ^{18}F-dopamine in the striatum (Leenders et al, 1991; Melega et al, 1990), but over the 90 minute duration of a PET scan it is reasonable to assume that ^{18}F remains trapped within the nerve terminals as ^{18}F-dopamine and its metabolites.

2.3.3 Patient preparation and scan protocol

Subjects were asked to have only a light breakfast on the morning 4 hours before the PET study to avoid potential competition between dietary amino acids and

^{18}F-dopa for the blood-brain transporter system. If the subjects were taking any anti-parkinsonian medication, this was stopped 12 hours prior to PET. They were given 150mg of carbidopa orally (100mg one hour and a further 50 mg 10 minutes) before scan start. During acquisition of the transmission scan a 22 gauge teflon cannula was placed in the right antecubital vein for administration of the tracer. ^{18}F-dopa (140–180 MBq in 10 ml of normal saline solution) was infused intravenously over 30 s. Dynamic scanning began at the start of the tracer injection with a protocol of 25 time frames (4 x 1 min, 3 x 2 min, 3 x 3 min, 15 x 5 min) over 94 minutes.

2.3.4 Data analysis

After transfer to a SPARC II workstation (Sun Microsystems, Europe Incorporated, Surrey, UK) , images were analysed using image-analysis software (ANALYZE^{TM} version 7.5 – Biodynamics Research Unit, Mayo Foundation, Rochester, MD, USA).

In all subjects the positions of striatal and occipital structures were defined by summing time frames to create an integrated image, representing activity collected 30-90 minutes after ^{18}F-dopa administration. Such an 'ADD' image facilitates the placement of regions. Figure 5 shows the appearance of such an image for a normal subject.

In order to quantify the data, time-activity curves (TACs) were calculated by placing regions of interest in a standard template arrangement. Circular regions of 10 mm diameter were placed over each dorsal head of caudate and an elliptical region of 10 x 24 mm over each dorsal putamen aligned to the long axis on three contiguous

transverse planes. One circular region of diameter 32.8 mm was placed over the occipital lobe of each hemisphere.

The data were analysed further by using an adaptation of the multiple time graphical analysis (MTGA), described by Patlak and co-workers (Patlak and Blasber 1985), using a nonspecific occipital reference tissue, rather than a plasma, input function (Brooks et al,1990). In brief, the MTGA assumes that there is an irreversible or bound region, into which a test substance enters during the study, but cannot leave. This corresponds to the striatum and the ^{18}F-dopa, respectively: The ^{18}F-dopa is effectively trapped by its conversion to ^{18}F-dopamine. In addition, equilibrium of the ^{18}F-dopa is assumed between the plasma and a so-called exchangeable, or not specific, region, represented by the occipital lobe. Irreversible tracer uptake into the striatum is measured by a comparison of the rate of change of activity in the striatum against a transformed and expanded time scale. An MTGA plot of striatal:occipital fluorine-18 uptake versus the transformed and expanded time scale of the integrated occipital/occipital fluorine-18 activity is linear between 30 and 90 minutes of 'real' time.

The gradient of this plot may be regarded as the influx constant, or Ki value, which reflects specific striatal fluorine-18 accumulation. The Ki value is, therefore, a composite rate constant reflecting striatal ^{18}F-dopa uptake, dopa decarboxylase activity and the rate of ^{18}F-dopa metabolism. Because regions of interest were placed over both caudate and putamen, independent Ki values could be derived for each of these structures.

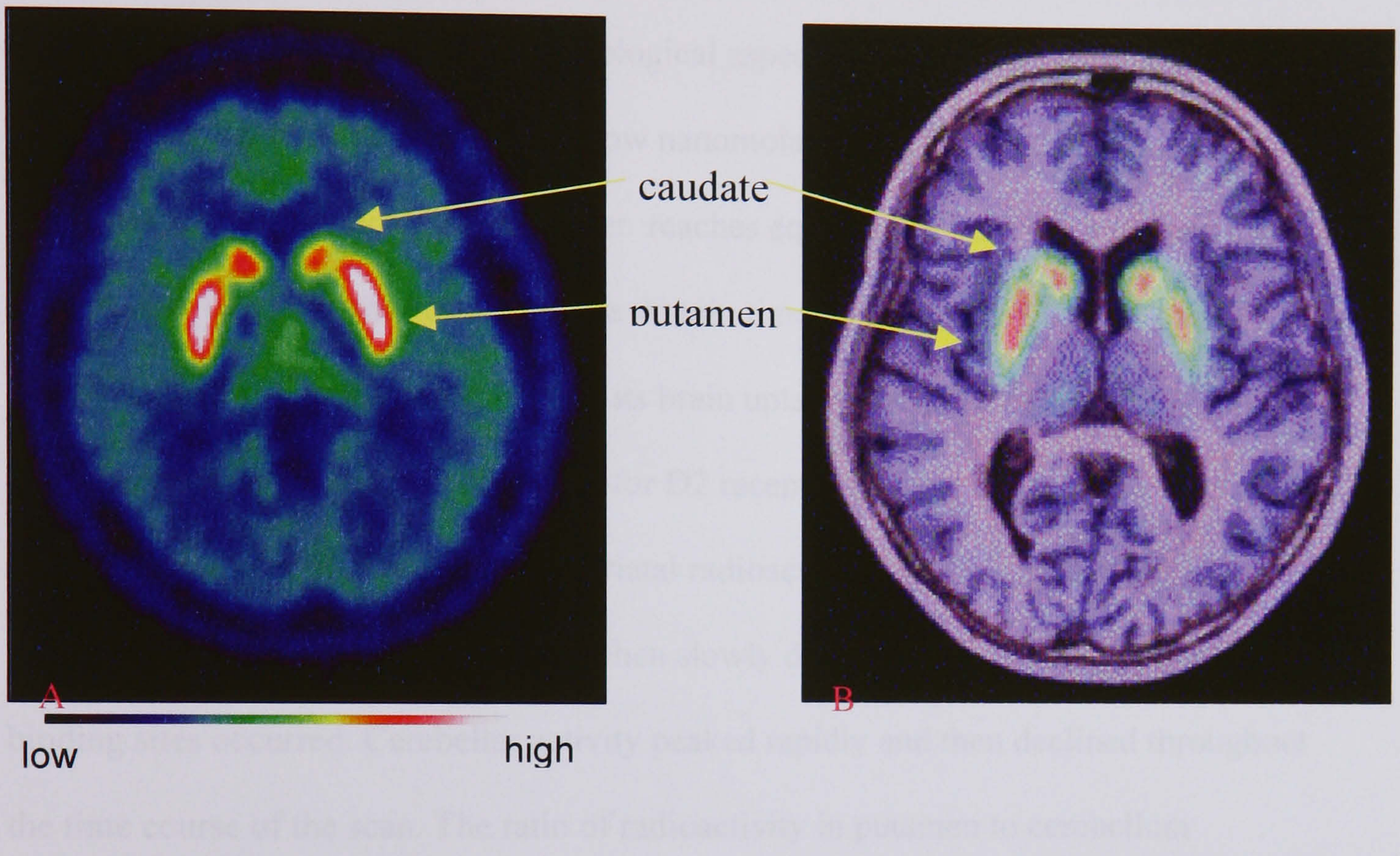


Figure 8.

Integral images of ^{18}F-dopa in a normal volunteer (A) superimposed onto the subject MRI. The yellow arrows point to the putamen and caudate nuclei.

2.4 ^{11}C-raclopride

2.4.1 Introduction

There are a number of pharmacological aspects which make ^{11}C-raclopride a suitable PET ligand. This ligand has a low nanomolar affinity for D2 and D3 receptors and low lipophilicity such that the tracer reaches equilibrium between brain and plasma after iv administration within the 90 min time course of a PET scan (Farde 1985). Unlike spiperone-based tracers, its brain uptake is also influenced by endogenous dopamine which competes for D2 receptor binding. Early studies reported a rapid uptake of ligand by the brain, striatal radioactivity reaching a peak at 25 minutes post intravenous injection and then slowly declining as dissociation from binding sites occurred. Cerebellar activity peaked rapidly and then declined throughout the time course of the scan. The ratio of radioactivity in putamen to cerebellum plateaued at 30 minutes indicating that equilibrium between specifically bound and free ligand compartments in the brain had been reached. As a consequence, (striatal - cerebellar)/cerebellar) activity at equilibrium can be taken to represent the binding potential or Bmax/Kd for the striatum.

The peripheral metabolism of raclopride comprises conjugation to form glucuronides and sulphates, both hydrophilic compounds. Following a bolus injection of raclopride in man, only 20% of the tracer is metabolised in plasma after 45 minutes.

It has been shown that a cerebellar time activity curve is a suitable input function for ^{11}C-raclopride delivery and can be used as a measure of non specific and free binding (Lammertsma 1996). As a consequence single injection studies of ^{11}C-raclopride without arterial cannulation can be employed for calculating D2 binding potentials.

2.4.2 Preparation

^{11}C-raclopride was prepared by the methylation of the desmethyl precursor analogue using ^{11}C-methyliodide (Ehrin 1987). This was prepared on site and checked for chemical purity using analytical high pressure liquid chromatography (HPLC) and mass spectrometry.

2.4.3 Safety and Tolerability

The tracer amounts of ^{11}C-raclopride injected in PET studies (5-10 μg) are not sufficient to cause pharmacological effects. Indeed if pharmacological effects were apparent the assumptions inherent in tracer kinetic modelling would be invalid. Nevertheless, injected doses are not associated with any dopamine antagonist like effects (Farde 1989).

2.5 Displacement studies

2.5.1 Introduction

It has been recognised for some years that imaging changes in neuroceptor availability to positron emission tomography (PET) ligands can be used to indirectly measure synaptic neurotransmitter fluxes in the living human brain. When endogenous dopamine (DA) binds to D2 receptors it competes with the reversible antagonist ^{11}C-raclopride. This phenomenon allows synaptic DA levels to be estimated indirectly from changes in tracer D2 receptor binding potentials (Ross et al., 1989).

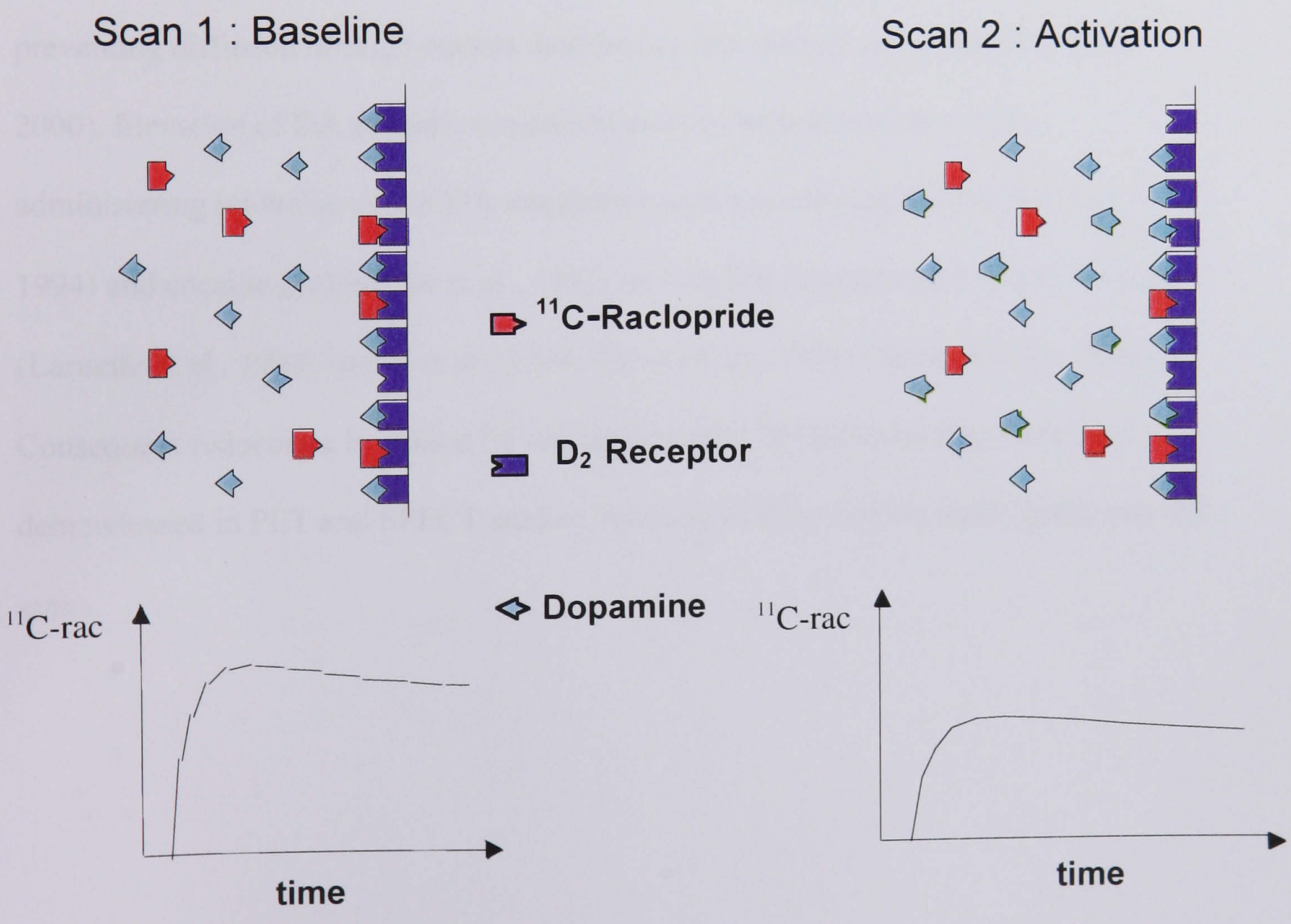


Figure 9. Two scan ^{11}C-raclopride model

Conventionally, specific D_2 binding of ^{11}C-raclopride is computed from regional brain time activity curves (TACs) using a simplified tissue reference model, which assumes that the cerebellum is devoid of DA receptors and so its TAC reflects non-specific binding levels in other brain regions. Following challenges that increase synaptic DA concentrations, reductions in radiotracer binding potential (BP) are assumed to directly reflect changes in availability of D_2 receptors due to occupancy by endogenous DA (Laruelle, 2000).

In reality the situation is probably more complex than this as binding of DA leads to internalisation of D_2 receptors (Chugani et al., 1988; Itokawa et al., 1996). However, internalisation of D_2 receptors following DA release does not invalidate the model as ^{11}C-raclopride can only bind to D2 receptors on the cell surface, its low lipophicility preventing diffusion through plasma membranes into the cell cytoplasm (Laruelle, 2000). Elevation of DA synaptic concentrations can be achieved *in vivo* by administering inhibitors of the DA transporter such as methylphenidate (Volkow et al., 1994) and cocaine (Schlaepfer et al., 1997) or with DA releasers such as amphetamines (Laruelle et al., 1995; Breier et al., 1997; Carson et al., 1998; Ginovart et al., 1999). Consequent reductions in striatal ^{11}C-raclopride and ^{123}I-IBZM binding have been demonstrated in PET and SPECT studies but none of these reports interrogated cortical areas.

2.5.2 Validation of the methods: studies on normal volunteers and patients with Parkinson's disease

2.5.2.1 Subjects

We studied six patients with advanced idiopathic Parkinson's disease (5 males and 1 female; age 65 ± 7.6 years) and six age-matched healthy male right-handed subjects (all males; age 57 ± 12 years, p= 0.14) (Table 3). Participants were not included if they had known current or past psychiatric or neurological disease, head trauma, diabetes or medical conditions that may alter cerebral functioning or a past or present history of alcohol or substance abuse. PD patients had a mean disease duration of 10.9 years (± 4.1) and mean Unified Parkinson's Disease Rating Scale (UPDRS) motor score in the practically defined 'off 'phase (12 hours withdrawn from medication) of 78.2 (± 15.6). They were all taking levodopa preparations (725 ± 150 mg/day). Patients were PET scanned in an "off" state after overnight withdrawal of antiparkinsonian medication. Written consent was obtained from all subjects after the nature and possible risks of the study were fully explained. Ethical permission for PET studies was obtained from the Hammersmith Hospitals Trust Ethics Committee. Approval to administer radiolabel ligands was obtained from the Administration of Radioactive Substances Advisory Committee (ARSAC) of the United Kingdom.

Table 3. Clinical characteristics of the Parkinson's disease patients.

Patient #	Sex	Age (yrs)	Disease Duration (yrs)	UPDRS Total motor score Off (max=108)	UPDRS Best side	UPDRS Worst side
1	M	76	15	98	32	36
2	M	58	9.5	64	20	23
3	M	61	7	70	24	27
4	M	73	17	86	22	31
5	M	63	8	60	8	34
6	F	59	9	91	18	35
Mean (±SD)		65.0 (7.6)	10.9 (4.1)	78.2 (15.6)	20.6 (7.8)	31.0 (5.1)

UPDRS= Unified Parkinson's disease rating scale assessed in the practically defined 'off' phase.

2.5.2.2 Experimental design

Normal volunteers and PD patients were scanned using the ECAT EXACT HR++ (CTI/Siemens 966) PET tomograph. Each subject was scanned twice in 3D mode, 2 to 3 days apart, and was assigned randomly to have an intravenous dose of normal saline in one scan and methamphetamine (0.3 mg/kg) in the other scan. Saline or methamphetamine was administered as a bolus over 30 s, 7 min before the injection of ^{11}C-raclopride. A dose of approximately 130 MBq (range 121-135) of ^{11}C-raclopride was then injected intravenously. Subjects did not know whether they would receive placebo or methamphetamine.

The six PD patients also had ^{18}F-dopa PET 1 to 2 days after their two ^{11}C-raclopride PET studies. A dose of approximately 110 MBq (range 75-87) of ^{18}F-dopa was administered intravenously over 30 seconds.

2.5.2.3 Data acquisition

Data were acquired in list mode (event-by-event) with post acquisition frame rebinning in order to obtain the following dynamic sequence 1*15sec, 1*5sec, 1*10sec, 1*30sec, 4*60sec, 10*300sec time-frames, for a total of 55 minutes. After reconstruction images had a spatial resolution of 5.1 mm (X) x 5.1 mm (Y) x 5.9 mm (Z) full-width half maximum.

2.5.2.4 Tracer kinetic modelling

Quantitative tracer kinetic modelling was performed using a simplified reference tissue compartmental model (Lammertsma and Hume 1996; Gunn et al., 1997). The cerebellum was used as the reference tissue. The model allows the estimation of the parameters R1 (relative rate of radioligands delivery normalised to the cerebellum) and binding potential (BP).

$$\mathbf{BP = f_2\ B_{MAX}/[K_D(1+ F_i / K_{Di})]}$$

Where f_2 is the free fraction of non specifically bound radioligands in the tissue, B_{MAX} is the total concentration of specific binding sites, K_D is the dissociation constant of the radioligands indicating its affinity, and F_i and K_{Di} are respectively the free concentration and the dissociation constant of competing endogenous ligand. The assumption on which the whole method is based is that changes in BP are attributed to changes in F_i for endogenous dopamine. The reference tissue model was applied at a voxel level using a basic function implementation, and parametric images of BP and R1 for the 55-minute scan period were calculated as described previously (Gunn et., 1997). The cerebellar reference region was generated within the Analyze™ software environment (Mayo biochemical Engineering, Rochester. MN) on a SUN Ultra 10 Workstation. Regular circular (15*15) region of interests (ROI) were defined for each

cerebellar hemisphere in five contiguous planes on an integrated PET images of brain activity from 1 to 30 minutes following the ^{11}C-raclopride injection for each individual scan.

2.5.2.5 Region of interest analysis

A volumetric magnetic resonance image (MRI) was obtained for each of the normal volunteer and PD patient. A 1.0 T Marconi Medical Systems HPQ scanner was used with a 3D RF spoiled sequence (TR = 24 ms, TE = 6ms, field of view = 25cm, slice thickness = 1.6mm, image matrix = 152 x 256, NEX = 2). To facilitate coregistration the brain was segmented from extra-cerebral tissue in MR image using AnalyzeTM software. Each MRI was then separately coregistered to saline and amphetamine associated ^{11}C-raclopride PET add images using coregistration software (MPR; Guy's Hospital, London, UK) (Studholme et al., 1997).

The pairs of coregistered MRIs and corresponding PET parametric images were visualized and regions were traced around the caudate and putamen of the left and the right hemispheres on the MRI for all planes where these structures were clearly defined. Regular elliptical ROIs were drawn on the head of the caudate and putamen of the left and right hemispheres. The five planes displaying maximum activity in the striatum were chosen for the analysis to obtain BP and R_1 values and the ROIs were then applied to the parametric ^{11}C-raclopride images.

2.6 $H_2{}^{15}O$

2.6.1 Measurement of regional cerebral blood flow (rCBF)

The most commonly used radiolabelled tracer for the measurement of rCBF is $H_2{}^{15}O$. The short half life of ^{15}O (2.05 min) allows 12 rCBF measurements to be performed in a single subject over 2 hours with limited radiation exposure (4.6 mSv). These features allow multiple experimental conditions to be performed in single subjects with good patient tolerability. The measurement of rCBF after bolus injection of $H_2{}^{15}O$ is based upon a model developed by Kety and colleagues (Kety, 1951). The model describes the *in vivo* behaviour of tracers that can equilibrate freely between blood and tissue.

Absolute quantitation of rCBF necessitates radial artery cannulation to determine the plasma input function for the radioisotope. It has been shown that there exists a near linear relationship between regional brain counts and rCBF, providing that a bolus $H_2{}^{15}O$ approach is used and scan durations are kept short (60 - 90 seconds). Indeed, the sensitivity and specificity of response detection and the accuracy of response localisation are similar whether $H_2{}^{15}O$ PET is used to image quantitative regional cerebral blood flow or regional tissue ^{15}O activity. In the activation study to be described comparisons are, therefore, made between levels of regional tissue ^{15}O activity rather than quantitative rCBF.

2.6.2 Relationship of rCBF to neuronal activity

The coupling of rCBF to the metabolic needs of functional neuronal activity has been a well documented tenet of neurophysiology dating from 1890. The rCBF response to a local change in neuronal synaptic activity occurs within 2-5 sec. Furthermore, rCBF responses in the primary somatosensory cortex have been shown to remain constant in magnitude throughout a period of sensory stimulation showing that in primary cortical areas, response habituation does not occur.

The close coupling of tissue metabolism and rCBF has been re-examined over the past ten years. In the resting state, levels of rCBF, regional cerebral metabolic rate for oxygen ($rCMRO_2$) and regional glucose consumption are closely coupled. However, during phasic neuronal activation induced by somatosensory and visual stimulation induced focal cortical increases in rCBF and glucose metabolism (50 and 51% respectively) greatly exceeded the increase in O_2 metabolism (5% increase). This suggests preferential aerobic glycolysis is occurring.

2.6.3 Interpretation of rCBF changes

It is generally agreed that the highest energy requirements in the brain are for active Na^+ transport through ATP dependent ion channels following neuronal depolarisation During neuronal firing an increase in glucose consumption by nerve terminals occurs due to their synaptic activity, whereas there is little change in the metabolism of their cell bodies. These observations have led to two important considerations when interpreting the results of rCBF activation studies: Firstly, an alteration in local metabolism and perfusion may be due in order to maintain ionic

gradients in synapses which are distant from the origin of their cell bodies. Activation of a particular brain area may, therefore, reflect afferent input along with intrinsic neuronal activity (Kadekaro et al., 1985). Failure to consider this may lead to incorrect interpretation of the functional anatomy underlying behaviour.

The second consideration is that both excitatory and inhibitory processes can lead to increases in synaptic activity (Nudo et al., 1986) and it is, therefore, not possible to distinguish between these processes with $H_2{}^{15}O$ PET. Caution must, therefore, be used in attributing excitatory or inhibitory roles to cerebral areas on the basis of changes in their rCBF.

2.6.4 Statistical analysis of rCBF activation studies

The localisation of significant rCBF changes associated with activation in this thesis utilises Statistical Parametric Mapping (SPM) software developed by Friston and colleagues at the MRC Cyclotron Unit and BIC, Wellcome Trust. It is now the most widely used method for localising significant changes during PET activation studies and many of the principles are applicable to ligand functional imaging studies. A feature of SPM is the use of the General Linear Model to describe the variation in voxel based regional activity as a linear combination of independent variables plus an error term. The use of a linear model greatly simplifies the variance of the data and reduces computational requirements.

There are a number of steps when applying SPM analysis to group studies of rCBF: These include image realignment, stereotaxic normalisation, ANCOVA to remove global rCBF variance as a nuisance variable, spatial smoothing to increase the signal to

noise ratio and performance of the relevant statistical comparisons. These will now be discussed in turn.

2.6.4.1 Realignment of rCBF studies

(Friston et al., 1991a; Woods et al., 1992; Friston et al., 1995)

One source of variance in activation studies is the change in brain's position within and between subjects. Participants lie in different positions in the scanner and also move during the duration of the experiment. Spatial realignment addresses the issue of continuity in brain position within subjects. For a voxel-by-voxel statistical analysis it is important that the images are in alignment. So that any particular voxel location corresponds to the same voxel across all emission scans and images. To correct for any possible movement of the subjects a realignment of the images is carried out. To achieve realignment the first image is taken as a reference and all other images are rotated and their axes translated to match the position and the orientation of the first image using a least square approach. This process is referred to as rigid body transformation and is expressed by three rotational (around the z-, y- and x-axes) and the three translational (along the z-, y- and x-axes) parameters. These parameters are then used to create a mean image and the whole process is repeated. The parameters resulting from the second procedure are referred to reslicing parameters. The parameters are used to resample all images realigned to the mean by a process called trilinear interpolation. After the realignment a voxel from one image corresponds to the same location of that voxel in another image from a particular scanning procedure.

2.6.4.2 Stereotaxic normalisation

To facilitate between subject comparisons of functional brain anatomy images of rCBF are usually transformed into standardized anatomical space (Talairach 1988).

The anatomical transformation relies upon an estimation of the position of the intercommisural line (the line passing through the centres of the anterior and posterior commisures or AC-PC line) directly from landmarks on the PET images, and the subsequent reslicing and reorientation of the images to lie parallel to this line. The landmarks used in the process consist of the ventral aspects of the anterior and posterior corpus callosum, the thalamus, and the occipital pole, all of which appear to have a consistent relationship to the AC-PC line (Friston 1991).

Variance due to linear differences in brain size is readily removed by proportional linear rescaling by interpolation of position vectors so that they correspond to the standardized brain co-ordinates. Plastic resampling of the data is also performed during the process of stereotaxic normalization to remove non-linear, morphological variance in brain shape and symmetry (Friston 1991).

The coordinates of foci reported in recent SPM software (SPM99) are based on a different coordinates system to Talairach space and use an MRI template derived from 152 normal brains studied at the Montreal Neurological Institute (Collins et al., 1994). This coordinate system is referred to as MNI space. Conversion from one system to the other is based on an algorithm developed by M.Brett which can be found at www.mrc-cbu.cam.ac.uk/imaging.

2.6.4.3 Smoothing

Convolution of the images with a Gaussian filter (smoothing) serves to minimize the effects of individual variations in structural and functional anatomy and to improve the signal to noise ratio of the images at the expense of spatial resolution. Smoothing essentially minimize variability in brain shape and function, as it increases the spatial extent of activity or signal at a particular brain location so that an area of

consistent activation across subjects even if differentially located a few millimetres apart can be robustly be detected.

2.6.4.4 Statistical analysis

When localising significant focal changes in ^{15}O activity during activation the confounding influence of global on local blood flow changes must be considered. These are assumed to be independent. The overall organisation of the statistical analysis is summarised in a mathematical model, referred to as the design matrix of the SPM, that is applied to each individual smoothed voxel. Overall the data is partitioned into components of interest (group and/or covariate of interest), covariates of no interest (the confounds of global flow and of scan order effects) and a non specific error term, The general linear model and standard least square approaches are used to estimate the contribution of these components to the observed physiological effect as specified in the design matrix. The general linear model is an equation that relates what one observes, to what one expected to see, by expressing the observations (response variable/rCBF [Y]) as a linear combination of expected components (or explanatory variables, i.e. the covariates of interest and no interest [X] and some residual error (ε) [$Y+X+\varepsilon$]). Specifically in SPM two other terms β and C are added [$Y=\beta X+C+\varepsilon$]. (C stands for a constant term, β is explained below). For example, designating the global blood flow as a confounding variable allows removal of the influence of the global flow variance with ANCOVA, leaving only the variance that is due to region specific activation (Friston et al., 1990). This process generates an adjusted mean rCBF value for each experimental condition together with its associated error variance. The other partitions of the design matrix (those of interest and those of no interest) are similarly estimated and are subsequently referred to as parameters estimates or betas.

Localisation of relative regional rCBF effects is assessed by specifying the differences among parameters estimates using appropriate weighted linear contrasts equivalent to experimental conditions. By dividing the change score between conditions by the error variance a Student's t statistic for each voxel is calculated. The null hypothesis is that the change in rCBF at a given location is not significantly different from zero. This process results in the definition of regional peaks and extent changes in rCBF for each particular contrasts. The mathematical outcome is a three-dimensional statistical parametric map of the t statistic (SPM $\{t\}$). The map indicates graphically the spatial extent (k) of individual activations. The height of the peak (μ) of the activation is indicated in the associated parametric z scores of the SPM. Z scores are derived from the t scores by transforming them to a normal or Gaussian distribution using a probability integral transformation (Poline et al., 1997). The Z scores, therefore, represents the maximal activation value (peak) divided by the distribution of the standard deviation of the mean.

2.6.4.5 Statistical inference

In SPM $\{t\}$, statistical analysis is applied to every voxel, which results in a high number of comparisons being made. It is important to note, however, that the effective number of comparisons being made is far lower than the actual number of existing voxels (Friston et al., 1991). This is because neighbouring voxels are not truly independent from each other as functional connectivity and smoothing lead to spatial correlation. If one is analysing data with a specific anatomically restricted *a priori* hypothesis in mind about which brain areas might activate based on previous knowledge, it is accepted that correction for multiple comparisons may not be necessary, as this would be deemed to be too conservative (Poline et al., 1997). Previous knowledge in this instance would be based on previous imaging experiments

or on reported findings. If such an approach is used, only changes at locations that were hypothesised can be validly reported and other localisations should be ignored. Related to this approach is the recently advocated method of using so-called small volume corrections (SVC) (Worsley et al., 1996). In SVC thresholding for significance corrected for multiple dependent comparisons is used where the null hypothesis is only tested at predefined brain locations.

Another possibility is to use a threshold for significance corrected for multiple dependent comparisons. This statistical inference is employed when one has no regional specific hypothesis about which brain areas might be activated during a particular condition or when an exploratory analysis is undertaken. The null hypothesis is, therefore, tested simultaneously at all locations throughout the brain. The correction employed is a Bonferroni-like adjustment that takes account of the fact that the activity of neighbouring voxels is correlated, that is not truly independent. Correlations are estimated according to a Gaussian probability density function. The theory of Gaussian fields is therefore used when correction for multiple comparisons is applied (Friston et al., 1991). Activations whose p values do not survive thresholding after correction for multiple comparisons can still be descriptively reported.

The role of PET in understanding the genetic contribution to the causes of Parkinson's disease

3

3.1 The role of inheritance in sporadic Parkinson's disease: Evidence from a longitudinal study of dopaminergic function in twins

3.1.1 Subjects

Over a period of eight years (from 1991 until 1998) 34 PD patients with asymptomatic co-twins, regardless of whether they were MZ or DZ were recruited by referral and from hospital clinics in the UK, in Italy, and in USA (New Brunswick, NJ, and Rochester, MN). Zygosity was confirmed by DNA fingerprinting. Eighteen MZ twin pairs (12 male and six female pairs with mean age 61.7 ± 13 .2 years) and 16 DZ pairs (five male/male pairs, four female/female pairs and seven male/female pairs; mean age 57.2 ± 15.1 years) were studied with ^{18}Fdopa PET. Over a seven year period (mean 4.2 ± 2.0 yr.) 10 MZ and 9 DZ asymptomatic co-twins were re-scanned.

At baseline clinically affected MZ twins (12M/6F) had mean disease duration of 5.6 ± 4.2 yr. and mean age at symptom onset of 56.1 ± 13.4 yr.; clinically affected DZ twins (8M/8F) had mean disease duration of 5.4 ± 5.5 yr. and mean age at symptom onset of 54.9 ± 13.3 yr. Three of the 34 (9%) twin pairs (2 MZ and 1 DZ) gave a family history of PD. One of the MZ pair had 1 affected first-degree and 1 affected second-degree relative, the other MZ pair had 2 affected first-degree relatives and the DZ pair had 2 affected first-degree and 1 affected second-degree relatives. Ethical permission for the study was obtained from the Ethics Committee of the Royal Postgraduate Medical School, Hammersmith Hospital. Approval to administer radiolabel ligands were obtained from the Administration of Radioactive Substances Advisory Committee of the United Kingdom. Written consent was obtained from all the subjects after a full explanation of the procedure.

3.1.2 Specific methods

^{18}F-dopa region of interest analysis was performed as previously described in methods 1.2.2.4 . ^{18}F-dopa Ki results for twin pairs were compared with those of 33 healthy volunteers matched for age and sex.

We used discriminant analysis to categorise individual asymptomatic co-twins as "normal" or "PD" on the basis of their pattern of caudate and putamen ^{18}Fdopa uptake. PD targets dopaminergic function in the putamen significantly more than in the caudate (2:1), while normal subjects have uniform levels of ^{18}F-dopa uptake throughout the striatum. For each subject in the five subgroups (healthy volunteers, PD MZ and DZ twins, asymptomatic MZ and DZ co-twins) the Ki values for left and right caudate and putamen were reclassified as the maximum and minimum putamen Ki values and the maximum and minimum caudate values. These four values together

with the diagnosis (normal or Parkinson's disease) were then used in a discriminant function analysis. We used maximum and minimum, rather than ipsilateral and contralateral (to the clinically most affected side) because we wished to apply the results of this analysis to asymptomatic subjects where neither side is clinically affected. In discriminant function analysis, each parameter is examined in turn to determine its power to discriminate between the different populations. The end product is a linear combination of the parameters (in this case the putamen and caudate ^{18}F-dopa uptake values) which, when applied to the original data set, enables calculation of a discriminant score for each subject. Each subject is then compared with all the other subjects to determine which of the diagnostic categories he or she is most likely to belong to (20). In this study, on the basis of the discriminant score, each subject is assigned a probability of being either normal or having PD.

3.1.3 Results

3.1.3.1 PD co-twins.

By discriminant function analysis all clinically affected PD twins and all healthy volunteers were assigned to the appropriate diagnostic category with a probability of 99% or greater. All clinically affected PD twins showed a pattern of striatal ^{18}F-dopa reduction characteristic of idiopathic disease (Brooks et al., 1990), putamen uptake being more affected than caudate uptake. There were no significant differences in mean putamen and caudate ^{18}F-dopa uptake between the clinically affected MZ and DZ cohorts (mean putamen: 3.7 ± 1.2 vs 3.2 ± 1.4 Ki min^{-1} x10^{-3}; mean caudate: 7.1 ± 2.5 vs 6.9 ± 2.8 Ki min^{-1} x10-^{3}).

3.1.3.2 Asymptomatic co-twins

3.1.3.2.1 Baseline.

At baseline, the mean ^{18}F-dopa putamen uptake was significantly lower for the 18 asymptomatic MZ co-twins compared with the 16 asymptomatic DZ co-twins ($p=0.02$) (table 4). Moreover, the MZ, but not the DZ co-twin group had mean ^{18}F-dopa putamen uptake significantly reduced compared with age-matched controls ($p< 0.0001$) (table 4).

Table 4. Mean putamen ^{18}F-dopa uptake in control subjects, in monozygotic and in dizygotic co-twins of clinically affected Parkinson's disease subjects. Differences between groups were calculated by unpaired t-test.

	Controls	MZ co-twins		DZ co-twins	
No of subjects	33	18	10	16	9
^{18}F-dopa putamen uptake		1st evaluation	2nd evaluation (4.0 ± 1.7 yr.)	1st evaluation	2nd evaluation (4.3 ± 2.2 yr.)
Mean (Ki min^{-1} x10^{-3})	10[I]	7.8*^	6.3*§	9.3	9.2
Std deviation	1.3	1.7	1.9	1.6	2.1

*$p < 0.0001$ vs controls, ^$p = 0.02$ vs DZ co-twins at 1st evaluation, $p = 0.005$ vs DZ co-twins at 2nd evaluation

Individually, 10 out of 18 asymptomatic MZ co-twins (6 M/4F) and 3 out of 16 asymptomatic DZ co-twins (2M/1F) were classified as "PD" by discriminant analysis with probabilities of 99-100% (Figure 10).

The concordance for nigro-striatal dopaminergic dysfunction at the time of the first scan was, therefore, 55% in the MZ twin pairs and 18% in the DZ pairs. These concordance levels were significantly different (p=0.03; Fisher exact test) (table 5).

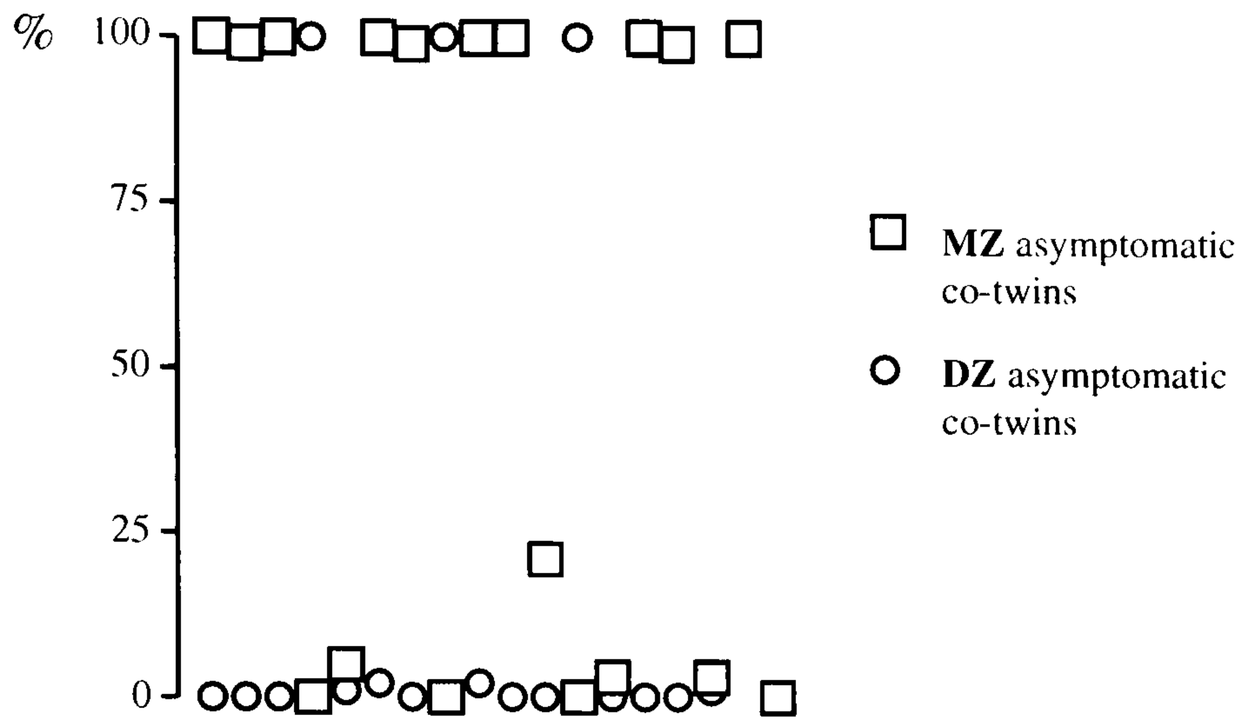


Figure 10. Discriminant analysis in 18 asymptomatic monozygotic and 16 dizygotic co-twins of Parkinson's disease patients. % probability of belonging to the Parkinson's disease diagnostic category on the basis of their ^{18}F-dopa caudate and putamen Ki values.

Since our intention was to specifically investigate the role of genetic factors in sporadic PD cases we also calculated concordance rates for dopaminergic dysfunction excluding those three twin pairs (2 MZ and 1 DZ) who gave a positive familial history for PD. Of the asymptomatic co-twins in these pairs the DZ co-twin and one of the 2 MZ co-twins were classified as PD by discriminant analysis on the basis of their ^{18}F-dopa uptake, so the concordance level of nigro-striatal dysfunction after excluding these subjects was 56% in the MZ pairs and 13% in the DZ pairs, (p=0.02). None of these 3 pairs with a positive family history was available for re-scanning.

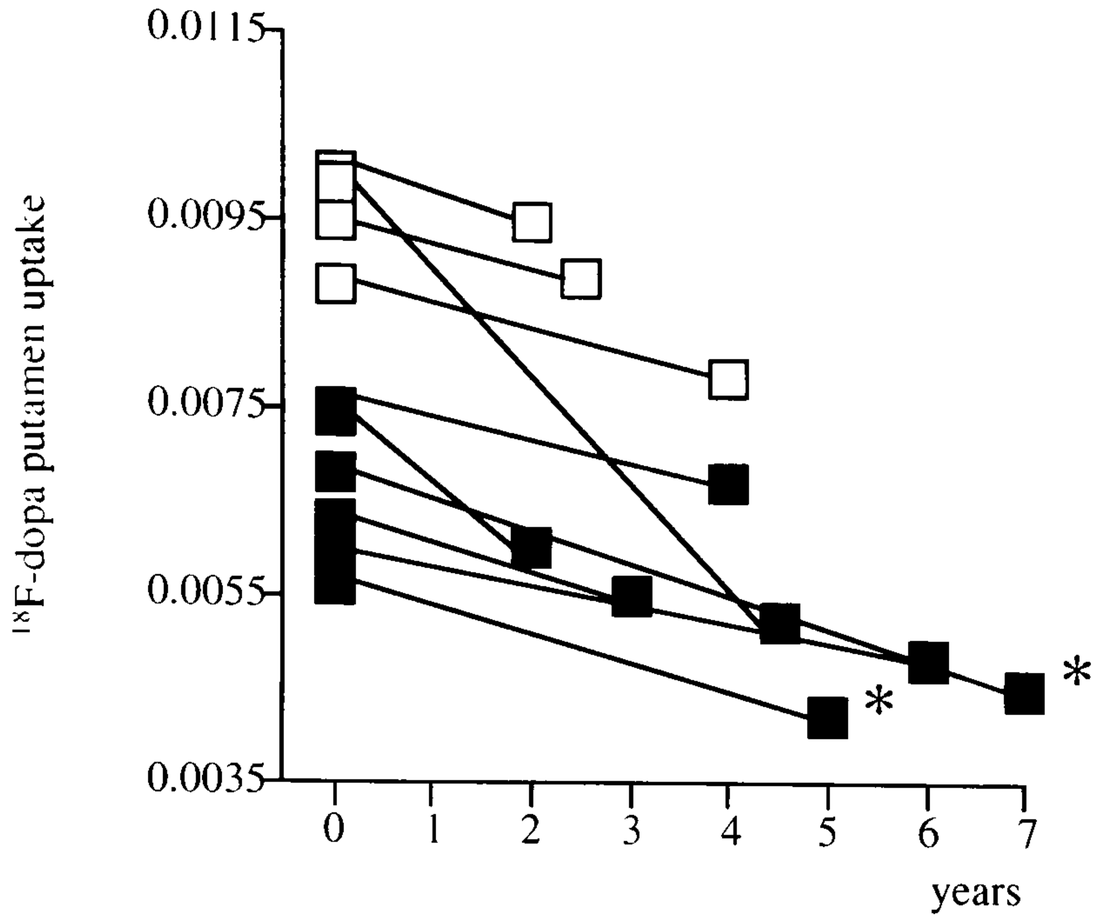
Table 5. Concordance levels of nigro-striatal dopaminergic dysfunction in monozygotic and dizygotic twin pairs at baseline discordant for clinical Parkinson's disease. At first evaluation individual asymptomatic monozygotic and dizygotic co-twins were identified as concordant with their clinically affected twins by discriminant analysis on the basis of the pattern of reduction in caudate and putamen ^{18}F-dopa uptake. Differences in concordance levels between twin pairs were calculated at 1st evaluation and follow up by Fisher exact test.

	MZ twin pairs		DZ twin pairs	
	1st evaluation	follow up (4.0 ± 1.7 yr.)	1st evaluation	follow up (4.3 ± 2.2 yr.)
No of subjects	18	12	16	9
Concordances				
PET DAergic dysfunction	55.5% (10/18)*	70% (7/10)	18.7% (3/16)	22.2% (2/9)
Clinical PD		33.3% (4/12)		0
Combined		75% (9/12) §		22.2% (2/9)

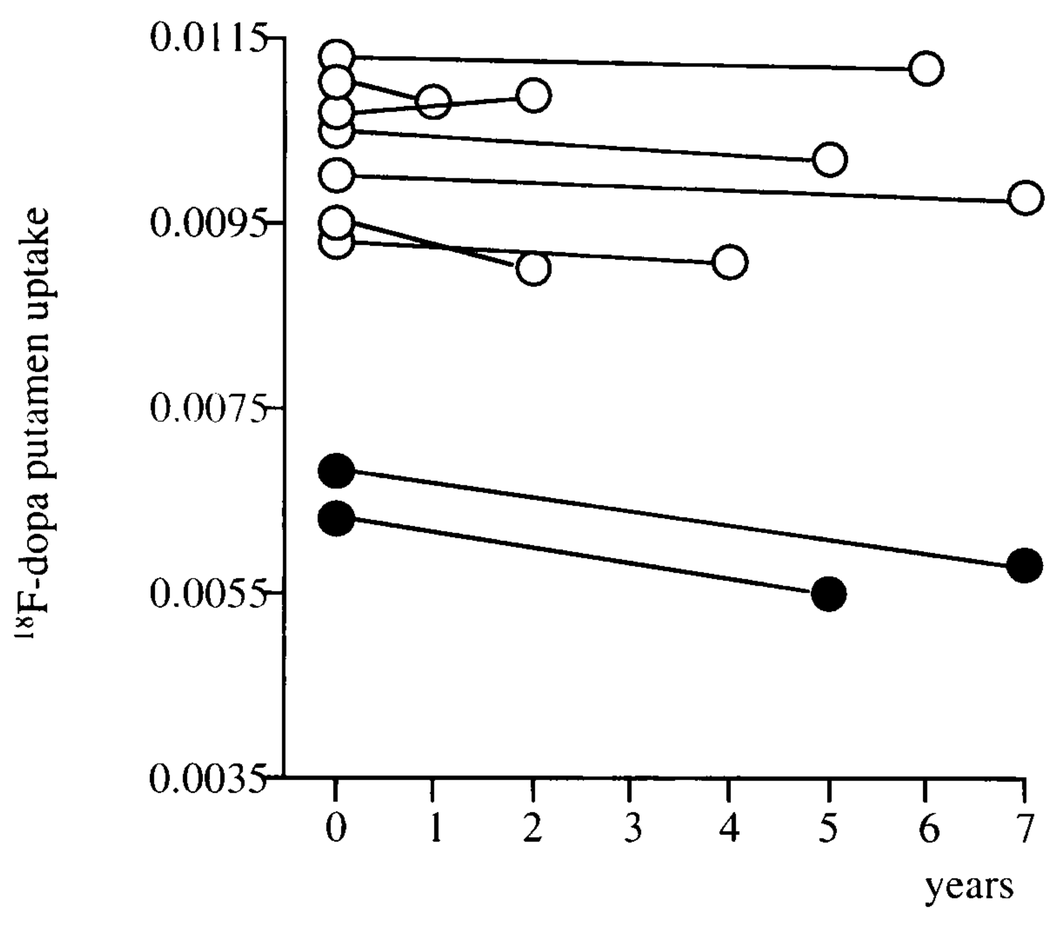
*p=0.03 vs DZ at 1st evaluation, §p=0.02 vs DZ at follow up

3.2.3.2.2 Repeat scanning

MZ co-twins. Of the asymptomatic 10 MZ co-twins (mean age 59.8 ± 12.1 yr.) that were scanned serially, four had been classified as PD and six as normal by discriminant analysis on the basis of their baseline ^{18}Fdopa scan. On repeat scanning, 4.0 ± 1.7 years after the first scan, three more MZ co-twins were classified as having PD by discriminant analysis (Figure 11A).



A .Monozygotic co-twins



B. Dizygotic co-twins

Figure 11. Putamen ^{18}F-dopa uptake in 10 asymptomatic monozygotic (A) and 9 dizygotic (B) co-twins of Parkinson's disease patients scanned twice. Subjects classified by discriminant analysis as having Parkinson's disease on the basis of their ^{18}F-dopa caudate and putamen Ki values are represented in black. The asterisks mark two of the monozygotic co-twins who developed clinical Parkinson's disease.

All 10 showed further decreases in putamen ^{18}Fdopa uptake (Figure 11A), the mean loss in putamen ^{18}Fdopa being $-4.6 \pm 2.5 \times 10^{-4}$ Ki min^{-1} per year, range -2.8, -11.

DZ co-twins. Of the nine asymptomatic DZ co-twins (mean age 56.7 ± 15.2 yr.) that were scanned serially two had been classified as PD and seven as normal by discriminant analysis on the basis of their baseline ^{18}Fdopa scan. On repeat scanning no other subject was classified as PD (figure 11B); as a group they showed a mean loss in putamen ^{18}Fdopa of -1.1 ± 2.1 x10^{-4} Ki min^{-1} per year, range +0.9, -3, over a period of 4.3 ± 2.2 years.

The mean annual loss in putamen ^{18}F-dopa Ki was significantly greater for the asymptomatic MZ than for the asymptomatic DZ co-twins (p=0.0007 unpaired *t* test; p=0.01 test for unequal variances) and the difference in mean putamen ^{18}F-dopa uptake between MZ and DZ co-twins became even more significant at follow-up (p=0.005) (table 4). If we considered the results of the discriminant analysis at the time of follow-up seven of the ten MZ and two of the nine DZ co-twins scanned twice were classified as PD so the concordance level for nigro-striatal dopaminergic dysfunction had risen to 70 % for the MZ pairs and 22.2% for the DZ pairs (p=0.05). Over the seven years of follow-up, two MZ and 1 DZ asymptomatic co-twins died without developing symptoms while four MZ co-twins, of which only two had been scanned twice (figure 11A), became clinically concordant for PD (at 64, 70, 72 and 78 years of age, 16, 21, 2 and 9 years after the onset of PD in their co-twin) resulting in a clinical concordance of 33.3 %. None of the DZ twin pairs became clinically concordant .The combined (subclinical and clinical) concordance levels was therefore 75% in the 12 MZ and 22% in the 9 DZ twin pairs evaluated at follow up (p=0.02; Fisher exact test) (table 5). The concordance for clinical PD was higher within the MZ pairs over 60 years of age (50%; 4 of 8) and the difference in clinical concordance levels between the MZ and DZ twin pairs in the 60-70 age group of age was significant (p=0.02; Fisher exact test).

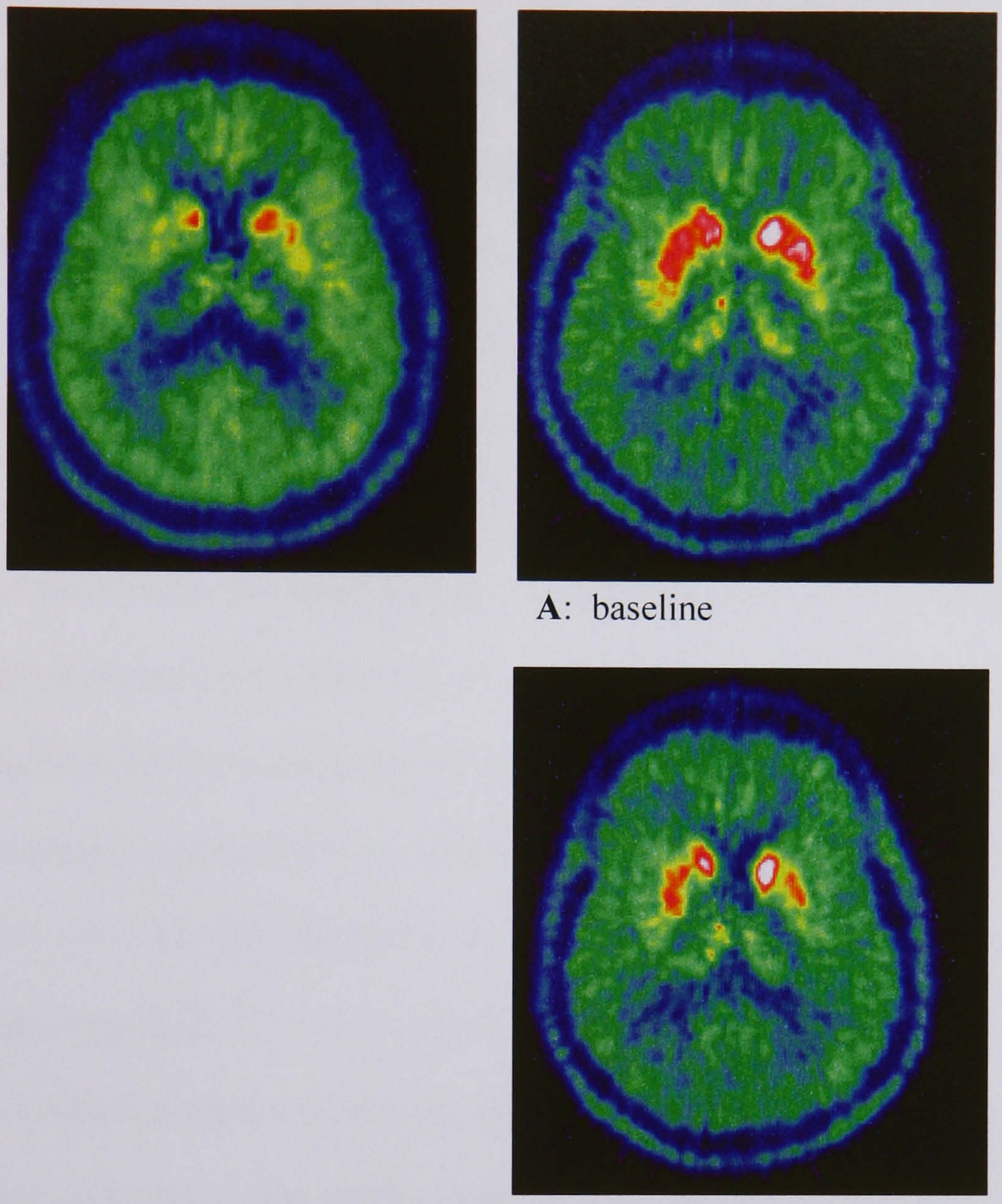


Figure 12. ^{18}F-dopa images in a twin with PD (Hoehn and Yahr 3.5) and in his asymptomatic MZ co-twins at baseline (A) and after 6 years (B).

3.1.4 Discussion

In support of a role for genetic factors in "sporadic" PD this study showed that concordance levels for dopaminergic dysfunction were significantly higher in MZ than in DZ twin pairs with no apparent history of familial aggregation for the disease; furthermore, the level of concordance in MZ pairs increased with time. Four asymptomatic MZ co-twins with abnormal baseline scans subsequently became concordant for clinical PD supporting the assumption that the nigro-striatal dopaminergic dysfunction identified by ^{18}F-dopa PET represents subclinical manifestation of the disease. The level of clinical concordance in MZ twins changed over a mean period of four years from 0% to 33%.

It has been suggested that the relationship between genetic susceptibility and the level of clinical concordance expected in twins with late-onset disorders will be different from that in early-onset diseases (Breitner et al., 1992, 1993). In diseases of late onset, any presumed genotype is likely to be expressed as a clinical phenotype in old age; therefore, if the proband develops clinical disease at an atypically early age the pair may only become concordant after years or even decades. It has been calculated that in Alzheimer's disease (AD), even if there is a strong genetic influence, the expected level of clinical concordance in identical twin pairs in their 60's and 70's would only be 20% to 40% while twin pairs in their late 70's and 80's would show concordances of 60% to 80% (Breitner et al., 1993).

Four of the MZ twin pairs in the present study became clinically concordant for PD at the ages of 65, 70, 72 and 78 (after a 14, 2, 9 and 20 year latency). The clinical concordance in MZ twins in their 60's and 70's was, therefore, 50% (4 of 8), a figure not dissimilar to the one estimated for AD. Furthermore, the clinical concordance

levels in this age group were significantly different between MZ and DZ twin pairs. All the asymptomatic MZ co-twins showed progressive loss of dopaminergic function over time: it is reasonable to assume that if all these identical MZ co-twins lived long enough, they might eventually become clinically concordant for PD. These data point to a significant genetic role in the development of nigro-striatal dopaminergic dysfunction; the variability *among* identical co-twins in rates of loss of dopaminergic function and the variability *within* identical twin pairs in length of pre-clinical phases, moreover, indicates that the genetic causes are heterogeneous and that there may be a modifying effect of the environment.

The reliability of twin studies for estimating the genetic components of diseases has been criticised (Phillips, 1993) on the basis that MZ pairs may share similar adverse uterine or early life environmental conditions that could be important in the aetiology of some diseases. However, epidemiological studies performed to date have not established any link between PD and low birth weight, birth order, congenital abnormalities, and perinatal risk factors (Vieregge et al., 1992; Martyn et al., 1995). There was no significant difference in mean age of our MZ and DZ twins and the pairs in both cohorts were reared at the same time and in a similar environment, apart from one of the MZ pairs that was separated at the age of 12: the asymptomatic co-twin in this pair had abnormal ^{18}F-dopa uptake and later developed clinical PD. Additionally, I have found no differences in later environmental conditions between the MZ and DZ cohorts; there were similar proportions of smokers and non-smokers and similar proportions of subjects living in a rural environment.

During the 1980's a genetic contribution to PD was thought to be unlikely when a series of cross-sectional clinical surveys of twins failed to demonstrate an increased concordance for PD in MZ versus DZ twins (Ward et al., 1983, Marttila et al., 1988).

A more recent study looking at a cohort of 250 twins with parkinsonism reported that while genetic factors do not seem to play a major role in causing PD after the age of 50 years, they are important when disease begins at or before age 50 years (Tanner et al., 1999).

As has been pointed out, however, cross-sectional studies are difficult to interpret since reliance on clinical diagnosis alone and a lack of follow-up makes the determination of concordance in PD twin cohorts extremely insensitive (Johnson et al., 1990).

A different epidemiological approach has been used in an Icelandic study by Sveinbjornsdottir et al. (2000) whose results suggested a greater role for genetics. They used a computerized database of genealogic information from the past 11 centuries to examine the genetic risk for PD. The database contained information on 610,920 persons including some from large families with complex interrelations, and allowed these authors to identify an effect that could be due to multifactorial interactions among several genes. Their results showed that subjects with PD had significantly higher "kindred coefficients" indicating inter-relatedness than non-affected individuals. This was true for patients with disease onset at age older than 50 years as well as for all patients even after first- and second-degree relatives were excluded from the analysis. Their results suggest that, at least in this interrelated Icelandic population, genetics may contribute substantially to development of PD, not only in 'young-onset' disease but also in disease with typical age at onset.

The present study is the first study in which clinical assessment and functional brain imaging have been used together in a longitudinal study of twin pairs. Taken together, the data demonstrate an important role of inheritance in the aetiology of PD.

3.2 Studies in *parkin*-linked parkinsonism

3.2.1 Progression of nigro-striatal dysfunction in a *parkin* kindred: an ^{18}F-dopa PET and clinical study

3.2.1.1 Subjects

Ten members of this family underwent a standardised neurological examination. A retrospective review of medical records and video material taken at the time of the first scan was used to estimate the Unified Parkinson's Disease Rating scale (UPDRS) (Fahn *et al.*, 1987) and the Hoehn and Yahr (H&Y) (Hoehn *et al.*, 1967) score at the time of the first scan. Scores on the H&Y scale and the UPDRS scale in a practically defined 'off' state (12 hours after withdrawal of medication) were used to rate the degree of parkinsonian disability at the time of the second scan. All subjects gave informed consent on both occasions and the project was approved by the Joint Ethics Committee of the National Hospital for Neurology and Neurosurgery, London, UK.

3.2.1.2 Specific methods

3.2.1.2.1 PARK2 molecular data

The molecular analysis was performed at the Institute of Neurology (Genetic laboratory) using a method previously described (Lucking et al., 2000; Kitada *et* al 1998).

Haplotype analysis in the region of *parkin* showed evidence of linkage (see figure 13). A deletion in exon 8 was identified in a paternal uncle II.3 and siblings III.1-5 and III.8. These cases were hemizygous for alleles at marker D6S411 confirming the presence of a deletion in exon 8 and segregating with the paternal haplotype 4-3-x-1.

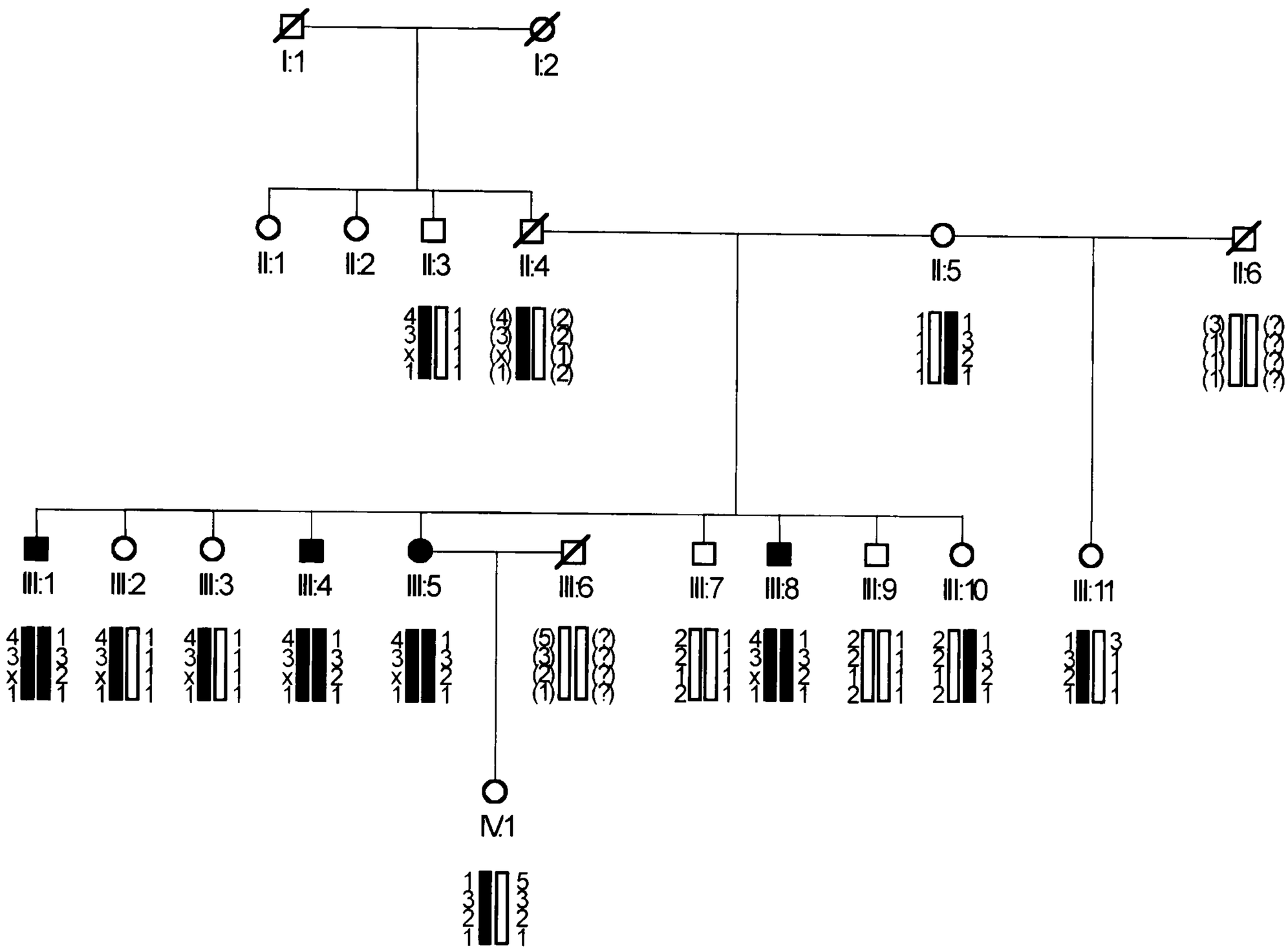


Figure 13. Pedigree of the family with *Parkin* disease. Haplotypes that segregate with *parkin* mutations are indicated in black such that the paternally inherited disease chromosome is indicated by 4-3-x-1 and the maternally inherited disease chromosome is indicated by 1-3-2-1. The position of the deletion on the paternal disease chromosome is indicated by an 'x'. Markers in parentheses were inferred on the basis of offspring data. Markers surrounded by question marks could not be phased with certainty.

The second mutation, an intron 5 +2 T->A splice mutation, was detected in the mother, II.5, siblings III.1, III.4, III.5, III.8, III.10, III.11 and offspring IV.1 and segregated with the maternal haplotype 1-3-2-1. The clinically affected individuals were compound heterozygotes having an exon 8 deletion and an intron 5 +2 T->A splice mutation and shared heterozygous haplotypes 4-3-x-1 and 1-3-2-1. Of the asymptomatic cases, three carried a paternally inherited *parkin*-associated haplotype (II.3, III.2 and III.3) and a detectable exon 8 mutation and one sibling (III.10), one half-sibling (III.11) and offspring (IV.1) inherited the maternal *parkin*-associated haplotype and a detectable intron 5 +2 T->A splice mutation. Siblings III.7 and III.9 did not inherit either of the *parkin*-associated haplotypes and did not have an exon 8 deletion nor an intron 5+2 T->A splice site mutation.

3.2.1.2 Scanning protocol

At the time of the first scan seven family members underwent ^{18}F-dopa PET on the CTI/ 931 scanner (Methods 1.3.9) while the second scan was performed on an CTI/953 scanner (Methods 1.3.10). A mean dose of 129.5 MBq ^{18}F-dopa was injected. Permission to perform these studies was obtained from the Ethics Committee of the Hammersmith Hospitals Trust, London, UK and from the Administration of Radioactive Substances Advisory Committee (ARSAC), UK.

Because two different scanners were used over the 10 year period, ^{18}F-dopa uptake was expressed as a percentage of the normal mean in healthy controls scanned with the respective scanners. On the first occasion 16 unrelated age matched controls (mean = 58.5±14.3 years, range = 28-75 years) scanned on the CTI 931 scanner were used as controls. For the second scan, 14 unrelated, age matched controls (mean = 54.6±13.9,

range = 30-71 years) scanned on the CTI/953 scanner with identical methods used for the *parkin* patients were used as controls. The controls reported no family history of parkinsonism and all had a normal neurological examination.

Seven patients with IPD, originally scanned on the 931 PET camera, with disease severity (evaluated on both clinical and ^{18}F-dopa striatum uptake ground) similar to the *parkin* group at the time of their first scan, were re-scanned on the 953 PET scanner after an interval of 5.04 (±1.73) years between scans. The clinical characteristics of the *parkin* and IPD patients are detailed in table 6.

Table 6. Clinical characteristics for each of the clinically affected subjects with *parkin* mutations and for a group of seven patients with idiopathic Parkinson's disease (IPD).

	Parkin patients					IPD (n=7)
	III.1	III.4	III.5	III.8	mean ±SD	mean ±SD
age of onset	28	27	31	32	29.0 ± 5.0	58.5 ± 4.8[1]
age at 1st scan	50	45	43	40	44.5 ± 4.2	68.7 ± 5.0[2]
duration of clinical symptoms at 1st scan (yrs)	22	18	12	8	15.0 ± 6.2	10.2 ± 2.4
interval between scans (yrs)	10	11	11	11	10.7± 0.5	7.0 ± 3.7
UPDRS 1st scan	39	57	42	59	49.2 ±10.2	50.3 ± 11.9
H&Y 1st scan	2	2	2	2	2	2.5 ± 0.6
UPDRS 2nd scan	59	108	74	90	82.7 ± 21.0	90.6 ± 12.7
H&Y 2nd scan	3	4	4	4	3.7 ± 0.5	4.1 ± 0.6

Wilcoxon test (*parkin* group vs IPD group) [1]p=0.0061, [2]p=0.0066

For those subjects who had repeat scans the percentage annual rate of decline of ^{18}F-dopa Ki (*r*) was calculated using the formula: r = [(mean Ki for the group of healthy

controls -subject Ki) / mean Ki of the group of healthy controls]/ number of years between consecutive scans) x 100.

The non-parametric Wilcoxon test was used for all comparisons between different groups of patients and controls.

3.2.1.3 Results

3.2.1.3.1 Clinical findings

Our *parkin* kindred originated from a small village in Southern Ireland. There was no known parental consanguineity and the parents did not have parkinsonism. The affected cases fulfilled the clinical diagnostic criteria of the UK Parkinson's Disease Society Brain Bank for PD except for the presence of a family history (Gibb *et al.*, 1988). Four (one woman and three men) out of ten siblings were affected at the time of the study in 1990 and no further members of this kindred have developed the disease. The mode of transmission was consistent with autosomal recessive inheritance. Mean age of onset of symptoms was 29 years (range 28-32 years). All affected siblings had a striking response to L-dopa therapy with levodopa-related dyskinesias after a mean interval of 2.4 years. Estimated mean clinical disease duration was 26 years (range 19-32 years) at the time of the second scan. The clinical presentation of the patients was comparable to that of juvenile-onset PD cases, however, currently their phenotype was indistinguishable from IPD with a common feature of severe resting leg tremor (abduction-adduction oscillations).

3.2.1.3.1.1 Patients

Patient III.1

This 60 year old man reported initial symptoms of fatigue, lower limb pain and slowness from the age of 28 years with subsequent in turning of both feet. At the time of the first scan he was H&Y stage II with a UPDRS 'off' score of 39. Following a 10 year interval, at the time of the second scan, disease duration was 32 years and he had now reached H&Y stage III and an UPDRS off score of 59. In the 'off' state he had a predominant abducting-adducting oscillatory tremor of both lower limbs at rest with asymmetrical bradykinesia and rigidity (left more than right). His posture was upright and he was unsteady on his feet. He had been receiving L-dopa for 14 years and continued to report a significant improvement taking 1000mg a day albeit with moderate inter dose dyskinesia and severe motor fluctuations. He was able to walk up to 3 miles at a time and maintain a job as a local handyman.

Patient III.4

This 55 year old man reported initial symptoms of slowness, right leg tremor and involuntary inversion of both feet from the age of 27 years. At the time of the first scan he was H&Y stage II with a UPDRS 'off'' score of 57. Following an 11year interval, at the time of the second scan, disease duration was 29 years and he had progressed to H&Y stage IV and a UPDRS 'off' score of 108. In the 'off' state he had a severe abducting-adducting oscillatory tremor of both lower limbs at rest with symmetrical bradykinesia and rigidity, postural instability and poor arm swing. At the time of the second scan he had been on L-dopa therapy for 23 years and continued to report significant improvement and dyskinesias with L-dopa, taking 1200mg a day. He was, however, no longer able to continue with employment as a landscape gardener; his disability had been exacerbated by lumbar canal stenosis such that he required walking sticks and at times, a wheelchair.

Patient III.5

This 54 year old housewife reported symptoms of slowness, leg pain and leg tremor from the age of 31. At the time of the first scan she was H&Y stage II and UPDRS 'off' score was 42. Following an 11 year interval, at the time of the second scan, disease duration was 19 years and she had progressed to H&Y stage IV and UPDRS 'off' score of 74. She had considerable motor fluctuations with her 'off periods' being characterised by marked generalised stiffness, pain, bilateral resting leg tremor, shuffling gait and poor balance such that she was barely able to mobilise independently and perform activities of daily living. She had been on L-dopa for 11 years and continued to report a significant improvement from L-dopa taking 500mg a day but had developed motor fluctuations and dyskinesias.

Patient III.8

This 51 year old former builder reported initial symptoms of bilateral leg tremor and involuntary inversion of the right foot from the age of 32. At the time of the first scan he was H&Y stage II with an UPDRS 'off' score of 59. He developed inter-dose painful dystonic cramps of the feet and severe chorea of the head, trunk and legs. Following an 11 year interval, disease duration was 19 years at the time of the second scan and he had progressed to H&Y stage IV and a UPDRS 'off' score of 90. 'Off' periods were associated with fatigue and distressing rest tremor of the legs and to a lesser degree the arms. Rigidity and bradykinesia were worse in the legs. At the time of the second scan he had been receiving L-dopa therapy for 18 years and continued to report a significant improvement , taking 1200mg a day.

3.2.1.3.1.2 Asymptomatic cases

None of the carriers of a single *parkin* mutation reported any symptoms. Individual IV.1 was first examined at the age of 19 years and then had ^{18}F-dopa PET when she was 24 and again when she was 30. At 19 years of age, individual IV.1 had a

postural tremor of the right arm. At follow up, eleven years later, there was a postural tremor of both hands (right more than left), rest tremor of both legs and reduced arm swing on the right. Tone was normal with no evidence of bradykinesia, hypomimia or micrographia. Despite these extrapyramidal signs the UK Brain Bank diagnostic criteria for PD (Gibb *et al.*, 1988) were not fulfilled.

Individual III.2, a housewife, had a normal examination in 1990 but at the time of the second scan had facial masking and reduced left arm swing.

Individual III.3, a housewife, had a history of diabetes, depression and schizophrenia that had been previously treated with chlorpromazine. Present treatment for depression included olanzapine, procyclidine and sertraline. Clinical examination at the time of the first scan was normal but at follow up there was a positive glabellar tap with normal tone, poor arm swing and mild paucity of facial expression with a bucco-lingual masticatory syndrome and stereotypies of the lower limbs.

The neurological examination of III.11 was normal.

Of those siblings with a normal genotype, III.7 had a normal neurological examination. Individual II.3, a 75 year old paternal uncle, was not examined on the second occasion nor scanned on either occasion.

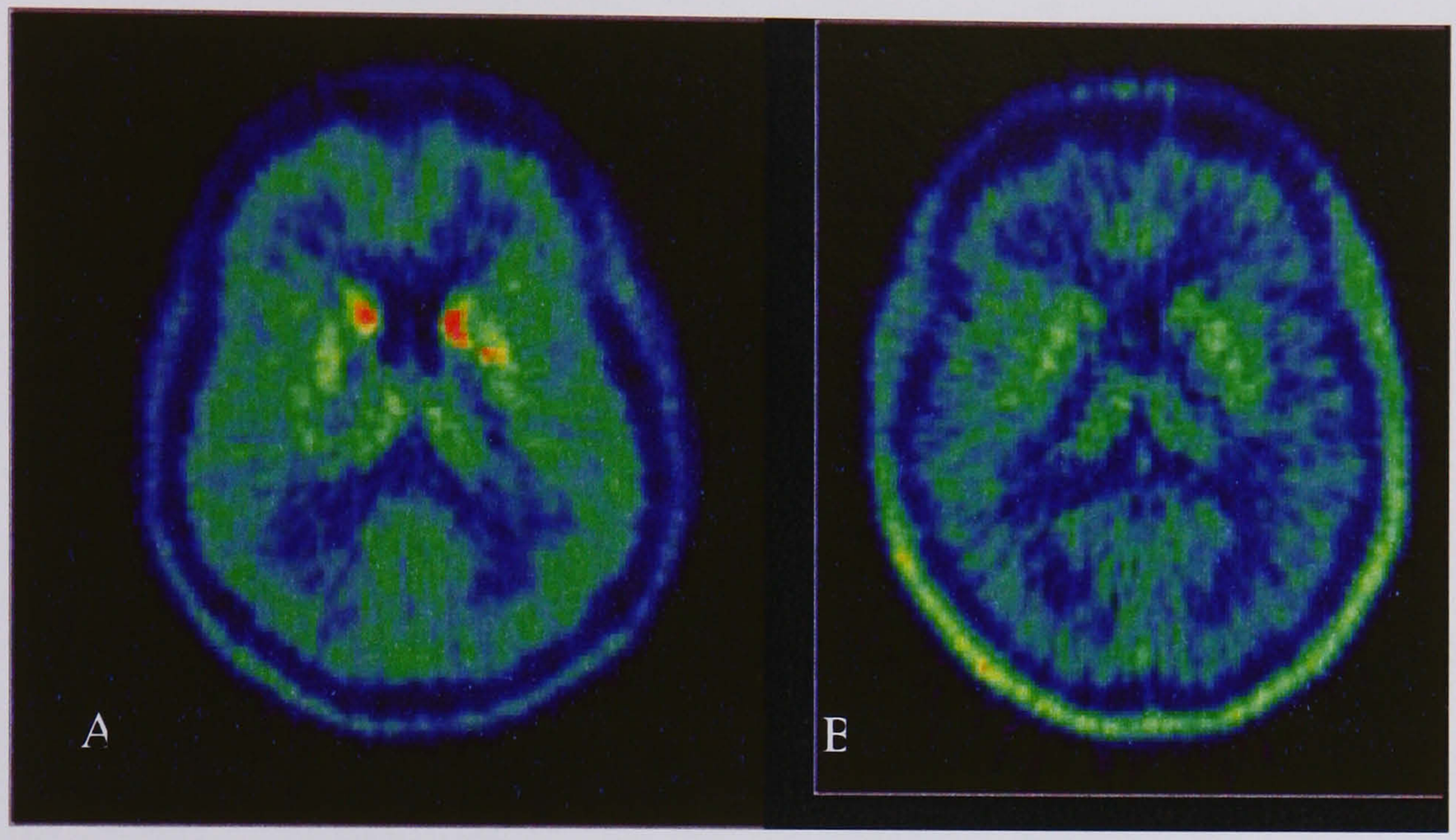


Figure 14. ^{18}F-dopa images for a patient with idiopathic PD (A) and for a patient with Parkin mutation (B) with similar age duration and similar disease severity.

3.2.1.3.2 PET data

3.2.1.3.2.1 Patients

Figure 14 shows examples of ^{18}F-dopa PET scans for a patient with idiopathic PD and a *parkin* patient. Mean values for ^{18}F-dopa caudate and putamen uptake, expressed as percentage reduction relative to the normal mean, at the first and second scan for the *parkin* and the IPD groups are shown in table 4. At the time of the first scan, percentage reductions below the normal mean in caudate ^{18}F-dopa uptake in the *parkin* and in the IPD groups were not significantly different (55±12 vs 43±5, p=0.109), similarly putamen percentage reductions below the normal mean were not significantly different in the two groups (64±4 in the *parkin* vs 58±8 in the PD patients, p=0.315) (table 7).

Table 7. Mean percentage reductions relative to the mean of normal subjects in caudate and putamen ^{18}F-dopa Ki values in the four *parkin* patients and in the group of seven patients with idiopathic Parkinson's disease (IPD), at the time of the first and the second scan with the interval in years between scans.

		% of ^{18}F-dopa Ki reductions				Interval
		Caudate		Putamen		
		1st scan	2nd scan	1st scan	2nd scan	years
Parkin patients	III.1	40	73	59	71	10
	III.4	50	56	67	75	11
	III.5	68	82	69	77	11
	III.8	62	71	62	82	11
	mean ±SD	55 ± 12	69 ± 13	64 ± 4	76 ± 4	10.7 ±0.5
IPD group (n=7)	mean ±SD	43 ± 5	51 ± 5	58 ± 8	79 ± 5	5.0 ± 1.7

Figure 15 shows the individual rates of decline in putamen ^{18}F-dopa uptake relative to the normal mean for the four *parkin* patients and the seven IPD patients.

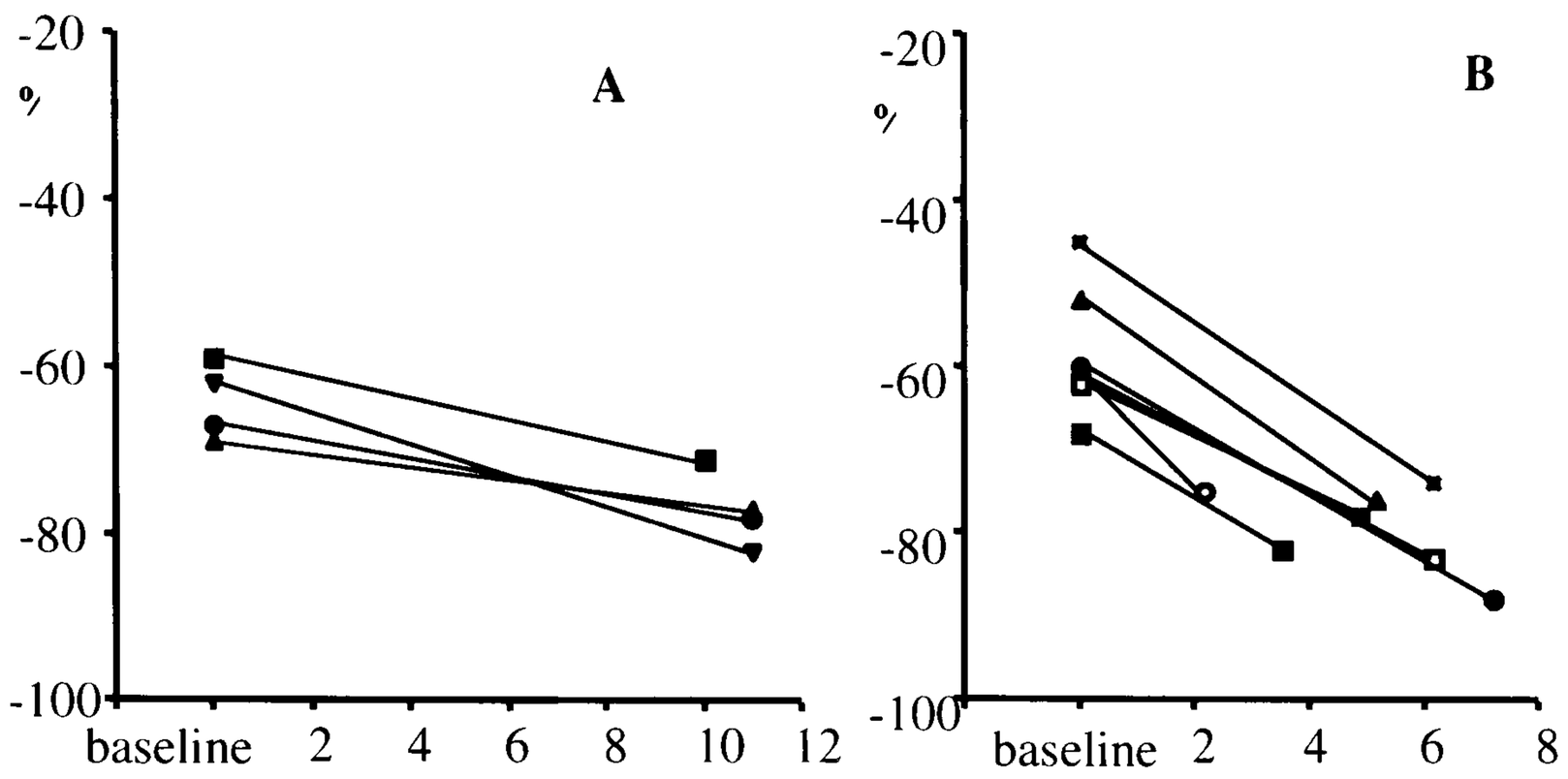


Figure 15. Individual rate of decline over time in ^{18}F-dopa putamen uptake in the four *parkin* patients (A) and in seven patients with idiopathic Parkinson's disease (IPD) (B) matched for clinical disease severity at the time of first scan. Values are expressed as percentage (%) reduction of the mean of normal controls.

The mean percentage rate of decline of putamen ^{18}F-dopa uptake relative to the normal mean was 1.47 (±05) per annum for the *parkin* group and 5.71 (±1.63) per annum for the IPD group. The rates of progression between these two groups was significantly different (p=0.0008) (Figure 15).

The mean percentage rate of decline of caudate ^{18}F-dopa uptake relative to the normal mean was 1.72 (±1.7) per annum in the *parkin* group and 3.51 (±1.04) per annum in the IPD group. This difference was not statistically significant (p=0.885) (Figure 16).

Within the *parkin* group the mean percentage rate of decline in caudate was not significantly different from that of putamen (1.72±1.7 and 1.47 ±05 respectively, p=0.16), while within the IPD group the mean percentage rate of decline was significantly slower in the caudate than in the putamen (3.51±1.04 and 5.71±1.63 respectively, p=0.006).

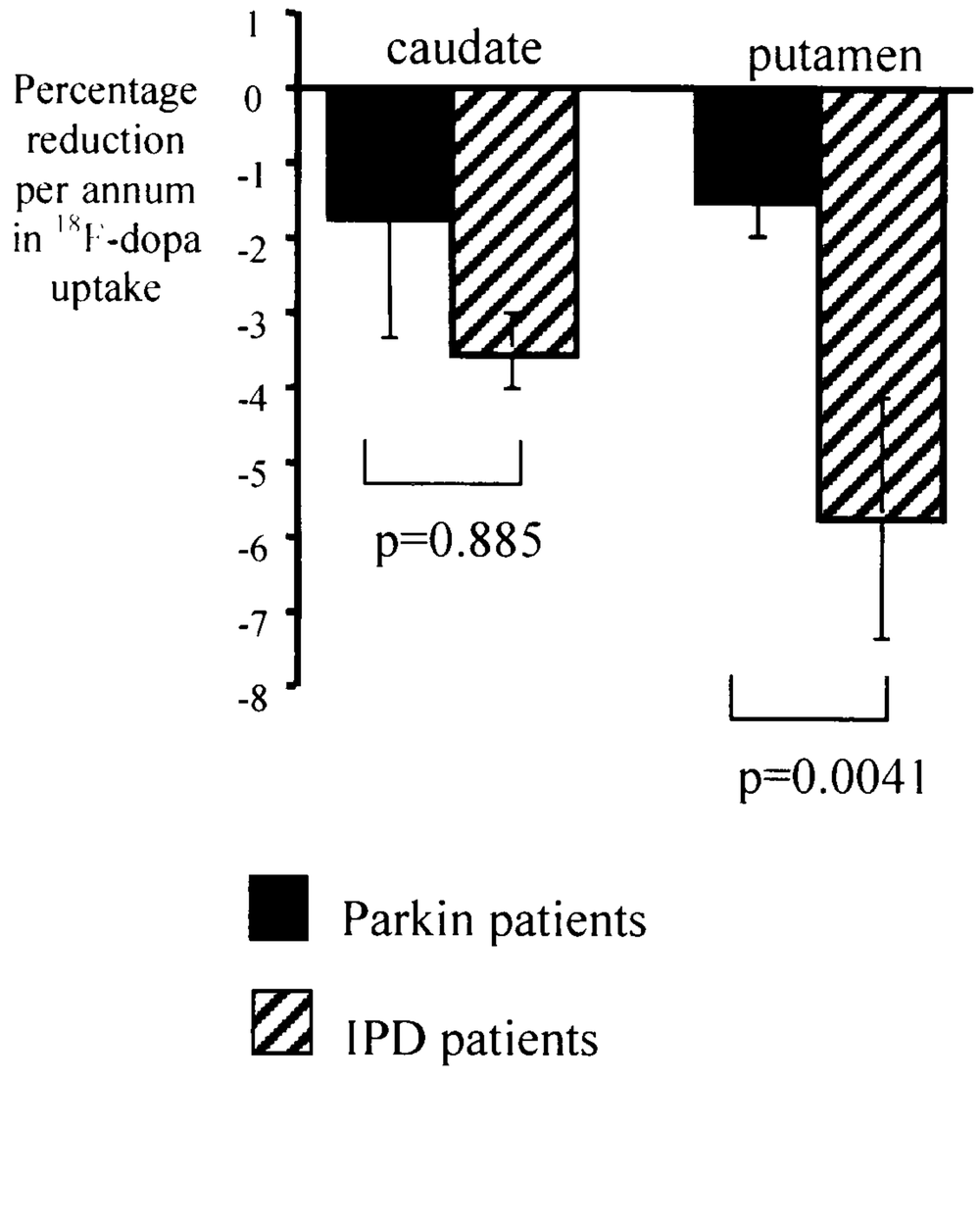


Figure 16. Mean percentage reductions per annum in ^{18}F-dopa caudate and putamen uptake in the group of *parkin* and in the IPD group. Patients were matched for disease severity at the time of first scan. Values are expressed as percentage reduction of the mean of normal controls. *Between groups Wilcoxon test.

3.2.1.3.2.2 Clinically asymptomatic cases

Sibling III.7, who had a normal genotype, had normal caudate and putamen ^{18}F-dopa uptake (Table 8) which remained normal after 6 years.

Table 8. Clinical, genetic and striatal ^{18}F-dopa PET characteristics of the asymptomatic members of the family.

	Controls (n=14) mean ± SD	III.2	III.3	III.11	IV.1	III.7
Age	54.6 ±13.9	59	58	69	30	52
Parkin carrier	-	yes	yes	yes	yes	no
Intron 5 +2 T->A mutation	-	no	no	yes	yes	no
Exon 8 deletion	-	yes	yes	no	no	no
Extrapyramidal signs	no	yes	yes *	no	yes	no
Right caudate	0.0152 ±0.0028	0.0131	0.0127	0.0109§	0.0119	0.0127
Left caudate	0.0154 ±0.0025	0.0112§	0.0117	0.0115	0.0123	0.0155
Right putamen	0.0168 ±0.0032	0.0123	0.0114§	0.0113§	0.0102§	0.0154
Left putamen	0.0169 ±0.0032	0.0125	0.0123	0.0115§	0.0121	0.0164

Caudate and putamen ^{18}F-dopa values are expressed as Ki min^{-1} § denotes Ki influx constants at least 1.5 standard deviations below normal mean. * denotes previous history of neuroleptic exposure

Individually, two *parkin* carriers showed low normal levels of caudate Ki (>1.5 SD below the normal mean) and three carriers had a low normal putamen Ki (>1.5 SD below the normal mean) (Table 8). As a group the four carriers had significantly reduced mean caudate and putamen ^{18}F-dopa uptake (0.0119±0.00047 and 0.0117 ± 0.00054 respectively) compared to mean caudate and putamen ^{18}F-dopa uptake of the healthy controls (0.0153±0.0026 and 0.0168±0.0031 respectively) (p=0.0126 and 0.009 respectively) (Figure 17).

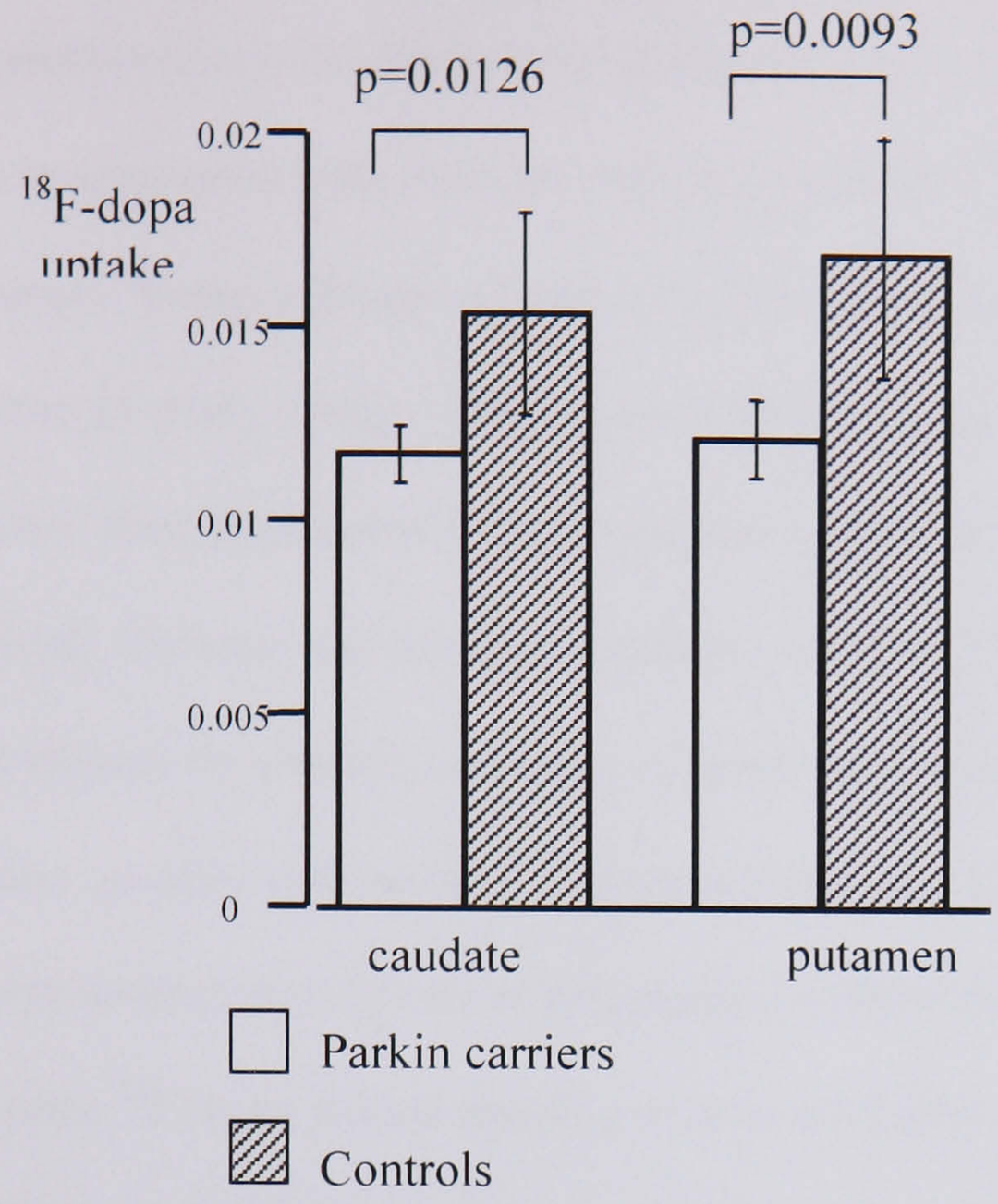


Figure 17. Mean caudate and putamen ^{18}F-dopa uptake in four *parkin* heterozygous carriers and in 14 age matched normal controls.
Values are expressed as Ki min^{-1}. *Between groups Wilcoxon test.

Two of the carriers (III.3 and IV.1) were scanned on two occasions (after 9 and 6 years respectively). The rate of changes in caudate and putamen ^{18}F-dopa uptake per annum was 0.14% and 0.09%, respectively, in carrier III.3 and 0.73% and 0.74%, respectively, in carrier IV.1.

3.2.1.4 Discussion

We have used serial ^{18}F-dopa PET to measure over a ten-year period the rate of loss of dopaminergic function in clinically affected members of a kindred with *parkin* disease. The mean annual loss of putamen ^{18}F-dopa Ki relative to the normal mean was

1.48 % in *parkin* disease compared to 5.71 % in the group with IPD suggesting that disease progression in established *parkin* disease is slower. Our findings for IPD patients are in agreement with previous studies which have reported a mean annual 6% loss of putamen ^{18}F-dopa storage relative to the normal mean or 12% relative to patient baseline (Morrish *et al.*, 1996). Although our IPD group were not age matched with the *parkin* patients, their duration of clinical symptoms at the time of the baseline scan was not significantly different and they had a similar severity of disease to the *parkin* group, as evidenced by similar reductions of putamen ^{18}F-dopa uptake and motor scores. Similar severity and duration of disease at baseline rather then age are the critical factors when assessing rate of progression of Parkinson's disease in two group of patients since ^{18}F-dopa striatal uptake *per se* is not influenced by age (Sawle *et al.*, 1990; Eidelberg *et al.*, 1993).

The rate of decline of putamen uptake amongst the symptomatic *parkin* patients was similar whilst we observed some variability in the rate of decline of caudate uptake. However, mean caudate Ki deteriorated at approximately the same rate as mean putamen Ki in the *parkin* group whereas in the IPD group caudate dopamine function was relatively spared at baseline and deteriorated at a slower rate than putamen. The finding that nigrostriatal dysfunction in *parkin* disease progresses more slowly than IPD is in keeping with the clinical observation that cases of young onset parkinsonism can have a normal lifespan and suggests that neurodegeneration in *parkin* disease is an indolent process.

Intra-sibling variability of both Ki values and degree of parkinsonian disability amongst clinically affected cases may be due to the influence of other unlinked genes (modifier genes) and undefined environmental influences. Generally however, the pattern and course of the affected cases was remarkably similar.

Because of the lapse of time, more then 10 years, we had to use two different PET cameras. We acknowledge that the procedure is not rigorous. We compensated for this by normalising patient data to control groups scanned with the respective scanners and by matching a group of IPD patients with similar disease severity and duration of clinical symptoms to that of the *parkin* group at the time of the first baseline scan. Our sample size was small and confined to a single family such that the rate and pattern of nigral cell loss that we found may be specific to this family. Our results require confirmation with a larger study.

In this study we also observed dopaminergic dysfunction in the group of asymptomatic *parkin* carriers. Abnormal nigrostriatal function in heterozygous carriers (clinically asymptomatic cases with a single mutant allele) may be attributed to *haplo-insufficiency* (Strachen *et al.*, 2000) such that a single mutant allele results in a reduction of up to 50% of ubiquitin ligase activity, which may not be sufficient for normal nigrostriatal activity. This would imply that *parkin*'s ligase activity is dosage sensitive and that sufficient relative levels of enzyme are required for interaction with other gene products of the ubiquitin-conjugating pathway. The effects of modifying genes particularly influence those cases in which the phenotype is dependent on haplo-insufficiency and environmental factors (Strachen *et al.*, 2000). An alternative explanation is a *dominant negative effect* (Strachen *et al.*, 2000), the non-functional mutant *parkin* polypeptide physically interferes with the function of the normal polypeptide suggesting that dimerization or oligomerization of the protein is requisite for normal function. Moderate reduction in protein function caused by either *haplo-insufficiency* or a *dominant negative* effect may produce nigrostriatal damage in heterozygous carriers. An alternative explanation is that the ^{18}F-dopa PET changes observed are of no clinical significance, however, the manifestation of subtle

extrapyramidal signs in three *parkin* carriers (one of whom, however, had a history of neuroleptic exposure) suggests that these individuals may well be 'manifesting heterozygotes' and raises the possibility that they may be at risk of developing *parkin* disease. Severe reduction, however. in ubiquitin ligase activity in homozygotes may produce the recessive condition, which results in marked nigrostriatal dysfunction and the clinical disease.

In the two carriers of a single *parkin* mutation, scanned 9 and 6 years apart, there were no significant changes in ^{18}F-dopa uptake with time, similar to their sibling with normal genotype (111.7) and to that seen in normal volunteers (Morrish *et al.*, 1996). This implies that either the two carriers have a fixed deficit that does not progress with time or that the rate of nigral cell death was too slow to be detected with PET over the time period. Alternatively, there may also be additional pathophysiological processes at the post synaptic receptor not detectable by ^{18}F-dopa PET. The clinical development of mild signs of basal ganglia dysfunction between the two examinations is, however, intriguing and suggests incipient nigral cell dysfunction. Repeated observation with clinical examination and repeat scanning over time in a much larger cohort will be necessary to confirm these findings.

In conclusion clinically affected cases with *parkin* mutations showed significantly slower progression of putamen dopamine terminal dysfunction, as evidenced by ^{18}F-dopa PET findings, compared to late onset idiopathic PD patients. Nigro-striatal dopaminergic dysfunction was found in a group of four asymptomatic heterozygous *parkin* carriers from the same family, three of whom manifested subtle extrapyramidal signs.

3.2.2 Striatal and cortical pre-and postsynaptic dopaminergic dysfunction in sporadic *parkin*-linked parkinsonism

3.2.2.1 Subjects

Thirteen patients homozygous or compound heterozygous for *parkin* gene mutations have been identified from a cohort of unrelated sporadic patients with disease onset below age 40 years (Table 9).

Table 9. *Parkin* mutations identified in 13 cases with young onset Parkinsons's disease.

Patient	*Parkin* mutation Allele 1	*Parkin* mutation Allele 2	PET scans
1	exon 8 deletion	intron 5 (+2 T>A)	Fdopa/Rac
2	exon 2 202-203 AG deletion	exon 2 202-203 AG deletion	Fdopa/Rac
3	exon 7 924c>t Arg275Trp	exon 12 1390g>a Gly430As	Fdopa/Rac
4	exon 7 924c>t Arg275Trp	exon 5/6 deletion	Fdopa/Rac
5	exon 6/7 deletion	uncharacterised	Fdopa/Rac
6	exon 3 40bp deletion>140stop	exon 11 1281g>a Asp394Asn	Fdopa/Rac
7	Cys268Stop	uncharacterised	Fdopa
8	exon 12 1390g>a Gly430Asp	uncharacterised	Fdopa
9	exon 7 905t>a Cys268stop	exon 2 202-203 AG deletion	Fdopa
10	exon 5 deletion	uncharacterised	Fdopa
11	exon 5 deletion	uncharacterised	Fdopa
12	exon 9 1101c>tArg334Cys	exon 7 939g>aAsp280Asn	Rac
13	exon 8 deletion	uncharacterised	Rac

Eleven of these 13 *parkin*-positive and ten *parkin*-negative young onset PD (YOPD) patients, matched for age, disease duration and severity, underwent ^{18}F-dopa PET (Table 10).

The PET findings for the YOPD patients were also compared with those of a group of 11 older IPD patients with similar disease severity but significantly shorter disease duration (Table 10).

Table 10. Demographic and clinical characteristics of *parkin* positive, *parkin* negative YOPD, IPD and control subjects.

	^{18}F-dopa PET						^{11}C-raclopride PET				
	Age years	Sex M/F	Disease duration	HY stage	UPDRS total off drug		Age years	Sex M/F	Disease duration	HY stage	UPDRS total off drug
Parkin pos. (n=11)						*Parkin* pos. (n=8)					
mean	44.8	7/4	17.9	2.9	40.1	mean	52.4	5/3	23.3	3.1	44.4
SD	±10.2		±7.4	±0.6	±13.3	SD	±6.1		±4.9	0.6	±11.3
Parkin neg. (n=10)						*Parkin* neg. (n=9)					
mean	52.7	8/2	18	2.9	36.3	mean	54	8/1	19.7	2.9	36.4
SD	±8.8		±8.7	±0.7	10.3	SD	±8.3		±7.3	0.7	±10.9
IPD (n=11)						IPD (n=7)					
mean	61.2*	6/5	8.6*	3.0	34.1	mean	53	4/3	7.9**	2.7	35.4
SD	±6.9		±3.2	±0.7	±9.5	SD	±4.7		±3.6	±0.5	9.5
Controls (n=16)						Controls (n=10)					
mean	47.1	16/0				mean	45.8	10/0			
SD	±14.4					SD	±10.3				

Values represent the means (± 1 SD). Intergroup differences were calculated by one-way ANOVA with post hoc LSD correction (least statistical significance).

*, ** indicates $p<0.01$ and $p<0.001$ vs. the *parkin* positive and *parkin* negative group.

Eight out of the 13 *parkin*-positive YOPD patients had ^{11}C-raclopride PET and findings were compared with those for 9 of the 10 YOPD patients negative for *parkin* mutations who were also scanned with ^{18}F-dopa PET. Additionally a group of seven older IPD patients with similar disease severity but significantly shorter disease

duration had ^{11}C-raclopride. ^{18}Fdopa and ^{11}C-raclopride findings for parkinsonian cases were also compared with those for groups of 16 and 10 normal control subjects, respectively, age-matched to YOPD. All *parkin*-positive and negative patients fulfilled the UK Parkinson's Disease Society Brain Bank diagnostic criteria for IPD (Gibb et al., 1988). In all patients, the disease severity was measured using the Hoehn and Yahr scale (Hoehn and Yahr, 1967).

3.2.2.2 Specific Methods

3.2.2.2.1 Molecular analysis

The molecular analysis was performed at the Institute of Neurology (Genetic laboratory) using a method previously described (Lucking et al., 2000; Kitada *et* al 1998). A brief description of the methods is reported in chapter 3.2.1.2.1

3.2.2.2.2 Scanning protocol

^{18}F-dopa and ^{11}C-raclopride scans were performed in patients and control subjects with the CTI-Siemens ECAT EXACT HR++/966 positron emission tomograph (see chapter 2.3 and 2.4).

Subjects were positioned such that their orbitomeatal line was parallel to the transaxial plane of the tomograph. Head position was carefully monitored with a video camera and by direct observation throughout. Each patient had his anti-parkinsonian medication stopped at least 12h before PET.

^{18}F-dopa-scan: Following a transmission scan, ^{18}F-dopa (100-111MBq in 10ml of normal saline solution) was infused intravenously as a bolus over 30s. Scanning began 30s prior to tracer injection with a protocol of 26 time frames over 94 min 30s (1 x 30s; 4 x 1min; 3 x 2min; 3 x 3min; 15 x 5min). Following correction for decay, parametric images of ^{18}F-dopa

influx rate constants (K_i) were generated using the multiple time graphical analysis approach with an occipital reference tissue input function. ^{18}F-dopa K_i^0 values, representing the rate of [^{18}F]dopa uptake and storage as [^{18}F]dopamine, were calculated for each voxel with in-house Kronos software (Dale Bailey) written in IDL (Research Systems, Inc., Boulder, Col., USA).

^{11}C-raclopride scans: Detailed methods of ^{11}C-raclopride scanning are reported in chapter 2.2.2. In brief, following the intravenous injection of a bolus of 110-129 MBq of ^{11}C-raclopride a dynamic time series of 26 frames over a period of 90min 30s (1 x 30s; 1 x 15s; 1 x 5s; 1 x 10s; 1 x 30s; 4 x 1min; 17 x 5min) was acquired starting 30s prior to injection. Parametric images of ^{11}C-raclopride binding potential were generated at a voxel level from the dynamic ^{11}C-raclopride scan time series using a basis function implementation of the simplified reference region compartmental model with the cerebellum as the reference tissue (Gunn et al., 1997).

3.2.2.2.3 Data analysis

Two methods of analysis were employed: (i) a region of interest (ROI) approach and (ii) SPM (statistical parametric mapping), allowing exploratory voxel-by voxel group comparisons throughout the entire brain volume without requiring an *a priori* hypothesis.

Four ROIs were outlined by inspection of integrated transversal ^{11}C-raclopride and ^{18}F-dopa PET images using Analyze software. These included the head of the caudate nucleus (circle 10 x 10mm), the anterior part of the putamen (circle 10 x 10mm), the posterior part of the putamen (circle 10 x 10mm) and the entire putamen (elliptical 10 x 24mm).

Caudate and putaminal asymmetry indices (AIs) were calculated, reflecting the percentage difference between the PET signal in the respective region of higher tracer-uptake compared with the contralateral region.

AI = (higher PET signal –lower PET signal / higher PET signal) *100.

Additionally, the hemispheric ratio between caudate and putaminal PET signal was measured. Right and left caudate and putaminal ^{18}F-dopa K_i and ^{11}C-raclopride -BP were averaged for each subject to allow for one-way analysis of variance (ANOVA) and post hoc LSD (least significance difference). Statistical analyses were carried out using a commercial software package (SPSS for Windows 8.0, SPSS UK, Surrey, England).

SPM was performed using the software package SPM99 (Wellcome Dept of Cognitive Neuroscience, Institute of Neurology, Queen Square, London, UK) implemented in Matlab 5.3 (Mathworks Inc., Sherborn, Mass., USA) (Friston et al., 1995).

In order to localise significant changes in ^{18}F-dopa K_i^0 and ^{11}C-raclopride -BP at a voxel level between groups, individual images were normalized into standard stereotaxic MNI (Montreal Neurological Institute) space with SPM. Spatial normalization of parametric maps was achieved by generating individual integrated "add images' (combined time frames 1-26 of the dynamic dataset) and normalizing those onto in-house made ^{18}F-dopa and RAC templates. Subsequently, the resulting transformation parameters were applied to the patient's corresponding parametric ^{18}F-dopa K_i and ^{11}C-raclopride BP images. A Gaussian kernel (6 x 6 x 6 mm) was then convolved with the spatially normalized parametric images to smooth them in order to accommodate inter-individual anatomic variability and to improve signal to noise for

the statistical analysis. Since dopamine uptake and D2 receptor density are known to be low in the occipital lobe and the cerebellum, a brain mask for those areas was created in order to minimize voxels of no-interest for multi-comparison corrections. The obtained datasets allowed for categorical comparisons of mean ^{18}F-dopa K_i values and ^{11}C-raclopride BP among the *parkin* positive, *parkin* negative and control groups.

3.2.2.3 Results

3.2.2.3.1 ROI analysis of ^{18}F-dopa

Regional mean ^{18}F-dopa K_i and ^{11}C-raclopride of the study groups and the intergroup statistics are illustrated in Table 11 One-way ANOVA showed a significant decrease of caudate ($p<0.001$) and putamen ($p<0.001$) ^{18}F-dopa uptake in *parkin* positive patients, *parkin* negative YOPD patients, and in IPD versus normal control subjects. *Parkin* positive and negative YOPD patients and IPD cases had similar levels and patterns of striatal ^{18}F-dopa uptake. Comparing parkinsonian patient groups with the normal control group, the asymmetry index of ^{18}F-dopa uptake was significantly increased in the caudate (*parkin* positive group, $p<0.01$; *parkin* negative YOPD group $p<0.01$; IPD group $p<0.05$) and putamen (*parkin* positive group, $p<0.05$; *parkin* negative YOPD group, $p<0.001$; IPD, $p<0.05$). No significant difference in striatal ^{18}F-dopa asymmetry was found between *parkin* positive, *parkin* negative YOPD and IPD patients. The caudate to putamen ratio of ^{18}F-dopa K_i was significantly increased in *parkin* positive ($p<0.001$), *parkin* negative ($p<0.001$) and IPD patients ($p<0.001$) versus control subjects. There was no significant difference in caudate and putamen ^{18}F-dopa uptake, the asymmetry indices and the ratio between caudate and putamen comparing *parkin* positive, negative YOPD, and IPD patients.

Table 11. Mean regional putamen (anterior, posterior) and caudate ^{18}F-dopa K_i min^{-1} and ^{11}C-raclopride binding potential values in *parkin* positive YOPD, *parkin* negative YOPD, idiopathic Parkinson's disease and control subjects.

	^{18}F-dopa $K_i$min^{-1}						
	Caudate	Putamen	Putamen ant.	Putamen pos.	AI (%) caudate	AI (%) putamen	Ratio caudate/putamen
Parkin pos. (n=11)							
mean	0.0099***	0.0056***	0.0072***	0.0049***	21**	11*	1.76***
SD	±0.0025	±0.001	±0.0015	±0.0011	±12	±10	±0.3
Parkin neg. (n=10)							
mean	0.0094***	0.0054***	0.0067***	0.0043***	19**	17***	1.77***
SD	±0.0023	±0.0011	±0.0019	±0.0006	±14	±12	±0.35
IPD (n=11)							
mean	0.0099***	0.0051***	0.0065***	0.0042***	16*	11*	2.02***
SD	±0.0019	±0.0015	±0.0021	±0.001	±14	±11	±0.4
Controls (n=16)							
mean	0.0165	0.0168	0.0179	0.0179	6	4	0.99
SD	±0.0024	±0.0028	±0.0029	±0.0037	±4	±2	±0.07
	^{11}C-raclopride BP						
Parkin pos. (n=8)							
mean	2.21***†	2.84***†	2.9***†	2.85**†	6	6	0.78**
SD	±0.35	±0.34	±0.31	±0.41	±5	±5	±0.09
Parkin neg. (n=9)							
mean	2.6**	3.37	3.31*	3.39	6	6	0.77**
SD	±0.5	±0.54	±0.54	±0.59	±3	±4	±0.06
IPD (n=7)							
mean	2.6**	3.38	3.37	3.51	5	5	0.78**
SD	±0.46	±0.69	0.59	0.83	±3	±5	0.07
Controls (n=10)							
mean	3.16	3.58	3.72	3.55	4	3	0.88
SD	±0.29	±0.3	±0.21	±0.35	±3	±3	0.06

Values represent the means (± 1 SD). Intergroup differences were calculated by one-way ANOVA with post hoc LSD correction (least statistical significance).

*, **, *** indicates $p<0.05$; $p<0.01$; $p<0.001$ vs. normal controls, respectively

† indicates $p<0.05$ vs *parkin* negative patients.

3.2.2.3.2 ROI analysis of ^{11}C-raclopride

One-way ANOVA revealed significant reductions in caudate and putamen ^{11}C-raclopride BP in *parkin* positive patients compared with *parkin* negative YOPD patients (caudate $p<0.05$ and putamen $p<0.05$) and control subjects (caudate and putamen $p<0.001$). *Parkin* negative YOPD patients showed significant decreases of

caudate ($p<0.01$) and anterior putamen BP ($p<0.05$) when compared to healthy controls. ^{11}C-raclopride BP was significantly decreased in the caudate of the IPD group versus control subjects ($p<0.01$). The asymmetry indices were not significantly different among the four groups, however we found significant decreases of the caudate-to-putamen ratio in the three patient groups when compared with the control group (*parkin* positive patients $p<0.01$; *parkin* negative patients $p<0.01$, IPD group $p<0.01$). There was no significant difference in caudate and putamen ^{11}C-raclopride BP and asymmetry indices and the ratio between caudate and putamen comparing *parkin* negative YOPD patients and the IPD group.

3.2.2.3.3 ^{18}F-dopa SPM findings

SPM of parametric ^{18}F-dopa K_i images confirmed the results of the putaminal ROI analysis. However significant relative decreases of Ki values were also detected bilaterally in the caudate of *parkin* positive compared with *parkin* negative YOPD patients (Figure 18., Table 12A). Furthermore, we found significant decreases in ^{18}F-dopa values in the ventral and dorsal midbrain in the *parkin* positive patients (areas of the red nucleus, substantia nigra and raphe nuclei) compared with both *parkin* negative YOPD patients and controls. No significant increases in ^{18}F-dopa uptake were detected in the *parkin* positive group versus the *parkin* negative YOPD and control groups.

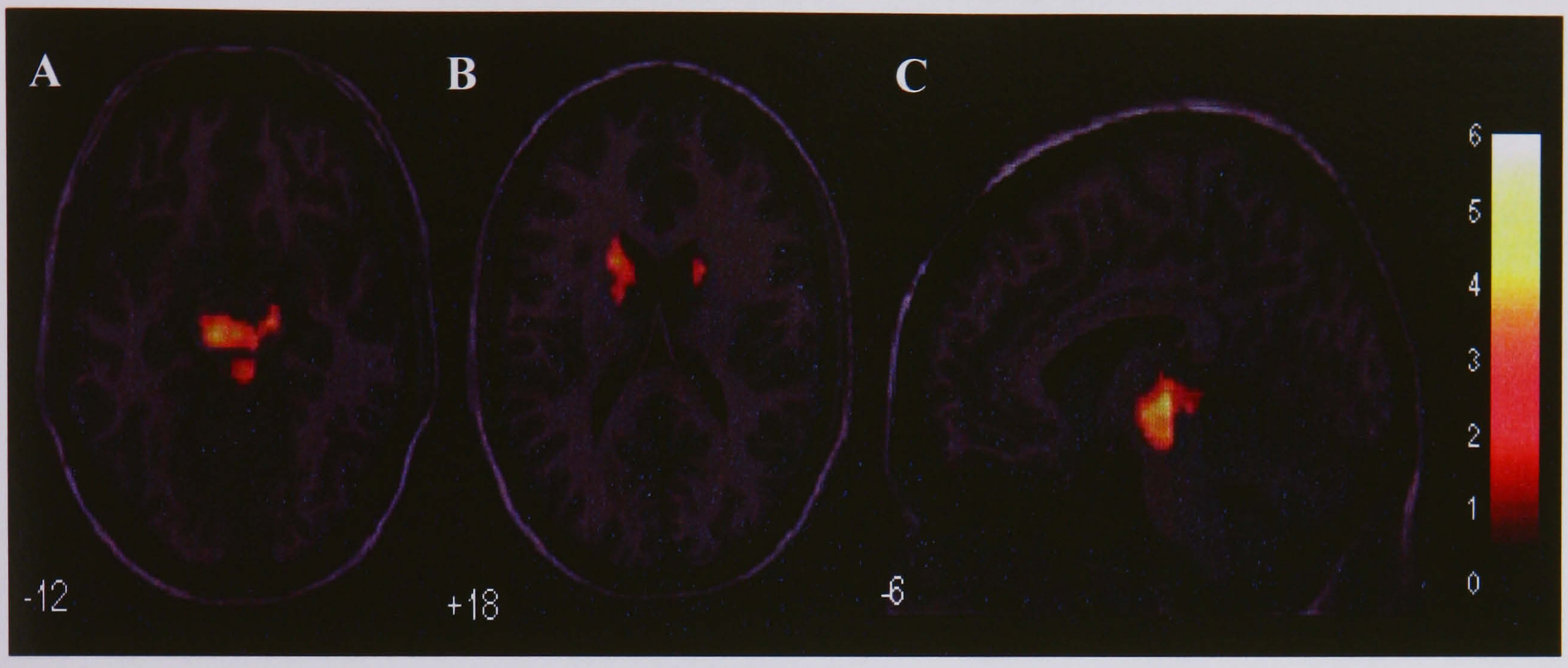


Figure 18. SPM transverse and sagittal maximum intensity projection maps rendered on to a stereotactically normalized MRI scan, showing areas of significant decreases in midbrain (A, axial slice; C, sagittal slice) and caudate (B, axial slice) ^{18}F-dopa K_i uptake in *parkin*-linked parkinsonism compared with *parkin* negative YOPD. Numbers in A and B correspond to the Z co-ordinate, number in C corresponds to X co-ordinate in Talairach space.

Comparing the *parkin* negative YOPD with the IPD group no significant differences were apparent (data not shown). When compared with control subjects, significant reductions of ^{18}F-dopa uptake were localized in the caudate and putamen in all three parkinsonian patient groups, whereas significant decreases in the dorsal and ventral midbrain ^{18}F-dopa uptake were observed only in the *parkin* positive group.

Table 12A. Between-group SPM findings showing the locations of significant decreases and increases of ^{18}F-dopa Ki in *parkin* positive, *parkin* negative YOPD, and control subjects.

^{18}F-dopa $K_i min^{-1}$ Area	Talairach co-ordinates			Z score	P values (corr.)	Height threshold
	x	y	z			
Decreases in *parkin* positive patients compared with *parkin* negative patients						
Left ventral midbrain (SN, NR, RN)	-14	-8	-8	4.03	0.0001	0.01
Right ventral midbrain (SN, NR, RN)	10	-20	-2	3.56	0.0001	
Right dorsal midbrain	8	-36	-15	3.23	0.0001	
Left caudate	-16	0	24	3.73	0.0001	0.05
Right caudate	22	11	20	3.32	0.0001	
Decreases in *parkin* positive patients compared with control subjects						
Left putamen	-30	0	0	∞	0.0001	0.001
Right putamen	30	-2	2	7.34	0.0001	
Right caudate	20	16	8	6.29	0.0001	
Left caudate	-14	16	0	6.05	0.0001	
Right ventral midbrain	6	-20	-11	5.35	0.0001	
Left ventral midbrain	-8	-16	-9	4.91	0.0001	
Dorsal midbrain	0	-31	-15	4.41	0.0001	
Decreases in *parkin* negative patients compared with control subjects						
Left putamen	-30	0	0	∞	0.0001	0.001
Right putamen	28	2	4	7.27	0.0001	
Left caudate	-16	8	9	6.44	0.0001	0.05
Right caudate	16	8	11	5.97	0.0001	

3.2.2.3.4 ^{11}C-raclopride SPM findings

The categorical comparison of striatal ^{11}C-raclopride BP between *parkin* positive and negative YOPD patients reflected the results obtained from the ROI analysis, showing significant relative reduction of ^{11}C-raclopride BP in the caudate and putamen in the *parkin* positive group. Additionally, significant reductions in ^{11}C-raclopride BP were localised in the parietal cortex, temporal cortex and bilaterally in the prefrontal cortex Figure 19, (table 12B). When compared with controls, *parkin* positive patients showed widespread decreases in ^{11}C-raclopride BP over cortical (Brodmann area (BA) 10; 21; 22; 40 (bilateral); 37 (right)), striatal and thalamic (medial dorsal nucleus, bilateral) areas. Significant reductions of ^{11}C-raclopride BP in *parkin* negative YOPD patients versus controls were localized in the left and right caudate and anterior putamen and the thalamus (medial dorsal nucleus, bilateral). No significant differences in ^{11}C-raclopride BP were observed in the group of *parkin* negative YOPD patients when compared with IPD patients.

Table 12B. Between-group SPM findings showing the locations of significant decreases of ^{11}C-raclopride BP in *parkin* positive, *parkin* negative YOPD, and control subjects.

^{11}C-raclopride BP Area	Talairach co-ordinates			Z score	P values (corr.)	Height threshold
	x	y	z			
Decreases in *parkin* positive patients compared with *parkin* negative patients						
Left area 40	-39	-48	45	4.61	0.038	0.01
Left putamen (ant.)	-26	6	9	4.3	0.0001	
Right putamen	29	-5	13	4.13	0.0001	
Right area 37	55	-49	-11	3.98	0.0001	
Right area 21	61	-24	-9	3.73	0.0001	
Left area 22	-50	-53	21	3.75	0.01	
Right area 22	53	-34	16	3.49	0.002	
Right caudate	16	9	20	3.32	0.0001	
Right area 40	57	-27	36	3.28	0.002	
Left caudate	-16	14	12	3.07	0.02	
Right area 10	26	48	20	3.45	0.0001	0.05
Left area 10	-10	58	-8	3.37	0.048	
Decreases in *parkin* positive patients compared with control subjects.						
Right putamen	28	8	3	6.04	0.0001	0.001
Left caudate	-16	19	-3	5.75	0.0001	
Right caudate	-26	12	-1	5.11	0.0001	
Left putamen	12	19	-1	5.64	0.0001	
Left area 40	-40	-50	47	4.86	0.029	
Right area 10	28	51	20	4.61	0.002	
Right area 37	46	-41	-13	4.48	0.0001	
Left thalamus (dm)	-4	-9	12	4.36	0.001	
Right area 40	46	-33	46	4.30	0.006	
Right area 21/22	57	-37	6	3.88	0.046	
Right thalamus (dm)	6	-22	8	3.74	0.0001	
Left area 21	-50	-12	-10	3.62	0.022	
Left area 22	-59	-31	7	3.58	0.025	

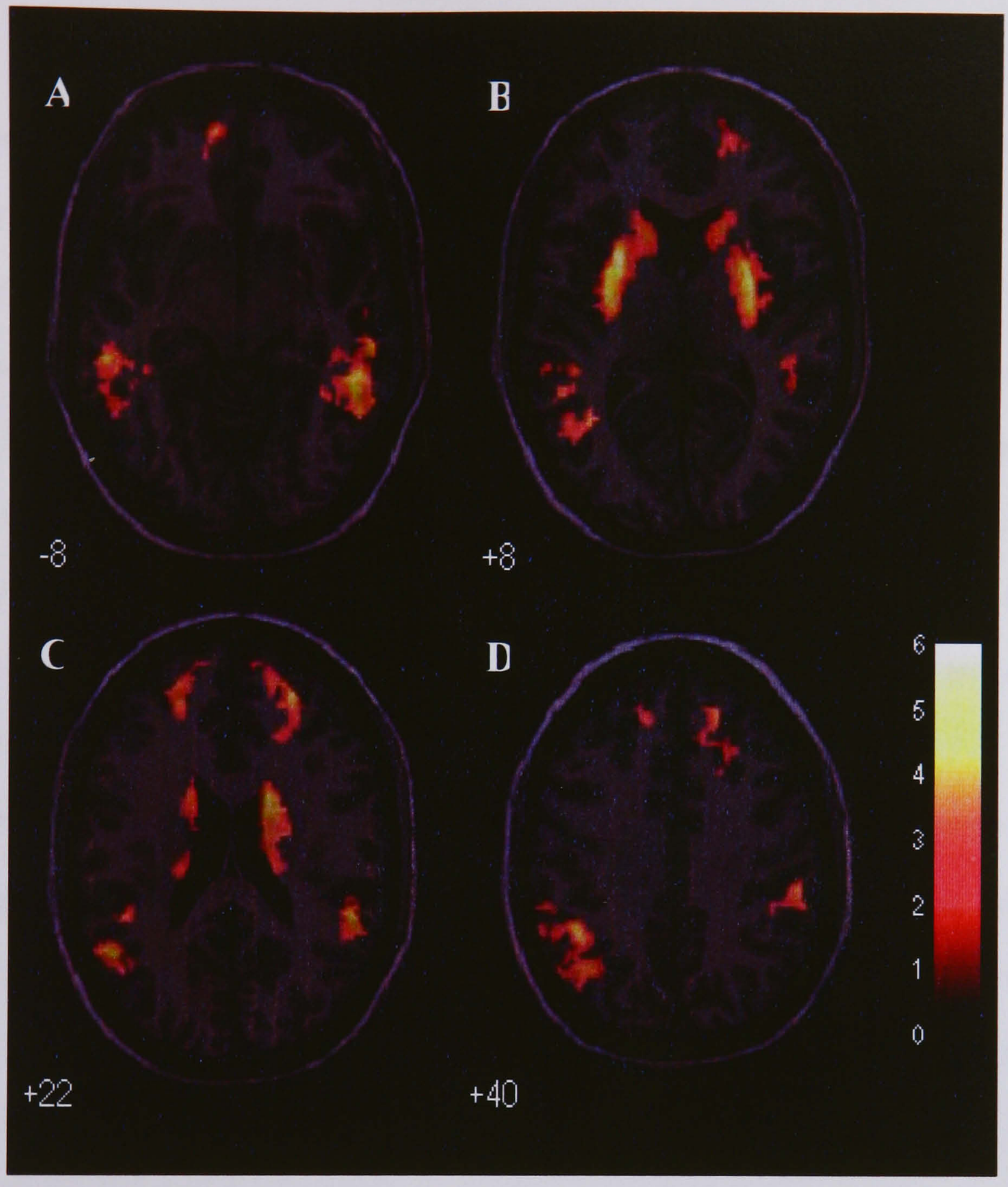


Figure 19. SPM transverse maximum intensity projection maps rendered on to a stereotactically normalized MRI scan, showing areas of significant decreases in temporal (A), striatal and temporal (B), frontal, striatal and parietal (C) and frontal and parietal (D) RAC-BP in parkin-linked parkinsonism compared with parkin negative YOPD.

3.2.2.4 Discussion

This is the first ^{18}F-dopa and ^{11}C-raclopride study to characterize, within the entire brain volume, abnormalities in pre- and post-synaptic dopaminergic function in a group of sporadic patients with *parkin*-linked parkinsonism.

ROI analysis revealed a severe reduction of caudate and putaminal ^{18}F-dopa uptake in *parkin* positive and negative YOPD patients and in IPD when compared to controls. A similar striatal pattern of reduced ^{18}F-dopa uptake in *parkin* positive and negative YOPD patients was evident, both groups showing the typical IPD anterior-posterior gradient with most prominent loss in the posterior part of the putamen. These findings are in line with previously published case reports (Broussolle et al.,2000; Hilker et al., 2001; Portman et al., 2001)

SPM interrogation of ^{18}F-dopa uptake comparing *parkin* positive and negative YOPD patients localised significant symmetrical relative reductions in the caudate and midbrain areas of *parkin* positive patients. A possible explanation for the failure of the ROI approach to detect these caudate decreases in the *parkin* positive cases may be that the ROIs sampled dorsal head of caudate whereas SPM localised relative reductions in the body of the nucleus. Furthermore, ROI analysis is based on sampling brain volumes with *a priori* categorical assumptions as to their size and shape whereas no *a priori* hypothesis regarding the localization of PET signal change is required by SPM.

Monoaminergic neurons in striatal regions are predominantly dopaminergic and so ^{18}F-dopa PET provides a marker of functional integrity of nigrostriatal dopaminergic neurons. However, in midbrain areas serotonergic and noradrenergic neurons also express AADC (Tison et al., 1991)and may take up ^{18}F-dopa . Consequently, reduced

^{18}F-dopa K_i^0 in the dorsal and ventral midbrain of the *parkin* positive group may imply a more widespread dysfunction of catecholaminergic and serotonergic neurotransmitter systems. This would be in line with the recently reported neuropathological findings of loss of pigmented neurons and gliosis in both the substantia nigra pars compacta and locus coeruleus in Parkinson's disease in the absence of Lewy bodies (Hayashi et al., 200). Decreases in midbrain ^{18}F-dopa uptake have, however, also been reported in advanced IPD patients so this finding is not specific to *parkin* cases (Rakshi et al.,1999).

No significant ^{18}F-dopa K_i^0 reductions were found in cortical regions comparing *parkin* positive and negative YOPD patients with normal controls. This finding is surprising given that postmortem data has shown a reduction in frontal dopamine and its metabolites in IPD (Scatton et al., 1982). In agreement with our findings, an ^{18}F-dopa-PET study in advanced IPD by Rakshi et al. using voxel-by-voxel based comparisons also detected no significant reductions in frontal ^{18}F-dopa K_i^0 suggesting that the AADC activity may be maintained in this area (Rakshi et al.,1999).

Both, ROI analysis and SPM detected significant and uniform decreases of ^{11}C-raclopride BP in the caudate and putamen of *parkin* positive patients compared with *parkin* negative cases. This finding in sporadic Parkinson's disease is in line with the study of Hilker et al. who reported decreases in caudate and putaminal ^{11}C-raclopride BP in five members of the same *parkin* kindred (Hilker et al., 2001). Compared to controls, ^{11}C-raclopride BP was significantly reduced in the caudate but not the putamen of *parkin* negative YOPD and IPD patients. These findings are in keeping with other ^{11}C-raclopride PET and neuropathological data indicating that putamen but not caudate dopamine D2 receptor binding remains normal in chronically treated patients with IPD (Guttman et al., 1985; Ahlskog et al., 1991; Brooks et al.,1992;

Griffiths et al., 1994; Antonini et al., 1997). While nigral degeneration of dopaminergic neurons results in an initial 10-20% upregulation of D2 receptor binding in early IPD, adaptive postsynaptic mechanisms and treatment exposure normalises this as the condition advances (Ahlskog et al., 1991; Brooks et al.,1992; Antonini et al., 1997). The presence of an adaptive mechanism is supported by animal studies: ^{11}C-raclopride BP was normal in four parkinsonian rhesus monkeys that had been treated with MPTP 6-7 years before PET and never received antiparkinsonian treatment (Doudet et al., 2000). As initial putamen D2 receptor upregulation normalises in chronically medicated patients with IPD, the reduced D2 availability found in *parkin*-linked Parkinsonism suggests that the genetic defect itself may be responsible rather than loss of dopamine projections or exposure to medication. Alternatively, the reduced D2 binding could reflect a greater susceptibility to dopaminergic medication. Longitudinal studies on striatal D2 site density in cohorts of untreated and treated parkin patients are required to clarify this issue.

Cortical D2 receptor binding. Autoradiography and PET studies with a dopamine D2/D3 receptor ligand ^{11}C-FLB 457 have shown that extrastriatal D2 density is highest in the thalamus, lower in prefrontal, temporal and parietal cortex, and lowest in the occipital cortex (Lidow et al., 1989; Kessler et al., 1993; Hall et al., 1996). Although the D2/D3 receptor affinity for ^{11}C-FLB is 100 times higher than it is for RAC (Halldin et al., 1995), recent improvement of PET-scanner sensitivity and use of SPM have revealed significant reductions in ^{11}C-raclopride BP in prefrontal, temporal, parietal and thalamic areas when patients receive D2-receptor antagonist neuroleptics (unpublished data). The location of the extrastriatal loss of D2 function in *parkin* linked parkinsonism with SPM is consistent with the distribution of D2 receptor

reported in post mortem studies of the human brain (Kessler et al., 1993; Hall et al., 1996; Joyce et al., 1998).

In the present study significant reductions in extrastriatal ^{11}C-raclopride BP were observed in thalamic, temporal, parietal and prefrontal brain areas of parkin patients when compared to controls and patients with *parkin* negative YOPD. ^{11}C-raclopride BP was also significantly decreased in thalamic, temporal, parietal and frontal brain areas of patients with YOPD versus control subjects. The latter finding is in line with a recently published study investigating FLB distribution in medicated patients with IPD (Kaasinen et al., 2000). To date, there are no studies correlating cortical D2 receptor status and clinical symptoms. It has been reported that patients with *parkin* mutations have an increased prevalence of behavioural and neuropsychiatric disorders in comparison to patients with IPD (Khan et al., 2003). A retrospective analysis of the clinical notes revealed a high incidence of symptoms such as depression (two patients), panic attacks (three patients) and paranoia (one patient) in our patients with *parkin*-linked parkinsonism. These behavioural disorders might be partially associated with the disruption of dopaminergic pathways interconnecting the prefrontal cortex and ventral striatum (Ribeyre et al., 1994; Farde et al., 1997; Joyce et al., 1997).

Conclusions. In contrast to equivalently disabled YOPD and IPD patients, *parkin*-linked Parkinsonism is associated with more widespread and severe disruption of striatal dopaminergic and midbrain catecholaminergic and serotoninergic pathways. Reductions of post-synaptic D2 receptors in *parkin*-linked Parkinsonism have been localised in striatal, thalamic and cortical areas. This may be a direct consequence of the genetic defect. However, as *parkin* patients generally exhibit an enhanced response to antiparkinsonian medication even after many years of disease, the uniform decrease

in D2 binding could equally be the result of a higher susceptibility to dopaminergic treatment.

Measuring striatal and cortical dopamine release in normals and Parkinson's disease patients.

4

4.1 Subjects

We studied six patients with advanced idiopathic Parkinson's disease (5 males and 1 female; age 65 ± 7.6 years) and six age-matched healthy male right-handed subjects (all males; age 57 ± 12 years, p= 0.14). Participants were not included if they had known current or past psychiatric or neurological disease, head trauma, diabetes or medical conditions that may alter cerebral functioning or a past or present history of alcohol or substance abuse.

PD patients clinical characteristics are shown in table 13. They were all taking levodopa/AADI (725 ± 150 mg/day) and COMT inhibitors (640 ± 120mg/day) preparations. Three of them were on levodopa/AADI and COMT inhibitors

preparations alone. Of the other three patients two were on ropinirole and a third on pergolide, in these three cases the dopamine agonists were stopped at least 2 weeks before PET studies.

Patients were PET scanned in an "off" state after overnight withdrawal of levodopa/AADI/COMTI medication. Written consent was obtained from all subjects after the nature and possible risks of the study were fully explained. Ethical permission for PET studies was obtained from the Hammersmith Hospitals Trust Ethics Committee. Approval to administer radiolabel ligands was obtained from the Administration of Radioactive Substances Advisory Committee (ARSAC) of the United Kingdom.

Table 13. Clinical characteristics of the Parkinson's disease patients.

Patient #	Sex	Age (yrs)	Disease Duration (yrs)	UPDRS Total motor score Off (max=108)	UPDRS Best side	UPDRS Worst side
1	M	76	15	98	32	36
2	M	58	9.5	64	20	23
3	M	61	7	70	24	27
4	M	73	17	86	22	31
5	M	63	8	60	8	34
6	F	59	9	91	18	35
Mean (±SD)		65.0 (7.6)	10.9 (4.1)	78.2 (15.6)	20.6 (7.8)	31.0 (5.1)

4.2 Specific methods

SPM voxel-by-voxel analysis. For the purpose of the statistical analysis, the ^{11}C-raclopride parametric images of those PD patients whose right limbs were clinically most affected were flipped so that the major putamen loss of DA function appeared in the left hemisphere in all cases. The parametric images were then spatially transformed to co-register with a normal ^{11}C-raclopride template in MNI space (Meyer et al., 1999). Images were spatially smoothed using a 6 x 6 x 6 mm (full width at half maximum) isotropic Gaussian kernel. Signficant changes were sought with the threshold set at $p<0.001$. For all the comparisons only those regional brain differences that survived correction for cluster size ($p < 0.05$) were considered. Within group categorical comparisons of mean ^{11}C-raclopride BP values obtained from the six saline scans and the six methamphetamine scans were performed for both the groups of normal subjects and PD patients. Then, a between-group comparison examined differences in mean ^{11}C-raclopride BP after methamphetamine between these two groups of subjects. Significant changes of BP were localised with SPM and displayed as Z scores. No global BP normalization was applied.

^{18}F-dopa. PET scans were performed as described in the methods section (2.3.3) and analysed using a standard region of interest (ROI) approach and multiple time graphical analysis with an occipital reference tissue input function (see chapter 2.3.4). ^{18}F-dopa normal values were obtained by selecting from our database a group of 16 healthy subjects matched for age and sex with the group of PD patients and scanned with the same scanner and scan protocol as the PD patients.

4.3 Results

4.3.1. Region of interest analysis.

All six normal volunteers individually showed reductions in caudate and putamen ^{11}C-raclopride BP after methamphetamine in comparison to saline (figure 20A). The mean percent reductions in BP after methamphetamine are shown in table 14.

In the normal group the mean BP reduction induced by methamphetamine in putamen (25.2%) was significantly greater then that in caudate (17.2%) ($p= 0.01$, unpaired parametric test). Figure 21 shows ^{11}C-raclopride BP parametric images after saline and methamphetamine administration for one of the normal subjects.

The six PD patients also showed individual reductions in both caudate and putamen ^{11}C-raclopride BP after methamphetamine (figure 20 B). Mean percentage reductions are shown in table 14. For the PD group the mean putamen BP reduction (6.8%) induced by methamphetamine was similar to that seen for caudate (7.9%) ($p= 0.48$, unpaired parametric test). Figure 23 shows images of ^{18}F-dopa uptake and ^{11}C-raclopride BP after saline and methamphetamine administration for one of the PD patients. The decreases in striatal ^{11}C-raclopride BP following methamphetamine administration were significantly lower for the PD patients than those observed for the normal volunteers ($p= 0.0001$ and $p= 0.00035$, caudate and putamen respectively).

Table 14. Mean caudate and putamen ^{11}C-raclopride BP (± SD) for the normal subjects and for the Parkinson' s disease (PD) patients after saline and after methamphetamine i.v. infusion.

	Normal volunteers (No=6)				PD patients (No=6)			
	caudate		putamen		caudate		putamen	
	R	L	R	L	R	L	R	L
Saline (±SD)	2.99 (0.21)	2.91 (0.25)	3.12 (0.21)	3.15 (0.22)	2.99 (0.22)	3.08 (0.26)	3.27 (0.23)	3.01 (0.28)
Methamphetamine (±SD)	2.45 * (0.17)	2.43 * (0.24)	2.35 * (0.16)	2.34 * (0.17)	2.77 * (0.22)	2.84 * (0.25)	3.00 * (0.25)	2.83 * (0.29)
Δ % (±SD)	-18.2% (3.81)	-16.3% (4.39)	-24.7% (1.54)	-25.6% (1.13)	-7.53% (1.60)	-7.94% (1.7)	-8.14% (3.02)	-5.83% (2.90)
	-17.24%		-25.20%		-7.90%		-6.84%	

R=right, L=left.

Δ % = changes in BP, given in percentage from values after saline.

*p<0.001 (Comparisons of ^{11}C-raclopride BP after saline versus after methamphetamine within the groups of Normals and PD patients; Two-way ANOVA with repeated measures).

Mean ^{18}F-dopa Ki 's for the PD group was 0.0067 min^{-1} (± 0.0023) and 0.0062 min^{-1} (± 0.0025) for right and left caudate, respectively, and 0.0048 min^{-1} (± 0.0021) and 0.0038 min^{-1} (± 0.0022) for right and left putamen. These values represent reductions of 56% and 59% (right and left caudate respectively) and 71.4% and 77% (right and left putamen respectively) from mean ^{18}F-dopa values of the normal subjects.

Normal volunteers

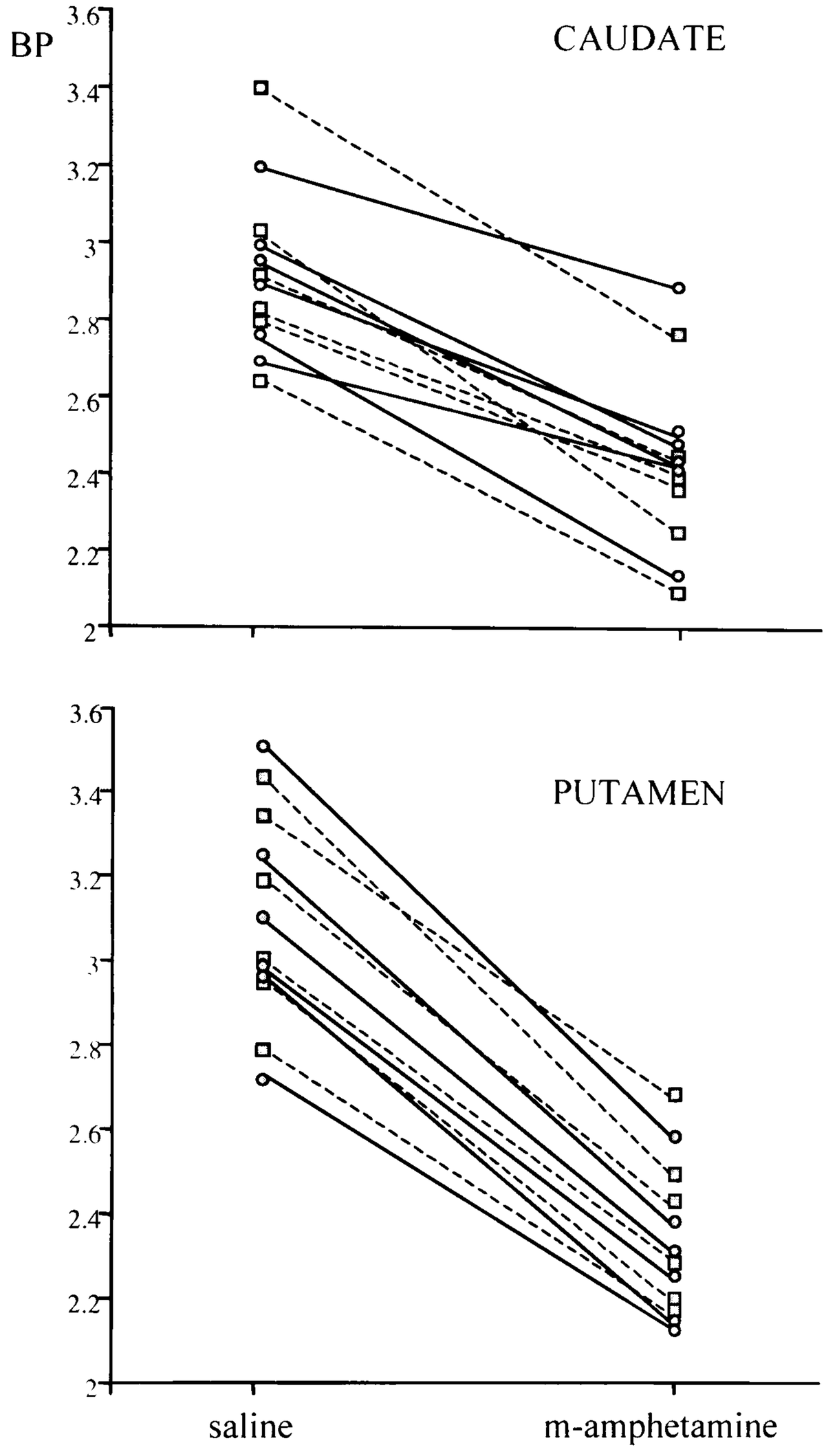


Figure 20 A. Individual caudate and putamen ^{11}C-raclopride binding potentials (BP) after injection of saline and after injection of m-amphetamine in the 6 normal volunteers. Squares indicate left side and circles right side.

PD patients

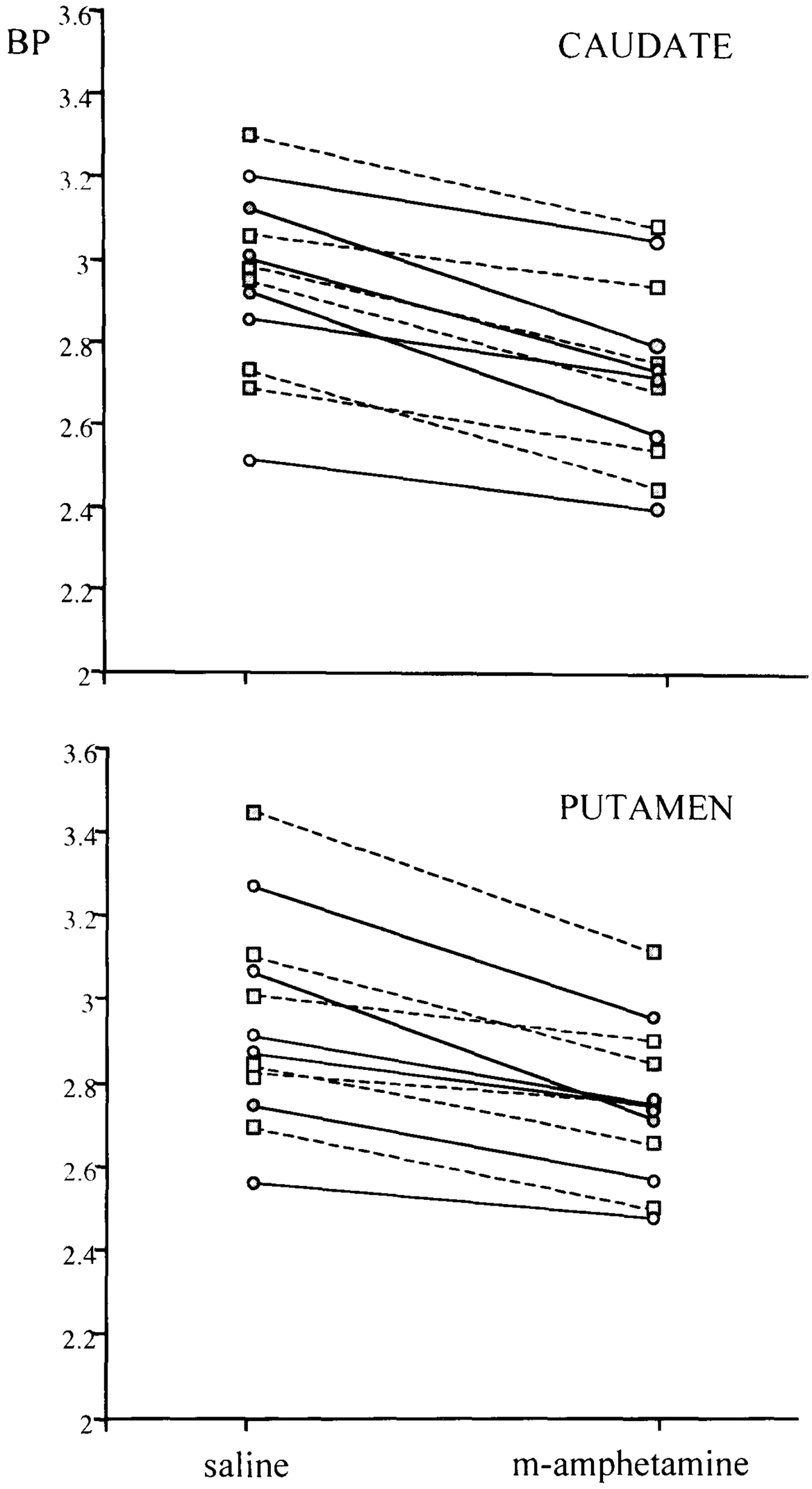


Figure 20 B. Individual caudate and putamen ^{11}C-raclopride binding potentials (BP) after injection of saline and after injection of m-amphetamine in the 6 patients with PD. Squares indicate left side and circles right side.

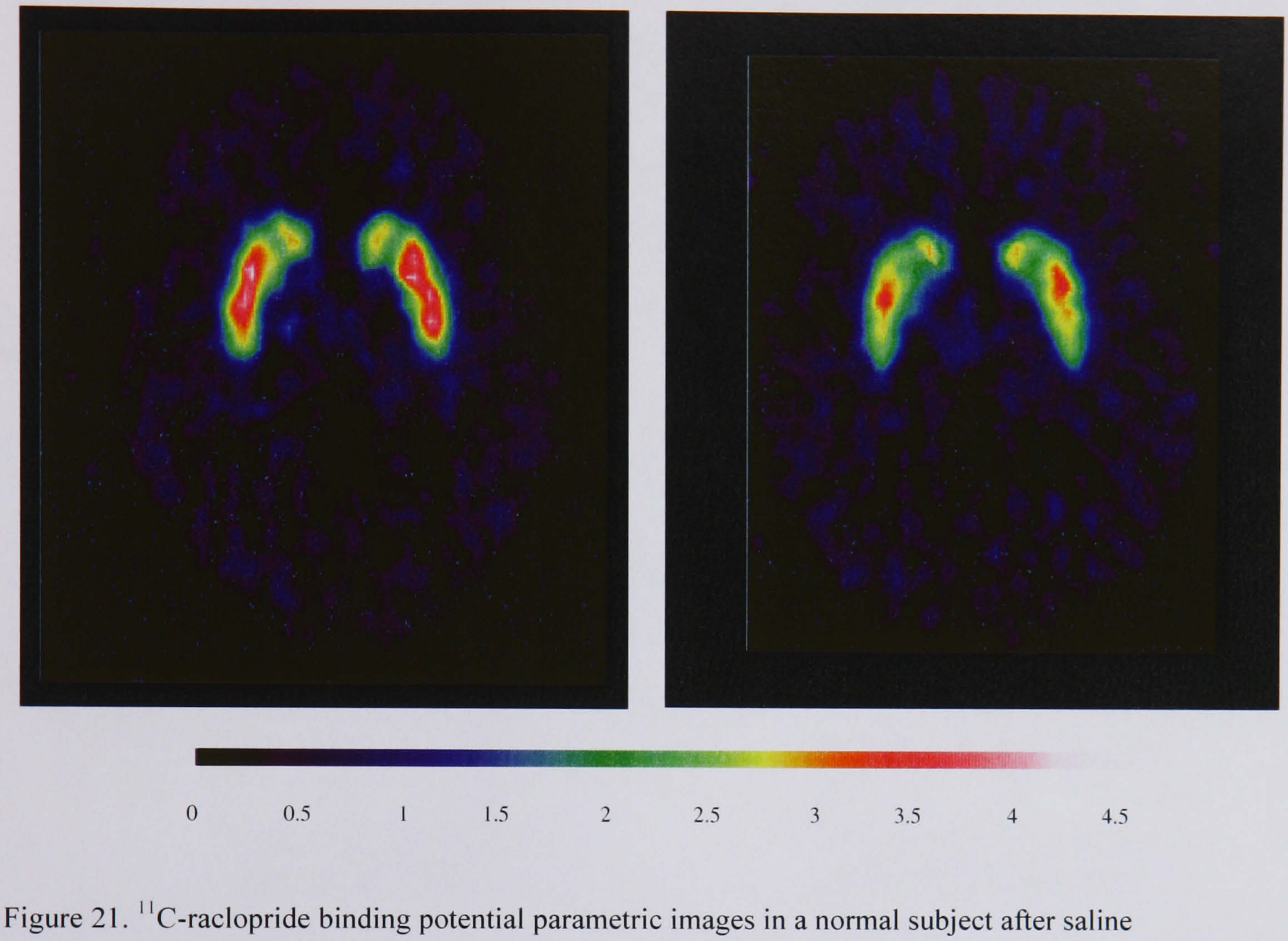


Figure 21. ^{11}C-raclopride binding potential parametric images in a normal subject after saline and after 0.3 mg/kg methamphetamine

The PD patients showed a significant positive correlation between left and right putamen ^{18}F-dopa uptake values and percentage reductions in left and right putamen ^{11}C-raclopride BP after methamphetamine [Correlation coefficient (r) = 0.86, r^2= 0.74, p = 0.02 and correlation coefficient (r) = 0.83, r^2= 0.69, p = 0.03; left and right side respectively] (figure 22). This correlation was not significant for caudate values (p= 0.45) (data not shown). We also observed a marginally significant correlation between "off" UPDRS motor score in the lesser and more affected sides and decreases in the respective contralateral putamen ^{11}C-raclopride BP values after methamphetamine

[Correlation coefficient (r) = 0.81, r^2= 0.66, p = 0.04 and correlation coefficient (r) = 0.79, r^2= 0.63, p = 0.05; best and worst side respectively] (data not shown).

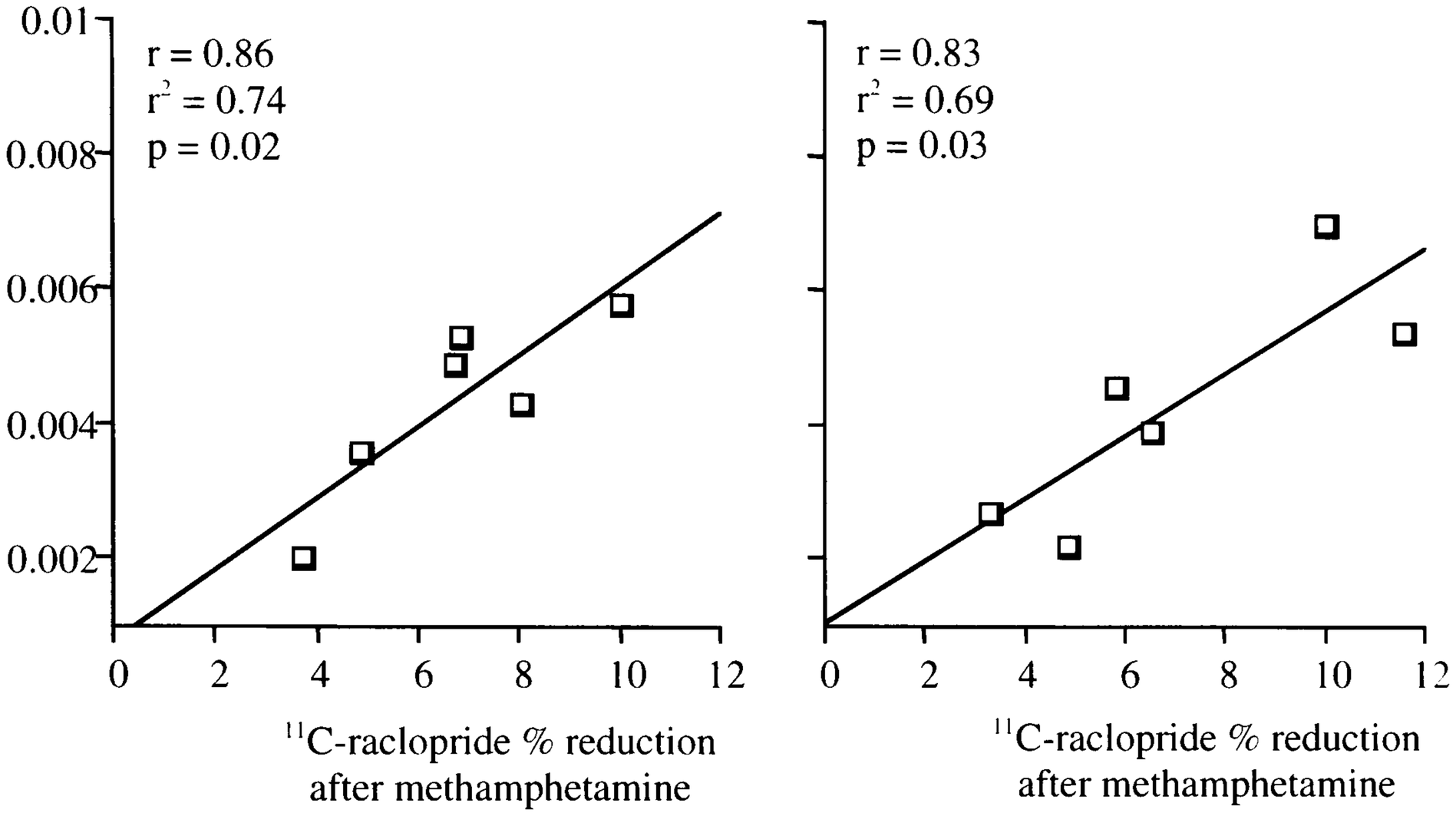


Figure -22

Correlation between left and right putamen ^{18}F-dopa uptake (Ki) and % reduction in left and right putamen ^{11}C-raclopride binding potentials (BP) after methamphetamine in individual patients with Parkinson's disease.

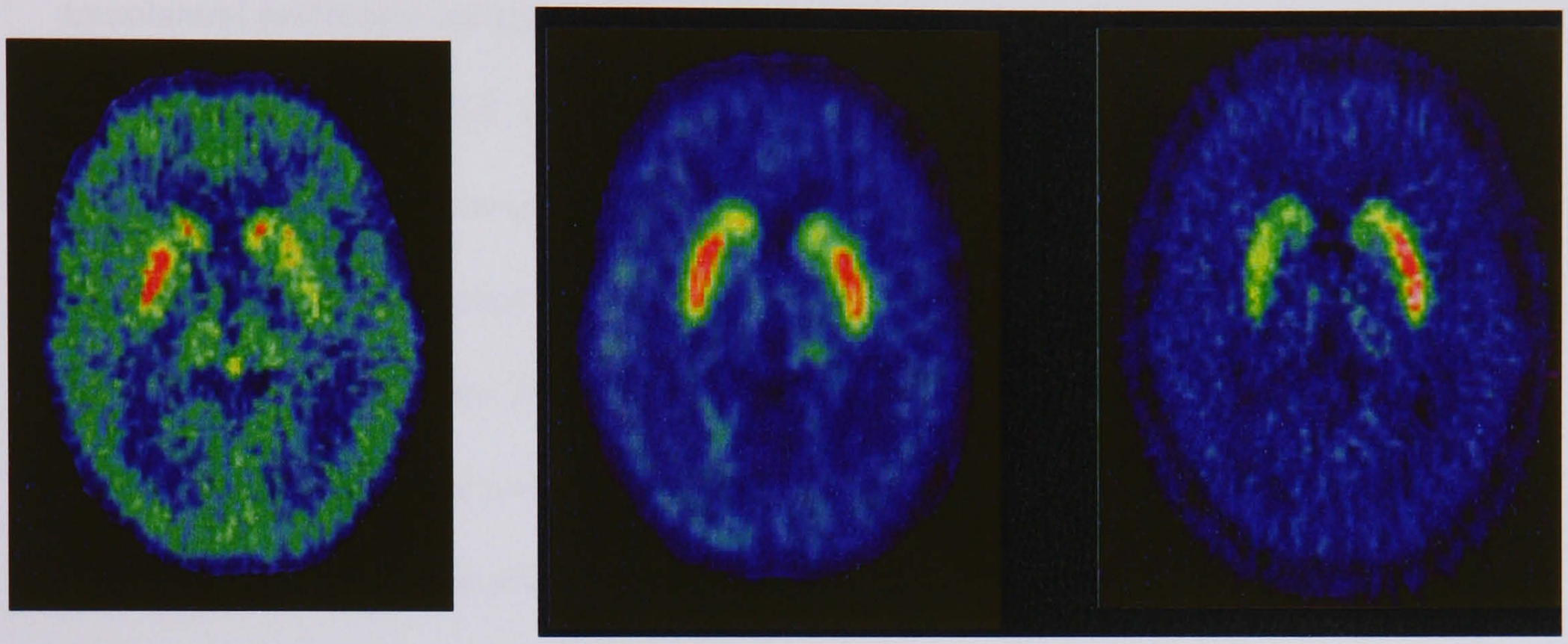


Figure 23 Images of ^{18}F-dopa uptake and ^{11}C-raclopride Binding Potential (BP) following administration of saline and following administration of 0.3 mg/kg methamphetamine in a PD patient. Note the asymmetry in ^{18}F-dopa uptake (higher on the right side) which is reflected in the asymmetric reduction in ^{11}C-raclopride BP following methamphetamine.(more release of endogenous dopamine and greater reduction in ^{11}C-raclopride BP on the right side)

4.3.2 Statistical parametric mapping.

Compared with saline, methamphetamine induced a significant decrease in ^{11}C-raclopride BP in striatal areas bilaterally and also in cortical areas (anterior cingulate, dorsolateral prefrontal cortex, dorso-frontopolar cortex, and orbito-frontal cortex) in normal subjects (table 15A, figure 24A). After methamphetamine the group of advanced PD patients showed significant reductions in ^{11}C-raclopride BP in the less affected caudate and anterior putamen and in the same prefrontal areas as the normal subjects (table 15A, figure 24A).

A between-group comparison between normals and PD showed significantly differences in DA release after methamphetamine in striatal areas but not in frontal regions (table 15B, figure 24B). Even at more lenient statistical thresholds significant differences in frontal DA release were not evident between the two groups of subjects.

Table 15. SPM co-ordinates

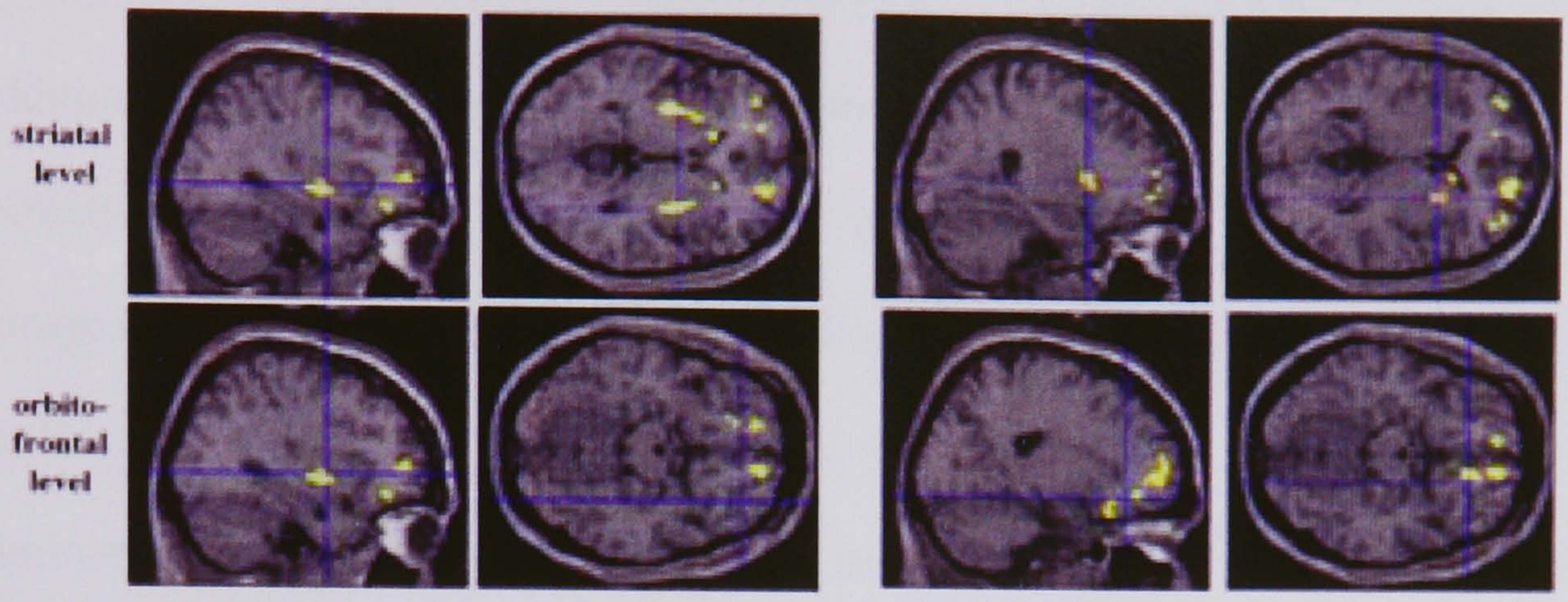
A. Within group comparison

Area	Co-ordinates MNI space			Co-ordinates Tailarach & Tournoux space*			*Z* *score*
	x	y	z	x	y	z	
Normal volunteers							
R putamen	28	-4	-2	27	-4	-2	4.45
L putamen	-26	2	-2	25	1.8	-2	4.38
R caudate	16	6	1	16	5.8	1	4.13
L caudate	-6	18	-6	-5.9	17	-5.9	4.21
Anterior cingulate gyrus (32)	-2	32	24	-1.9	24.7	28.2	3.99
Dorso-lateral prefrontal cortex (9)	-45	20	36	-44.5	21	32	3.48
Dorso-frontopolar cortex (10)	38	38	2	38	38	0	3.13
Orbito-frontal cortex (11)	-14	46	-14	-13.8	43	-13.8	3.59
PD patients							
R putamen	20	0	0	19	1.8	0	3.27
R caudate	18	6	1	17	5.8	1	3.18
Anterior cingulate gyrus (32)	-2	28	30	1.98	30.3	24.8	3.85
Dorso-lateral prefrontal cortex (9)	40	18	36	39.9	19	32	3.35
Dorso-frontopolar cortex (10)	-40	46	6	-39.6	45	3.8	3.48
Orbito-frontal cortex (11)	10	36	-12	9.9	35	11.8	3.73
B. Between group comparison							
R putamen	25	0	4	24	0	-4	3.24
L putamen	-20	0	-2	-19	1.8	-2	3.27
R caudate	12	14	-4	11.8	14.7	-3.4	3.12
L caudate	-6	16	-4	-5.9	15.3	-3.4	3.13

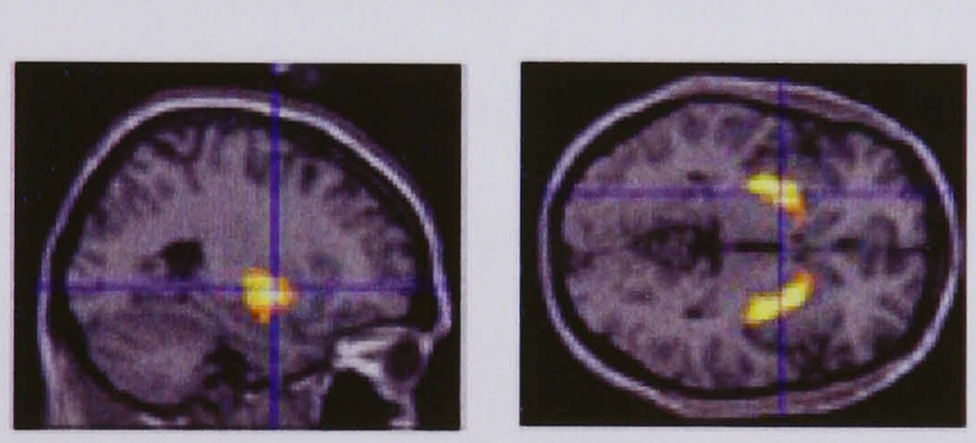
(A). Within group comparison: Co-ordinates for the areas of significant decrease in ^{11}C-raclopride binding potential after methamphetamine as compared to saline in 6 normal volunteers and in 6 patients with Parkinson's disease. **(B)**. Between group comparison: Co-

ordinates for the areas of significant differences in ^{11}C-raclopride binding potential after methamphetamine between the groups of normal subjects and of patients with Parkinson's disease. Converted from MNI (Montreal Neurological Institute) co-ordinates into Tailarach & Tournoux co-ordinates (www.mrccbu.cam.ac.uk/Imaging).

A



B



Normal volunteers vs PD patients

Figure 24

Sagittal and transaxial projections of statistical parametric maps.

A. Within group comparisons: Areas of significant decreases in ^{11}C-raclopride binding potential after methamphetamine as compared to after saline in 6 normal volunteers and in 6 patients with Parkinson's disease. B. Between group comparisons: Areas of significant differences in ^{11}C-raclopride binding potential after methamphetamine between the groups of normal subjects and patients with Parkinson's disease. The areas are superimposed on a standard MRI template.

4.4 Discussion

The findings of this study indicate that significant endogenous striatal DA release, can still be induced by a pharmacological challenge in advanced stages of PD. Additionally, we have shown that the endogenous DA release in putamen is directly correlated with putaminal DA storage capacity as measured by ^{18}F-dopa, although the storage capacity in PD patients was reduced by more than 70% from the normal values. Studies with microdialysis in non-human primates have shown that amphetamine administration induces a marked increase in extracellular DA levels in the striatum, which lasts for at least 150 minutes and is dose-dependent (Brier et al., 1997; Tsukada et al., 1999). Following an i.v. dose of 0.3 mg/kg of amphetamine a 13.5 fold peak increase over baseline DA was achieved. Concomitant ^{11}C-raclopride PET suggested that a 2% reduction in ^{11}C-raclopride BP reflects around 100% increase in extracellular DA levels (Brier et al., 1997; Tsukada et al., 1999). Consequently, the 25% reduction in striatal ^{11}C-raclopride BP following 0.3 mg/kg methamphetamine observed with our normal subjects is likely to reflect a 12.5 fold peak increase in DA, similar to the changes observed in non-human primates after equivalent amphetamine exposure. In the PD patients reductions in striatal ^{11}C-raclopride BP following methamphetamine ranged from 4% to 12% and probably reflect 2 to 6 fold peak increases in extracellular DA levels, although direct extrapolation from normal subjects need to be cautious as changes in D2 receptor affinity in PD patients cannot be completely excluded.

Our group of normal volunteers showed release of endogenous dopamine after methamphetamine greater in putamen than caudate. This differential release was reversed with the PD patients, reductions in binding after methamphetamine being slightly higher in the caudate indicating a greater release of DA in this structure than in

putamen. Correspondingly, in PD patients ^{18}F-dopa uptake was significantly higher in caudate than in putamen. A relative sparing of DA levels in caudate compared with putamen in PD is well documented: the less pigmented ventrolateral substantia nigra cells are most susceptible to degeneration in PD and these cells project mainly to the posterior dorsal putamen, while the less affected rostral and medial cells of the subtantia nigra project to the anterior dorsal putamen and dorsal head of caudate[23, 24]; the relative greater storage and greater release of dopamine in caudate than putamen observed in our patients confirms *in vivo* these pathological observations.

In the PD patients, side-to -side differences in methamphetamine-induced ^{11}C-raclopride BP putamen reductions also correlated with the disability withdrawn from medication rated with the UPDRS, the lowest release of DA occurring from the putamen contralateral to the more clinically affected limbs. A significant inverse correlation between ^{18}F-dopa uptake and UPDRS has been shown in PD patients in several studies [25-27]. Our findings of a correlation between both these parameters and the release of dopamine from putamen provide further evidence that ^{18}F-dopa uptake is a reliable measure of dopaminergic pre-synaptic function not only as a marker of dopamine storage but also as an indirect indicator of the residual capacity of releasing dopamine.

Interestingly, exogenous levodopa administration results in a different pattern of striatal ^{11}C-raclopride BP reductions in PD, the most pronounced fall being observed in putamen rather than in caudate and contralateral to the side of most severe clinical involvement (Bernheimer et al., 1973; Kish et al., 1988). Taken together these observations indicate that in PD patients the most denervated striatal regions that release least endogenous DA are also least able to take up and store extracellular synaptic DA generated from exogenous levodopa treatment.

In this study, statistical parametric mapping also revealed methamphetamine -induced DA release in prefrontal and anterior cingulate areas in both normal subjects and PD patients. Microdialysis studies in human primates have already shown that amphetamine exposure increases extracellular levels of DA in many cerebral areas. The magnitude of these increases is less profound in cortical regions compared to putamen, as dopamine innervation is less dense, but medial frontal and dorsolateral prefrontal cortex levels of DA have been reported to increase 5 fold over baseline (Moghaddam et al.,1993).

The between-group categorical comparison of methamphetamine -induced reductions in ^{11}C-raclopride BP for the normal and parkinsonian subjects applying statistical parametric mapping at a voxel level showed highly significant differences in levels of DA release in striatal regions but no differences in cortical regions. This finding indicates that even advanced PD patients are in principle able to release normal levels of DA in frontal areas though this may only be the case in the face of extreme challenges such as amphetamine exposure. Our observations are in accordance with post-mortem studies that have reported only mild depletion of DA in the prefrontal cortex in PD (Scatton et al., 1982; Scatton et al., 1983. Studies *in vivo* with ^{18}F-dopa PET have also shown either a small decline (Rinne et al., 2000) or no changes in prefrontal tracer uptake in advanced PD patients in comparison to controls (Rakshi et al., 1999).

Prefrontal deficits of executive functions, such as planning and spatial working memory, have been reported in PD (Morris et al., 1988; Owen et al., 1993; Robbins et al., 1994) even early in the disease process (Owen et al., 1995). However, it is not clear whether these functional deficits reflect cortical and/or striatal pathological changes

given that these areas are interconnected. In an elegant PET activation study (Owen et al., 1998) levels of regional cerebral blood flow (rCBF) were measured in normal subjects and in PD patients while they solved easy and difficult Tower of London planning problems and also performed a visual memory task. Normal subjects increased while PD patients decreased levels of rCBF in the internal globus pallidus during these tasks, whereas in other cortical areas, including dorsolateral prefrontal cortex differential task-specific rCBF modifications were not found. The authors concluded that frontal cognitive deficits in PD are the result, not of intrinsic prefrontal dysfunction *per se*, but rather of abnormal processing of the prefrontal input through malfunctioning basal ganglia circuitry.

The finding of a normal release of endogenous DA from prefrontal regions after a pharmacological challenge in our PD patients suggests that presynaptic DA terminals in these areas are able to compensate for the disease process.

In conclusion, in this study I have reported that endogenous DA release can be induced *in vivo* by a pharmacological challenge in normals and in PD patients with advanced stages of disease. Striatal levels of DA release, as reflected by methamphetamine-induced reductions in ^{11}C-raclopride binding, are directly proportional to levels of DA storage capacity, as reflected by uptake of ^{18}F-dopa, and levels of disability when patients are withdrawn from medication. I have also showed for the first time that even in advanced PD patients methamphetamine -induced DA release in prefrontal regions does not differ from that of normal subjects indicating that presynaptic DA terminals in these areas are able to compensate for the disease.

PET studies on the efficacy of cell transplantation therapy in Parkinson's disease

5

5.1 Demonstrating dopamine release from striatal implants in a Parkinson's disease patient.

5.1.1 The subject

The patient was 69-years-old with typical PD which started as rigidity and tremor in the left arm in 1980. L-dopa treatment was successful until 1986 when he developed severe "on-off" motor fluctuations. In 1989, he was grafted with human embryonic mesencephalic tissue in the right putamen (Lindvall et al., 1992; Lindvall et al., 1994). During the first three postoperative years, the patient showed gradual, major clinical improvement. Rigidity and hypokinesia were reduced bilaterally but most markedly contralaterally to the graft. "On-off" fluctuations disappeared and L-dopa could be withdrawn after 32 months (figure 25). Immunosuppressive treatment was stopped at 64 months (Lindvall et al., 1994). Low-dose L-dopa (1/3 of preoperative

dose) was reintroduced at 74 months due to progression of symptoms axially and in the limbs ipsilateral to the graft. He responded well to this medication, and motor function and L-dopa dose have been unchanged thereafter. At the time of the present study, 10 years after transplantation, he exhibits continuous marked benefit with virtually no rigidity, minor hypokinesia, intermittent, mild resting tremor and no "on-off" fluctuations.

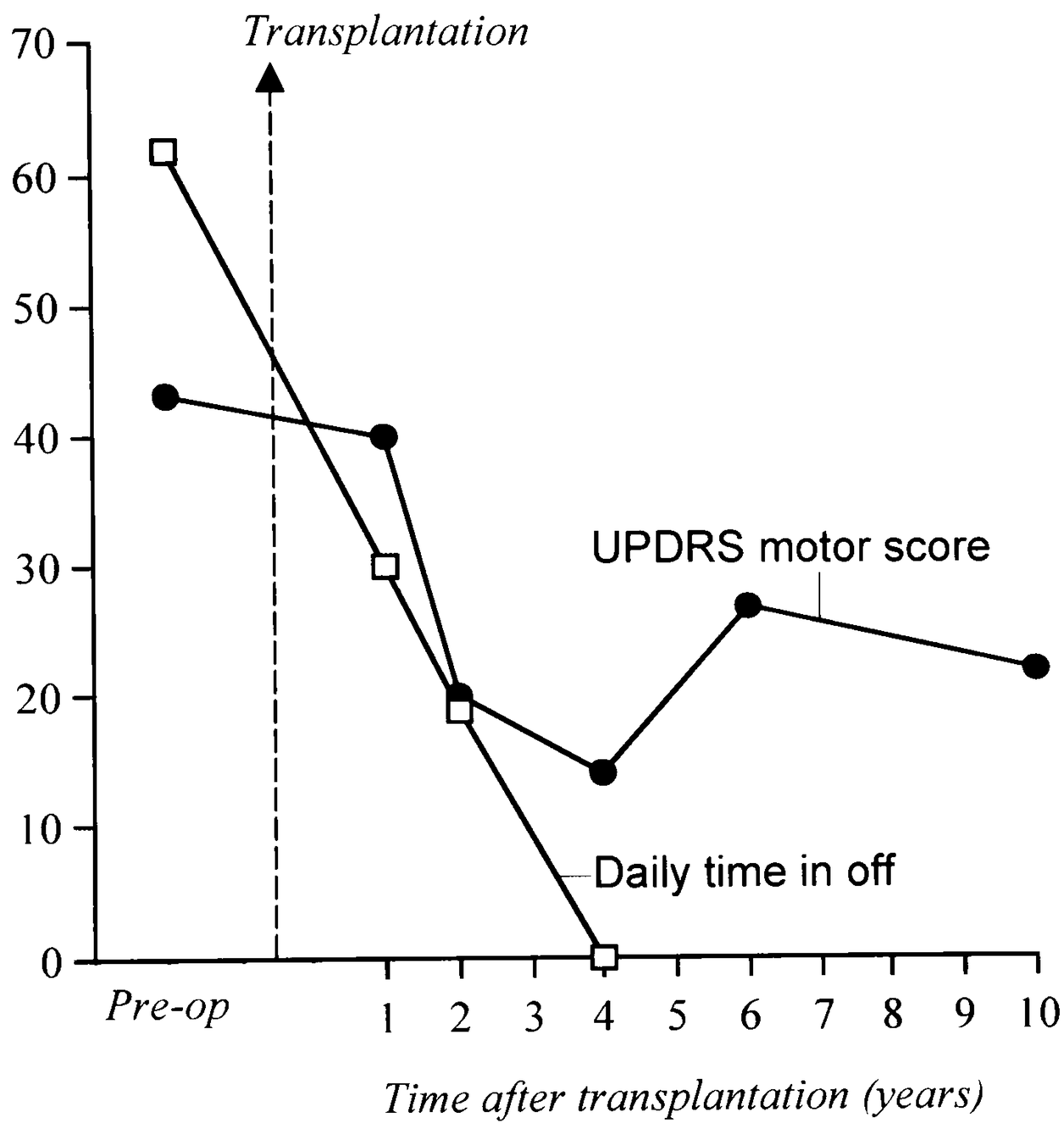


Figure 25. Percentage of the day spent in "off" (open squares) and UPDRS motor score (filled circles) in the practically defined "off" phase.

5.1.2 Specific Methods

Ethical permission was obtained from the Hammersmith Hospital Trusts Research Ethics Committee and the Research Ethical Committee of the Medical

Faculty at the University of Lund, Sweden. Approval to administer radiolabel ligands was obtained from the Administration of Radioactive Substances Advisory Committee of the United Kingdom. Written consent was obtained after full explanation of the procedure.

5.1.2.1 Transplantation procedure .

Details have been given elsewhere (Rehncrona, 1997; Brundin et al., 2000). Briefly, dissociated ventral mesencephalic tissue was implanted stereotaxically in the anterior, middle and posterior part of the right putamen (contralateral to the most affected limbs). Implantation was performed along three trajectories, 8, 12, and 12 mm long. The tissue was procured from 4 human embryos (aged 6 to 7 weeks postconception) obtained at routine suction abortions, with informed consent from the women and approval by the Research Ethical Committee of the Medical Faculty at the University of Lund, Sweden. The patient was given immunosuppressive treatment with cyclosporin, prednisolone and azathioprine

5.1.2.2 Clinical evaluation.

Motor fluctuations ("on-off" phenomena) were recorded continuously by the patient who scored his symptoms every 30 min. Clinical assessments were performed in the morning after a drug-free period overnight ("practically defined off"). The test battery included UPDRS motor examination score, timed motor tasks and a single-dose L-dopa test (Langston et al., 1992). Clinical evaluations were carried out on six occasions during the year before surgery, monthly during the first postoperative year, and 4 to 5 times annually thereafter.

5.1.2.3 Scanning procedure.

^{18}F-dopa PET scans were performed on a CTI 953 (CTI, Knoxville, TN) camera after intravenous injection of 166.5-185 MBq of ^{18}F-dopa.Analysis of ^{18}F-dopa scans has been described in another chapter of this thesis (2.3.4). The subject had two ^{11}C-raclopride scans and was given an intravenous dose of saline in one scan and methamphetamine (0.3 mg/kg) in the other scan. The ^{11}C-raclopride scanning procedure and analysis for normal volunteers and the PD patient has been described in other chapters (Methods section, 2.5).

5.1.3 Results

The regional ^{18}F-dopa influx constant values in the grafted putamen increased over 3 years post-surgery by which time ^{18}F-dopa uptake had reached normal levels. There were only minor additional changes at 6 and 10 years after transplantation (table 16, figure 26). In contrast, ^{18}F-dopa uptake values in the caudate nuclei on both sides and in the non-grafted putamen (table 16) decreased gradually compared with the normal values.

Table 16. ^{18}F-dopa uptake in a PD patient before and after unilateral transplantation of fetal mesencephalic cells in the right putamen.

	^{18}F-dopa K_i (min $^{-1}$)				
ROI	1988 (pre-implant)	1990	1992	1995	1999
R Caudate	0.0059	0.0055	0.0052	0.0046	0.0039
L Caudate	0.0067	0.0053	0.0058	0.0050	0.0037
R Putamen (grafted side)	0.0030	0.0063	0.0105	0.0109	0.0121
L Putamen	0.0037	0.0035	0.0030	0.0023	0.0012

In order to monitor basal and drug-induced transmitter release from grafted dopaminergic neurons, the patient underwent two ^{11}C-raclopride PET scans at 10 years after grafting, one after a saline infusion and the other after a 0.3mg/kg methamphetamine (m-amphetamine) bolus infusion. Binding of ^{11}C-raclopride to dopamine D2 receptors was measured in the putamen and caudate nucleus on each side.

^{11}C- raclopride binding was upregulated by 30% compared with normal subjects in the non-grafted putamen but was normal in the grafted putamen (Table 17, Fig. 27 and 28). In the non-transplanted caudate nuclei, ^{11}C- raclopride binding was increased bilaterally. Following m-amphetamine administration, there was only a 5% reduction of ^{11}C- raclopride binding in the non-grafted putamen (Table 17, Fig. 26 and 27).

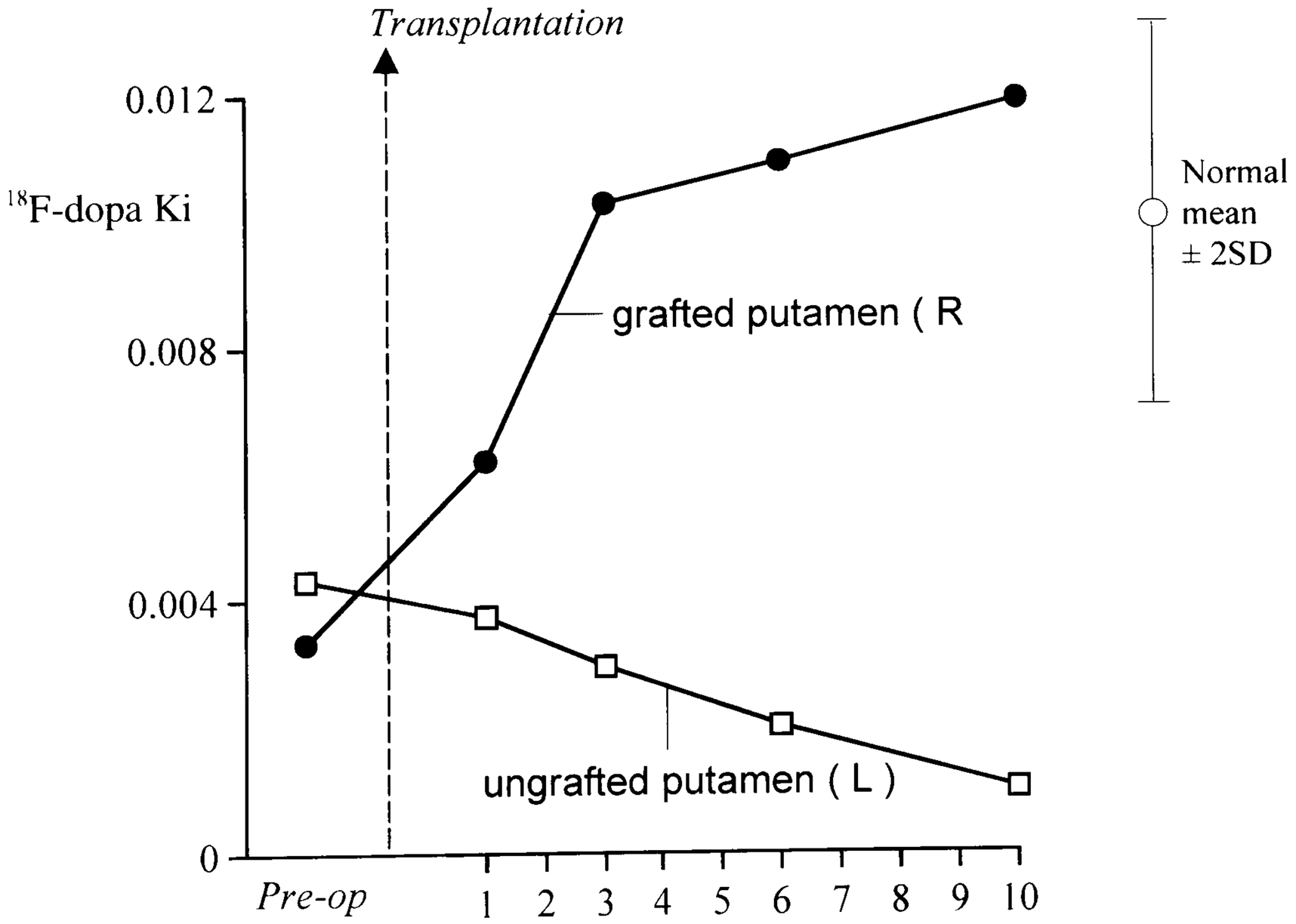


Figure 26 ^{18}F-dopa uptake in the grafted (filled circles) and in the ungrafted putamen (open squares) before transplantation and at one, three, six and ten years follow-up.

In contrast, the binding reduction was much more pronounced (26.6 %) in the grafted putamen and similar to the m-amphetamine-induced decrease of ^{11}C- raclopride binding in the putamen of normal controls (24% and 23% in the left and right putamen, respectively; Table 17). No side-to-side difference in the decrease of ^{11}C- raclopride binding induced by m-amphetamine was observed between the caudate nuclei.

Table 17. Values of striatal ^{11}C-raclopride BP and relative tracer delivery (R_I) after intravenous infusion of m-amphetamine or saline in a PD patient 10 years after transplantation of embryonic mesencephalic tissue into the right putamen.

	^{11}C-raclopride							
	R-caudate		L-caudate		R-putamen		L-putamen	
	BP	R_I	BP	R_I	BP	R_I	BP	R_I
Saline	3.22	0.99	3.28	1.02	2.89	1.01	4.21	1.04
m-amphetamine	2.9	0.96	2.99	0.98	2.12	0.97	4.02	1
D %	-9.9%	-3%	-8.8%	-3.9%	-26.6%	-3.9%	-4.6%	-3.8%

R=right, L=left; SD=standard deviation; D %=percentage difference (m-amphetamine-placebo/placebo x100).

Reductions in R_I are not correlated to reductions in BP (r^2 =0.03; p=0.45).

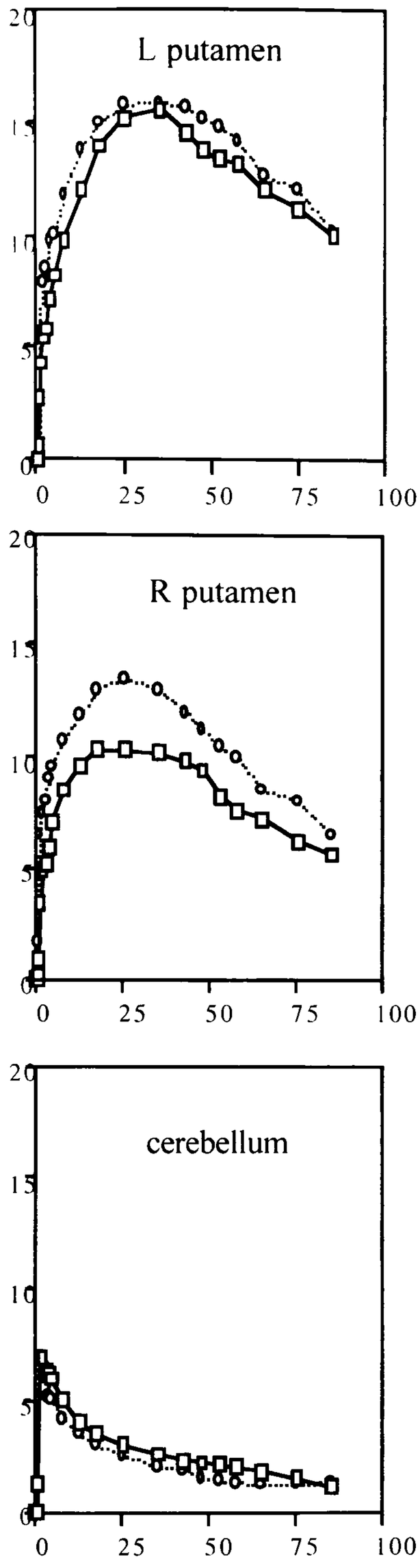


Figure 27. ^{11}C-raclopride time active curves after saline and after methamphetamine injection in a PD patient with transplantation of embryonic mesencephalic tissue to the right putamen. Open squares: methamphetamine, open circles: saline.

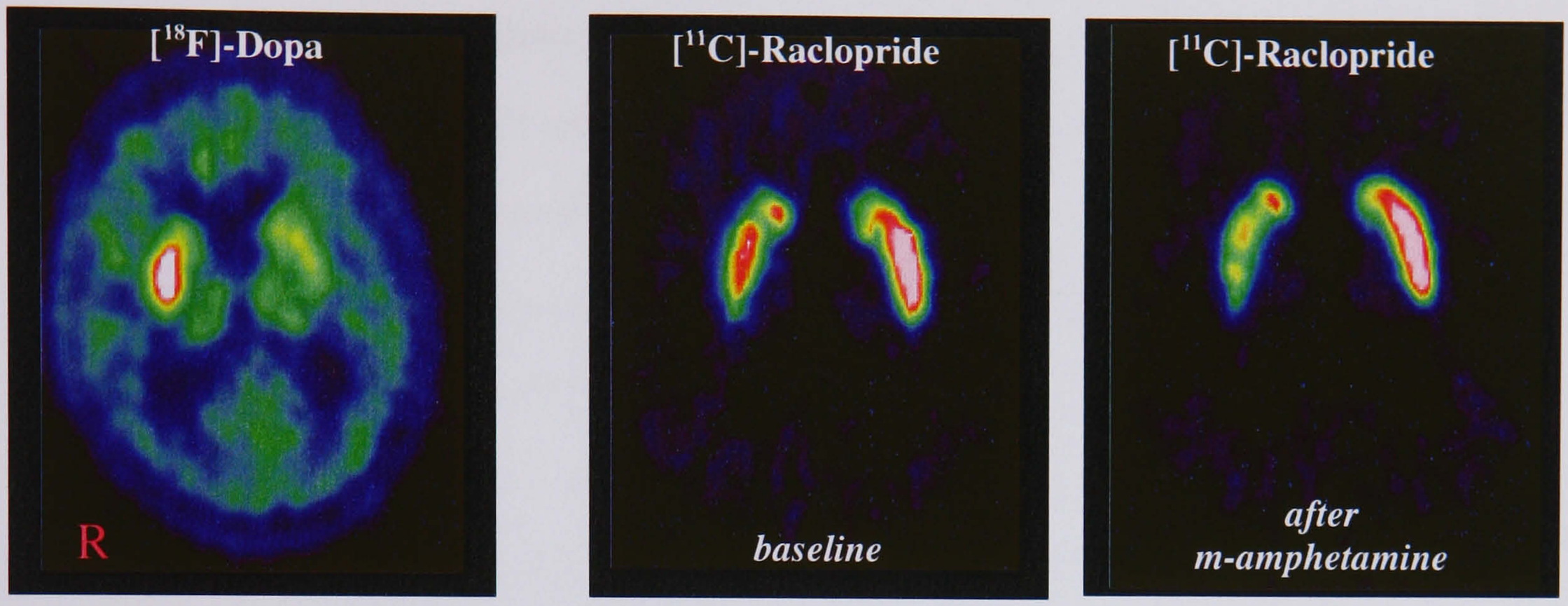


Figure 28. Integral images of ^{18}F-dopa and parametric images of ^{11}C-raclopride binding potential (BP) at the level of the basal ganglia for the PD patient 10 years after transplantation of embryonic mesencephalic tissue into the right putamen. In the baseline condition (after saline infusion) ^{11}C-raclopride BP is increased in the non-grafted putamen and normal on the grafted side. After administration of methamphetamine the binding reduction in the grafted putamen is similar to that seen in normal subjects whereas it is negligible in the non-grafted putamen

5.1.4 Discussion

By use of non-invasive imaging of D2 receptor availability, I have demonstrated, for the first time, that dopamine release from intrastriatal grafts of human embryonic mesencephalic tissue can be visualized *in vivo* in patients with PD. Measurement of dopamine D2 receptor occupancy by endogenous dopamine using ^{11}C- raclopride PET has previously shown changes of dopamine receptor availability consistent with transmitter release in the striatum of normal volunteers during performance of a rewarded goal-directed motor task (Koepp et al., 1998). This technique has also been used to detect increases in the amphetamine-evoked release of dopamine in the striatum of schizophrenic patients compared with controls (Laruelle et al., 1996).

The grafted putamen showed normal ^{11}C- raclopride binding, whereas D2 site availability was upregulated by 30% in the non-grafted putamen. ^{18}F-dopa uptake, which is a good measure of the overall storage capacity of dopaminergic terminals in the striatum, was restored to normal levels in the grafted putamen compared to a level of 10% of normal on the non-grafted side. Taken together, these data indicate that the new transplant-derived innervation tonically releases sufficient dopamine to restore D2 receptor occupancy to a normal level throughout a large part of the previously denervated striatum. Lesions of the nigrostriatal dopaminergic system in animals lead to upregulation of dopamine D2 receptor binding in the striatum (Creese et al., 1977; Neve et al., 1984; Savasta et al., 1988; Gerfen et al., 1990; Elsworth et al., 1998). In untreated early PD patients, the majority of PET and post-mortem autoradiographic studies have also shown 10-20% upregulation of dopamine D2 receptor binding in the putamen (contralateral to the more affected limbs) (Lee et al., 1978; Guttman et al.,

1986; Seeman et al., 1987; Rinne et al., 1990), which reverses after L-dopa treatment (Antonini et al.; 1994). The elevated D2 receptor binding in the non-grafted putamen of this patient, however, was not reversed by his recent low-dose L-dopa treatment. The normal level of D2 receptor binding in the grafted putamen (contralateral to the limbs which exhibited the most severe parkinsonian symptoms preoperatively) is consistent with studies after transplantation in animal models of PD. In both rats and monkeys dopaminergic grafts which reinnervate the striatum have been shown to normalize the upregulated D2 receptor binding (Elsworth et al., 1998; Dawson et al., 1991; Blunt et al., 1992; Chritin et al., 1992), most probably due to restored continuous stimulation of postsynaptic sites by dopamine released from the axon terminal network established by the grafted neurons. *In vivo* monitoring of dopamine release, by microdialysis or voltammetry, has demonstrated that rat and human embryonic nigral implants are able to restore baseline striatal dopamine levels to control values in the rat PD model (Strecker et al., 1987; Nishino et al., 1990; Rioux et al., 1991). Furthermore, the lesion-induced increase of striatal D2 mRNA in rats can be reversed by a D2 agonist (Gerfen et al., 1990) and L-dopa treatment normalizes putaminal D2 receptor binding in PD patients (Antonini et al., 1994).

The pronounced side-to-side difference in the amphetamine-induced reduction of putaminal ^{11}C- raclopride binding in our PD patient is compatible with a marked increase of extracellular dopamine levels in the grafted compared to the non-grafted striatum leading to a greater reduction of the number of D2 receptor sites available for ^{11}C- raclopride binding on the implanted side. Based on microdialysis studies in non-human primates, it has been proposed that a 25-30% decrease in striatal D2 receptor binding after administration of amphetamine measured by single-photon emission computed tomography (SPECT) reflects a 2- to 10-fold peak increase from baseline in

extracellular dopamine levels (Laruelle et al., 1996). Therefore, the 26 % reduction in ^{11}C- raclopride binding detected in the grafted putamen of this patient following m-amphetamine is likely to reflect a similar level of increase in extracellular dopamine derived from the transplanted neurons. The small, 5% reduction of ^{11}C- raclopride binding in the non-grafted putamen confirms the low capacity for dopamine release in this severely denervated structure. Our interpretation is supported by *in vivo* microdialysis studies in animals, which have demonstrated that grafted neurons of rodent or human origin reinnervating the striatum release several-fold increased amounts of dopamine when the rat hosts are challenged with amphetamine (Zetterström et al., 1986; Nishino et al., 1990; Rioux et al., 1991; Herman et al., 1993). Histopathological observations in another two patients with nigral transplants (Kordower et al., 1996; Kordower et al., 1998) have confirmed that increased striatal fluorodopa uptake is well correlated with dopamine neuron survival and extent of reinnervation of the host striatum. Our data in this patient suggest that in the best cases, nigral transplants reinnervate the putamen extensively, to a level sufficient to normalize both ^{18}F-dopa uptake and D2 receptor occupancy throughout the grafted putamen. The restoration of dopamine neurotransmission, unilaterally within the putamen, was reflected by a sustained improvement of the UPDRS motor score by about 50%. The level of disability in this patient at 10 years after transplantation and nearly 20 years after the onset of the disease was similar to that seen in early stages of PD. We found that grafts can survive for at least 10 years without any evidence of destruction by the disease process. The decrease of ^{18}F-dopa uptake values in non-grafted striatal regions most likely reflects the progressive degeneration of the patient's own dopamine neurons. The long-term stability of the grafted neurons suggests that PD is not caused by an endogenously produced neurotoxin, but rather argues for an

intrinsic deficit in nigral dopamine neurons in patients with PD. There were no signs of rejection even 7 years after cessation of cyclosporine treatment and 4.5 years following complete withdrawal of immunosuppression. This indicates that even if well-developed dopaminergic allografts may contain various immune markers, it is possible for them to survive seemingly unimpaired for several years in the absence of immunosuppression.

In conclusion, this study provides the first evidence that well-developed and clinically efficacious nigral transplants can restore both basal and drug-induced dopamine release in the striatum of PD patients. Moreover, the results obtained in the present patient show that this capacity can be maintained for at least a decade, despite the fact that the grafted neurons are exposed to an ongoing disease process. This indicates that efficient restoration of dopamine release throughout the grafted putamen in this patient underlies his major clinical improvement. These results have now been reproduced in other transplanted patients. Figure 29 shows images of ^{18}F-dopa uptake and ^{11}C-raclopride BP after saline and after methamphetamine in another PD patient who was studied before and eight months after transplantation.

These findings thus demonstrate the usefulness of ^{11}C- raclopride PET for *in vivo* analysis of dopamine release from grafted dopamine-producing cells after transplantation. This imaging technique is needed because, in addition to embryonic mesencephalic tissue, other sources of dopamine-producing cells have been considered potentially useful for transplantation in patients, including carotid body and genetically engineered fibroblasts or stem cells. The ^{11}C- raclopride PET method is a novel powerful tool in the further development of cell replacement strategies in PD.

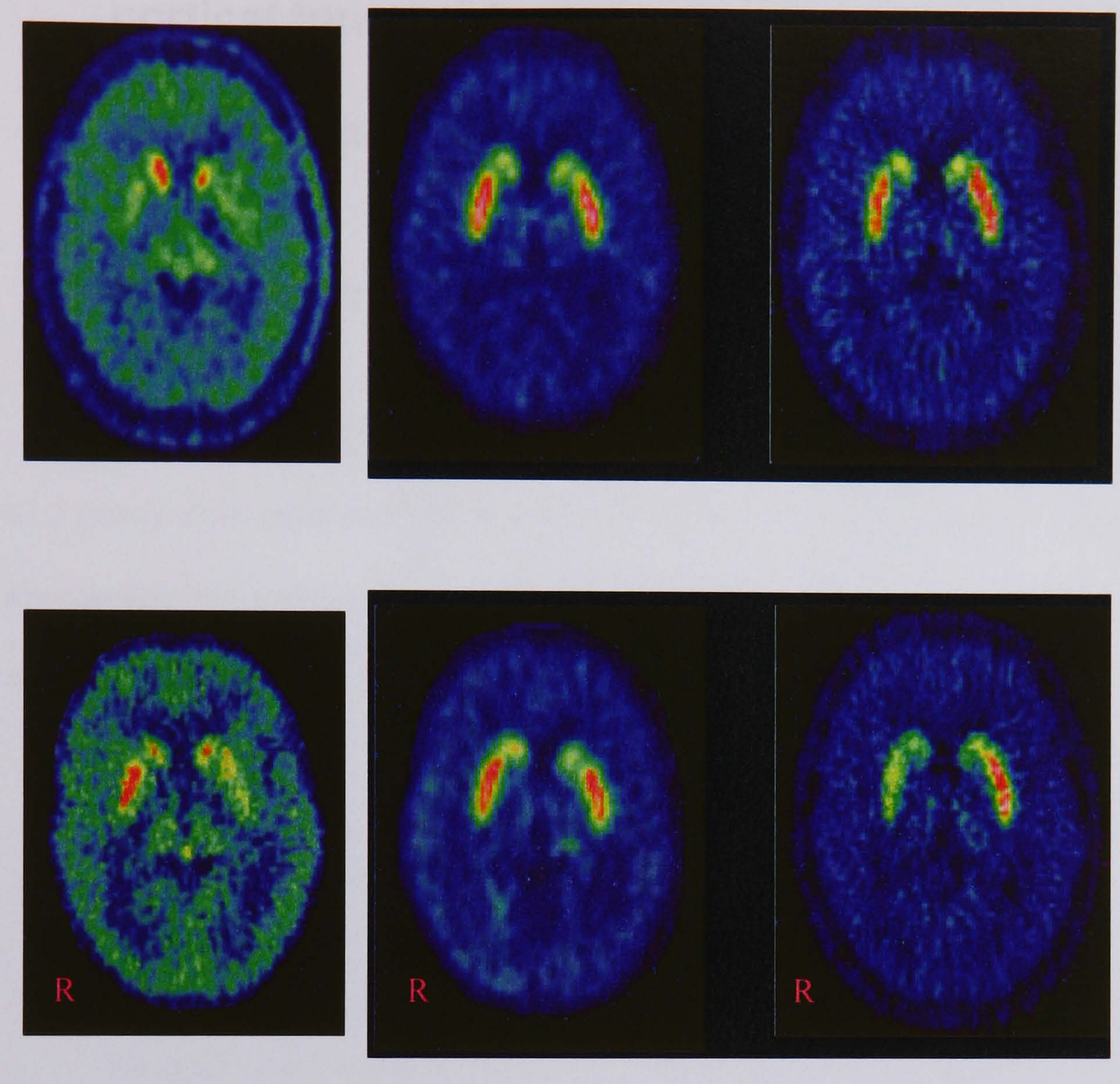


Figure 29. Images of ^{18}F-dopa uptake and ^{11}C-raclopride Binding Potential (BP) following administration of saline and following administration of 3 mg/kg methamphetamine in a PD patient before and after transplantation of human embryonic mesencephalic cells into the right putamen.

Note the increase in ^{18}F-dopa signal in the right putamen post-transplantation. Before grafting ^{11}C-raclopride BP was not modified by the methamphetamine challenge in comparison to saline. Eight months after transplantation there was a clear reduction of ^{11}C-raclopride BP in the right putamen indicating that the graft is releasing endogenous dopamine.

5.2 Delayed recovery of movement-related cortical function in Parkinson's disease following striatal dopaminergic grafts.

5.2.1 Subjects

Four patients with idiopathic PD (age 49.2 ±5.9 years; disease duration 12.8 ±1.7 years) were implanted with human embryonic mesencephalic tissue bilaterally into caudate nucleus and putamen. Their clinical characteristics and number of donors are reported in table 18.

Table 18. Characteristics of PD patients

	Mean (range)
Age (years)	53 (41-68)
Disease duration (years	12.6 (11-15)
Treatment duration (years)	11 (8-15)
Hoehn and Yahr	3.5 (3-5)
Preoperative clinical scores	
UPDRS motor score	41.7 (23-67)
Percent time in off	29.9 (11.2-50.4)
Percent time in "on" with dyskinesias	28.9 (3.9-50.4)
Time to perform tapping test	32.2 (11.1-156.6)
Upper limb rigidity	2 (1-4)
Daily L-dopa dose (mg)	825.0 (225-1500)
Duration of L-dopa induced "on" (min)	115.1 (67-157)
Number of donors	2.8 (2.2-3.6)

5.2.2 Specific Methods

Clinical evaluations, ^{18}F-dopa PET and $H_2{}^{15}O$ PET activation studies were performed 1-5 months prior to transplantation and at 6.5 (±2.7) and 18.3 (±3.4) months after surgery. The patients' informed consent was obtained according to the Declaration of Helsinki and the procedures were approved by the local Ethical Committees in Lund (Research Ethics Committee, Lund University) and London (Hammersmith Hospitals Trusts Research Ethics Committee).

5.2.2.1 Graft preparation and neurosurgical procedure.

Detailed descriptions are available elsewhere (Rehncrona, 1997; Wenning et al., 1997; Brundin et al., 2000). Briefly, dissociated ventral mesencephalic tissue from seven to nine aborted human embryos (aged 5 to 7 weeks postconception, crown to rump length 13 to 27 mm) was implanted in each patient. The ventral mesencephalon was dissected from each embryo and cut into 6-10 pieces. These were stored for 2-5 hrs during the retrieval and dissection of donor tissue in a hibernation medium (Sauer and Brundin, 1991) supplemented with 3.0 μM tirilazad mesylate. Tissue pieces from multiple embryos were then incubated at 37^0 C for 20 min in Hanks balanced solution with 0.1% trypsin and 0.05% deoxyribonuclease supplemented with 3.0 μM tirilazad mesylate. After incubation, the pieces were rinsed five times using HBSS containing 0.0% DNase and 3.0 μM tirilazad mesylate. Immediately before transplantation, the pieces were mechanically dissociated using fire-polished Pasteur pipette in HBSS with 0.05% DNase and 3.0 μM tirilazad mesylate.

Implantation of embryonic mesencephalic tissue was performed in Lund using CT- and MRI-guided stereotaxic neurosurgery. In all the patients the grafts were placed

bilaterally in the dorsal putamen and head of the caudate nucleus along five and two trajectories, respectively. Twenty microlitres of cell suspension were deposited along each trajectory. Patients 12 and 16 were grafted bilaterally in one session, whereas patient 14 and 15 were operated with an interval of 4 and 2 weeks, respectively, between the two sides. Patient 13 received his second graft (right striatum) six month after the first graft (left striatum).

Tirilazad mesylate was given intravenously to the patients four times a day (1.5 mg/kg) for 3 days, starting preoperatively at the time of the first implantation. All the patients were immunosuppressed with cyclosporine, azathioprine and prednisolone according to a standard regime (Lindvall et al., 1989). Apart from patient 14 (azathioprine discontinued during the first month due a liver reaction), this regimen was maintained for 12-24 months.

5.2.2.2 Clinical evaluation.

Patients were assessed clinically according to the Unified Parkinson's Disease Rating Scale (UPDRS) (Fahn et al., 1987) in the practically defined 'off' phase (Langston et al., 1992) at the time of PET scanning. In addition, they underwent clinical assessments according to the Core Assessment Program for Intracerebral Transplantation (CAPIT) (Langston et al., 1992); detailed description of these clinical observations has been published previously (Brundin et al., 2000).

5.2.2.3 PET scanning procedures and data analysis.

Patients were scanned in the practically defined "off" condition after overnight withdrawal of anti-parkinsonian medication. $H_2{}^{15}O$ PET activation studies comprised 12 measurements of rCBF; six at rest and six while performing paced joystick movements in freely selected directions using the left hand. The motor paradigm

performed during PET, therefore, consisted of two tasks: 'rest' and 'movement'. The order of the task was balanced in order to eliminate the effects of time and habituation. During the 'movement' task the patients were instructed to move a joystick with their left hand in one of four freely chosen directions: left, right, forwards or backwards. They were instructed to make a single movement as soon as possible after a pacing tone. The pacing frequency was set to one tone every four seconds. The 'rest' condition involved the patients holding the joystick loosely with the right hand. They were instructed not to move and to ignore the pacing tones and to avoid repetitions. Scans were performed using a CTI 953 PET camera and data acquired in 3D mode. An intravenous bolus of 3 ml saline containing 11.5 mCi of $H_2{}^{15}O$ was injected for each measurement of rCBF. Scanning commenced 30 s after the start of tracer infusion and there was a 10 min interscan interval. ^{18}F-dopa PET was performed 1-2 days after the $H_2{}^{15}O$ studies. A dose of approximately 80 MBq of ^{18}F-dopa was administered intravenously over 30 seconds. Scanning began at the start of tracer infusion with 25 time frames over 93 min. ^{18}F-dopa PET scans were analysed using a standard region of interest (ROI) approach and multiple time graphical analysis with an occipital reference tissue input function (see chapter 3).

$H_2{}^{15}O$ PET activation data were interrogated with statistical parametric mapping (SPM) in order to localise significant movement-related focal blood flow increases in brain areas. Realignment and normalisation were performed using SPM98 package (Wellcome department of Cognitive Neurology, London, UK) and statistical analysis was performed with SPM95 (Friston et al., 1995). The images were realigned using the mean of all twelve scans as reference and transformed into standard stereotaxic space to allow for comparison of scan data in identical voxels across different subjects and scans. The images were then smoothed using a Gaussian filter of 12-mm FWHM in

order to remove high- frequency noise and to accommodate differences in gyral anatomy between subjects. Global blood flow was normalised following ANCOVA across the entire data set to a mean of 50 ml/100ml/min. The normalisation process adjusted the rCBF values for each voxel after taking into account variations in global activity across subjects pre- and postoperatively. The adjusted rCBF voxel values were used for the statistical analysis.

The patterns of regional cerebral activation associated with joystick movements pre- and post-operatively were determined by comparing the adjusted mean rCBF values during the movement task with the rest task. To investigate the effects of transplantation on movement-associated activation we conservatively considered the pre-operative scans and the two sets of post-operative scans (at 6.5 and at 18.3 months) as originating from three separate patient groups. We then tested for relative increases and decreases by comparing the post-operative movement-associated rCBF increases at 6.5 months with the pre-operative movement-associated rCBF, the post-operative movement-associated rCBF increases at 18.3 months with the pre-operative movement-associated rCBF, and the post-operative movement-associated rCBF increases at 18.3 months with those at 6.5 months. All comparisons were specified by appropriately weighted categorical contrast and performed on a voxel-by-voxel basis using an ANOVA. This generates SPM {t} maps for the activation associated with each comparison. The SPM {t} were subsequently transformed into SPM {Z} maps and the levels of significance of areas of activation was assessed by the peak height of their foci using estimations based on the theory of random Gaussian fields.

Significance was accepted if voxel survived a threshold of $p<0.01$ with correction for multiple non-independent comparisons.

5.2.3 Results

Before transplantation, the brain areas where there was significant activation associated with performance of joystick movements in freely chosen directions included right sensorimotor cortex, bilateral lateral premotor areas and SMA, inferior parietal association area (Brodmann area 40), medial parietal cortex (area 7), and left cerebellum (Figure 30 left). The pattern of activation induced increases in rCBF was similar to that described in previous studies on PD patients 'off' medication and, in contrast to normal subjects performing this motor task, no significant activation in DLPFC was evident.

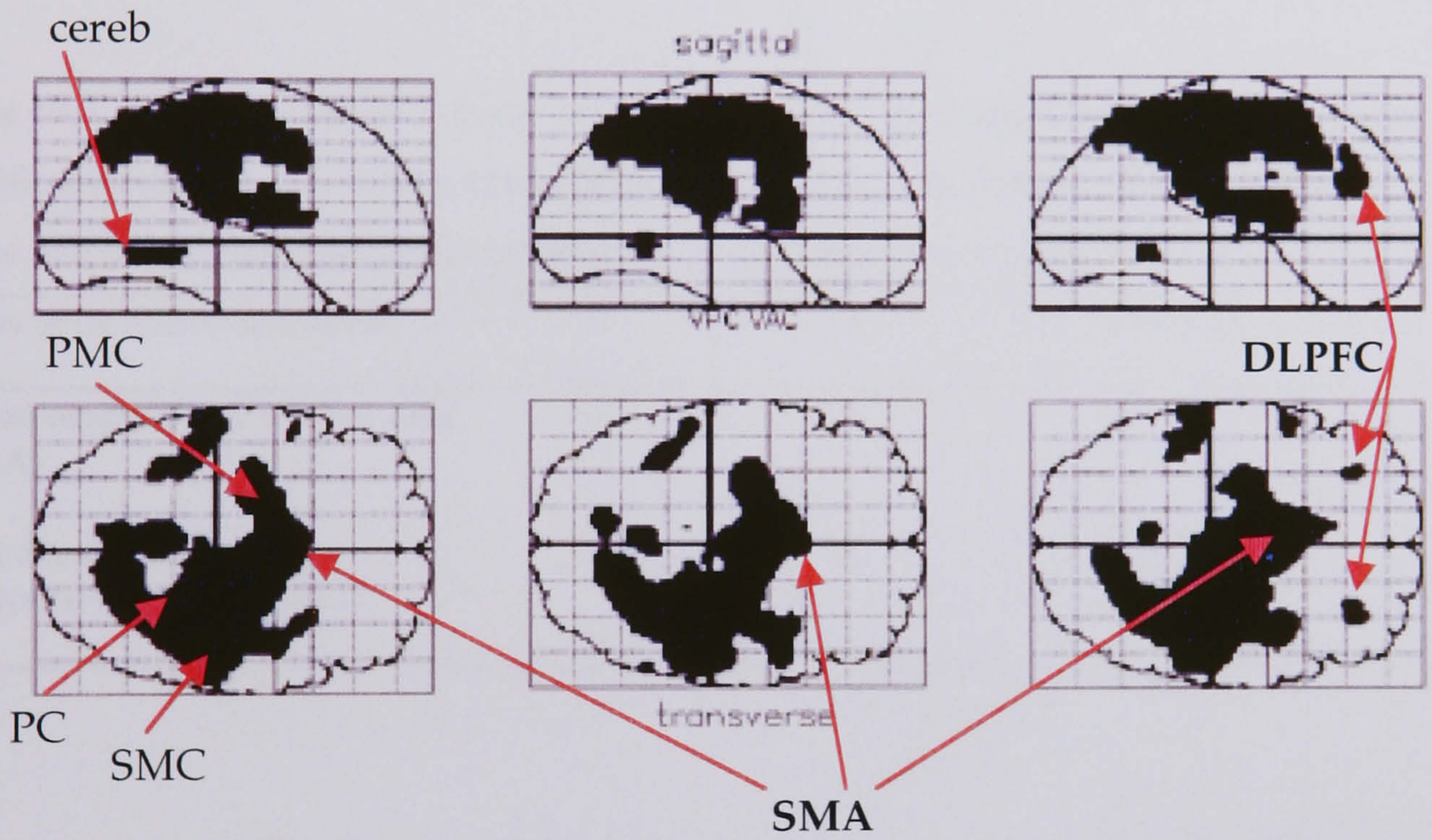


Figure 30. Areas of activation associated with freely selected joystick movements before (left), at 6.5 months (centre), and at 18.3 months (right) after bilateral implantation of embryonic mesencephalic tissue into the caudate nucleus and putamen in four PD patients. Note that at a mean of 18.3 months after implantation, there is a further significant increase in activation of rostral SMA and additional significant activation of DLPFC compared to preoperatively and 6.5 months postoperatively. Threshold $p < 0.01$, with correction for multiple no independent comparisons. SMC = sensorimotor cortex; PMC = lateral premotor cortex; PC = parietal cortex (Brodmann area 40); cereb = cerebellum; BG = basal ganglia; SMA = supplementary motor area; DLPFC = dorsolateral prefrontal cortex.

No significant differences in cortical activation were observed in our PD patients at 6.5 months compared with preoperatively (Figure 30 centre), while $H_2{}^{15}O$ PET performed 18.3 months after grafting showed significant increases in rostral SMA and bilateral DLPFC activation during the task compared with rest (Figure 30 right).

The comparison between increases in movement-associated activation before transplantation and at 18.3 months confirmed a significant increase in activation in rostral SMA and in the right DLPFC at 18.3 months after surgery (Table 19, Figure 31).

Table 19. Locations and peak-Z-scores of areas in which rCBF during joystick movements was significantly greater 18.3 months after bilateral implantation of embryonic mesencephalic tissue into caudate and putamen as compared to preoperatively in four PD patients.

Areas of increased activation	x	y	z	Z-score
rostral supplementary motor area (SMA)	-1	1	54	4.31
right dorsolateral prefrontal cortex (DLPFC)	30	36	32	4.09

In contrast, mean ^{18}F-dopa uptake values in striatum were significantly elevated already by6.5 months (putamen +78%, caudate +27% compared to preoperatively) with no further change at 18.3 months after grafting (Table 20; Figure 33). The increases in putaminal ^{18}F-dopa uptake were more pronounced than those in the head of caudate.

Table 20. Mean striatal ^{18}F-dopa uptake in four PD patients before and after bilateral implantation of embryonic mesencephalic tissue in the caudate nucleus and putamen.

	preoperatively		1st post-operative evaluation [a]		2nd post-operative evaluation [a]	
^{18}F-dopa K_i	*putamen*	*caudate*	*putamen*	*caudate*	*putamen*	*caudate*
mean	0.0043	0.0086	0.0076*	0.0109*	0.0077*	0.0111*
SD	0.0010	0.0013	0.0016	0.0013	0.0014	0.0012

K_i = ^{18}F-dopa influx rate constant. The K_i values for each subject were given as the average of the left and right side value on three consecutive planes.

[a] months after surgery; * $p < 0.001$ compared to preoperatively, paired *t-test*

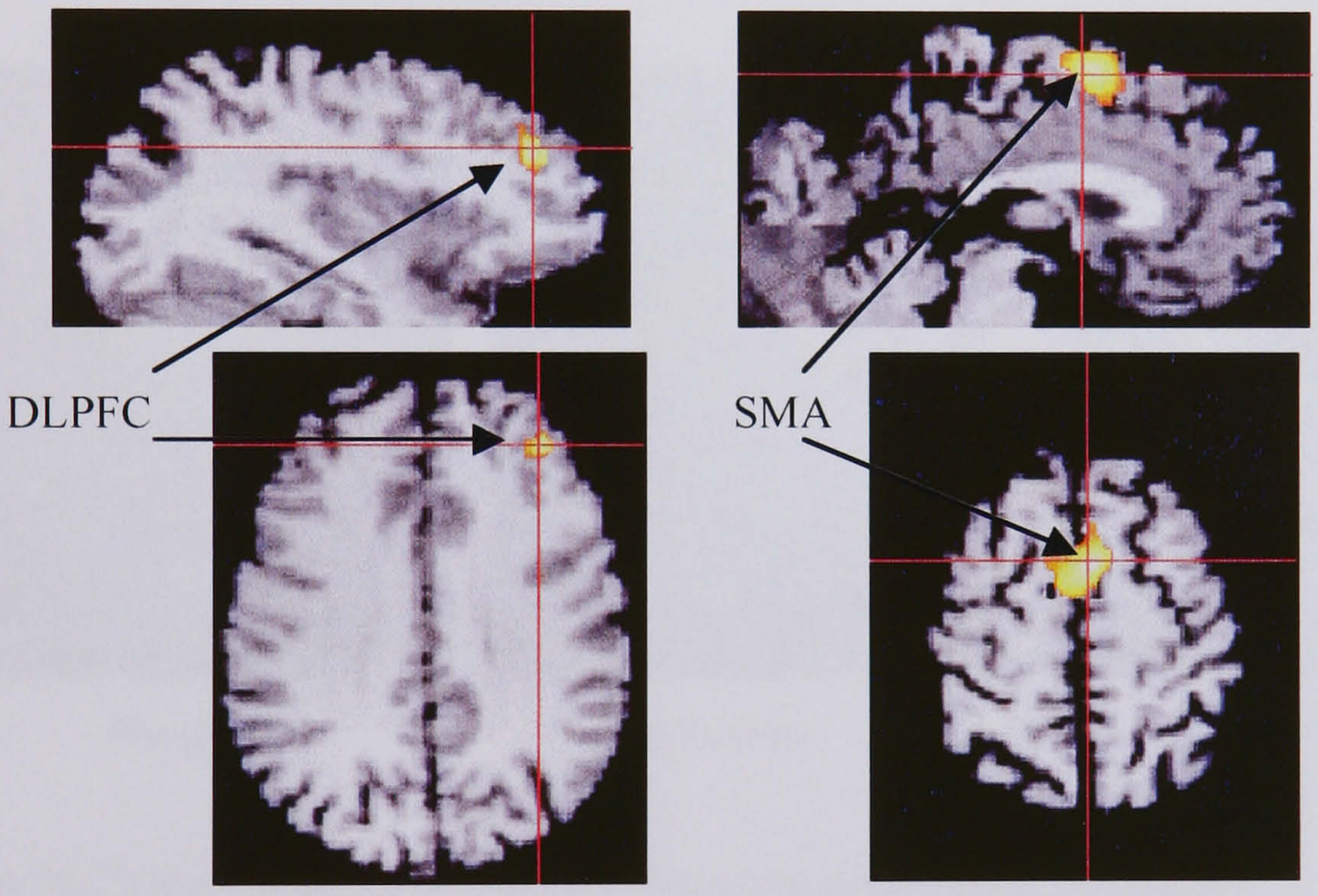
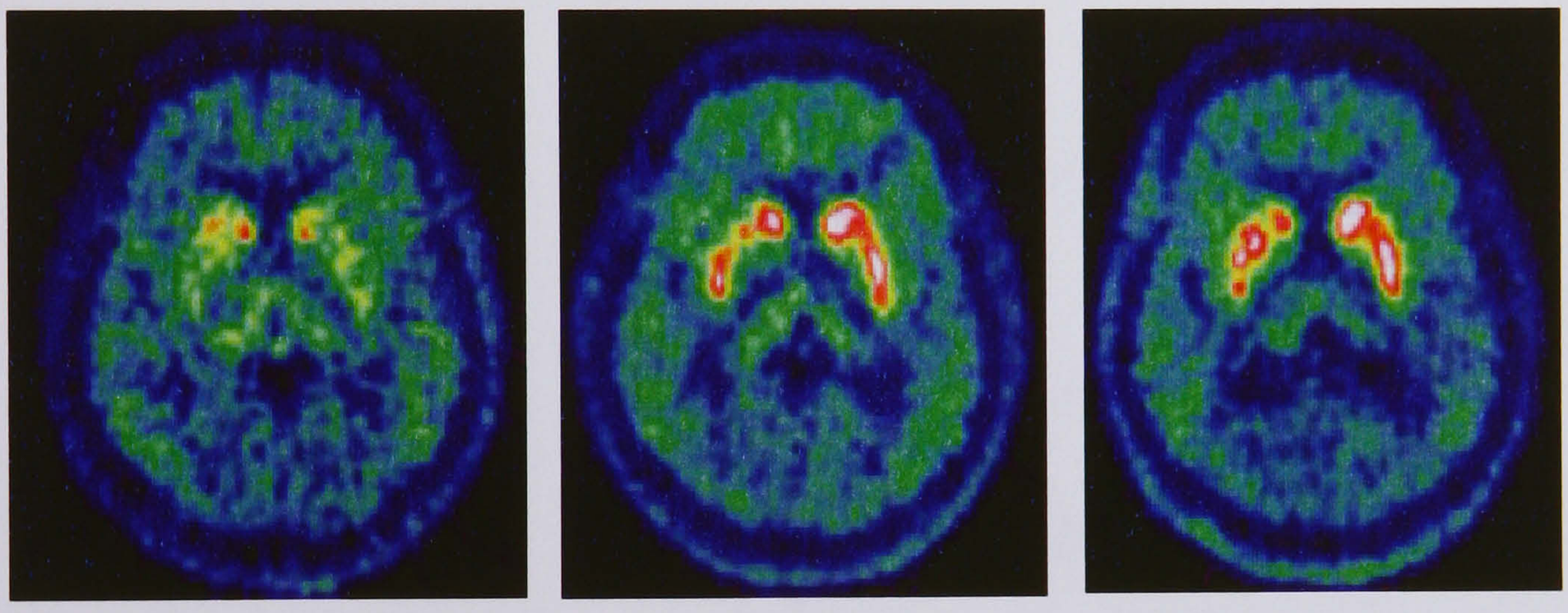


Figure 31. Areas of increased movement-related activation at a mean of 18.3 months after bilateral implantation of embryonic mesencephalic tissue into the caudate nucleus and putamen as compared to preoperatively in four PD patients. Activated regions (threshold $p < 0.001$ with correction for multiple no independent comparisons) have been superimposed onto a normalized T_1-weighted MRI scan. SMA = supplementary motor area; DLPFC = right dorsolateral prefrontal cortex.

The time course of clinical improvement paralleled that of the increases in task-induced activation of rostral SMA and DLPFC. Although symptomatic improvement

was observed in the four patients already at 6.5 months (25% reduction in UPDRS motor score), the patients continued to improve over the subsequent year and by 18.3 months the reduction in the UPDRS motor score (50%) was highly significant (Figure 33). Mean response times (time from the pacing tone to the completion of the joystick movement during scans) were faster at both 6.5 months (10%, p=0.06) and 18.3 months (19%, p=0.02) in comparison to baseline after grafting.

At 18.3 months, daily levodopa intake was reduced by a mean of 60% and one patient had been able to withdraw from levodopa treatment completely.



Pre-graft 8 months 21 months

Figure 32. ^{18}F-dopa scans for a PD patient before and after bilateral implantation of human foetal dopamine cells in caudate and putamen bilaterally.

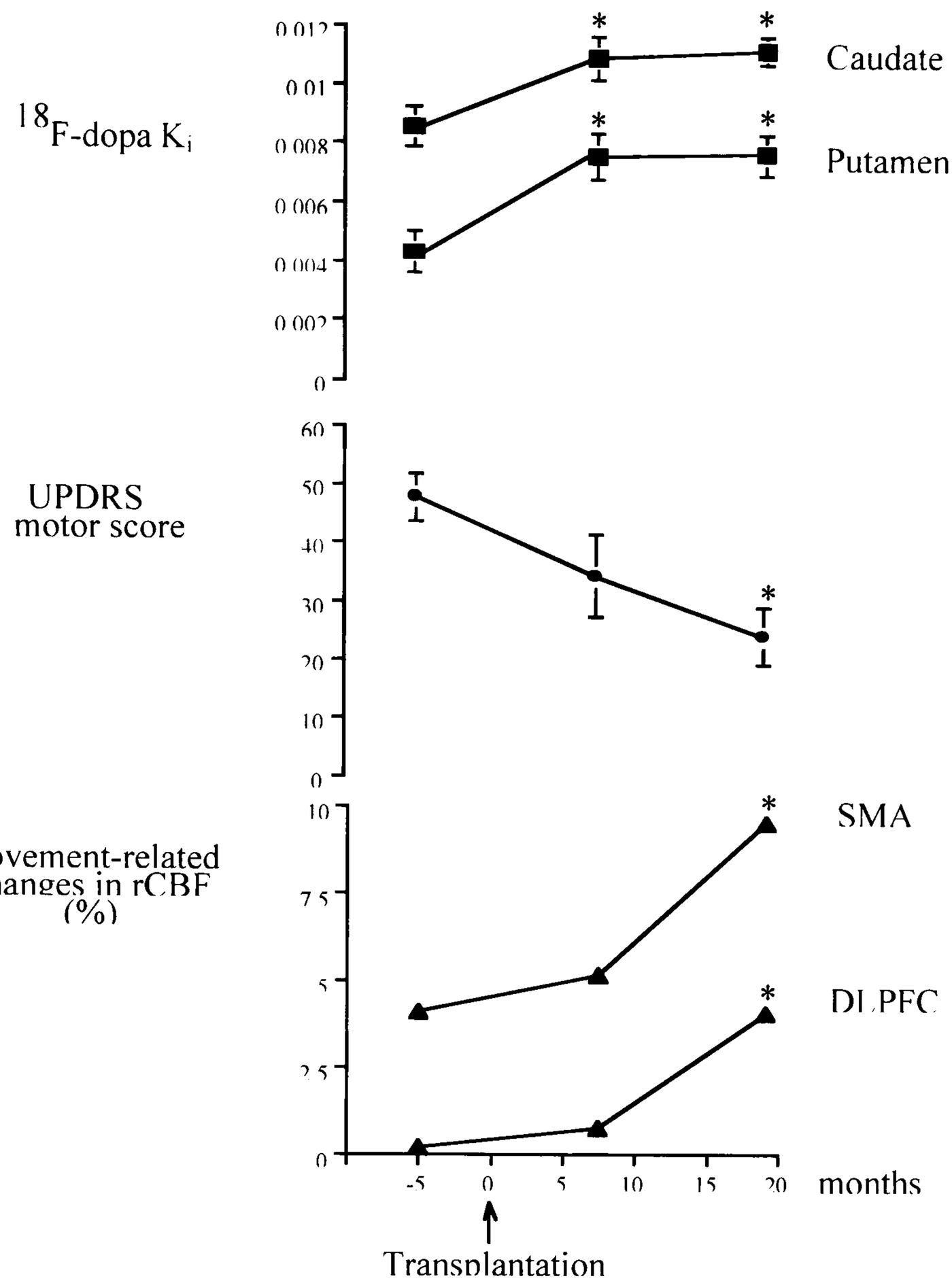


Figure 33. Caudate and putaminal ^{18}F-dopa K_i values, UPDRS motor score and percentage of movement-associated levels of rCBF in comparison to rest in SMA and DLPFC preoperatively and at 6.5 and 18.3 months after bilateral implantation of embryonic mesencephalic tissue into the caudate nucleus and putamen. Significant increase in ^{18}F-dopa uptake occur already at 6.5 months after grafting, without any changes thereafter. Although modest symptomatic relief is observed at 6.5 months, the development of significant clinical improvement is delayed and coincides with the restoration of movement-related activation. The voxels selected for these results (SMA= -1, 1, 54; right DLPFC= 30, 36, 32 [*x, y, z*]) were those showing peak-Z-scores (table 10).

K_i values and UPDRS motor scores are mean ± SE. *p < 0.001, compared to preoperatively, Student's unpaired *t*-test.

5.2.4 Discussion

This study demonstrates that intrastriatal grafts of human embryonic mesencephalic tissue in PD patients can reverse specific deficits in brain function associated with degeneration of the nigrostriatal dopaminergic system. The grafts restored activation of DLPFC and increased activation of rostral SMA during arm movements in freely selected directions. These frontal areas are known to be important in the preparation and selection of voluntary movements (Alexander et al., 1990;Deiber et al., 1991), their function is influenced by basal ganglia-thalamo-cortical circuitries (Widner et al., 1992), and their impairment is believed to underlie parkinsonian akinesia. Improvements in frontal activation and UPDRS motor scores occurred in parallel in our patients and continued over 18 months of follow-up despite no further significant increase in striatal ^{18}F-dopa uptake after 6 months. These data indicate that the significant clinical improvements in our patients were associated with more efficient cortical motor programming.

Previous clinical trials in parkinsonian patients have shown that the dopamine storage capacity in the striatum, as evaluated by ^{18}F-dopa PET, increases during the first few months after transplantation and in most cases reaches maximal values within the first postoperative year (Remy et al., 1995; Freeman et al., 1995; Hagell et al., 1999; Hauser et al., 1999). Post-operative clinical recovery typically becomes evident 2 to 6 months after transplantation (Kordower et al., 1995; Defer et al., 1996; Wenning et al., 1997). Some patients exhibited maximum symptomatic relief already at 12 months (Freeman et al., 1995), whereas, others have continued to improve beyond this time point (Hauser et al., 1999; Wenning et al., 1997; Lindvall et al., 1994). Interestingly, the clinical improvement after grafting seems to show varying time courses for different

symptoms in individual patients. Thus, rigidity has been observed to improve significantly as early as 4-7 months after surgery, in contrast to the slowness of simple and complex arm and hand movements which shows a slower and continued improvement well beyond the first postoperative year in the same patient (Lindvall et al., 1992; Lindvall et al., 1994).

Similar observations have been reported in animal experiments. In both the rat and marmoset PD models, the development of the capacity for dopamine synthesis and storage in grafts precedes the more gradual improvements in complex sensorimotor behaviour by several months (Annett et al., 1995; Winkler et al., 1999). The establishment of a new dopamine-storing terminal network in the host striatum is closely correlated to the onset of graft-derived dopamine release (Forni et al., 1989) and reversal of dopamine receptor supersensitivity in the rat PD model (Dunnett et al., 1987; Winkler et al., 1999. These early effects may all be mediated by tonic, non-regulated release of dopamine from spontaneously active grafted neurones. The later development of more pronounced functional effects suggest, however, a continued further maturation of the transplants and/or their synaptic connections with neuronal elements in the host. Fisher et al. (1991) have shown that embryonic dopamine neurones grafted to the striatum in rats still retain immature electrophysiological features at 4-5 months after surgery, and continue to mature over the subsequent months. This indicates that graft maturation may be a slow and protracted process, which continues many months after the initial formation of the graft-derived dopamine-containing fiber projections (Clarke et al., 1988) Substantia nigra neurones *in situ* exert their functions in the striatum not only through tonic dopamine release but also by phasic changes in activity controlled by regulatory afferent inputs.

Interestingly, in the study of Fisher et al. (1991), a large proportion (about 50 %) of the

grafted dopamine neurones received functional afferent inputs from the host cortex and thalamus. Burst firing, which is a critical feature of the phasic type of dopamine release that depends, at least in part, on cortical afferents developed in some of the grafted neurones (Grace et al., 1991). This suggests that functional integration into the host cortico-striatal circuitry may be important for the full expression of the functional capacity of the grafted dopamine neurones. On the basis of these animal data it seems likely, therefore, that the protracted functional improvement seen in transplanted patients depends not only on graft survival and striatal reinnervation, but also on the degree of graft-host integration.

In conclusion, results from the present study show that embryonic dopaminergic transplants can restore cortical activation during freely selected movements in severely affected PD patients and provide new evidence that the functional effects of the grafted neurones go beyond those of a simple dopamine delivery system. It appears that restoration of non-regulated dopamine release during the early stages of maturation of the transplants is not sufficient to restore movement-related cortical activation and, therefore, only induces partial symptomatic relief. The ability of the grafted dopamine neurones to increase striato-cortical neurotransmission and movement-related cortical activation, and to give rise to substantial clinical improvement is likely to require the establishment of both afferent and efferent synaptic contacts with the host. Differences between patients in the degree and pattern of symptomatic recovery following transplantation could then be partly explained by variability in the magnitude of functional integration of the grafts in the host brain.

5.3 Dyskinesias following neural transplantation in Parkinson's disease.

5.3.1 Subjects

Of the18 patients transplanted in Lund, four with non-idiopathic PD were excluded from this analysis: Three had MPTP-induced parkinsonism (patient N 5, 6 and N 8) and one had suspected multiple system atrophy (patient N 11) (table 21). Of the 14 patients considered 12 were grafted stereotaxically with fresh dissociated VM tissue from six to nine weeks old (postconception) human embryos. In two patients (N 17 and N 18), the tissue was stored in a hibernation medium containing tirilazad mesylate and GDNF for one to eight days prior to implantation.Details for these surgical procedures have been reported elsewhere; Lindvall et al., 1989;Lindvall and Hagell 2000). Grafts were placed unilaterally in the putamen in two patients and in putamen and caudate in two patients, bilaterally in putamen and unilaterally in caudate in one patient, bilaterally in the putamen in four patients and bilaterally in the putamen and caudate in five patients. Table 21 details the clinical characteristics of individual patients at the time of transplantation, the implantation site and the number of donors per side.

5.3.2 Specific Methods

Dyskinesias were retrospectively scored from videos assessed in randomised order with the global clinical dyskinesia rating scale (CDRS) score.

CDRS. This scale has been described in details elsewhere (Hagell and Widner, 1999). In brief: Assessments were performed during the practically defined "off" phase and the "on" state while the patient was performing standardized timed motor tests

(Langston et al., 1992; Morris et al., 1998) and being rated with the UPDRS motor subcsale (UPDRS III). Each video sequence consisted of (a) patient at rest silent as well as speaking (b) rigidity testing of the patients' wrists, elbow and knees performed by an examiner with the patient sitting in a chair, (c) bilateral performance of 20 pronations/ supinations of the hands against the ipsilateral thigh with the patient sitting in a chair and (d) the patient standing up, walking 7 meters, turning around and walking back again.

During the scoring sequence the highest severities of hyperkinesias and dystonia observed in the face (including tongue), neck, trunk, and left and right upper and lower extremities were scored. Ratings were performed according to a defined 5-grade severity code with definition partly adopted from a modification of the Rush dyskinesia scale (Goetz et al., 1994) (0 = *none* observed; 1 *mild*: no interference with voluntary motor acts involved in the task; 2 = *moderate*: interference with voluntary motor acts involved in the task, but it can be completed; 3 = *severe*: intense interference with voluntary motor acts involved in the task, and completion is greatly limited; 4 = *extreme*: no completion of the voluntary motor acts involved in the rated task is possible). The scores were assigned to the body part in which the dyskinesias were observed: ballism was assigned to the arm or leg while lingual dyskinesias, blepharospasm, and grimaces were assigned to the face. The exception was dyskinesias causing head movements which were assigned to the neck. In this way the maximum score possible was 28 (face= 4, neck =4, trunk =4, left arm = 4, right arm = 4, left leg =4, right leg =4).

The most recent preoperative video and those recorded 12, and 24 months after grafting plus the most recent postoperative recordings were examined. Preoperative videos during 'on' and 'off' periods were unavailable for two patients.

Table 21. PD patients transplanted in Lund included in this study.

	At the time of transplantation					
Patient No	Age (years)	Disease Duration (years)	Hoehn & Yahr stage	Daily L-dopa mg	Implantation sites	No of donors
1	48	14	V	1200	L put + L cn	4
2	55	14	IV	350	R put	4
3	48	12	III	700	L put/ R put	4/5
4	58	9	III	450	R put	4
7	49	10	II	200	L put/ R put	5/5
9	52	10	IV	950	L put/ R put	4/7
10	43	9	IV	850	R put + cn/ L put	7/4
12	53	15	V	1500	R put + cn/ L put + cn	3/4
13	41	13	III-IV	225	L put + cn / R put + cn	4/5
14	49	11	III	425	R put + cn/ L put + cn	4/4
15	54	12	III	900	L put + cn / R put + cn	4/4
16	68	12	III	1075	R put + cn/ L put + cn	4/3
17	60	16	III	900	L put/ R put	4/5
18	51	10	V	1250	R put	4
	52.07 ± 6.92	11.93 ± 2.23	3.57 ± 0.93	783.93 ± 405.33		4.21/ 4.60

Patients 5, 6 and 11 had MPTP-induced parkinsonism and patient 8 developed signs of multiple system atrophy; there were not included in this study. Put = putamen, Cn =caudate, L= left, R = right

5.3.3 Results

All 14 patients showed peak "on" dyskinesias before grafting (Table 22, Figure 34).

Six, out of 11 cases for whom preoperative video recordings during "off" were available, also displayed some degree of "off" dyskinesias prior to transplantation.

Mild to moderate foot or neck dystonia was observed in three cases, and a fourth suffered from severe foot dystonia. In a fifth patient, very mild repetitive hyperkinetic movements of the right lower limb and generalized dystonic postures were observed. Finally, one patient exhibited mild, activity-induced choreic neck movements and hand dystonia.

Table 22. Clinical characteristics of the patients (n = 14) at the time of transplantation group and at the time of maximum post-operative 'off' phase dyskinesias

	At transplantation	At maximum postoperative "off" phase dyskinesias [f]
Daily dose of L-dopa equivalents [a]	932.5 ± 477.9	565.4 ± 474.9 (p = 0.0004)
UPDRS motor score[b]	42.5 (40.25 – 55) [d]	27 (19.25 – 36) (p = 0.002)
Percent time spent in "off" [c]	36.6 ± 21.1	24.7 ± 20.2 (p = 0.095)
Percent time spent in "on" with dyskinesias [c]	20.6 ± 16.7	14.4 ± 16.6 (P = 0.227)
No. of VM implanted in the putamen / caudate nucleus [e]	6.3 ± 2.8 / 1.1 ± 1.0	

VM, ventral mesencephalic grafts in putamen and caudate per patients. UPDRS, motor score was assessed in practically defined "off" (in the morning ≥ 12 h after the last dose of anti-parkinsonian medication).

[a] 100 L-dopa equivalents = 100 mg standard L-dopa = 133 mg controlled-release L-dopa = 10 mg bromocriptine = 1 mg pergolide = 5 mg ropinirole = 2 mg apomorphine.

[b] Overall parkinsonian symptomatology assessed using the UPDRS motor examination score.

[c] Mean daily time, as recorded by the patients during the preceding month.

[d] Median (inter-quartile range).

[e] Per patient.

[f] Highest postoperative "off" phase dyskinesia scores for each patient.

Data are mean ± standard deviation except where indicated. Comparisons are paired t-tests and, for the UPDRS, Wilcoxon Signed Ranks Test; alpha = 0.05 (2-tailed).

Hyperkinesias and dystonias increased significantly during "off" after transplantation (Fig. 34), both reaching maximum at 39.8 (range 11-132) months. In contrast, there were no significant alterations either in the severity of peak "on" dyskinesias (Fig. 34), or in the percent time spent in "on" with dyskinesias (Table 22). Also when the overall level of dyskinesias in each patient was expressed as a global CDRS score, there was a significant increase in "off" but not during peak "on". The maximum "off" global CDRS scores after grafting correlated with peak "on" scores at the same time point, but not with preoperative "off" or "on" scores (Table 23).

The hyperkinesias and dystonias in "off" typically appeared concurrently, either in the same or different body part(s), as choreic movements intermingled with brief dystonic postures. Repetitive, stereotypic or ballistic, movements were also observed.

In a group of eight patients, maximum postoperative "off" global CDRS scores ranged between 0.5-4.5 (median [inter-quartile range]: 2.5 [1.1-3.8]). Dyskinesias were mild in these patients and caused no distress or disability.

Table 23. Exploratory correlation analyses for the highest observed postoperative "off" phase global CDRS score [a,b] *

Preoperative variables: [c]	Spearman's Rho (*P*-value)
Age	0.028 (0.925)
Duration of PD (years)	-0.365 (0.199)
Daily dose of L-dopa equivalents	0.334 (0.234)
UPDRS motor score in "off" [d]	0.251 (0.388)
Percent time in "off"	-0.359 (0.207)
Percent time in "on" with dyskinesias	-0.015 (0.958)
Global CDRS score in "off" [d]	0.426 (0.191)
Global CDRS score during peak "on"	0.266 (0.403)
Putaminal FD-uptake (% of normal mean)	**-0.549 (0.064)**
Surgical variables: [e]	
No. of VM in the caudate nucleus	-0.241 (0.406)
No. of VM in putamen	**0.562 (0.037)**
No. of implantation sites in the caudate nucleus	-0.263 (0.363)
No. of implantation sites in putamen	0.492 (0.074)
Postoperative variables: [f]	
Daily dose of L-dopa equivalents	0.185 (0.526)
UPDRS motor score in "off" [d]	-0.213 (0.465)
Decrease of UPDRS motor score in "off" [d]	**-0.003 (0.991)**
Percent time in "off"	-0.166 (0.606)
Percent time in "on" with dyskinesias	-0.271 (0.393)
Global CDRS score during peak "on"	**0.634 (0.015)**
Putaminal FD-uptake (% of normal mean)	**-0.132 (0.652)**
Increase of putaminal FD-uptake	**-0.267 (0.401)**
Decrease of daily dose of L-dopa equivalents	**0.573 (0.032)**

[a] The global CDRS score (the sum of the highest hyperkinesia or dystonia ratings from each body part; maximum score = 28) was derived as an overall measure of dyskinesias (intra-rater reliability = 0.98).

[b] **Correlations highlighted in bold are discussed in the text**.

[c] At the time of the first transplantation

[d] As assessed in practically defined "off"

[e] Per patient

[f] At the time point of the highest postoperative "off" phase dyskinesia scores for each patient

CDRS, Clinical Dyskinesia Rating Scale; FD, fluorodopa; other abbreviations, see Table 18.

In another group of six patients, maximum postoperative "off" global CDRS scores ranged between 9 and 18 (12 [10.1-15.4]), constituting a clinical therapeutic problem in one case, and leading to some degree of disability and/or annoyance in the others. Also "on" dyskinesias were more pronounced in the latter group (13.8 [6.8-20.2] vs 5.2 [3-6.6]), whereas there was no difference preoperatively.

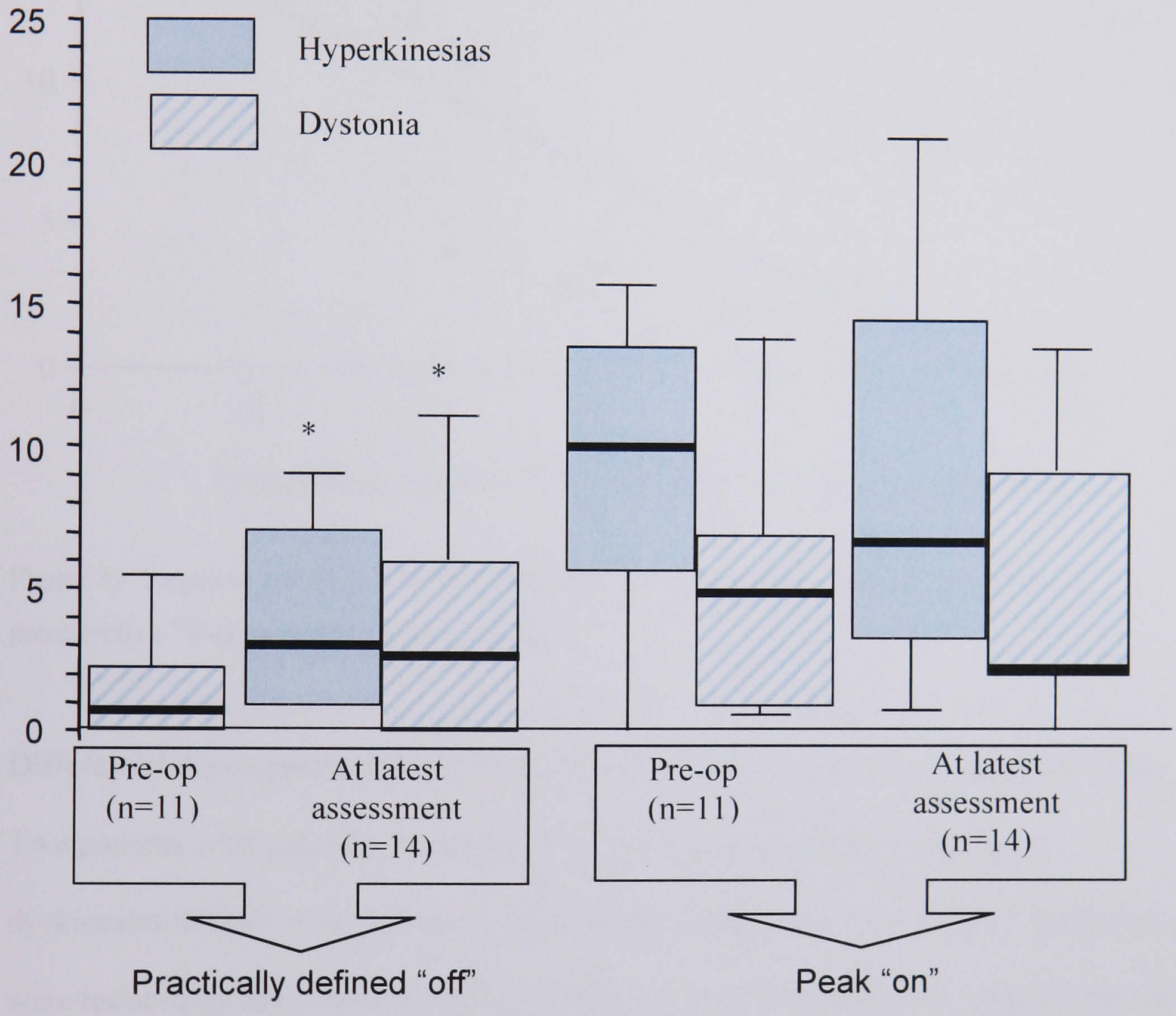


Figure 34. Hyperkinesias and dystonia during practically defined "off" and peak "on" phases before transplantation and the latest assessment after transplantation (mean 44.6 months). Solid horizontal lines are median values, boxes are inter-quartile ranges, error bars are ranges.

Of the six patients with preoperative "off" dyskinesias, three patients showed increased and three patients decreased dystonia after grafting, whereas hyperkinesias increased in all cases.

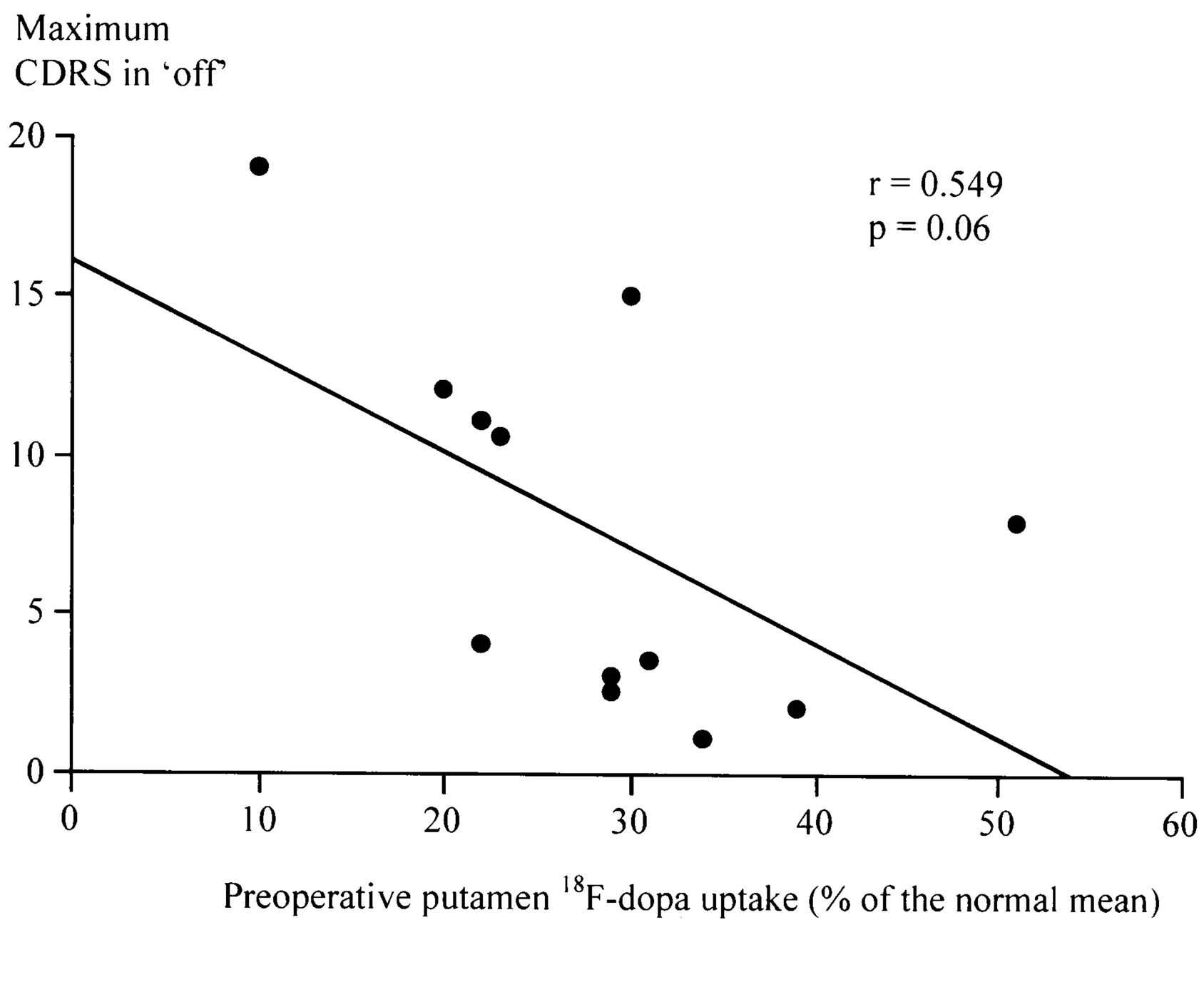


Figure 35. Negative correlation between severity of postoperative "off" dyskinesias and preoperative ^{18}F-dopa uptake in the putamen.

Differential developments of "off" and "on" dyskinesias were observed post-grafting. Two patients with virtually no preoperative "off" dyskinesias developed mild dyskinesias in "off". Concomitantly, their preoperatively pronounced "on" dyskinesias were reduced by more than 50% after grafting. In another patient with no preoperative but pronounced postoperative "off" dyskinesias, virtually no change in peak "on" dyskinesias was observed. In one of the patients with the most pronounced postoperative "off" dyskinesias, L-dopa and dopamine agonists were withdrawn for up to 9 weeks with no apparent effect on the severity of the dyskinesias.

There was a trend for the severity of postoperative "off" dyskinesias to correlate negatively with preoperative ^{18}F-dopa uptake in the putamen (Table 23; Figure. 35; r =-0.549, p = 0.064).

5.3.4 Discussion

The findings from this study suggest that the manifestation of "off" dyskinesias following grafting, similar to that of L-dopa-induced "on" dyskinesias (Boyce et al., 1999; Nutt, 2000; Lee et al., 2000) can be related to the degree of striatal dopaminergic denervation and to the resultant postsynaptic alterations before surgery. However, our observations argue against the idea that L-dopa-induced "on" and graft-evoked "off" dyskinesias have identical underlying mechanisms. Although occurring during "off" in rare cases of non-grafted patients (Cubo et al., 2001) the mixed type of dyskinesias seen in "off" after transplantation are different from the dyskinesias observed during "off" and "on" in non-grafted PD patients (Luquin et al., 1992; Cubo et al., 2000). At the time of maximum "off" dyskinesias, our patient group showed no change in the severity of peak "on" dyskinesias as compared to preoperatively. There was a significant correlation between the severity of peak "on" and "off" dyskinesias postoperatively, and the peak "on" dyskinesia scores were higher in patients with more pronounced as compared to those with mild "off" dyskinesias. Thus, in several cases these adverse effects appear additive after transplantation. However, in some patients, there was a gradual reduction or no change of peak "on" dyskinesias after grafting despite continued development of "off" dyskinesias. This finding suggest that grafts can induce or worsen "off" dyskinesias while ameliorating L-dopa-induced peak "on" dyskinesias (Widner et al 1992; Hauser et al., 1999; Lee et al., 2000).

"Off" dyskinesias were not associated with the most marked symptomatic relief. No correlation was found between "off" phase motor improvement, as assessed using UPDRS motor score, and maximum postoperative "off" CDRS scores There was a positive correlation with the decrease in antiparkinsonian treatment following surgery . The degree of motor improvement and reduction in medication did not differ between patients with mild and more pronounced postoperative dyskinesias. The evolution of "off" dyskinesias typically followed a time course different from that of the symptomatic relief. In the three bilaterally grafted patients who showed the highest postoperative "off" dyskinesia scores, maximum improvement of UPDRS motor scores had occurred already by12 months after transplantation, whereas "off" dyskinesias reached their maximum at 24 to 48 months.

Taken together, our data indicate that the mechanisms of graft-derived clinical improvement, believed to be restoration of striatal dopaminergic neurotransmission, are most likely different from those of "off" dyskinesias.

No evidence was obtained for the notion that "off" dyskinesias are caused by overgrowth of grafted dopamine neurons. Neither the FD uptake in the scan performed closest in time to maximum postoperative "off" phase dyskinesias nor the increase of putaminal FD uptake as compared to the preoperative scan correlated with "off" global CDRS scores (Table 23), or differed between the mild and severe groups of patients. Nevertheless, such dyskinesias could still be related to dopaminergic mechanisms in the striatum. Small grafts could give rise to dopamine spillover that reaches supersensitive receptors outside restricted islands of reinnervated striatal tissue. Alternatively, "off" dyskinesias might be dependent on transplantation-evoked changes in the host striatum or non-dopaminergic components in the grafts. Thus,

postoperative "off" CDRS scores correlated with the number of VM implanted in the putamen (Table 23). Conspicuously, the two patients who received tissue that had been stored for 1 to 8 days in the presence of glial cell line-derived neurotrophic factor (GDNF) developed more pronounced "off" dyskinesias (global CDRS score 12 and 18 respectively) than patients implanted with fresh tissue (CDRS median: 3.5). Similarly, the most dramatic post-grafting "off" dyskinesias have been observed after implantation of tissue cultured for up to 4 weeks, despite low numbers of surviving dopaminergic neurons (Greene et al., 1999; Freed et al., 2001).

Our findings argue against the notion that "off" dyskinesias are a characteristic feature of dopamine cell replacement *per se*, and provide no evidence that this side effect should stop the further development of a cell therapy for PD.

Conclusions: Review of the Major Findings

6

6.1 The role of PET in understanding the genetic contribution to the causes of Parkinson's disease

The contribution of genetic factors to the pathogenesis of PD continues to be debated. One of the major findings of this thesis has been the demonstration that the concordance for nigro-striatal dopaminergic dysfunction as assessed by ^{18}F-dopa PET is higher in monozygotic twins than in dizygotic twins and tends to increase over time. This finding indicates that in the pathogenesis of PD genetic factors play a more important role than is appreciated when clinical criteria alone are used to detect cases. One of these genetic "factors", *parkin* gene mutations, is thought to be responsible for up to 49% of early onset parkinsonism with clear autosomal recessive inheritance, but only 18% of isolated parkinsonism occurring below the age of 45. One of the aims of this thesis has been to investigate whether *parkin* disease causes similar nigro-striatal dysfunction to PD and whether these mutations are relevant to the pathogenesis of idiopathic PD. I found that, in comparison to *parkin* negative PD patients with similar disease severity, *parkin* patients have more diffuse disease affecting dopaminergic

terminals in caudate and midbrain nuclei more severely but that their disease progression was slower. *Parkin* patients also have decreased striatal and cortical D_2 binding in comparison to non-parkin patients. Despite this, they remain l-dopa responsive.

In addition to these data, I have observed a significant reduction in striatal and midbrain ^{18}F-dopa uptake in asymptomatic heterozygous carriers in a similar pattern to that reported for patients with clinical *parkin* disease. This would suggest that having a single mutant *parkin* allele may be a risk factor for the development of late-onset disease. Repeated observation over time will be necessary to confirm this. The incidence and prevalence of *parkin* heterozygotes in the general and late-onset PD population remains unclear. There is new evidence that asymptomatic parkin heterozygotes are at risk of developing late-onset PD if the mutation is is in exon 7 (Oliveira et al., 2003) . It is possible that different parkin mutations impart different degrees of susceptibility to developing clinical signs by working in concert with other genes and perhaps environmental risk factors.

Taken together the results of this section of the thesis suggest that genetic factors and particularly *parkin* mutations contribute to the prevalence of general sporadic PD.

6.2 PET studies on the efficacy of cell transplantation therapy in Parkinson' s disease.

Neural transplantation in PD is based on the idea that dopamine supplied from cells implanted into the striatum can substitute for the loss of the nigro-striatal dopaminergic neurones. To date, several open label clinical trials as well as two

double-blind, sham surgery-controlled studies have shown in PD patients that grafts survive and store dopamine (Freed et al., 2001; Olanow et al., 2003). Symptomatic relief after intrastriatal implantation of human foetal mesencephalic tissue has been variable. In the most successful cases patients have experienced major clinical improvement and levodopa requirements have fallen.

Two major achievements of this thesis have been the "*in vivo*" demonstrations that foetal mesencephalic grafts are able to release endogenous dopamine and that are able to restore movement-related frontal cortical–activation .

Recently, severe and intractable 'off' dyskinesias and facial dystonia that persisted despite reduction or even elimination of dopaminergic therapy have been described in patients transplanted with human foetal mesencephalic cells. These "runaway" dyskinesias were observed approximately 1 to 2 years after surgery (Freed et al., 2001; Olanow et al., 2003).

The concern about this severe side-effect has stimulated widespread media and scientific interest with serious implications for the further development of neural transplantation.

A chapter of the thesis has been dedicated to the clinical and ^{18}F-dopa re-evaluation of 14 patients who were given neural transplants during the past 11 years.

Overall, I have observed in these patients mild-to-moderate dyskinesias, in no case as severe and disabling as those reported after 12 months by Freed and colleagues study, and found no correlation between severity of dyskinesias and increases in striatal ^{18}F-dopa values after transplantation. Rather, a trend towards a negative correlation was observed between the severity of post-operative dyskinesias and the preoperative putamen ^{18}F-dopa uptake, i.e., the extent of putamen dopaminergic denervation before surgery.

Taken together the observations from this thesis have important implications into the further progress of dopamine cell transplantation. They provide no evidence that severe dyskinetic side-effects are characteristic of dopamine cell replacement per 'se'. There are, however, still many issue that need to be addressed: for neural transplantation to develop from an experimental procedure into a clinically useful treatment for PD. The optimal amount of dopaminergic cells to be transplanted is not known. Do neuroprotective agents such as antioxidant, anti-excitoxic, anti-apoptotic and trophic factors need to be included in transplantation protocols to provide higher dopamine cells survival? Is immunosuppression effective and necessary? Probably most important of all is the issue about possible sources of dopamine producing cells. It is in fact unlikely for practical, biological and ethical reasons that human mesencephalic embryonic tissue will be used in large clinical trials, however, whether other sources of cells, such as embryonic stem cells or neural precursor cells, can consistently generate populations of dopamine cells which are able to survive and function in the brain host is not yet known. The combined efforts of laboratory experiments and clinical/imaging trials hopefully will be able to provide indication of the direction of the future research in this area.

References

7

1) Abbas N, Lucking CB, Ricard S, Durr A, Bonifati V, De Michele G, Bouley S, Vaughan JR, Gasser T, Marconi R, Broussolle E, Brefel-Courbon C, Harhangi BS, Oostra BA, Fabrizio E, Bohme GA, Pradier L, Wood NW, Filla A, Meco G, Denefle P, Agid Y, Brice A. A wide variety of mutations in the parkin gene are responsible for autosomal recessive parkinsonism in Europe. French Parkinson's Disease Genetics Study Group and the European Consortium on Genetic Susceptibility in Parkinson's Disease. Hum Mol Genet. 1999;8(4):567-74.

2) Adam MJ, Ruth TJ, Grierson JR, Abeysekera B, Pate BD. Routine synthesis of L-[18F]6-fluorodopa with fluorine-18 acetyl hypofluorite. J Nucl Med 1986;27:1462-1466.

3) Agid Y. Neuroanatomy of dopaminergic system in the human brain. In: Baron JC, Comar D, Farde L, Martinot JL, Mazoyer B, eds. Brain dopaminergic systems: Imaging with positron emission tomography. Dordrecht: Kluwer Academic, 1991:1-4.

4) Ahlskog JE, Richelson E, Nelson A, Kelly PJ, Okazaki H, Tyce GM, van Heerden JA, Stoddard SL, Carmichael SW. Reduced D2 dopamine and

muscarinic cholinergic receptor densities in caudate specimens from fluctuating parkinsonian patients. Ann Neurol 1991; 30(2):185-191.

5) Alexander GE, Crutcher MD, DeLong MR. Basal ganglia-thalamocortical circuits: parallel substrates for motor, oculomotor, prefrontal and limbic functions. Prog Brain Res 1990; 85: 119-146.

6) Annett L. Functional studies of neural grafts in parkinsonian primates. In: Functional Neural Transplantation, Dunnett SB and Björklund A, Eds. Raven Press, New York 1994; pp. 71-102.

7) Annett LE, Torres EM, Ridley RM, Baker HF, Dunnett SB. A comparison of the behavioural effects of embryonic nigral grafts in the caudate nucleus and in the putamen of marmosets with unilateral 6-OHDA lesions. Exp Brain Res. 1995;103(3):355-71.

8) Antonini A, Schwarz J, Oertel WH, Pogarell O, Leenders KL. Long-term changes of striatal dopamine D2 receptors in patients with Parkinson's disease: a study with positron emission tomography and [11C]raclopride. Mov Disord 1997; 12(1):33-38.

9) Antonini, A. et al. [^{11}C]-raclopride and positron emission tomography in previously untreated patients with Parkinson's disease: influence of L-dopa and lisuride therapy on striatal dopamine D2 receptors. Neurology 44, 1325-1329 (1994).

10) Backlund EO, Granberg PO, Hamberger B, Knutsson E, Martensson A, Sedvall G, Seiger A, Olson L. Transplantation of adrenal medullary tissue to striatum in parkinsonism. First clinical trials. J Neurosurg. 1985;62(2):169-73.

11) Bartholini G, Pletscher A. Cerebral accumulation and metabolism of C-14-dopa after selective inhibition of peripheral decarboxylase. J Pharmacol Exp Ther 1968;161:14-20.

12) Bennett DA, Beckett LA, Murray AM, et al. Prevalence of parkinsonian signs and associated mortality in a community population of older people. N Engl J Med 1996; 334: 71-73.

13) Bernheimer H, Birkmayer W, Hornykiewicz O, Jellinger K, Seitenberger F. Brain dopamine and the syndromes of Parkinson and Huntington: Clinical, morphological and neurochemical correlations. J Neurol Sci 1973; 20: 415-455.

14) Biratarri C, Bonardi M, Ferarri A et al. Biomedical applications of cyclotrons and review of commercially available models. Journal of Medical Engineering and Technology 1987;11:166 - 176.

15) Blunt, S.B., Jenner, P., Marsden, C.D. Autoradiographic study of striatal D1 and D2 dopamine receptors in 6-OHDA-lesioned rats receiving foetal ventral mesencephalic grafts and chronic treatment with L-dopa and carbidopa. *Brain Res*. 582, 299-311 (1992).

16) Boer GJ. Ethical guidelines for the use of human embryonic or fetal tissue for experimental and clinical neurotransplantation and research. Network of European CNS Transplantation and Restoration (NECTAR). J Neurol. 1994;242(1):1-13.

17) Bonifati V, Fabrizio E, Vanacore N, De Mari M, Meco G. Familial Parkinson's disease: a clinical genetic analysis. Can J Neurol Sci. 1995 Nov;22(4):272-9

18) Bonifati V, Rizzu P, van Baren MJ, Schaap O, Breedveld GJ, Krieger E, Dekker MC, Squitieri F, Ibanez P, Joosse M, van Dongen JW, Vanacore N, van Swieten JC, Brice A, Meco G, van Duijn CM, Oostra BA, Heutink P.

Mutations in the DJ-1 gene associated with autosomal recessive early-onset parkinsonism. Science. 2003;299(5604):256-9

19) Bower JH, Maraganore DM, McDonnell SK, Rocca WA. Incidence of Parkinson's disease in Olmsted County, Minnesota. *Neurology* 1998; 50: A98.

20) Boyce S, Rupniak NM, Steventon MJ, Iversen SD. Nigrostriatal damage is required for induction of dyskinesias by L-DOPA in squirrel monkeys. Clin Neuropharmacol. 1990;13(5):448-58.

21) Breier A, Su TP, Saunders RC, Carson RE, et al. Schizophrenia is associated with elevated amphetamine induced synaptic dopamine concentrations: evidence from a novel positron emission tomography method. Proc Natl Acad Sci USA 1997; 94: 2569-2574.

22) Breitner JCS and Murphy EA. Twin studies of Alzheimer's disease: some prediction using a genetic model. Am J Med Genet 1992;44:628-634.

23) Breitner JCS, Gatz M, Bergem ALM, et al. Use of twin cohorts for research in Alzheimer's disease. Neurology 1993;43:261-267.

24) Brooks DJ, Ibanez V, Sawle GV, et al. Differing patterns of striatal ^{18}F-dopa uptake in Parkinson's disease, multiple system atrophy, and progressive supranuclear palsy. Ann Neurol 1990; 28: 547-555.

25) Brooks DJ, Salmon EP, Mathias CJ, et al. The relationship between locomotor disability, autonomic dysfunction, and the integrity of the striatal dopaminergic system in patients with multiple system atrophy, pure autonomic failure, and Parkinson's disease studied with PET. Brain 1990;113:1539-1552.

26) Broussolle E, Lucking CB, Ginovart N, et al. [18F]-dopa PET study in patients with juvenile-onset PD and *parkin* gene mutations. Neurology 2000;26:877-879.

27) Brundin P, Duan WM, Sauer H. Functional effects of mesencephalic dopamine neurons and adrenal chromaffin cells grafted to the rodent striatum. In: Functional Neural Transplantation, SB Dunnett and A Björklund, Eds. New York, NY: Raven Press. 1994; pp. 9-46.

28) Brundin P, Karlsson J, Emgard M, Schierle GS, Hansson O, Petersen A, Castilho RF. Improving the survival of grafted dopaminergic neurons: a review over current approaches.Cell Transplant. 2000 9(2):179-95. Review.

29) Brundin P, Pogarell O, Hagell P, et al. Bilateral caudate and putamen grafts of embryonic mesencephalic tissue treated with lazaroids in Parkinson's disease. Brain 2000; 123: 1380-1390.

30) Burn DJ, Mark MH, Playford ED, et al. Parkinson's disease in twins studied with ^{18}F-dopa and positron emission tomography. Neurology 1992;42:1894-1900

31) Calne DB, Langston JW, Martin WRW, et al. Positron emission tomography after MPTP: observations relating to the cause of Parkinson's disease. Nature 1985;317:246-248.

32) Carlsson A Towards a new understanding of dopamine receptors. Clin Neuropharmacol 1995; 18: S6-S13

33) Carson R.E., et al. Quantification of amphetamine-induced changes in [^{11}C]Raclopride binding with continuos infusion.J. Cereb. Blood Flow Metab. 17, 437-447 (1997).

34) Carson RE, Breier A, deBartolomeis A, et al., Quantification of amphetamine-induced changes in [C-11]raclopride binding with continuous infusion. J Cereb Blood Flow Metab 1998; 17:437-447.

35) Chan P, Jiang X, Forno LS, Di Monte DA, Tanner CM, Langston JW. Absence of mutations in the coding region of the alpha-synuclein gene in pathologically proven Parkinson's disease. Neurology. 1998; 50(4):1136-7.

36) Cherry SR, Woods RP, Hoffman EJ et al. Improved detection of focal cerebral blood flow changes using 3D positron emission tomography. J Cereb Blood Flow & Metab 1993;13:630 - 638.

37) Chritin, M. et al. Intrastriatal dopamine-rich implants reverse the increase of dopamine D2 receptor mRNA levels caused by lesion of the nigrostriatal pathway: a quantitative in situ hybridization study. Eur. J. Neurosci. 4, 663-672 (1992).

38) Chugani DC, Ackerman RF, Phelps ME. In vivo [3H]spiperone binding: evidence for accumulation in corpus striatum by agonist mediated receptor internalization. J Cereb Blood Flow Metab 1988; 8: 291-303.

39) Clarke DJ, Brundin P, Strecker RE, et al. Human foetal dopamine neurons grafted in a rat model of Parkinson's disease: ultrastructural evidence for synapse formation using tyrosine hydroxylase immunocytochemistry. Exp Brain Res 1988; 73: 115-126.

40) Collins DL, Neelin P, Peters TM, Evans AC. Automatic 3D intersubject registration of MR volumetric data in standardized Talairach space. J Comput Assist Tomogr. 1994; 18(2): 192-205

41) Creese, I., Burt, D.R., Snyder, S.H. Dopamine receptor binding enhancement accompanies lesion-induced behavioral supersensitivity. Science 197, 596-598 (1977).

42) Cubo E, Gracies JM, Benabou R, Olanow CW, Raman R, Leurgans S, Goetz CG. Early morning off-medication dyskinesias, dystonia, and choreic subtypes. Arch Neurol. 2001; 58(9):1379-1382.

43) Cumming P, Häusser M, Martin WRW, et al. Kinetics of *in vitro* decarboxylation and the *in vivo* metabolism of 2-18F- and 6-18F-Fluorodopa in the hooded rat. Biochem Pharmacol 1988;37:247-250.

44) Dawson, T.M et al. Functional recovery of supersensitive dopamine receptors after intrastriatal grafts of fetal substantia nigra. Exp. Neurol. 111, 282-292 (1991).

45) De Michele G, Filla A, Volpe G, De Marco V, Gogliettino A, Ambrosio G, Marconi R, Castellano AE, Campanella G. Environmental and genetic risk factors in Parkinson's disease: a case-control study in southern Italy. Mov Disord. 1996 Jan;11(1):17-23.

46) De Rijk M, Tzourio C, Breteler M. Prevalence of parkinsonism and Parkinson's disease in Europe: the EUROPARKINSON Collaborative Study. European Concerted Action on the Epidemiology of Parkinson`s disease. J Neurol Neurosurg Psych. 1997; 62: 10-15

47) Defer GL, Geny C, Ricolfi F, et al. Long-term outcome of unilaterally transplanted parkinsonian patients. I. Clinical approach. Brain 1996; 119: 41-50.

48) Defer GL, Widner H, Marie RM, Remy P, Levivier M. Core assessment program for surgical interventional therapies in Parkinson's disease (CAPSIT-PD). Mov Disord. 1999;14:572-84. Review.

49) Deiber MP, Passingham RE, Colebatch JG, et al. Cortical areas and the selection of movement: a study with positron emission tomography. Exp Brain Res 1991; 84: 393-402.

50) DeLong MR. Primate models of movement disorders of basal ganglia origin. Trends Neurosci. 1990;13(7):281-5. Review

51) Dick JP, Rothwell JC, Day BL, Cantello R, Buruma O, Gioux M. Benecke R, Berardelli A, Thompson PD, Marsden CD. The Bereitschaftspotential is abnormal in Parkinson's disease. Brain. 1989; 112 :233-44.

52) Doudet DJ, Holden JE, Jivan S, McGeer E, Wyatt RJ. In vivo PET studies of the dopamine D2 receptors in rhesus monkeys with long-term MPTP-induced parkinsonism. Synapse 2000; 38(2):105-113.

53) Doudet DJ, McLellan CA, Aigner TG, et al. Postinjection L-phenylalanine increases basal ganglia contrast in PET scans of 6-[18F]-dopa. J Nucl Med 1991;32:1408-1413.

54) Dunnett SB, Bjorklund A In Functional Neural transplantation. Eds Dunnett SB, Bjorklund A. Raven New York. 1994; pp531-567

55) Dunnett SB, Bjorklund A, Lindvall O. Cell therapy in Parkinson's disease - stop or go? Nat Rev Neurosci. 2001; 2:365-9. Review.

56) Dunnett SB, Bjorklund A, Stenevi U, Iversen SD. Behavioural recovery following transplantation of substantia nigra in rats subjected to 6-OHDA lesions of the nigrostriatal pathway. II. Bilateral lesions. Brain Res. 1981 229(2):457-70.

57) Dunnett SB, Whishaw IQ, Rogers DC, Jones GH. Dopamine-rich grafts ameliorate whole body motor asymmetry and sensory neglect but not

independent limb use in rats with 6-hydroxydopamine lesions. Brain Res 1987: 415: 63-78.

58) Dyson NA. The annihilation coincidence method of localising positron-emitting isotopes and a comparison with parallel counting. Phys Med Biol 1960;4:376 - 390.

59) Eidelberg D, Moeller JR, Dhawan V, et al. The metabolic anatomy of Parkinson's disease: complementary [18F]fluorodeoxyglucose and [18F]fluorodopa positron emission tomographic studies. Movement disord 1990;5:203-213.

60) Elbaz A, Grigoletto F, Baldereschi M, Breteler MM, Manubens-Bertran JM, Lopez-Pousa S, Dartigues JF, Alperovitch A, Tzourio C, Rocca WA. Familial aggregation of Parkinson's disease: a population-based case-control study in Europe. EUROPARKINSON Study Group. Neurology. 1999 Jun 10;52(9):1876-82.

61) Elsworth, J.H. et al. Upregulation of striatal D2 receptors in the MPTP-treated vervet monkey is reversed by grafts of fetal ventral mesencephalon: an autoradiographic study. Brain Res 795, 55-62 (1998).

62) Fahn S, Elton RL and members of the UPDRS Development Committee. Unified Parkinson's disease Rating Scale. In Recent developments in Parkinson's disease. S Fahn, CD Marsden, DB Calne, M Goldstein, Eds. Florham Park, NJ: MacMillan. 1987; pp. 153-163.

63) Farde L, Gustavsson JP, Jonsson E. D2 dopamine receptors and personality traits. Nature 1997; 385(6617):590.

64) Farrer LA, O'Sullivan DM, Cupples LA, Growdon JH, Myers RH. Assessment of genetic risk for Alzheimer's disease among first-degree relatives. Ann Neurol. 1989 May;25(5):485-93.

65) Farrer M, Gwinn-Hardy K, Muenter M, DeVrieze FW, Crook R, Perez-Tur J, Lincoln S, Maraganore D, Adler C, Newman S, MacElwee K, McCarthy P, Miller C, Waters C, Hardy J. A chromosome 4p haplotype segregating with Parkinson's disease and postural tremor. Hum Mol Genet. 1999;8(1):81-5

66) Farrer M, Maraganore DM, Lockhart P, Singleton A, Lesnick TG, de Andrade M, West A, de Silva R, Hardy J, Hernandez D. alpha-Synuclein gene haplotypes are associated with Parkinson's disease. Hum Mol Genet. 2001;10(17):1847-51

67) Farrer M, Wavrant-De Vrieze F, Crook R, Boles L, Perez-Tur J, Hardy J, Johnson WG, Steele J, Maraganore D, Gwinn K, Lynch T. Low frequency of alpha-synuclein mutations in familial Parkinson's disease. Ann Neurol. 1998;43(3):394-7

68) Feany MB, Bender WW. A Drosophila model of Parkinson's disease. Nature. 2000;404(6776):394-8

69) Firnau G, Sood S, Chirakal R, Nahmias C, Garnett SE. Metabolites of 6-[18F]fluoro-L-dopa in human blood. J Nucl Med 1988;29:363-369.

70) Fisher LJ, Young SJ, Tepper JM, et al. Electrophysiological characteristics of cells within mesencephalon suspension grafts. Neuroscience 1991; 40: 109-122.

71) Forni C, Brundin P, Strecker RE, et al. Time-course of recovery of dopamine neuron activity during reinnervation of the denervated striatum by fetal

mesencephalic grafts as assessed by in vivo voltammetry. Exp Brain Res 1989; 76: 75-87.

72) Freed CR, Greene PE, Breeze RE, Tsai WY, DuMouchel W, Kao R, Dillon S, Winfield H, Culver S, Trojanowski JQ, Eidelberg D, Fahn S. Transplantation of embryonic dopamine neurons for severe Parkinson's disease. N Engl J Med. 2001;344(10):710-9.

73) Freed CR. Will embryonic stem cells be a useful source of dopamine neurons for transplant into patients with Parkinson's disease? Proc Natl Acad Sci U S A. 2002 19;99(4):1755-7.

74) Freeman TB, Olanow CW, Hauser RA, et al. Bilateral fetal nigral transplantation into the postcommissural putamen in Parkinson's disease. *Ann Neurol* 1995; 38: 379-388.

75) Friston KJ, Frith CD, Liddle PF, Frackowiak RS. Plastic transformation of PET images. J Comput Assist Tomogr. 1991 Jul-Aug;15(4):634-9

76) Friston KJ, Frith CD, Liddle PF, Frackowiak RS. Comparing functional (PET) images: the assessment of significant change. J Cereb Blood Flow Metab. 1991 Jul;11(4):690-9.

77) Friston KJ, Frith CD, Liddle PF, Frackowiak RS. Functional connectivity: the principal-component analysis of large (PET) data sets. J Cereb Blood Flow Metab. 1993 Jan;13(1):5-14

78) Friston KJ, Ashburner J, Frith CD, Poline JB, Heather JD, Frackowiak RSJ. Spatieal registration and normalization of images. Hum Brain Mapp 1995a; 2: 1165-189.

79) Friston KJ, Holmes AP, Worsley KJ, Poline JB, Frith CD, Frackowiak RSJ. Statistical parametric maps in functional imaging: a general linear approach. Hum Brain Mapp 1995b; 2: 189-210.

80) Frodl EM, Sauer H, Lindvall O, Brundin P. Effects of hibernation or cryopreservation on the survival and integration of striatal grafts placed in the ibotenate-lesioned rat caudate-putamen.Cell Transplant. 1995;4(6):571-7.

81) Funayama M, Hasegawa K, Kowa H. A new locus for Parkinson's disease (PARK8) maps to chromosome 12p11.2-q13.1. Ann Neurol. 2002;51(3):296-301

82) Gai WP, Power JH, Blumbergs PC, Blessing WW. Multiple-system atrophy: a new alpha-synuclein disease? Lancet. 1998;352(9127):547-8

83) Galvin JE, Lee VM, Trojanowski JQ. Synucleinopathies: clinical and pathological implications. Arch Neurol. 2001;58(2):186-90.

84) Garnett ES, Firnau G, Nahmias C. Dopamine visualised in the basal ganglia of living man. Nature 1983;305:137-138.

85) Gasser T, Muller-Myhsok B, Wszolek ZK, Oehlmann R, Calne DB, Bonifati V, Bereznai B, Fabrizio E, Vieregge P, Horstmann RD. A susceptibility locus for Parkinson's disease maps to chromosome 2p13. Nat Genet. 1998;18(3):262-5.

86) Gerfen, C.R. *et al.* D1 and D2 dopamine receptor-regulated gene expression of striatonigral and striatopallidal neurons. *Science* 250, 1429-1432 (1990).

87) Gibb W, Lees A. The relevance of the Lewy body to the pathogenesis of idiopathic Parkinson's disease. J Neurol Neurosurg Psychiatry 1988;51:745-52.

88) Ginovart N, Farde L, Haldin C, Swahn CG. Changes in striatal D2-density following chronic treatment with amphetamine assessed with PET in nonhuman primates. Synapse 1999; 31:154-162.

89) Goetz CG, Stebbins GT, Shale HM, Lang AE, Chernik DA, Chmura TA, Ahlskog JE, Dorflinger EE. Utility of an objective dyskinesia rating scale for Parkinson's disease: inter- and intrarater reliability assessment. Mov Disord. 1994 ; 9(4):390-394.

90) Golbe LI. The genetics of Parkinson's disease: a reconsideration. Neurology 1990;40 (Suppl 3):7-14

91) Goldberg G. Supplementary motor area structure and function: review and hypotheses. Behav Brain Sci 1985; 8: 567-569.

92) Grace AA. Phasic versus tonic dopamine release and the modulation of dopamine system responsivity: a hypothesis for the aetiology of schizophrenia. Neuroscience 1991; 44: 1-24.

93) Green PE, Fahn S, Tsai WY, Breeze RE, Eidelberg D, Winfield H, Dillon S, Kao R, Winfield L, Freed CR. Severe spontaneous dyskinesias: a disabling complication of embryonic dopaminergic tissue implants in a subset of transplanted patients with advanced Parkinson's disease. Mov Disord 1999; 14(5):904.

94) Griffiths PD, Perry RH, Crossman AR. A detailed anatomical analysis of neurotransmitter receptors in the putamen and caudate in Parkinson's disease and Alzheimer's disease. Neurosci Lett 1994; 169(1-2):68-72.

95) Grootoonk S, Spinks TJ, Jones T. Correection for scatter using a dual energy window technique with a tomograph operated without septa. IEEE Medical Imaging Conf 1992; 3:1569 - 1573.

96) Gunn, R.N., Lammertsma, A.A., Hume, S.P., Cunningham V.J. Parametric imaging of ligand-receptor binding in PET using a simplified reference region model. Neuroimage 6, 279-287 (1997)

97) Guttman M, Seeman P. L-dopa reverses the elevated density of D2 dopamine receptors in Parkinson's diseased striatum. J Neural Transm 1985; 64(2):93-103.

98) Guttman M, Yong VW, Kin SU, et al. . Asymptomatic striatal dopamine depletion: PET scans in unilateral MPTP monkeys. Synapse 1988;2:469-473.

99) Guttman, M., Seeman, P. Dopamine D2 receptor density in parkinsonian brain is constant for duration of disease, age, and duration of L-dopa therapy. Adv. Neurol. 45, 51-57 (1986).

100) Hagell P, Schrag A, Piccini P, Jahanshahi M, Brown R, Rehncrona S, Widner H, Brundin P, Rothwell JC, Odin P, Wenning GK, Morrish P, Gustavii B, Bjorklund A, Brooks DJ, Marsden CD, Quinn NP, Lindvall O. Sequential bilateral transplantation in Parkinson's disease: Effects of the second graft. Brain 1999; 122: 1121-1132.

101) Hagell P, Widner H. Clinical rating of dyskinesias in Parkinson's disease: use and reliability of a new rating scale. Mov Disord. 1999; 14(3):448-55.

102) Hall H, Farde L, Halldin C, Hurd YL, Pauli S, Sedvall G. Autoradiographic localization of extrastriatal D2-dopamine receptors in the human brain using [125I]epidepride. Synapse 1996; 23(2):115-123.

103) Halldin C, Farde L, Hogberg T, Mohell N, Hall H, Suhara T, Karlsson P, Nakashima Y, Swahn CG. Carbon-11-FLB 457: a radioligand for extrastriatal D2 dopamine receptors. J Nucl Med 1995; 36(7):1275-1281.

104) Hasegawa K, Kowa H. Autosomal dominant familial Parkinson disease: older onset of age, and good response to levodopa therapy. Eur Neurol. 1997;38 Suppl 1:39-43.

105) Hashimoto M, Masliah E. Alpha-synuclein in Lewy body disease and Alzheimer's disease. Brain Pathol. 1999;9(4):707-20.

106) Hattori N, Kitada T, Matsumine H, Asakawa S, Yamamura Y, Yoshino H, Kobayashi T, Yokochi M, Wang M, Yoritaka A, Kondo T, Kuzuhara S, Nakamura S, Shimizu N, Mizuno Y. Molecular genetic analysis of a novel Parkin gene in Japanese families with autosomal recessive juvenile parkinsonism: evidence for variable homozygous deletions in the Parkin gene in affected individuals. Ann Neurol 1998; 44(6):935-941.

107) Hauser RA, Freeman TB, Snow BJ, et al. Long-term evaluation of bilateral fetal nigral transplantation in Parkinson`s disease. Arch Neurol 1999; 56: 179-187.

108) Hayashi S, Wakabayashi K, Ishikawa A, et al. An autopsy case of autosomal recessive juvenile parkinsonism with a homozygous exon 4 deletion in the *parkin* gene. Mov Dis 2000;15:884-888.

109) Herman, J.P., Rouge-Pont, F., Le Moal, M. & Abrous, D.N. Mechanisms of amphetamine-induced rotation in rats with unilateral intrastriatal grafts of embryonic dopaminergic neurons: a pharmacological and biochemical analysis. Neuroscience 53,1083-1095 (1993).

110) Hernit-Grant CS, Macklis JD. Embryonic neurons transplanted to regions of targeted photolytic cell death in adult mouse somatosensory cortex re-form specific callosal projections. Exp Neurol. 1996;139(1):131-42.

111) Hilker R, Klein C, Ghaemi M, et al. Positron Emission Tomographic Analysis of the Nigrostriatal Dopaminergic System in Familial Parkinsonism associated with Mutations in the *Parkin* gene. Ann Neurol 2001;49:367-376.

112) Hoehn MM, Yahr MD. Parkinsonism: onset, progression and mortality. Neurology 1967; 17:427-442.

113) Hoffer BJ, Leenders KL, Young D, Gerhardt G, Zerbe GO, Bygdeman M, Seiger A, Olson L, Stromberg I, Freedman R. Eighteen-month course of two patients with grafts of fetal dopamine neurons for severe Parkinson's disease.Exp Neurol. 1992;118(3):243-252.

114) Hoffman EJ, Huang S-C, Phelps ME. Quantitation in positron computed tomography. 1. Effect of object size. J Comp Assist Tomogr 1979;3:299 - 302.

115) Irwin I, Langston JW, DeLanney LE. 4-Phenylpyridine (4PP) and MPTP: the relationship between striatal MPP+ concentrations and neurotoxicity. Life Sci. 1987 Feb 23;40(8):731-40.

116) Ishikawa A, Tsuji S. Clinical analysis of 17 patients in 12 Japanese families with autosomal-recessive type juvenile parkinsonism. Neurology. 1996;47(1):160-6.

117) Itokawa M, Toru M, Ito K, et al. Sequestration of the short and long isoforms of dopamine D2 receptors expressed in Chinese hamster ovary cells. Mol Pharmacol 1996; 49: 560-566.

118) Jahanshahi M, Jenkins IH, Brown RG, Marsden CD, Passingham RE, Brooks DJ. Self-initiated versus externally triggered movements. I. An investigation using measurement of regional cerebral blood flow with PET and movement-related potentials in normal and Parkinson's disease subjects. Brain. 1995;118: 913-33.

119) Jenkins IH, Fernandez W, Playford ED, Lees AJ, Frackowiak RS, Passingham RE, Brooks DJ. Impaired activation of the supplementary motor

area in Parkinson's disease is reversed when akinesia is treated with apomorphine. Ann Neurol 1992; 32: 749-757.

120) Johnson WG, Hodge SE, Duvoisin RC. Twin studies and the genetics of Parkinson's disease. Mov Disord 1990;3:187-194

121) Jones AC, Yamamura Y, Almasy L, Bohlega S, Elibol B, Hubble J, Kuzuhara S, Uchida M, Yanagi T, Weeks DE, Nygaard TG. Autosomal recessive juvenile parkinsonism maps to 6q25.2-q27 in four ethnic groups: detailed genetic mapping of the linked region.Am J Hum Genet. 1998;63(1):80-7.

122) Joyce JN, Goldsmith SG, Gurevich EV. Limbic circuits and monoamine receptors: dissecting the effects of antipsychotics from disease processes. J Psychiatr Res 1997; 31(2):197-217

123) Joyce JN, Myers AJ, Gurevich E. Dopamine D2 receptor bands in normal human temporal cortex are absent in Alzheimer's disease. Brain Res 1998; 784(1-2):7-17.

124) Kaasinen V, Nagren K, Hietala J, Oikonen V, Vilkman H, Farde L, Halldin C, Rinne JO. Extrastriatal dopamine D2 and D3 receptors in early and advanced Parkinson's disease. Neurology 2000; 54(7):1482-1487.

125) Kadekaro M, Crane AM, Sokoloff L. Differential effects of electrical stimulation of sciatic nerve on metabolic activity in spinal cord and dorsal root ganglion in the rat. Proc Natl Acad Sci U S A. 1985; 82(17): 6010-3.

126) Kessler RM, Whetsell WO, Ansari MS, Votaw JR, de Paulis T, Clanton JA, Schmidt DE, Mason NS, Manning RG. Identification of extrastriatal dopamine D2 receptors in post mortem human brain with [125I]epidepride. Brain Res 1993; 609(1-2):237-243.

127) Khan NL, Graham E, Critchley P, Schrag AE, Wood NW, Lees AJ, Bhatia KP, Quinn N. Parkin disease: a phenotypic study of a large case series. Brain. 2003;126:1279-92.

128) Kitada T, Asakawa S, Hattori N, Matsumine H, Yamamura Y, Minoshima S, Yokochi M, Mizuno Y, Shimizu N. Mutations in the parkin gene cause autosomal recessive juvenile parkinsonism. Nature. 1998;392(6676):605-8.

129) Kish SJ, Shannak K, Hornykiewicz O, Uneven pattern of dopamine in the striatum of patients with idiopathic Parkinson's disease: pathophysiologic and clinical implications. N Engl Med 1988; 318: 876-880.

130) Klein C, Vieregge P, Hagenah J, Sieberer M, Doyle E, Jacobs H, Gasser T, Breakefield XO, Risch NJ, Ozelius LJ. Search for the PARK3 founder haplotype in a large cohort of patients with Parkinson's disease from northern Germany. Ann Hum Genet. 1999;63 (Pt 4):285-91.

131) Koepp, M.J. *et al*. Evidence for striatal dopamine release during a videogame. Nature 393, 266-268 (1998).

132) Kordower JH, Freeman TB, Chen EY, et al. Fetal nigral grafts survive and mediate clinical benefit in a patient with Parkinson's disease. Mov Disord 1998; 13: 383-393.

133) Kordower JH, Freeman TB, Snow BJ, et al. Neuropathological evidence of graft survival and striatal reinnervation after the transplantation of fetal mesencephalic tissue in a patient with Parkinson's disease. N Engl J Med 1995; 332: 1118-1124.

134) Kordower JH, Rosestein JM, Collier TJ, et al. Functional fetal nigral grafts in a patient with Parkinson`s disease: chemoanatomic, ultrastructural, and metabolic studies. J Comp Neurol 1996; 370: 203-230.

135) Kruger R, Eberhardt O, Riess O, Schulz JB. Parkinson's disease: one biochemical pathway to fit all genes? Trends Mol Med. 2002;8(5):236-40.

136) Kruger R, Kuhn W, Muller T, Woitalla D, Graeber M, Kosel S, Przuntek H, Epplen JT, Schols L, Riess O. Ala30Pro mutation in the gene encoding alpha-synuclein in Parkinson's disease. Nat Genet. 1998;18(2):106-8

137) Kruger R, Vieira-Saecker AM, Kuhn W, Berg D, Muller T, Kuhnl N, Fuchs GA, Storch A, Hungs M, Woitalla D, Przuntek H, Epplen JT, Schols L, Riess O. Increased susceptibility to sporadic Parkinson's disease by a certain combined alpha-synuclein/apolipoprotein E genotype. Ann Neurol. 1999;45(5):611-7

138) Laihinen A, Rinne JO, Rinne UK, et al. [18F]-6-Fluorodopa PET scanning in Parkinson's disease after selective COMT inhibition with nitecapone (OR-462). Neurology 1992;42:199-203.

139) Langston JW, Widner H, Goetz CG, Brooks D, Fahn S, Freeman T, Watts R. Core assessment program for intracerebral transplantations (CAPIT). Mov Disord. 1992;7(1):2-13

140) Laruelle M, Abi-Dargham A, Van Dyck CH, et al. SPECT imaging of striatal dopamine release after amphetamine challenge. J Nucl Med 1995: 36: 1182-1190.

141) Laruelle M. Imaging synaptic neurotransmission with in vivo binding competition techniques: a critical review. J Cereb Blood Flow Metab 2000; 20:423-451.

142) Laruelle M. Imaging synaptic neurotransmission with in vivo binding competition techniques: a critical review. J Cereb Blood Flow Metab 2000: 20:423-451.

143) Laruelle M., *et al.* Microdialysis and SPECT measurements of amphetamine-induced release in nonhuman primates. Synapse 25, 1-14 (1997).

144) Lazzarini AM, Myers RH, Zimmerman TR Jr, Mark MH, Golbe LI, Sage JI, Johnson WG, Duvoisin RC. A clinical genetic study of Parkinson's disease: evidence for dominant transmission. Neurology. 1994;44:499-506

145) Lee CS, Cenci MA, Schulzer M, Bjorklund A. Embryonic ventral mesencephalic grafts improve levodopa-induced dyskinesia in a rat model of Parkinson's disease. Brain. 2000;123:1365-79.

146) Lee, T., Seeman, P., Rajput, A., Farley, I.J. & Hornykiewicz, O. Receptor basis for dopaminergic supersensitivity in Parkinson's disease. Nature 273, 59-61(1978).

147) Leenders KL. [18F]Fluorodopa uptake in brain. In: Baron JC, Comar D, Farde L, Martinot JL, Mazoyer B, eds. Brain dopaminergic systems: Imaging with positron emission tomography. Dordrecht: Kluwer Academic, 1991:97-110.

148) Leroy E, Anastasopoulos D, Konitsiotis S, Lavedan C, Polymeropoulos MH. Deletions in the Parkin gene and genetic heterogeneity in a Greek family with early onset Parkinson's disease. Hum Genet. 1998;103(4):424-7

149) Leroy E, Boyer R, Auburger G, Leube B, Ulm G, Mezey E, Harta G, Brownstein MJ, Jonnalagada S, Chernova T, Dehejia A, Lavedan C, Gasser T, Steinbach PJ, Wilkinson KD, Polymeropoulos MH. The ubiquitin pathway in Parkinson's disease. Nature. 1998;395(6701):451-2.

150) Lidow MS, Goldman-Rakic PS, Rakic P, Innis RB. Dopamine D2 receptors in the cerebral cortex: distribution and pharmacological characterization with [3H]raclopride. Proc Natl Acad Sci U S A 1989; 86(16):6412-6416.

151) Lindvall O, Widner H, Rehncrona S, et al. Transplantation of fetal dopamine neurons in Parkinson's disease: one-year clinical and neurophysiological observations in two patients with putaminal implants. Ann Neurol 1992; 31: 155-165.

152) Lindvall O, Brundin P, Widner H, et al. Grafts of fetal dopamine neurons survive and improve motor function in Parkinson` s disease. Science 1990; 247: 574-577.

153) Lindvall O, Hagell P. Clinical observations after neural transplantation in Parkinson's disease. Prog Brain Res. 2000;127:299-320. Review.

154) Lindvall O, Rehncrona S, Brundin P, Gustavii B, Astedt B, Widner H, Lindholm T, Bjorklund A, Leenders KL, Rothwell JC, et al. Human fetal dopamine neurons grafted into the striatum in two patients with severe Parkinson's disease: A detailed account of methodology and a 6-month follow-up. Arch Neurol. 1989;46(6):615-631

155) Lindvall O, Sawle GV, Widner H, et al. Evidence for long-term survival and function of dopaminergic grafts in progressive Parkinson`s disease. Ann Neurol 1994; 35: 172 -180.

156) Lindvall, O. Cerebral implantation in movement disorders: State of the art. Mov. Disord. 14, 201-205 (1999).

157) Lippa CF, Schmidt ML, Lee VM, Trojanowski JQ. Antibodies to alpha-synuclein detect Lewy bodies in many Down's syndrome brains with Alzheimer's disease. Ann Neurol. 1999;45(3):353-7

158) Lucking CB, Abbas N, Durr A, Bonifati V, Bonnet AM, de Broucker T, De Michele G, Wood NW, Agid Y, Brice A. Homozygous deletions in parkin gene in European and North African families with autosomal recessive juvenile parkinsonism. The European Consortium on Genetic Susceptibility in Parkinson's Disease and the French Parkinson's Disease Genetics Study Group. Lancet. 1998;352(9137):1355-6.

159) Lucking CB, Durr A, Bonifati V, Vaughan J, De Michele G, Gasser T, Harhangi BS, Meco G, Denefle P, Wood NW, Agid Y, Brice A. Association between early-onset Parkinson's disease and mutations in the parkin gene. French Parkinson's Disease Genetics Study Group. N Engl J Med. 2000;342(21):1560-7.

160) Luquin MR, Scipioni O, Vaamonde J, Gershanik O, Obeso JA. Levodopa-induced dyskinesias in Parkinson's disease: clinical and pharmacological classification. Mov Disord. 1992;7(2):117-24.

161) Madrazo I, Drucker-Colin R, Diaz V, Martinez-Mata J, Torres C, Becerril JJ. Open microsurgical autograft of adrenal medulla to the right caudate nucleus in two patients with intractable Parkinson's disease. N Engl J Med. 1987;316(14):831-4.

162) Madrazo I, Leon V, Torres C, Aguilera MC, Varela G, Alvarez F, Fraga A, Drucker-Colin R, Ostrosky F, Skurovich M, et al. Transplantation of fetal substantia nigra and adrenal medulla to the caudate nucleus in two patients with Parkinson's disease. N Engl J Med. 1988;318(1):51

163) Maraganore DM, Farrer MJ, Hardy JA, Lincoln SJ, McDonnell SK, Rocca WA. Case-control study of the ubiquitin carboxy-terminal hydrolase L1 gene in Parkinson's disease. Neurology. 1999;53(8):1858-60

164) Marder K, Tang MX, Mejia H, Alfaro B, Cote L, Louis E, Groves J, Mayeux R. Risk of Parkinson's disease among first-degree relatives: A community-based study. Neurology. 1996 Jul;47(1):155-60

165) Marsden CD, Linazasoro G, Obeso JA. An introduction to the new surgery for Parkinson's disease. Past and present problems. Adv Neurol. 1997;74:143-7. Review.

166) Marsden CD, Parkes JD. Success and problems of long-term levodopa therapy in Parkinson's disease. Lancet. 1977;1(8007):345-9.

167) Martin WRW, Palmer MR, Patlak CS, Calne DB. Nigrostriatal function in humans studied with positron emission tomography. Ann Neurol 1989;26:535-542.

168) Marttila RJ, Kaprio J, Koskenvuo MD, Rinne UK. Parkinson's disease in a nationwide twin cohort. Neurology 1988;38:1217-1219.

169) Martyn CN and Osmond C. Parkinson's disease and the environment in early life. J Neurol Sci 1995;132;201-206.

170) Maruyama M, Ikeuchi T, Saito M, Ishikawa A, Yuasa T, Tanaka H, Hayashi S, Wakabayashi K, Takahashi H, Tsuji S. Novel mutations, pseudo-dominant inheritance, and possible familial affects in patients with autosomal recessive juvenile parkinsonism. Ann Neurol 2000; 48(2):245-250.

171) Masliah E, Rockenstein E, Veinbergs I, Mallory M, Hashimoto M, Takeda A, Sagara Y, Sisk A, Mucke L. Dopaminergic loss and inclusion body

formation in alpha-synuclein mice: implications for neurodegenerative disorders. Science. 2000;287(5456):1265-9

172) Matsumine H, Saito M, Shimoda-Matsubayashi S, Tanaka H, Ishikawa A, Nakagawa-Hattori Y, Yokochi M, Kobayashi T, Igarashi S, Takano H, Sanpei K, Koike R, Mori H, Kondo T, Mizutani Y, Schaffer AA, Yamamura Y, Nakamura S, Kuzuhara S, Tsuji S, Mizuno Y. Localization of a gene for an autosomal recessive form of juvenile Parkinsonism to chromosome 6q25.2-27. Am J Hum Genet. 1997;60:588-596.

173) Melega WP, Luxen A, Perlmutter MM, Nissenson CHK, Phelps ME, Barrio JR. Comparative in vivo metabolism of 6-[18F]fluoro-L-dopa and [3H]L-dopa in rats. Biochem Pharmacol 1990;39:1853-1860.

174) Mendez I, Dagher A, Hong M, Hebb A, Gaudet P, Law A, Weerasinghe S, King D, Desrosiers J, Darvesh S, Acorn T, Robertson H. Enhancement of survival of stored dopaminergic cells and promotion of graft survival by exposure of human fetal nigral tissue to glial cell line--derived neurotrophic factor in patients with Parkinson's disease. Report of two cases and technical considerations. J Neurosurg. 2000; 92(5):863-869.

175) Meyer JH, Gunn RN, Myers R, Grasby PM. Assessment of spatial normalization of PET ligand images using ligand-specific templates. Neuroimage 1999; 9: 545-553.

176) Moghaddam B, Berridge CW, Goldman-Rakic PS, Bunney BS, Roth RH. In vivo assessment of basal and drug-induced dopamine release in cortical and subcortical regions of the anaesthetized primate. Synapse 1993; 13: 215-222.

177) Mori H, Kondo T, Yokochi M, et al. Pathologic and biochemical studies of juvenile parkinsonism linked to chromosome 6q. Neurology 1998;51:890-892.

178) Morris ME, Churchyard A, Iansek R. How to conduct a dose rensponse trial of Parkinson's disease medication. Austrialian Journal of Physiotherapy. 1998; 44: 131-133.

179) Morris RG, Downes JJ, Sahakian BJ, Evenden JL, Heald A, Robbins TW. Planning and spatial working memory in Parkinson's disease. J Neurol Neurosurg Psychiatry 1988; 51: 757-766.

180) Nahmias C, Garnett ES, Firnau G, Lang A. Striatal dopamine distribution in Parkinsonian patients during life. J Neurol Sci 1985;69:223-230.

181) Neve, K.A., Altar, C.A., Wong, C.A., Marshall, J.F. Quantitative analysis of 3H-spiroperidol binding to rat forebrain sections: plasticity of neostriatal dopamine receptors after nigrostriatal injury. Brain Res. 302, 9-18 (1984).

182) Nishino, H. *et al.* Long-term survival of grafted cells, dopamine synthesis/release, synaptic connections, and functional recovery after transplantation of fetal nigral cells in rats with unilateral 6-OHDA lesions in the nigrostriatal dopamine pathway. Brain Res. 534, 83-93 (1990).

183) Nudo RJ, Masterton RB. Stimulation-induced [14C]2-deoxyglucose labeling of synaptic activity in the central auditory system. J Comp Neurol. 1986; 245(4): 553-65.

184) Nutt JG. Clinical pharmacology of levodopa-induced dyskinesia. Ann Neurol. 2000; 47(4 Suppl 1):S160-1644. Review.

185) Olanow, C.W., Kordower, J.H. & Freeman, T.B. Fetal nigral transplantation as a therapy for Parkinson's disease. Trends Neurosci. 19, 102-109 (1996).

186) Olanow CW, Goetz CG, Kordower JH, Stoessl AJ, Sossi V, Brin MF, Shannon KM, Nauert GM, Perl DP, Godbold J, Freeman TB. A double-blind controlled trial of bilateral fetal nigral transplantation in Parkinson's disease. Ann Neurol. 2003; 54(3):403-14.

187) Oliveira SA, Scott WK, Martin ER, et al. Parkin mutations and susceptibility alleles in late-onset Parkinson's disease. Ann Neurol. 2003; 53: 624-629.

188) Olson L, Malmfors T. Growth characteristics of adrenergic nerves in the adult rat. Fluorescence histochemical and 3H-noradrenaline uptake studies using tissue transplantations to the anterior chamber of the eye. Acta Physiol Scand Suppl. 1970;348:1-112.

189) Olson L, Seiger A. Brain tissue transplanted to the anterior chamber of the eye. 1. Fluorescence histochemistry of immature catecholamine and 5-hydroxytryptamine neurons reinnervating the rat iris. Z Zellforsch Mikrosk Anat. 1972;135(2):175-94

190) Otsuka M, Ichiya Y, Hosokawa S, et al. Striatal blood flow, glucose metabolism and 18F-dopa uptake: difference in Parkinson's disease and atypical parkinsonism. J Neurol Neurosurg Psychiatry 1991;54:898-904.

191) Owen AM, Roberts AC, Hodges JR, Summers BA, Polkey CE, Robbins TW. Contrasting mechanisms of impaired attentional set-shifting in patients with frontal lobe damage or Parkinson's disease. Brain 1993; 116: 1159-75.

192) Owen AM, Sahakian BJ, Hodges JR, Summers BA, Polkey CE. Robbins TW. Dopamine-dependent frontostriatal planning deficits in early Parkinson's disease. Neuropsychology 1995; 9:126-140.

193) Owen AM, Doyon J, Dagher A, Sadikot A, Evans AC Abnormal basal ganglia outflow in Parkinson's disease identified with PET: implication for higher cortical functions. Brain 1998; 121: 949-965.

194) Papadimitriou A, Veletza V, Hadjigeorgiou GM, Patrikiou A, Hirano M, Anastasopoulos I. Mutated alpha-synuclein gene in two Greek kindreds with familial PD: incomplete penetrance? Neurology. 1999;52(3):651-4.

195) Parkinson J. An essay on the shaking palsy. Sherwood, Neely and Jones. London 1817.

196) Patlak CS, Blasberg RG. Graphical evaluation of blood-to-brain transfer constants from multiple time uptake data. Generalisations. J Cereb Blood Flow Metab 1985;5:584-590.

197) Payami H, Larsen K, Bernard S, Nutt J. Increased risk of Parkinson's disease in parents and siblings of patients. Ann Neurol. 1994 Oct;36(4):659-61.

198) Perlow MJ, Freed WJ, Hoffer BJ, Seiger A, Olson L, Wyatt RJ. Brain grafts reduce motor abnormalities produced by destruction of nigrostriatal dopamine system. Science. 1979;204(4393):643-7.

199) Peschanski M, Defer G, N'Guyen JP, et al. Bilateral motor improvement and alteration of L-dopa effect in two patients with Parkinson's disease following intrastriatal transplantation of foetal ventral mesencephalon. Brain 1994; 117: 487-499.

200) Phelps ME Emission computed tomography. Seminars in Nuclear Medicine 1977;7;337 - 365.

201) Phillips DIW. Twin studies in medical research :can they tell us whether diseases are genetically determined? Lancet 1993; i:1008-1009.

202) Piccini P, Brooks DJ, Bjorklund A, et al. Dopamine release from nigral transplants visualized *in vivo* in a Parkinson`s patient. Nat Neuroscience 1999; 2(12): 1137-1140.

203) Piccini P, Morrish PK, Turjanski N, et al. Dopaminergic function in familial Parkinson's disease: a clinical and ^{18}F-dopa positron emission tomography study. Ann Neurol 1997;41:222-228

204) Playford ED, Jenkins IH, Passingham RE, Nutt J, Frackowiak RS, Brooks DJ. Impaired mesial frontal and putamen activation in Parkinson's disease: a positron emission tomography study.Ann Neurol. 1992;32:151-61.

205) Poewe W and Granata R. in Movement Disorders, Neurological Principles and practice. Eds Watts RL and Koller WC. McGraw-Hill, New York; 1997 pp 201-209

206) Poline JB, Holmes AP, Worsley K, Friston KJ. Making statistical infereces. In: Human Brain Function. Frackowiak RSJ, Friston KJ, Frith CD, Dolan RF, Mazziotta JC (eds.) Academic Press. 1997, pp 85-106.

207) Pollak P, Benabid AL, Limousin P, Benazzouz A. Chronic intracerebral stimulation in Parkinson's disease. Adv Neurol. 1997;74:213-20.

208) Polymeropoulos MH, Higgins JJ, Golbe LI, Johnson WG, Ide SE, Di Iorio G, Sanges G, Stenroos ES, Pho LT, Schaffer AA, Lazzarini AM, Nussbaum RL, Duvoisin RC. Mapping of a gene for Parkinson's disease to chromosome 4q21-q23. Science. 1996;274(5290):1197-9.

209) Polymeropoulos MH, Lavedan C, Leroy E, Ide SE, Dehejia A, Dutra A, Pike B, Root H, Rubenstein J, Boyer R, Stenroos ES, Chandrasekharappa S,

Athanassiadou A, Papapetropoulos T, Johnson WG, Lazzarini AM, Duvoisin RC, Di Iorio G, Golbe LI, Nussbaum RL. Mutation in the alpha-synuclein gene identified in families with Parkinson's disease. Science. 1997;276(5321):2045-7.

210) Portman AT, Giladi N, Leenders KL, Maguire P, Veenma-van der Duin L, Swart J, Pruim J, Simon ES, Hassin-Baer S, Korczyn AD. The nigrostriatal dopaminergic system in familial early onset parkinsonism with parkin mutations. Neurology 2001; 56(12):1759-1762.

211) Pramstaller PP, Kunig G, Leenders K, Kann M, Hedrich K, Vieregge P, Goetz CG, Klein C. Parkin mutations in a patient with hemiparkinsonism--hemiatrophy: A clinical--genetic and PET study. Neurology 2002; 58(5):808-810.

212) Raisman G. Use of Schwann cells to induce repair of adult CNS tracts. Rev Neurol (Paris). 1997;153(8-9):521-5. Review.

213) Rakshi JS, Uema T, Ito K, et al. Frontal, midbrain and striatal dopaminergic function in early and advanced Parkinson's disease. A 3D [18F]dopa-PET study. Brain 1999; 122: 1637-50.

214) Rehncrona S. A Critical review of the current status and possible developments in brain transplantation. Adv Tech Stand Neurosurg 1997; 23: 3-46.

215) Reith J, Dyve S, Kuwabara H, Guttman M, Diksic M, Gjedde A. Blood-brain transfer and metabolism of 6-[18F]fluoro-L-dopa in rat. J Cereb Blood Flow Metab 1990;10:707-719.

216) Remy P, Samson Y, Hantraye P, et al. Clinical correlates of ^{18}F-dopa uptake in five grafted parkinsonian patients. Ann Neurol 1995; 38: 580-588.

217) Ribeyre JM, Lesieur P, Varoquaux O, Dollfus S, Pays M, Petit M. A comparison of plasma homovanillic acid in the deficit and nondeficit subtypes of schizophrenia. Biol Psychiatry 1994; 36(4):230-236.

218) Rinne, U.K. et al. Positron emission tomography demonstrates dopamine D2 receptor supersensitivity in the striatum of patients with early Parkinson's disease. Mov. Disord. **5,** 55-59 (1990).

219) Rinne JO, Portin R, Ruottinen H, et al. Cognitive impairment and the brain dopaminergic system in Parkinson disease: [18F]fluorodopa positron emission tomographic study. Arch Neurol 2000; 57: 470-5.

220) Rioux, L. *et al.* Correlation of functional recovery after a 6-hydroxydopamine lesion with survival of grafted fetal neurons and release of dopamine in the striatum of the rat. Neuroscience 40, 123-131 (1991).

221) Robbins TW, James M, Owen AM, et al. Cognitive deficits in progressive supranuclear palsy, Parkinson's disease, and multiple system atrophy in tests sensitive to frontal lobe dysfunction. J Neurol Neurosurg Psychiatry 1994; 57: 79-88.

222) Ross SB, Jackson DM. Kinetic properties of the in vivo accumulation of the dopamine D2 receptor antagonist raclopride in the mouse brain. Naunyn Schmiedebergs Arch Pharmacol 1989; 340: 6-12

223) Ross SB, Jackson DM. Kinetic properties of the in vivo accumulation of the dopamine D2 receptor antagonist raclopride in the mouse brain. Naunyn Schmiedebergs Arch Pharmacol 1989; 340: 6-12.

224) Samuel M, Ceballos-Bauman AO, Turjanski N, et al. Pallidotomy in Parkinson`s disease increases supplementary motor area and prefrontal

activation during performance of volitional movements. An H215O PET study. Brain 1997; 120: 1301-1313.

225) Sauer H, Brundin P. Effects of cool storage on survival and function of intrastriatal ventral mesencephalic grafts. Rest Neurol Neurosci 1991: 2: 123-135.

226) Savasta, M., Dubois, A., Benavides, J., Scatton, B. Different plasticity changes in D-1 and D-2 receptors in rat striatal subregions following impairment of dopaminergic transmission. Neurosci Lett 85, 119-124 (1988).

227) Sawle GV, Bloomfield PM, Bjorklund A, Brooks DJ, Brundin P, Leenders KL, Lindvall O, Marsden CD, Rehncrona S, Widner H, et al. Transplantation of fetal dopamine neurons in Parkinson's disease: PET [18F]6-L-fluorodopa studies in two patients with putaminal implants. Ann Neurol. 1992 Feb;31(2):166-73.

228) Sawle GV, Colebatch JG, Shah A, Brooks DJ, Marsden CD, Frackowiak RSJ. Striatal function in normal ageing: Implications for Parkinson's disease. Ann Neurol 1990;28:799-804.

229) Sawle GV, Playford ED, Burn DJ, et al. Separating Parkinson's disease from normality. Discriminant function analysis of fluorodopa F18 positron emission tomography data. Arch Neurol 1994;31:237-243.

230) Sawle GV, Wroe SJ, Lees AJ, et al. The Identification of Presymptomatic Parkinsonism: Clinical and [18F]-dopa Positron Emission Tomography studies in Irish Kindred. Ann Neurol 1992;32:609-617.

231) Sawle, G.V., Playford, E.D., Brooks, D.J., Quinn, N., & Frackowiak R.S.J. Asymmetrical pre-synaptic and post-synaptic changes in the striatal dopamine projection in dopa naive parkinsonism. Brain. 116, 853-867 (1993).

232) Scatton B, Rouquier L, Javoy-Agid F, Agid Y. Dopamine deficiency in the cerebral cortex in Parkinson disease. Neurology 1982; 32(9):1039-1040.

233) Scatton B, Javoy-Agid F, Rouquier L, Dubois B, Agid Y. Reduction of cortical dopamine, noradrenaline, serotonin and their metabolites in Parkinson's disease. Brain Res 1983; 275: 321-328.

234) Schlaepfer TE, Pearlson GD, Wong DF, Marenco S, Dannals RF. PET study of competition between intravenous cocaine and [C-11]raclopride at dopamine receptors in human subjects. Arch J Psychiatry 1997; 154: 1209-1213.

235) Seeman, P. *et al.* Human brain D1 and D2 receptors in schizophrenia, Alzheimer's, Parkinsons's and Huntingtons's diseases. Neuropsychopharmacology 1, 5-15 (1987).

236) Shimura H, Schlossmacher MG, Hattori N, Frosch MP, Trockenbacher A, Schneider R, Mizuno Y, Kosik KS, Selkoe DJ. Ubiquitination of a new form of alpha-synuclein by parkin from human brain: implications for Parkinson's disease. Science 2001; 293(5528):263-269.

237) Snow BJ, Peppard RF, Guttman M, et al. Positron emission tomography scanning demonstrates a presynaptic dopaminergic lesion in Lytico-Bodig. The amyotrophic lateral sclerosis-parkinsonism-dementia complex of Guam. Arch Neurol 1990;47:870-874.

238) Snyder EY, Yoon C, Flax JD, Macklis JD. Multipotent neural precursors can differentiate toward replacement of neurons undergoing targeted apoptotic degeneration in adult mouse neocortex. Proc Natl Acad Sci U S A. 1997;94(21):11663-8.

239) Sotelo C, Alvarado-Mallart RM. The reconstruction of cerebellar circuits. Trends Neurosci. 1991;14(8):350-5. Review

240) Spillantini MG, Schmidt ML, Lee VM, Trojanowski JQ, Jakes R, Goedert M. Alpha-synuclein in Lewy bodies. Nature. 1997;388(6645):839-40

241) Spinks TJ, Bailey DL, Bloomfield PM, Miller M, Murayama H et al. Performanc eof a new 3D-only PET scanner – the EXACT 3D. IEEE Nuclear Science symposium and Medical Imaging conference. Anaheim , California:Piscataway, NJ. 1996;2:1275-1279.

242) Spinks TJ, Tones T, Bailey D et al. Physical performance of a positron tomograph for brain imaging with retractable septa. Phys Med Biol 1992;37:1637 - 1655.

243) Starr PA, Vitek JL, Bakay RA. Ablative surgery and deep brain stimulation for Parkinson's disease. Neurosurgery. 1998;43(5):989-1013; discussion 1013-5. Review.

244) Stenevi U, Bjorklund A, Svendgaard NA. Transplantation of central and peripheral monoamine neurons to the adult rat brain: techniques and conditions for survival. Brain Res. 1976;114(1):1-20.

245) Strecker, R.E. et al. Autoregulation of dopamine release and metabolism by intrastriatal nigral grafts as revealed by intracerebral microdialysis. Neuroscience 22, 169-178 (1987).

246) Studholme C., Derek L.G., Hawkes D.J. Automated three-dimensional registration of magnetic resonance and positron emission tomography brain images by multiresolution optimization of voxel similarity measures. Med. Psys. 24, 25-35 (1997).

247) Sveinbjornsdottir S, Hicks AA, Jonsson T, Petursson H, Gugmundsson G, Frigge ML, Kong A, Gulcher JR, Stefansson K. Familial aggregation of Parkinson's disease in Iceland. N Engl J Med. 2000; 343(24): 1765-1770.

248) Takahashi H, Ohama E, Suzuki S, Horikawa Y, Ishikawa A, Morita T, Tsuji S, Ikuta F. Familial juvenile parkinsonism: clinical and pathologic study in a family. Neurology. 1994;44:437-41.

249) Tanner CM, Ottman R, Goldman SM, Ellenberg J, Chan P, Mayeux R, Langston JW. Parkinson disease in twins: an etiologic study. JAMA. 1999 Jan 27;281(4):341-346.

250) Tassin J, Durr A, de Broucker T, Abbas N, Bonifati V, De Michele G, Bonnet AM, Broussolle E, Pollak P, Vidailhet M, De Mari M, Marconi R, Medjbeur S, Filla A, Meco G, Agid Y, Brice A. Chromosome 6-linked autosomal recessive early-onset Parkinsonism: linkage in European and Algerian families, extension of the clinical spectrum, and evidence of a small homozygous deletion in one family. The French Parkinson's Disease Genetics Study Group, and the European Consortium on Genetic Susceptibility in Parkinson's Disease. Am J Hum Genet. 1998;63(1):88-94.

251) Taylor JR, Elsworth JD, Roth RH, Sladek JR Jr, Collier TJ, Redmond DE Jr. Grafting of fetal substantia nigra to striatum reverses behavioral deficits induced by MPTP in primates: a comparison with other types of grafts as controls. Exp Brain Res. 1991;85(2):335-48.

252) Tison F, Normand E, Jaber M, Aubert I, Bloch B. Aromatic L-amino-acid decarboxylase (DOPA decarboxylase) gene expression in dopaminergic and serotoninergic cells of the rat brainstem. Neurosci Lett 1991: 127(2):203-206.

253) Townsend DW, Spinks TJ, Jones T et al. Fully three-dimensional reconstruction for a PET camera with retractable septa. Eur J Nucl Med 1989;15:741 - 745.

254) Tsukada H, Nishiyama S, Kakiuchi T, Ohba H, Sato K, Harada N. Is synaptic dopamine concentration the exclusive factor which alters the in vivo binding of [11C]raclopride?: PET studies combined with microdialysis in conscious monkeys. Brain Res 1999; 84: 160-169.

255) Valente EM, Bentivoglio AR, Dixon PH, Ferraris A, Ialongo T, Frontali M, Albanese A, Wood NW. Localization of a novel locus for autosomal recessive early-onset parkinsonism, PARK6, on human chromosome 1p35-p36. Am J Hum Genet. 2001;68(4):895-900

256) Valente EM, Brancati F, Ferraris A, Graham EA, Davis MB, Breteler MM, Gasser T, Bonifati V, Bentivoglio AR, De Michele G, Durr A, Cortelli P, Wassilowsky D, Harhangi BS, Rawal N, Caputo V, Filla A, Meco G, Oostra BA, Brice A, Albanese A, Dallapiccola B, Wood NW. PARK6-linked parkinsonism occurs in several European families. Ann Neurol. 2002;51(1):14-8

257) van de Warrenburg BP, Lammens M, Lucking CB, Denefle P, Wesseling P, Booij J, Praamstra P, Quinn N, Brice A, Horstink MW. Clinical and pathologic abnormalities in a family with parkinsonism and parkin gene mutations. Neurology. 2001;56(4):555-7

258) van Duijn CM, Dekker MC, Bonifati V, Galjaard RJ, Houwing-Duistermaat JJ, Snijders PJ, Testers L, Breedveld GJ, Horstink M, Sandkuijl LA, van Swieten JC, Oostra BA, Heutink P. Park7, a novel locus for autosomal

recessive early-onset parkinsonism, on chromosome 1p36. Am J Hum Genet. 2001;69(3):629-34

259) Vaughan JR, Farrer MJ, Wszolek ZK, Gasser T, Durr A, Agid Y, Bonifati V, DeMichele G, Volpe G, Lincoln S, Breteler M, Meco G, Brice A, Marsden CD, Hardy J, Wood NW. Sequencing of the alpha-synuclein gene in a large series of cases of familial Parkinson's disease fails to reveal any further mutations. The European Consortium on Genetic Susceptibility in Parkinson's Disease (GSPD). Hum Mol Genet. 1998a;7(4):751-3.

260) Vieregge P, Schiffke KA, Friedrich HJ, et al. Parkinson`s disease in twins. Neurology 1992;42:1453-1461.

261) Volkow ND, Wang GJ, Fowler JS, et al. Imaging endogenous dopamine competition with [^{11}C]raclopride in the human brain. Synapse 1994; 15: 255-262.

262) Ward CD, Duvoisin RC, Ince SE, et al. Parkinson`s disease in 65 pairs of twins and in a set of quadruplets. Neurology 1983;33: 815-824.

263) Wenning GK, Odin P, Morrish P, et al. Short- and long-term survival and function of unilateral intrastriatal dopaminergic grafts in Parkinson`s disease. Ann Neurol 1997; 42: 95-107.

264) West AB, Zimprich A, Lockhart PJ, Farrer M, Singleton A, Holtom B, Lincoln S, Hofer A, Hill L, Muller-Myhsok B, Wszolek ZK, Hardy J, Gasser T. Refinement of the PARK3 locus on chromosome 2p13 and the analysis of 14 candidate genes. Eur J Hum Genet. 2001;9(9):659-66

265) Widner H, Tetrud J, Rehncrona S, et al. Bilateral fetal mesencephalic grafting in two patients with parkinsonism induced by 1-methyl-4-phenyl-1,2,3,6-tetrahydropyridine (MPTP). N Engl J Med. 1992; 327: 1556-1563.

266) Winkler C, Bentlaage C, Nikkhah G, et al. Intranigral transplants of GABA-rich striatal tissue induce behavioral recovery in the rat parkinson model and promote the effects obtained by intrastriatal dopaminergic transplants. Exp Neurol 1999; 155: 165-186.

267) Woods RP, Cherry SR, Mazziotta JC. A rapid automated algorithm for accuartely aligning nad reslicing positron emission tomography images. J Comput Assis Tomogra 1992; 16: 620-633.

268) Worsley KJ, Marret S, Neelin P, Vanda AC, Friston KJ, Evans AC. A unified statistical approach to determining significnat signals in images of cerebral activation. Hum Brain Mapp 1996; 4: 58-73.

269) Yamamura Y, Sobue I, Ando K, Iida M, Yanagi T. Paralysis agitans of early onset with marked diurnal fluctuation of symptoms. Neurology 1973; 23(3):239-244.

270) Zetterström, T. et al. *In vivo* measurement of spontaneous release and metabolism of dopamine from intrastriatal nigral grafts using intracerebral microdialysis. Brain Res. 362, 344-349 (1986).

271) Zhang ZX, Roman GC. Worldwide occurrence of Parkinson's disease: an updated review. Neuroepidemiology. 1993;12(4):195-208. Review.

272) Zimmerman TR, Bhati M, Calne DB, Duvoisin RC. Parkinson's disease in monozygotic twins: a follow up. Neurology 1991;41 (Suppl 1):225.

BIBL.
LONDIN.
UNIV.